Komitet Krystalografii PAN
Instytut Niskich Temperatur i Badań Strukturalnych PAN
Uniwersytet Kardynała Stefana Wyszyńskiego
Polskie Towarzystwo Krystalograficzne

62 Konwersatorium Krystalograficzne

Polish Crystallographic Meeting

Edycja on-line, 24 - 25 VI 2021

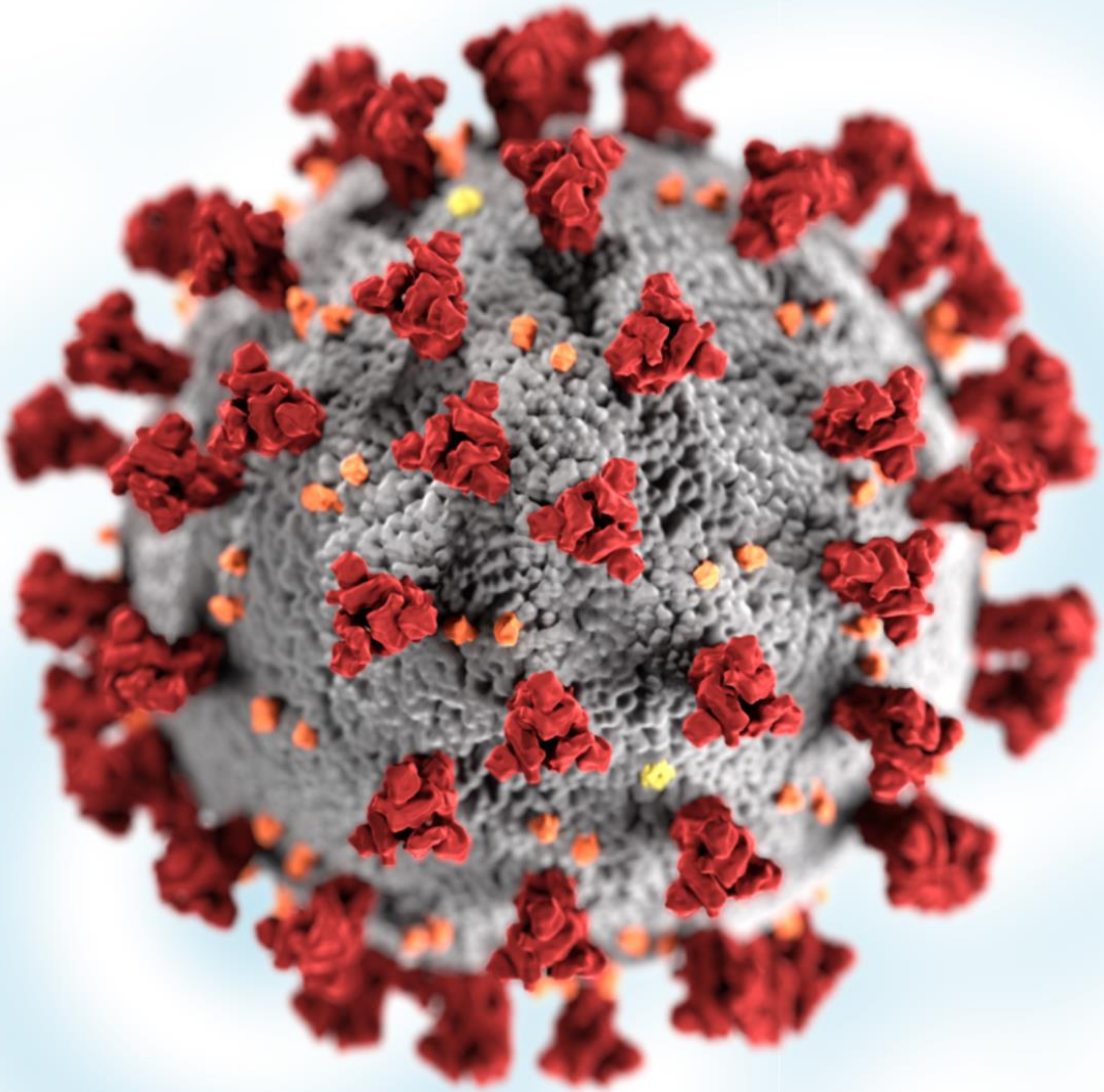

62 Konwersatorium Krystalograficzne

Edycja on-line, 24 – 25 VI 2021 r.

Program
Streszczenia komunikatów
Lista uczestników i autorów prac

Organizatorzy:
Komitet Krystalografii PAN
Instytut Niskich Temperatur i Badań Strukturalnych PAN we Wrocławiu
Uniwersytet Kardynała Stefana Wyszyńskiego w Warszawie
Polskie Towarzystwo Krystalograficzne

Sponsor:
Polska Akademia Nauk z Funduszu Upowszechnienia i Promocji Nauki

Komitet Organizacyjny:
Marek Wołcyrz – przewodniczący, Kinga Suwińska, Marek Daszkiewicz - zastępca przewodniczącego, Anna Gągor, Daniel Lis, Vasyl Kinzhybalo, Dorota Kowalska, Tamara Bednarchuk, Volodymyr Medviediev, Piotr Rejnhardt, Dawid Drozdowski

Redakcja:
Marek Wołcyrz, Dorota Kowalska

Wydawca:
Instytut Niskich Temperatur i Badań Strukturalnych PAN, Wrocław
oraz Komitet Krystalografii PAN

ISBN 978-83-939559-5-4

Tematyka Konwersatorium obejmuje badania podstawowe i stosowane dotyczące idealnej i realnej struktury kryształów prowadzone za pomocą promieniowania rentgenowskiego uzyskiwanego zarówno tradycyjnymi metodami jak i w synchrotronach, badania przy użyciu neutronów i elektronów, zagadnienia symetrii, przemian fazowych i wzrostu kryształów, nowe metody badawcze i obliczeniowe oraz wszelkie inne aspekty krystalografii. Konwersatorium stanowi forum wymiany poglądów wszystkich polskich krystalografów.

Cover illustration, created at the Centers for Disease Control and Prevention (CDC), reveals ultrastructural morphology exhibited by coronaviruses. Note the spikes that adorn the outer surface of the virus, which impart the look of a corona surrounding the virion, when viewed electron microscopically. A novel coronavirus, named Severe Acute Respiratory Syndrome coronavirus 2 (SARS-CoV-2), was identified as the cause of an outbreak of respiratory illness first detected in Wuhan, China in 2019. The image by Alissa Eckert and Dan Higgins is in the public domain and free of any copyright restrictions. See: https:// phil.cdc.gov/details.aspx?pid=23312.

PROGRAM KONWERSATORIUM
PROGRAM OF THE MEETING

Czwartek, 24 czerwca 2021 r. / Thursday, June 24, 2021

9:00 – 9:20 **Otwarcie Konwersatorium i uroczyste wręczenie nagród laureatom IV Ogólnopolskiej Olimpiady Krystalograficznej / Opening of the conference and the ceremonial awarding of prizes to the winners of the 4th Polish Crystallographic Olympiad**

SESJA PLENARNA / PLENARY SESSION

9:20 – 9:50 Angela B. Grommet, Oksana Yanshyna, Hema Kuntrapakam, Oleg V. Chashchikhin, **Michał J. Białek**, Rafal Klajna **O-1**
Faculty of Chemistry, Weizmann Institute of Science, Rehovot, Israel; Department of Chemistry, University of Wrocław
Host-guest interactions under molecular confinement within a flexible coordination cage – solid state vs. solution

9:50 – 10:10 **Piotr A. Guńka**, Janusz Zachara **O-2**
Wydział Chemiczny Politechniki Warszawskiej
Novel bond-valence-based coordination number definitions and their application to high-pressure crystal structures

10:10 – 10:30 **Jakub Drapała**, Radosław Kamiński, Krzysztof Durka, Katarzyna N. Jarzembska **O-3**
Warsaw University of Technology, Faculty of Chemistry: University of Warsaw, Faculty of Chemistry
Structural trends in bisphosphine complexes of coinage metals at first oxidation state

10:30 – 10:50 **Marta Otręba**, Katarzyna Ślepokura **O-4**
University of Wrocław, Faculty of Chemistry
Crystallochemical analysis of adenosine hypodiphosphate ester and related organic hypodiphosphates

10:50 – 11:00 **Kunal Kumar Jha**, Florian Kleemiss, Michał Leszek Chodkiewicz, Paulina M. Dominiak **O-5**
Electron Density Modelling Group, Department of Chemistry, University of Warsaw; Universität Regensburg, Fakultät für Chemie und Pharmazie, Regensburg, Germany
Aspherical atom refinements on X-ray and electron diffraction data of diverse structures including disorder and COF systems: a time-accuracy trade off

11:00 – 11:30 **PRZERWA / BREAK**

11:30 – 12:00	**Felix Hennersdorf, Marcus J. Winter** Rigaku Europe SE, Neu Isenburg, Germany **Rigaku advances in X-ray and electron crystallography**	**O-6**
12:00 – 12:30	**Tadeusz Glenc** Testchem, Pszów **Prezentacja najnowszego dyfraktometru proszkowego firmy Rigaku**	**O-7**
12:30 – 12:50	**Jarosław Serafińczuk** Department of Nanometrology, Wrocław University of Science and Technology; Łukasiewicz Research Network – PORT Polish Center for Technology Development, Wrocław **High resolution X-ray diffraction measurements carried out from the edge of the sample**	**O-8**
13:00 – 14:00	**PRZERWA / BREAK**	
14:00 – 14:20	Agnieszka Kiliszek, Leszek Błaszczyk, Magdalena Bejger, **Wojciech Rypniewski** Institute of Bioorganic Chemistry, Polish Academy of Sciences, Poznań **Broken symmetry between RNA enantiomers in a crystal lattice**	**O-9**
14:20 – 14:40	**Joanna Loch**, Barbara Imiołczyk, Joanna Śliwiak, Anna Wantuch, Mirosław Gilski, Mariusz Jaskólski Jagiellonian University, Faculty of Chemistry, Kraków; Polish Academy of Sciences, Institute of Bioorganic Chemistry, Poznań; A. Mickiewicz University, Faculty of Chemistry, Poznań **Structural and functional studies of novel L-Asparaginase from *Rhizobium etli*** **Małgorzata K. Cabaj**, Paulina M. Dominiak Electron Density Modelling Group, Biological and Chemical Research Centre, Department of Chemistry, University of Warsaw **Frequency and hydrogen bonding geometry of nucleobase homopairs in small molecule crystal structures**	**O-10** **O-11**
15:00 – 16:00	**Alexander Wlodawer**, Marek Grabowski, Joanna M. Macnar, Marcin Cymborowski, David R. Cooper, Ivan G. Shabalin, Mirosław Gilski, Dariusz Brzeziński, Marcin Kowiel, Zbigniew Dauter, Bernhard Rupp, Mariusz Jaskólski, and Wladek Minor Center for Structural Biology, National Cancer Institute, Frederick, MD, USA; Department of Molecular Physiology and Biological Physics, University of Virginia, Charlottesville, VA, USA; Faculty of Chemistry, University of Warsaw; Faculty of Chemistry, A. Mickiewicz University, Poznań; Institute of Bioorganic Chemistry, Polish Academy of Sciences, Poznań; Institute of Computing Science, Poznań University of Technology; k.-k Hofkristallamt, San Diego, CA, USA; Institute of Genetic Epidemiology, Medical University Innsbruck, Austria **One thousand structures of SARS-CoV-2 proteins, or how the Polish crystallographic mafia joined the fight against Covid-19**	**O-12**
16:00 – 16:30	**PRZERWA / BREAK**	
16:30 – 18:30	**SESJA PLAKATOWA A / POSTER SESSION A**	

Piątek, 25 czerwca 2021 r. / Friday, June 25, 2021

SESJA PLENARNA / PLENARY SESSION

9:00 – 9:20 **O-13**
Wiesław Świętnicki, Ewa Brzozowska
Instytut Immunologii i Terapii Doświadczalnej PAN im. L. Hirszfelda, Wrocław
Analiza *in silico* białek kanalikowych ogonka bakteriofaga sugeruje przypuszczalne miejsce wiązania cukru i mechanizm katalityczny

9:20 – 9:30 **O-14**
Marta Kulik, Michał L. Chodkiewicz, Paulina M. Dominiak
Centrum Nauk Biologiczno-Chemicznych Uniwersytetu Warszawskiego, Wydział Chemii, Uniwersytet Warszawski
From electron density maps to electrostatic potential density maps of macromolecules with MATTS databank

9:30 – 9:40 **O-15**
Anna Cociurovscaia, Agnieszka Pietrzyk-Brzezińska
Instytut Biotechnologii Molekularnej i Przemysłowej, Wydział Biotechnologii i Nauk o Żywności, Politechnika Łódzka
Identyfikacja potencjalnych efektorów bakteryjnego czynnika transkrypcyjnego RcdA

9:40 – 10:10 **O-16**
Krzysztof Woźniak, Marcin Stachowicz, Roman Gajda, Jan Parafiniuk
Chemistry Department., University of Warsaw; Institute of Geochemistry, Mineralogy and Petrology, University of Warsaw
Experimental charge densities of minerals under pressure

10:10 – 10:20 **O-17**
Daniel Tchoń, Anna Makal
Biological and Chemical Research Centre, Faculty of Chemistry, University of Warsaw
Completeness in high-pressure XRD experiments

10:20 – 10:30 **O-18**
Svitlana V. Shishkina, Yevhenii A. Vaksler, Abdenacer Idrissi
SSI "Institute for Single Crystals" NAS of Ukraine, Kharkiv, Ukraine; V.N. Karazin Kharkiv National University, Kharkiv, Ukraine; Laboratoire de Spectroscopie pour les Interactions, la Réactivité et L'environnement, Université de Lille, Villeneuve d'Ascq, France
High-pressure influence on piracetam crystals: studying by quantum chemical methods

10:30 – 10:40 **O-19**
Yevhenii A. Vaksler, Abdenacer Idrissi, Svitlana V. Shishkina
SSI "Institute for Single Crystals" NAS of Ukraine, Kharkiv, Ukraine; V.N. Karazin Kharkiv National University, Kharkiv, Ukraine; Laboratoire de Spectroscopie pour les Interactions, la Réactivité et L'environnement, Université de Lille, Villeneuve d'Ascq, France
Computational analysis of pressure-induced shear in R,S-ibuprofen

10:40 – 10:50 **O-20**
Piotr Rejnhardt, Jan K. Zaręba, Ida Moszczyńska, Marek Daszkiewicz
Institute of Low Temperature and Structure Research, Polish Academy of Sciences, Wrocław; Advanced Materials Engineering and Modelling Group, Faculty of Chemistry, Wrocław University of Science and Technology; Faculty of Chemistry, Adam Mickiewicz University, Poznań
Non-linear optical properties and negative area compressibility of (S)-2-amino-3-guanidinopropanoic acid monochloride

10:50 – 11:00 **Michał Duda**, Marta Grzesiak-Nowak, Marcin Oszajca, Wiesław Łasocha **O-21**
Wydział Chemii Uniwersytetu Jagiellońskiego, Kraków; Instytut Katalizy i Fizykochemii Powierzchni im. Jerzego Habera PAN, Kraków
Synteza i badania strukturalne połączeń bromku kadmu z diaminami alifatycznymi z wykorzystaniem techniki rentgenowskiej dyfrakto-metrii proszkowej

11:00 – 11:30 **PRZERWA / BREAK**

11:30 – 11:50 **Henryk Drozdowski**, Małgorzata Śliwińska-Bartkowiak, Stefan Jurga **O-22**
Faculty of Physics, Adam Mickiewicz University, Poznań
Application of crystallography in studies of soft materials

11:50 – 12:10 **Anna A. Hoser**, Marcin Sztylko, Anders Ø. Madsen **O-23**
Biological and Chemical Research Centre, Faculty of Chemistry, University of Warsaw; Department of Pharmacy, University of Copenhagen, Denmark
Theoretically derived thermodynamic properties can be improved by the refinement of low-frequency modes against X-ray diffraction data

12:10 – 12:35 **Iwona Lazar**, Andrzej Majchrowski, Krystian Roleder **O-24**
Institute of Physics, University of Silesia, Katowice; Institute of Applied Physics, Military University of Technology, Warsaw
Phase transitions in a $PbZr_{0.87}Ti_{0.13}O_3$ single crystal

12:35 – 12:50 **Irena Jankowska-Sumara**, Marek Paściak, Andrzej Majchrowski **O-25**
Institute of Physics, Pedagogical University of Cracow; Institute of Physics of the Czech Academy of Sciences, Prague, Czech Republic; Institute of Applied Physics, Military University of Technology, Warsaw
Modulated structures in $Pb(Hf_{1-x}Sn_x)O_3$ single crystals by X-ray diffraction

12:50 – 13:00 **Konrad Dyk**, Łukasz Baran, Wojciech Rżysko, Marek Stankevič, Daniel Kamiński **O-26**
Katedra Chemii Ogólnej, Koordynacyjnej i Krystalografii; Katedra Chemii Teoretycznej; Katedra Chemii Organicznej, Uniwersytet Marii Curie-Skłodowskiej w Lublinie
Wzajemne oddziaływanie między stabilnością kryształów a energią konformacji molekuły

13:00 – 14:00 **PRZERWA / BREAK**

14:00 – 16:00 **SESJA PLAKATOWA B / POSTER SESSION B**

16:00 – 16:10 **ZAKOŃCZENIE KONWERSATORIUM**

REFERATY PLENARNE
ORAL SESSIONS

O-01

HOST-GUEST INTERACTIONS UNDER MOLECULAR CONFINEMENT WITHIN A FLEXIBLE COORDINATION CAGE – SOLID STATE VS SOLUTION

Angela B. Grommet,[a] Oksana Yanshyna,[a] Hema Kuntrapakam,[a] Oleg V. Chashchikhin,[a] Michał J. Białek,[a,b] Rafal Klajn[a]

[a]Faculty of Chemistry, Weizmann Institute of Science, Herzl 245, 76100 Rehovot, Israel
[b]Department of Chemistry, University of Wrocław, F. Joliot-Curie 14, 50383 Wrocław

I will introduce an elegant model system of enzymatic centers in a shape of a simple flexible coordination cage **1** [1]. The concept of the molecular confinement is an important contributor to a way of thinking about molecular reactivity [2]. In the talk, I will focus on the confined space inside the hydrophobic cavity of cage **1**. The mutual interactions with guests enforce conformational changes leading to maximization of interaction.

These, at a significant degree depending on the guest molecule, provide a metastable, previously unknown conformer **2** that yielded single crystals for diffraction [3]. The fact that bent guests are effective for the transformation allows for light-driven modulation of cage shape while using photoresponsive azobenzenes. But is this conformer what we see in solution after encapsulation of certain guests? Further enrichment of the mixture with the other cage species provides an answer to its true identity.

On the other hand, the importance of host-guest interactions manifests itself by altering physical and chemical properties of the later one as well. In a study of fluorescent dye resorufin (RF) and its redox counterparts we noticed that upon encapsulation of two guest molecules (RF_2⊂**1**), their fluorescent properties diminish thus forming the smallest nonfluorescent dimer protected by the cage walls [4]. The story is quite different in the solid state when we investigated a series of single crystals obtained from (Guest)$_2$⊂**1** crystallization.

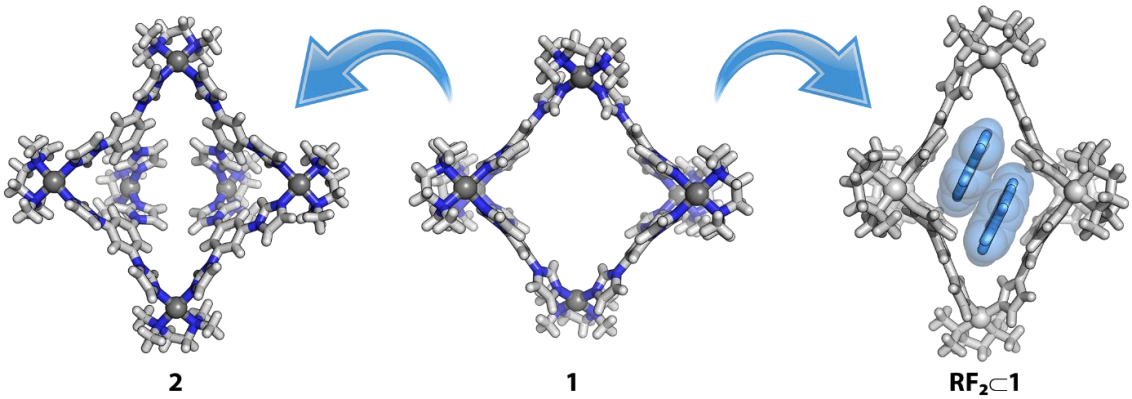

References

[1] D. Samanta, S. Mukherjee, Y.P. Patil, P.S. Mukherjee, *Chem. Eur. J.* **18** (2012) 12322.
[2] A.B. Grommet, M. Feller, R. Klajn, *Nat. Nanotech.*, **15** (2020) 256.
[3] A.B. Grommet, H. Kuntrapakam, M.J. Białek, R. Klajn, in preparation.
[4] O. Yanshyna, M.J. Białek, O.V. Chashchikhin, R. Klajn, in review.

O-02

NOVEL BOND-VALENCE-BASED COORDINATION NUMBER DEFINITIONS AND THEIR APPLICATION TO HIGH-PRESSURE CRYSTAL STRUCTURES

Piotr A. Guńka, Janusz Zachara

Wydział Chemiczny Politechniki Warszawskiej, ul. Noakowskiego 3, 00-664 Warszawa

Coordination number is one of the basic concepts in structural and general chemistry and yet it lacks a precise and straightforward definition [1]. Problems arise, for instance, when one wants to compare a series of structures determined at increasing pressures and the coordination center forms *n* strong primary and *m* weak secondary bonds and its coordination number is described as *n* + *m*. Herein novel definitions of coordination number based on bond valence and aimed at solving these difficulties will be described. Firstly, the definitions of valence entropy and valence diversity coordination numbers (VECN and VDCN) will be given. Subsequently, their properties will be briefly studied, and the new coordination numbers will be compared to the established Hoppe's effective coordination number (ECoN) [2]. Finally, an application of VECN to structural data of arsenic(III) oxocompounds including high-pressure data of arsenic(III) oxide polymorphs will be presented [3].

Literatura

[1] R. Hoppe, *Angew. Chem. Int. Ed.*, **9** (1970) 25.
[2] R. Hoppe, *Z. Kristallogr.*, **150** (1979) 23.
[3] P. A. Guńka, J. Zachara, *Acta Crystallogr. Sect. B*, **75** (2019) 86.

O-03

STRUCTURAL TRENDS IN BISPHOSPHINE COMPLEXES OF COINAGE METALS AT FIRST OXIDATION STATE

Jakub Drapała[a,b], **Radosław Kamiński**[b], **Krzysztof Durka**[a], **Katarzyna N. Jarzembska**[b]

[a]*Warsaw University of Technology, Faculty of Chemistry, Noakowskiego 3, 00-664 Warsaw, Poland*
[b]*University of Warsaw, Faculty of Chemistry, Pasteura 1, 02-093, Warsaw, Poland*

Transition metal complexes are perpetually a widely studied class of compounds. Due to specific metal-ligand interactions they are often source of unique properties such as phosphorescence or catalytic activity. Structural chemistry of coordination compounds is constantly progressing since it allows understanding the mechanisms of structure organisation which, together with structure-property relationship analysis, plays a crucial role in designing of novel materials.

A series of Au^{I} and Cu^{I} chloride complexes with bisphosphine ligands were structurally and spectroscopically examined. Imposing structural changes affecting rigidity and aromaticity of the organic ligand core played a primal role in complex organisation. Additionally, the influence of metal cation polarizability was reviewed. Increase of hardness of the Lewis acid drives competition between anion and ligand heteroatoms in binding to the metallic centre, which dramatically affects the complex structure. Strong cation-anion interactions led to formation of multicentre complexes in most cases of Cu^{+} compounds, whereas more labile $Au^{+}\cdots Cl^{-}$ interactions had minor influence on the complex organisation.

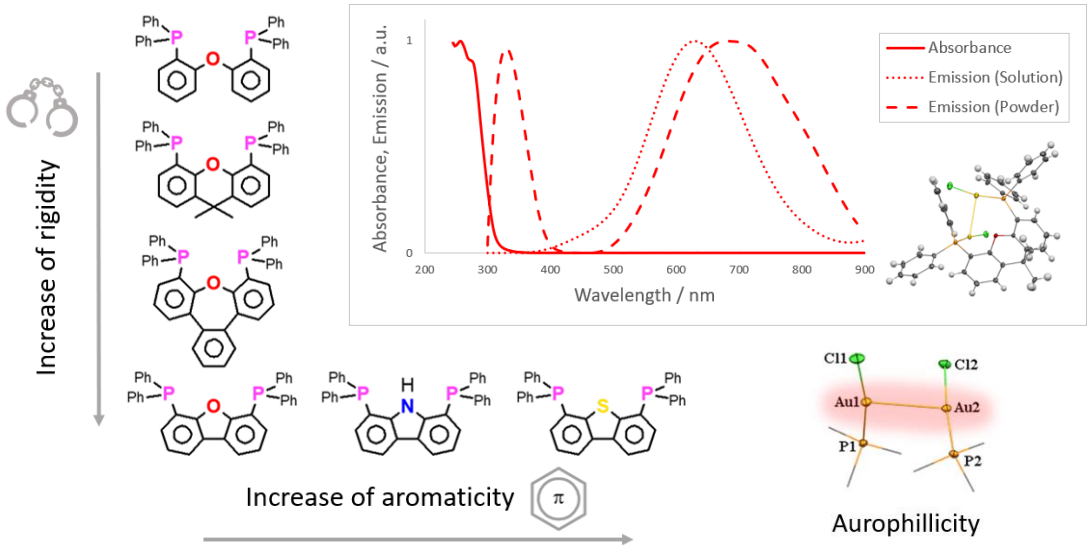

Spectroscopic analysis revealed bathochromical shift in absorption spectra of metal complexes in DCM solution with the increase with ligand rigidity. Formation of new charge-transfer bands with respect to pure ligand was also observed. Analysis of complexes emissive properties in solution proves the presence of phosphorescent properties, while in most cases powder samples occurred non-emissive.

Structural and spectroscopic analyses were also fortified with computational studies. DFT methods were useful in determination of the mechanism of complex excitation upon irradiation. The lowest-energy absorption bands were attributed to metal-to-ligand charge transfer. QTAIM analysis revealed immense influence of weak-type intramolecular interactions in the formation of a complex structure. This extremely important conclusion indicate the necessity of taking into consideration C–H···π, π–stacking, halogen-halogen and metalophillic interactions while designing metal complexes.

The authors would like to acknowledge the SONATA grant (No. 2014/15/D/ST4/02856) from the National Centre in Poland for financial support. The in-house X-ray diffraction experiments were performed at the Department of Physics, University of Warsaw, on a Rigaku Oxford Diffraction SuperNova diffractometer, which was co-financed by the European Union within the European Regional Development Fund (POIG.02.01.00-14-122/09). The authors thank the Wroclaw Centre for Networking and Supercomputing, Wroclaw, Poland (Grant No. 285) for providing computational facilities.

References

[1] Gemma M. Adams, Andrew S. Weller, *POP-type ligands: Variable coordination and hemilabile behaviour*, *Coord. Chem. Rev*., **355** (2018) 150-172.

[2] V. Balzani, S. Campagna, *Photochemistry and Photophysics of Coordination Compounds I*, Berlin: Springer-Verlag, 2007. ISBN 978-3-540-73346-1.

[3] L. J. Farrugia, P. Macchi, *Bond Orders in Metal–Metal Interactions Through Electron Density Analysis; Electron Density and Chemical Bonding I. Structure and Bonding*, vol. 146, Springer, Berlin, 2010, ISBN: 978-3-642-30802-4, 127-158

O-04

CRYSTALLOCHEMICAL ANALYSIS OF ADENOSINE HYPODIPHOSPHATE ESTER AND RELATED ORGANIC HYPODIPHOSPHATES

Marta Otręba, Katarzyna Ślepokura

University of Wrocław, Faculty of Chemistry, F. Joliot - Curie 14 St., 50-383 Wrocław

Pyrophosphoric esters of nucleosides, e.g. ADP or GDP, play crucial role in biochemical pathways of living organisms, especially as energy storage agents, substrates in biosynthesis reactions or enzymatic activity regulators. In the search of compounds which could replace naturally occurring pyrophosphates, structural analogues are considered. Those are hypodiphosphates which contain direct P^{IV}–P^{IV} bond instead of pyrophosphate P^{V}–O–P^{V} linkage. Initial biochemical research shows that hypodiphosphate analogues of ATP or ADP act as inhibitors or substrates in selected enzymatic reactions of natural substrates.[1-2] It has been proven that even hypodiphosphoric acid ($H_4P_2O_6$) is recognized by some enzymes and can replace pyrophosphoric acid ($H_4P_2O_7$) in its pathways, producing more resistant product which inhibits further reactions.[3]

While undertaking the challenge of structural investigations in hypodiphosphate nucleoside esters we decided to synthesize and characterize hypodiphosphate analogues of ADP (Fig. 1).[4] A series of crystals with organic cations has also been synthesised to thoroughly investigate crystallochemical behaviour of hypodiphosphate group. Purine and pyrimidine nucleosides (adenosine, cytidine, deoxycytidine and cytarabine) accompanied with purine bases (adenine, xanthine, theophylline, theobromine and caffeine) have been chosen as organic counterpart to characterize interactions that could play major role in esters. Additionally, series of hypodiphosphate sodium salts has been synthesised and analysed to illustrate inorganic ion interactions that could be found in living cells.

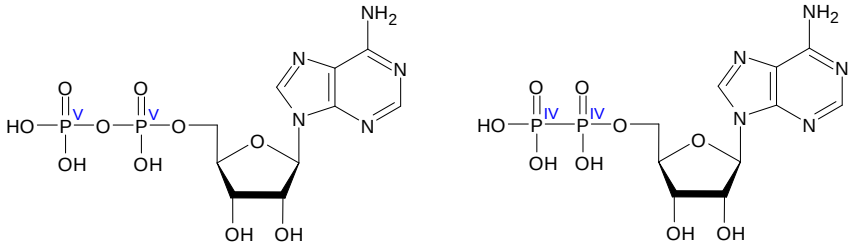

Figure 1. Structural formulae of adenosine 5′-diphosphate (1, ADP) and adenosine 5′-hypodiphosphate (2, AhDP).

In organic hypodiphosphate crystals supramolecular interactions are mainly realized by base–hypodiphophate hydrogen bonds (with structural ring motif $R^2_2(8)$, consisting of two N–H···O bonds) supported by $\pi\cdots\pi$ stacking interactions between purine or pyrimidine rings. Other observed hydrogen bonds are realized as hypodiphosphate–hypodiphosphate, sugar–hypodiphosphate, base–sugar or sugar–sugar

contacts. In many crystals lone pair–π (lp–π) interactions occur between electron-rich oxygen atoms (mostly carbonyl or hypodiphosphate) and nucleobases aromatic rings.

In the analysed crystals hypodiposphate groups (PP) adopt different ionization states, i.e. $H_4P_2O_6$, $H_3P_2O_6^-$, $H_2P_2O_6^{2-}$ and $P_2O_6^{4-}$ in organic salts or O5′–$P_2O_5H_3$, O5′–$P_2O_5H_2^-$ and O5′–$P_2O_5H^{2-}$, in esters. Through the network of hydrogen bonding, PP anions can build up 3*D* inorganic networks, 2*D* layers, 1*D* chains or exist as isolated anions. Their mutual interactions play important role for nucleotide self-assembly.

References

[1] J. Setondji; P. Remy; J. P. Ebel, G. Dirheimer, *Biochim. Biophys. Acta* **232** (1971) 585.
[2] T. Godefroy-Colburn, J. Setondji, *Biochim. Biophys. Acta* **272** (1972) 417.
[3] M. K. Kukhanova, N. F. Zakirova, A. V. Ivanov, L. A. Alexandrova, M. V. Jasco, A. R. Khomutov, *Biochem. Biophys. Res. Commun.* 338 (2005), 1335.
[4] M. Otręba, D. Budzikur, Ł. Górecki & K. A. Ślepokura, *Acta Crystallogr. C.*, **74** (2018) 571.

O-05

ASPHERICAL ATOM REFINEMENTS ON X-RAY AND ELECTRON DIFFRACTION DATA OF DIVERSE STRUCTURES INCLUDING DISORDER AND COF SYSTEMS: A TIME-ACCURACY TRADE OFF

Kunal Kumar Jha[1], Florian Kleemiss[2], Michał Leszek Chodkiewicz[1], Paulina M. Dominiak[1]

1) Electron Density Modelling Group, Department of Chemistry, University of Warsaw, ul. Żwirki i Wigury 101, 02-089, Warszawa, Poland,
2) Universität Regensburg, Fakultät für Chemie und Pharmazie, Universitätsstr. 31, 93053 Regensburg, Germany.
Email of communicating author: k.jha@uw.edu.pl

The recent advances in quantum crystallography facilitated a shift from the most common but improper independent atom model (IAM) used in structure determination to more appropriate aspherical atom model. With IAM, which is based on scattering factors precomputed for isolated, spherically averaged atoms or ions, the structural information is limited to nucleus position only. During aspherical refinement, information on chemical bonding, lone pairs, partial charges, etc. is taken into account. A lot of experimental or computational effort is however required to get such information with high accuracy. Parametrization of aspherical models from experimental data is a very time consuming and tedious process. The computational efforts have been focused on achieving highly accurate aspherical models and at the same time on reducing the computational cost. A convenient and computationally cheap approach was developed in which transferable aspherical atom model (TAAM) is used for the refinement. TAAM refinement have been applied on both X-ray and electron diffraction (ED) data largely improving the physical representation and refinement statistics of the crystal structure.[1-3] With the new developments, Hirshfeld atom refinement (HAR) in NoAspherA2[4] using the Olex2 software, it is now possible to integrate TAAM with NoAspherA2 and perform the refinement on X-ray and electron diffraction data of even disordered structures in a quick time. Here we'll highlight the results of TAAM refinement on large molecules, co-crystals, disordered structures. A comparison of accuracy and time taken in refinement resulting from HAR in NoAspherA2 and TAAM in NoAspherA2 will be presented. Refinement of network and polymeric structure can also be performed efficiently using TAAM in NoAspherA2 and the results will be discussed.

Acknowledgement: This work is supported by the National Centre of Science (Poland) through grant OPUS No.UMO-2017/27/B/ST4/02721.

References

[1] Jha, K. K.; Gruza, B.; Kumar, P.; Chodkiewicz, M. L.; Dominiak, P. M. TAAM: A Reliable and User Friendly Tool for Hydrogen-Atom Location Using Routine X-Ray Diffraction Data. *Acta Crystallogr. Sect. B Struct. Sci. Cryst. Eng. Mater.* **2020**, *76* (3).
[2] Gruza, B.; Chodkiewicz, M.; Krzeszczakowska, J.; Dominiak, P. M. Refinement of Organic Crystal Structures with Multipolar Electron Scattering Factors. *Acta Crystallogr. Sect. A Found. Adv.* **2020**, *76* (1).
[3] Jha, K. K.; Gruza, B.; Chodkiewicz, M. L.; Jelsch, C.; Dominiak, P. M. Refinements on electron

diffraction data of β-glycine in MoPro: A quest for improved structure model. *J. Appl. Cryst.* **2021**, Accepted Manuscript.

[4] Kleemiss, F.; Dolomanov, O. V; Bodensteiner, M.; Peyerimhoff, N.; Midgley, L.; Bourhis, L. J.; Genoni, A.; Malaspina, L. A.; Jayatilaka, D.; Spencer, J. L.; et al. Accurate Crystal Structures and Chemical Properties from NoSpherA2. *Chem. Sci.* **2021**.

O-06

RIGAKU ADVANCES IN X-RAY AND ELECTRON CRYSTALLOGRAPHY

Felix Hennersdorf, Marcus J. Winter

Rigaku Europe SE, Hugenottenallee 167, 63263 Neu-Isenburg, Germany
E-mail: felix.hennersdorf@rigaku.com

The latest range of Rigaku Oxford Diffraction instrument configurations will be summarised, and illustrated with a number of particular example applications.

The XtaLAB Synergy-ED is a new and fully integrated electron diffractometer, creating a seamless workflow from data collection to structure determination of three-dimensional molecular structures. The XtaLAB Synergy-ED is the result of an innovative collaboration to synergistically combine our core technologies: Rigaku's high-speed, high-sensitivity photon-counting detector (HyPix-ED) and state-of-the-art instrument control and single crystal analysis software platform (CrysAlisPro for ED), and JEOL's long-term expertise and market leadership in designing and producing transmission electron microscopes.

Furthermore, our X-ray diffraction instruments will be presented. The XtaLAB Synergy platform with microfocus or rotating anode sources on one side and a series of Hybrid Photon Counting (HPC) X-ray area detectors on the other side of the four-circle goniometer allows for versatile configurations perfectly adapted to the researcher's needs. These systems can be further equipped with the sample changing robot (XtaLAB Synergy Flow), an Intelligent Gonoimeter Head (IGH) for automated crystal centering, the plate scanning device XtalCheck-S or a high pressure unit.

O-07

PREZENTACJA NAJNOWSZEGO DYFRAKTOMETRU PROSZKOWEGO FIRMY RIGAKU

Tadeusz Glenc

Testchem sp. z o.o.

Firma Rigaku, jeden z kluczowych producentów aparatury do dyfrakcji rentgenowskiej wprowadziła na rynek nowy dyfraktometr proszkowy przeznaczony przede wszystkim do laboratoriów przemysłowych, a szczególnie do kontroli jakości, ale również do celów badawczych i edukacyjnych.

Dyfraktometr z goniometrem theta/theta i promieniu 150 mm jest wyposażony w generator 800W. Taka konfiguracja zapewnia dużą intensywność wiązki dyfrakcyjnej oraz wystarczającą rozdzielczość w przypadku wielu zastosowań.

W dyfraktometrze zastosowano nową, kompaktową lampę rentgenowską i detektor paskowy D/tex Ultra250. System chłodzenia lampy rentgenowskiej jest umieszczony wewnątrz obudowy dyfraktometru.

Obróbka danych dyfrakcyjnych jest realizowano za pomocą nowego oprogramowania EasyX. Oprogramowanie oparte jest na standardowym oprogramowaniu firmy Rigaku o nazwie SmartLab Studio2. Celem nowego oprogramowania jest ekstremalne uproszczenie analizy ilościowej, opartej na metodzie Rietvelda. Dyfraktometr może być wyposażony w system do automatycznego wprowadzania próbek .

Rysunek przedstawia widok nowego dyfraktometru.

O-08

HIGH RESOLUTION X-RAY DIFFRACTION MEASUREMENTS CARRIED OUT FROM THE EDGE OF THE SAMPLE

Jarosław Serafińczuk

Department of Nanometrology, Wrocław University of Science and Technology, Janiszewskiego 11/17, 50-372 Wrocław, Poland
ŁUKASIEWICZ Research Network – PORT Polish Center for Technology Development, Stablowicka 147, 54-066 Wrocław, Poland

High resolution X-ray diffractometry is the primary structural method used in the investigations of epitaxial layers and structures. In high resolution configuration a 4-bounce Ge(220) Bartels monochromator gives an incidence beam divergence of 12 arcsec. In the diffracted beam path, open detector configuration is used for rocking curves (RC) measurements or triple-axis analyser crystal before the detector is used for reciprocal lattice maps (RLM) measurements. Such configurations allow investigations of the single crystals semiconductor structures including: low-dimensional quantum well (QW), quantum dots (QDs), laser structures etc. The analysis of the results such as RC and RLM allow determination of the basic parameters of the structure: thickness and composition of the layers, degree of relaxation, lattice parameters, size of crystalline blocks and mosaicity of the highly mismatched structures but also dislocations density and strain in the epitaxial layers. In such analysis the main problem is the measurement of planes perpendicular to the sample surface. In standard XRD configuration it is practically impossible to measure such planes for such highly oriented samples. In order to avoid this problem, planes with a large inclination angle, (e.g. over 60 deg) are investigated using the skew geometry (Fig. 1).

The application of measurements carried out from the edge of the sample allows analysis of such structures, above all, spatial separation of the effects shown in the investigation results. In particular, it allows independently determination of the lattice parameter perpendicular to the growth direction, separation of tilt and twist mosaicity [1], calculation of the edge dislocations density [2] or residual strains [3] in the structure. Furthermore, such type of measurements reveals the difference in lattice parameters of the specific layers [4], which are not always visible with conventional measurements performed from the surface of the sample. This type of measurements were developed in Structural Research Laboratory in Wroclaw University of Science and Technology and has been used for years in the analysis of epitaxial structures - mainly mismatched III-N materials like (Ga, Al)N but also low dimensional structures (QW and QDs)of the III-V materials.

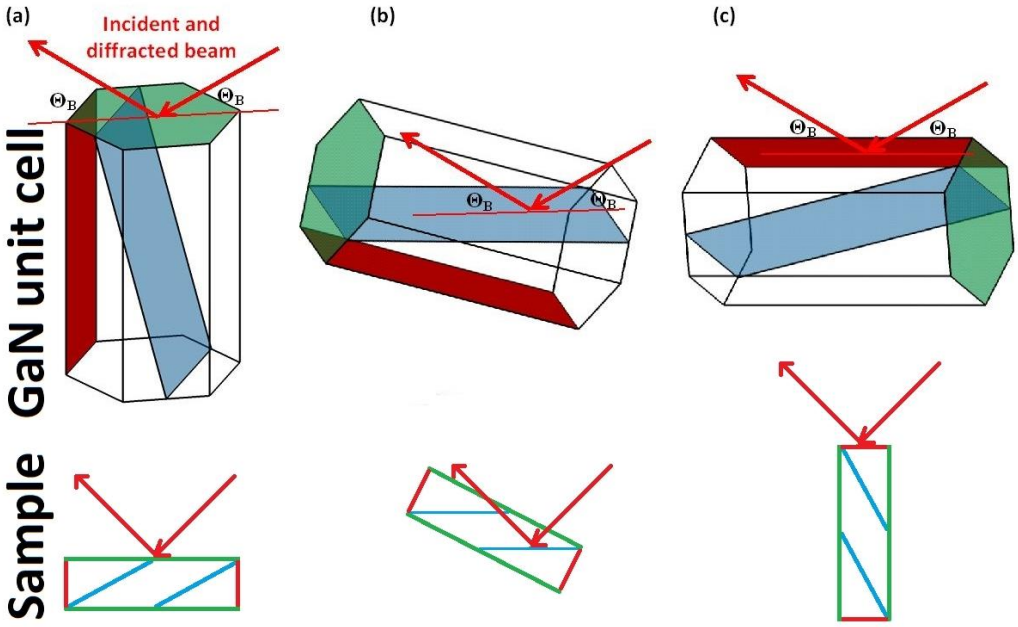

Fig. 1. XRD measurements geometry: a) classical measurements from the surface of the sample; b) skew geometry; c) edge measurements geometry

References

[1] J. Serafinczuk, *Cryst. Res. Technol*., **51** (2016), 276–281.
[2] J. Serafinczuk, K. Moszak, L. Pawlaczyk, W. Olszewski, D. Pucicki, R. Kudrawiec, D. Hommel, *J. Alloys Compd.*, **825** (2020), 153838
[3] J. Serafinczuk, L. Pawlaczyk, K. Moszak, D. Pucicki, R. Kudrawiec, D. Hommel, submitted to *Materials Characterisation* (2021)
[4] R. Kucharski, M. Zajac, A. Puchalski, T. Sochacki, M. Bockowski, JL. Weyher, M. Iwinska, J. Serafinczuk, R. Kudrawiec, Z. Siemiątkowski, *J. Cryst. Growth*, **427** (2015), 1-6.

O-09

BROKEN SYMMETRY BETWEEN RNA ENANTIOMERS IN A CRYSTAL LATTICE

Agnieszka Kiliszek, Leszek Błaszczyk, Magdalena Bejger, Wojciech Rypniewski

Institute of Bioorganic Chemistry, Polish Academy of Sciences, ul. Noskowskiego 12/14, 61-704 Poznań

Explaining the origin of the homochirality of biological molecules requires a mechanism of disrupting the natural equilibrium between enantiomers and amplifying the initial imbalance to significant levels. Authors of existing models have sought an explanation in the parity-breaking weak nuclear force, in some selectively acting external factor, or in random fluctuations that subsequently became amplified by an autocatalytic process. We have obtained crystals in which L- and D-enantiomers of short RNA duplexes assemble in an asymmetric manner. These enantiomers make different lattice contacts and have different exposures to water and metal ions present in the crystal. Apparently, asymmetry between enantiomers can arise upon their mutual interactions and then propagate via crystallization. Asymmetric racemic compounds are worth considering as possible factors in symmetry breaking and enantioenrichment that took place in the early biosphere.

O-10

STRUCTURAL AND FUNCTIONAL STUDIES OF NOVEL L-ASPARAGINASE FROM *RHIZOBIUM ETLI*

Joanna Loch[1], Barbara Imiołczyk[2], Joanna Śliwiak[2], Anna Wantuch[1], Mirosław Gilski[2,3], Mariusz Jaskólski[2,3]

[1]Jagiellonian University, Faculty of Chemistry, Krakow, Poland
[2]Polish Academy of Sciences, Institute of Bioorganic Chemistry, Poznan, Poland
[3]A. Mickiewicz University, Faculty of Chemistry, Poznan, Poland

L-Asparaginases have been known to form two unrelated structural families: bacterial-type and plant-type [1]. Among them, only enzymes from a periplasmic subclass of the former family have sufficiently high L-Asn affinity to be effective as antileukemic drugs. In 2001, we predicted that the bacterium *Rhizobium etli*, a symbiont of legume plants, should possess another, structurally unrelated L-asparaginase [2], currently termed ReAV. After nearly 20 years of efforts, the crystal structure of ReAV has been solved by the application of S-SAD.

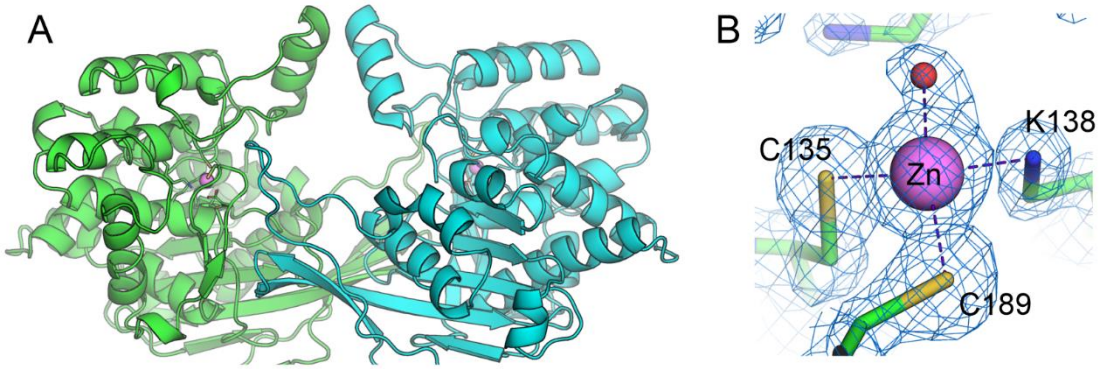

Fig. 1. (A) Structure of ReAV dimer with subunits A and B colored green and cyan. (B) 2Fo-Fc electron density (1.5σ) around the zinc coordination sphere in the orthorhombic structure (1.29 Å resolution).

We present several high-resolution crystal structures of recombinant ReAV solved in different space groups ($P2_1$, $C2$, $P2_12_12_1$). ReAV is a homodimeric enzyme (Fig. 1), with a catalytic center built around two Ser-Lys dyads. In close vicinity of the dyads, a zinc ion was identified, coordinated by a lysine and two cysteine residues (Fig. 1). The topology of ReAV resembles the fold of some bacterial glutaminases or β-lactamases and is entirely different from the structures of other known L-asparaginases. Biophysical studies revealed that ReAV has micromolar affinity for L-Asn and that it is a thermolabile enzyme with T_m ~51°C.

Work supported by National Science Centre (NCN, Poland) grant 2020/37/B/NZ1/03250

References

[1] K. Michalska, M. Jaskolski, *Acta Biochim. Polon.* **53** (2006) 627-640.
[2] D. Borek, M. Jaskólski, *Acta Biochim. Polon.* **48** (2001) 893-902.

O-11

FREQUENCY AND HYDROGEN BONDING GEOMETRY OF NUCLEOBASE HOMOPAIRS IN SMALL MOLECULE CRYSTAL STRUCTURES

Małgorzata K. Cabaj, Paulina M. Dominiak

Electron Density Modelling Group, Biological and Chemical Research Centre, Department of Chemistry, University of Warsaw, ul. Żwirki i Wigury 101, 02-089 Warsaw, Poland

Nucleobases are mostly known as vital parts of macromolecules such as DNA and RNA, in which they are encoding the genetic information. Their role does not end there – nucleobases also act as parts of active centers of enzymes and facilitate various biochemical reactions. Because of these aspects, nucleobases are thoroughly studied as potential pharmaceutical active ingredients. The question of their pairing is a prominent one since the day of their discovery as a part of DNA.

The first discovered base pairs – adenine:thymine and guanine:cytosine – were historically named as the canonical base pairs. From that time the number of base pairs found inside living organisms only grows, giving the scientists a plethora of material to study.

One of the methods good for investigating the problem of base pair formation can be analysis of the frequency of their occurrence in various environments. Many groups already tackled this problem and their methods can be divided into two approaches. First – analysis of base pair types and frequencies found in RNA crystal structures. Second – analysis of possible base pairs and their energies obtained in quantum-mechanical simulations. Both of these approaches are bound to have some limitations.

In our work [1] we choose the third possible path, which means an analysis of base pair types and frequencies found in small molecule crystal structures deposited in the Cambridge Structural Database. Such approach let us both reliably look into the protonation patterns found among base pairs, and to evaluate the influence of the environment on the base pair formation.

To facilitate more robust and precise way of referring to each base pair, we devised a new naming scheme for them (Fig. 1). It encompasses both the traditional way of referring to the interacting edges, which makes it more familiar to those already working with base pairs, and adds a way of numbering the interacting atoms, which makes it able to unequivocally describe particular interactions.

Basing on the frequencies of base pairs, it can be seen that the pairs often occurring in crystals of small molecules also often occur in RNA crystals. In addition to the presence of a substituent at the site of the glycosidic bond, protonation is also one of the factors that determines what type of pair will be formed, and its effects go well beyond steric clash or possibility of hydrogen bonding due to the presence of an additional proton. The possibility of creating higher-order structures as well as the presence of accompanying molecules in the crystal also influences the formation of pairs – it is clearly visible in the differences between the energies of nucleobase pairs calculated by other research groups using quantum chemistry methods, and the frequencies of the given pairs in the crystals.

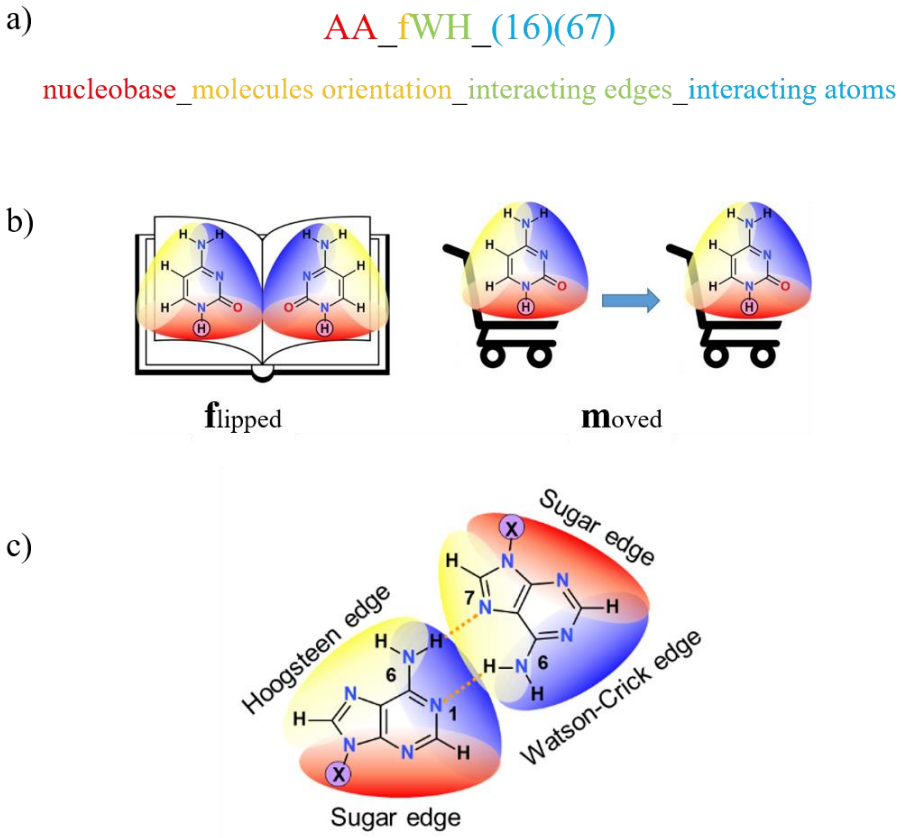

Fig. 1. Schematic representation of the new naming scheme; a) the partition of the new base pair name; b) explanation for the abbreviation of relative orientation; c) the named base pair.

In conclusion, we managed to find and explain many general trends characteristic to all the bases considered, but many pairs were individual cases that had to be discussed separately.

Bibliography

[1] M. K. Cabaj, P. M. Dominiak, *Nucleic Acids Research*, **48** (2020) 8302.

O-12

ONE THOUSAND STRUCTURES OF SARS-COV-2 PROTEINS, *OR* HOW THE POLISH CRYSTALLOGRAPHIC MAFIA JOINED THE FIGHT AGAINST COVID-19

Alexander Wlodawer[1], Marek Grabowski[2], Joanna M. Macnar[3], Marcin Cymborowski[2], David R. Cooper[2], Ivan G. Shabalin[2], Miroslaw Gilski[4,5], Dariusz Brzezinski[2,5,6], Marcin Kowiel[5], Zbigniew Dauter[1], Bernhard Rupp[7,8], Mariusz Jaskolski[4,5], and Wladek Minor[2]

[1]Center for Structural Biology, National Cancer Institute, Frederick, MD, USA; [2]Department of Molecular Physiology and Biological Physics, University of Virginia, Charlottesville, VA, USA; [3]Faculty of Chemistry, University of Warsaw, Poland; [4]Faculty of Chemistry, A. Mickiewicz University; [5]Institute of Bioorganic Chemistry, Polish Academy of Sciences, Poznan, Poland; [6]Institute of Computing Science, Poznan University of Technology, Poland; [7]k.-k Hofkristallamt, San Diego, CA, USA; [8]Institute of Genetic Epidemiology, Medical University Innsbruck, Austria

The response of the scientific community to the COVID-19 pandemic has been remarkable, with over 1000 structures related to SARS-CoV-2 submitted to the Protein Data Bank by mid-April 2021. With structural data obtained very rapidly by many groups using different techniques and varied experimental approaches, such efforts may lead to inevitable mistakes, errors, and interpretational problems. To help biomedical researchers, who may not be experts in structural biology, navigate through and absorb the flood of structural information, we have created an online resource, covid19.bioreproducibility.org, that aggregates expert-validated information about SARS-CoV-2-related macromolecular models. A number of protein complexes with inhibitors, which are most vital for drug design, were found to pose significant problems. Our critical analysis of a large number of protein structures that are potential or actual targets for drug design, all determined within about a year using modern experimental tools, is important not only in a current medical emergency but should be also useful as a paradigm study for future projects of high interest to biomedical community.

Supported in part by the NIGMS grant R01-GM132595, by the Polish National Agency for Academic Exchange (grant PPN/BEK/2018/1/00058/U/00001), by the Polish National Science Center (grants 2020/01/0/NZ1/00134 and 2018/29/B/ST6/01989), by the Intramural Research Program of the NIH, NCI, CCR, and by the Austrian Science Foundation grant P 32821.

O-13

ANALIZA IN SILICO BIAŁEK KANALIKOWYCH OGONKA BAKTERIOFAGA SUGERUJE PRZYPUSZCZALNE MIEJSCE WIĄZANIA CUKRU I MECHANIZM KATALITYCZNY

Wieslaw Swietnicki i Ewa Brzozowska

Instytut Immunologii i Terapii Doświadczalnej PAN im. L. Hirszfelda, ul. Weigla 12, 53-114 Wrocław

Niedawno odkryto, że podstawowe białka płytki ogonowej bakteriofaga wykazują aktywność hydrolityczną wobec disacharydów. Przypuszczalne przypisanie miejsc wiązania cukru oparto na znanych strukturach lektyn i zidentyfikowanych resztach a.a. 40-120 jako potencjalny region wiążący disacharydy [1]. Aby zweryfikować przewidywania, przeprowadzono analizę in silico struktury podstawowego białka gp31 płytki ogonowej z bakteriofaga Klebsiella pneumoniae KP32 (PDB: 5MU4), które wykazuje aktywność wobec maltozy, ale nie trehalozy [1]. Na podstawie tych informacji przeprowadzono pełne dokowanie powierzchniowe dla obu cukrów, które zidentyfikowały 2 regiony inne niż pierwotnie przewidywano. Pierwszy region wyraźnie faworyzował maltozę podczas fazy dokowania, podczas gdy drugi pozwalał na energetycznie równoważne wiązanie trehalozy. Aby zweryfikować przypisanie, przeprowadzono symulację dynamiki molekularnej w celu oceny stabilności zadokowanych substratów. Symulacje MD sugerowały, że pierwsze miejsce zawierało reszty D131, D133 i E134, a także było lepsze pod względem wiązania maltozy, podczas gdy wyraźnie nie sprzyjało trehalozie. Analiza przypuszczalnego mechanizmu katalitycznego sugerowała reszty D131, D133 i E134 jako krytyczne dla wiązania substratu. Reszta D133 uczestniczyła w stabilnym wiązaniu substratu i była umieszczona w pobliżu wiązania odcinającego, potencjalnie czyniąc z niej resztę katalityczną. Reszty katalityczne to najprawdopodobniej D131 i D133, jedna z dwóch opcji zaproponowanych przez Pyra et al. [1]. Porównanie ze znanymi mechanizmami hydrolazy sugeruje, że enzym najprawdopodobniej zachowuje konfigurację podczas hydrolizy maltozy. Odkrycia omówiono dla innych białek bakteriofagowych pod kątem ich potencjalnej swoistości i mechanizmów katalitycznych.

Literatura

[1] A. Pyra, E. Brzozowska, K. Pawlik, A. Gamian, M. Dauter, Z. Dauter. Tail tubular.protein A: a dual-function tail protein of Klebsiella pneumoniae bacteriophage, KP32. *Sci. Rep*., **7** (2017), p. 2223.

O-14

FROM ELECTRON DENSITY MAPS TO ELECTROSTATIC POTENTIAL DENSITY MAPS OF MACROMOLECULES WITH MATTS DATABANK

Marta Kulik, Michał L. Chodkiewicz, Paulina M. Dominiak

Centrum Nauk Biologiczno-Chemicznych Uniwersytetu Warszawskiego, Wydział Chemii, Uniwersytet Warszawski, ul. Żwirki i Wigury 101, 02-089 Warszawa

Structure factors in the X-ray diffraction experiment enable the calculation of the density of the core and valence electrons in the studied crystal. In the electron diffraction experiment, the structure factors convey the information about the electrostatic potential density map. Such density maps are being obtained in micro-electron diffraction at atomic resolution. An important difference between the atomic scattering factors for X-rays and electrons is that the latter are strongly dependent on scattering angle and at low scattering angle may become negative. Modeling of the structure factors can be done in a spherical way, using Independent Atom Model (IAM) and in aspherical way with the Multipolar Atom Types from Theory and Statistical clustering (MATTS) databank (successor of UBDB2018 [1]), which gathers atom types, useful for deriving the multipolar electron scattering factors. MATTS is a database universal for various macromolecules as the atom types are transferable between similar chemical environments. Using MATTS it is possible to recreate the electron density distribution of macromolecules via structure factors [2] or to calculate the accurate electrostatic potential maps for small molecules [3]. MATTS is able to reproduce the molecular electrostatic potential of molecules within their entire volume better than the simple point charge models used in molecular mechanics or neutral spherical models used in electron crystallography.

Here, we calculate both the electron density maps and the electrostatic potential maps for two model proteins and compare the latter with experimental maps from micro-electron diffraction. We apply the multipolar electron scattering factors and advance the knowledge how the theoretically-obtained potential maps of proteins should look like. We also consider the influence of atomic displacement parameters on the theoretical maps as their physical meaning in cryo-electron microscopy is not as well established as in X-ray crystallography.

The authors acknowledge NCN UMO-2017/27/B/ST4/02721 grant.

References

[1] Kumar *et al*., *Acta Cryst*., A**75** (2019) 398-408.
[2] Chodkiewicz *et al*., *J. Appl. Cryst*., **51** (2018) 193-199.
[3] Gruza *et al*., *Acta Cryst.*, A**76** (2019) 92-109.

O-15

IDENTYFIKACJA POTENCJALNYCH EFEKTORÓW BAKTERYJNEGO CZYNNIKA TRANSKRYPCYJNEGO RcdA

Anna Cociurovscaia i Agnieszka Pietrzyk-Brzezińska

Instytut Biotechnologii Molekularnej i Przemysłowej, Wydział Biotechnologii i Nauk o Żywności, Politechnika Łódzka, Stefanowskiego 2/22, 90-537 Łódź

Bakterie posiadają rozbudowaną sieć systemów regulatorowych, które pozwalają im na szybkie przystosowanie się do szkodliwych lub limitujących wzrost warunków środowiska [1]. Czynnik transkrypcyjny RcdA, który bierze udział między innymi w regulacji syntezy biofilmu, należy do rodziny czynników transkrypcyjnych TetR. Regulator ten posiada dwie domeny: domenę końca N, oddziałującą z DNA, i domenę końca C, odpowiedzialną za rozpoznawanie cząsteczek sygnałowych i dimeryzację [2]. Wcześniejsze badania nad RcdA pozwoliły na zidentyfikowanie genów, które są pod kontrolą tego regulatora [3]. Jednak nadal nie wiadomo, jakie efektory są rozpoznawane przez RcdA.

Podczas badań mających na celu identyfikację potencjalnych ligandów dla RcdA, rozwiązano pierwsze struktury kompleksów tego białka z małymi cząsteczkami – Tris (2-amino-2-(hydroksymetylo)-1,3-propanodiol) i TMAO (N-tlenek trimetyloaminy). Dodatkowo, rozwiązano strukturę natywną o rozdzielczości 1.80 Å. Na podstawie tych struktur szczegółowo opisano kieszeń wiążącą RcdA oraz określono stopień konserwatywności tego czynnika transkrypcyjnego w stosunku do zidentyfikowanych białek homologicznych. Oddziaływanie z TMAO i Tris może wskazywać na udział RcdA w komórkowej odpowiedzi na stres alkaliczny.

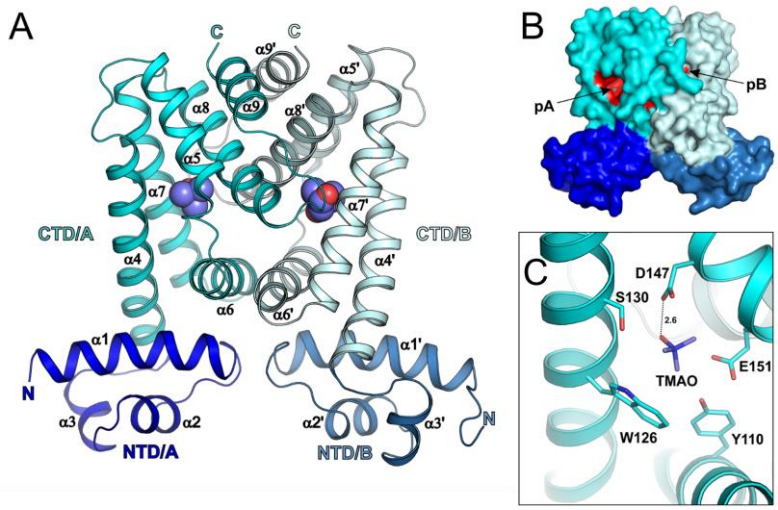

Rys. 1. Oddziaływanie RcdA z ligandem. A) Struktura kompleksu RcdA i TMAO. B) Przedstawienie kieszeni wiążących ligandy w białku RcdA. C) Reszty aminokwasowe domeny końca C oddziałujące z TMAO.

Literatura

[1] Ishihama A, *FEMS Microbiol. Rev.*, **34 (5)** (2010) 628–645.
[2] Shimada T, Katayama Y, Kawakita S, et al. *Microbiologyopen*, **1** (2012) 381–394.
[3] Shimada T, Fujita N, Maeda M, et al. *Genes to Cells*, **10** (2005) 907–918.

O-16

EXPERIMENTAL CHARGE DENSITIES OF MINERALS UNDER PRESSURE

Krzysztof Woźniak[1]*, Marcin Stachowicz[2], Roman Gajda[1], Jan Parafiniuk[2]

[1]Chemistry Deptm., Univ. of Warsaw, 02-093 Warszawa, Poland
[2]Institute of Geochem., Miner. and Petrology, Univ. of Warsaw, Poland
**e-mail: kwozniak@chem.uw.edu.pl*

This is quite a paradox that a century after introduction of the spherical Independent Atom Model (IAM, 1914 [1]), 99.7% of all *ca.* 1.5mln known crystal structures, including almost all structures of minerals, have been refined using IAM which suffers from severe methodological deficiencies. Far better results can be obtained when new approaches of quantum crystallography ustilising aspherical atomic factors are applied. This also is possible in the case of high pressure studies. A short wavelength (0.4Å) od X-radiation and a special type of Diamond Anvil Cell (DAC) with large opening angle allow us to collect data with extremaly high resolution (up to *ca.* 0.4 Å) and 100% completeness.

We have successfully refined quantitative experimental electron densities [2] for crystals of several minerals such as fluorite, grossular and hsianghualite. We will present the most interesting results such as onset of F…F interactions (charge-shift bonding) in fluorite[3], results of our successful experimental quantitative charge density feasibility study of grossular under pressure[4] and flow of charge among ions in the structure of hsianghualite, $Ca_3Li_2(Be_3Si_3O_{12})F_2$, under high pressure (Fig. 1). Up to our best knowledge, these are the very first successful experimental determinations of quantitative charge density distributions in mineral crystals under high pressure. They allow for quantitative characterisation of electron density in crystals of minerals including studies of changes of electron density under pressure.

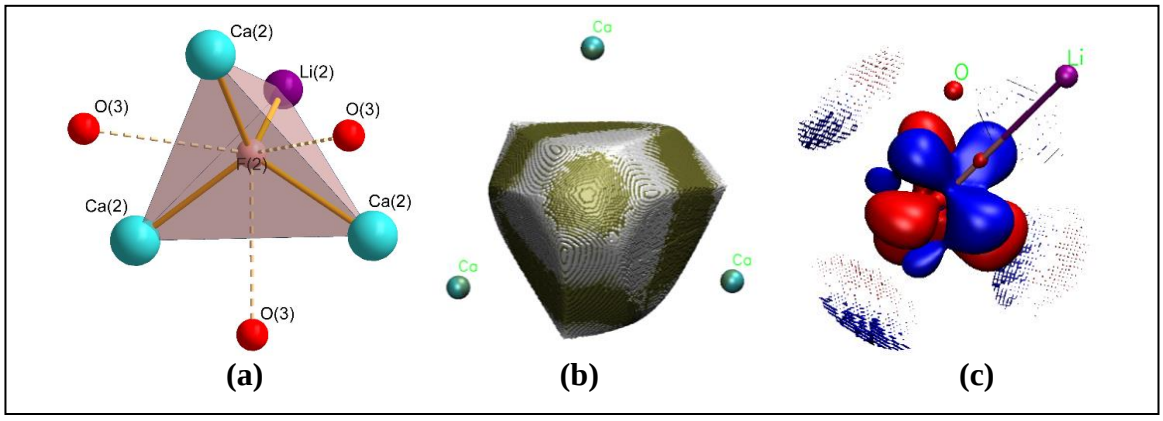

Fig.1. Structure of hsianghualite: (a) classic F2 tetrahedron, (b) projection of the atomic basin of F2 under 1.1GPa and RT (greenish) on the surface of the F2 atomic basin at the ambient pressure and 100K (gray colour) and (c) difference in the total electron densities of the F2 ion (inside atomic basin) at ambient pressure and 100K and at 1.1GPa (at RT) illustrated at the contour lines +0.1e/Å^3 (blue) and -0.1e/Å^3 (red) and showing how electron density redistributes from the blue space region to the red one when temperature is increased from 100K to RT and pressure is raised from ambient to 1.1GPa.

Such studies open a new field of mineralogical subatomic investigations (at the level of changes of electron density properties) of different mineralogical processes in the Earth mantle by simulating them in DAC in laboratory conditions.

KW acknowledges a financial support within the Polish National Science Centre (NCN) OPUS17 grant number DEC-2019/33/ B/ST10/02671

References:

[1] Compton, A.H., (1915) *Nature.*, **95**, pp. 343-344.
[2] Hansen, N. K., & Coppens, P., (1978) *Acta Cryst.*, **A34,** 909–921.
[3] Stachowicz, M., Malinska, M., Parafiniuk, J., &Woźniak, K., (2017) *Acta Cryst.*, **B73,** 643–653.
[4] Gajda, R., Stachowicz, M., Makal, A., Sutuła, S., Parafiniuk, J., Fertey, P., & Wozniak, K., (2020) *IUCRJ*, **7(3),** 383-392.

O-17

COMPLETENESS IN HIGH-PRESSURE XRD EXPERIMENTS

Daniel Tchoń and Anna Makal

Biological and Chemical Research Centre, Faculty of Chemistry,
University of Warsaw, Żwirki i Wigury 101, 02-089 Warsaw, Poland

Quality of data obtained from high-pressure diffraction experiments has become a sort of a taboo topic in the community. Any mentions of high-pressure in experimental tables tend to be followed with higher discrepancy factors, and it is so not without reason [1]. Presence of bulky steel body and two diamonds does not only affect the reliability of collected data, but more importantly limits the number of collectable reflections altogether. This often hampers investigation and forces researchers to rely on distorted or restrained models, which may lead to oversights and false conclusions.

While anvil cell is expected to increase background noise, and diamond signals can be considered a necessary evil, the completeness of obtained datasets can be vastly improved by carefully planning experimental strategy. The most straightforward way to do that is to increase coverage of reciprocal space using a cell with higher aperture [2], though this may come with a cost of limiting maximum attainable pressure. A much more affordable approach relies on utilising internal sample symmetry and increasing the final completeness by exposing as much independent reciprocal space as possible.

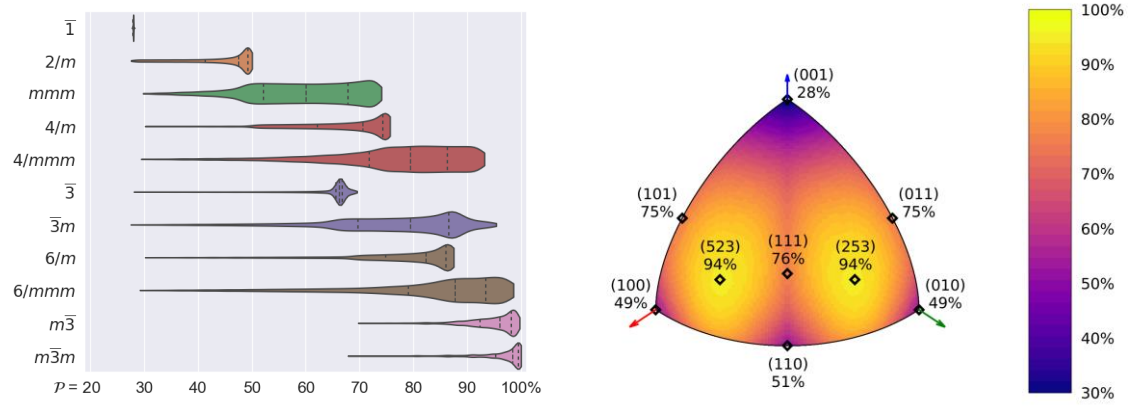

Fig. 1. Distribution of data completeness obtainable in high-pressure experiments: integrated (left) and as a function of crystal orientation (right), simulated assuming MoKα radiation and 35° anvil cell aperture. In some cases well-thought sample placement may increase completeness even by a factor of 4.

In this work an impact of diamond anvil cell aperture, incident radiation wavelength and sample placement on completeness of collected data is discussed. Range of data completeness obtainable using the most common incident sources and anvil cells, predicted using new software designed with this task in mind, is presented. Sample preparation protocols and data collection strategies, allowing to obtain the highest quality of results at virtually no expense, are suggested.

References

[1] a) N. Casati *et al.*, Nat Commun **7**, 10901 (2016); b) A. Jaffe *et al.*, ACS Cent. Sci., **2**, 201 (2016); c) S. A. Moggach *et al.* Crystallogr. Rev., **14**, 143 (2008)
[2] L. Merrill and W. Basset, Rev. Sci. Instrum. **45**, 290 (1974).

O-18

HIGH-PRESSURE INFLUENCE ON PIRACETAM CRYSTALS: STUDYING BY QUANTUM CHEMICAL METHODS

Svitlana V. Shishkina[a,b], **Yevhenii Vaksler**[a,b,c], **Abdenacer Idrissi**[c]

[a] *SSI "Institute for Single Crystals" NAS of Ukraine, 60 Nauky ave., Kharkiv, 61001, Ukraine*
[b] *V.N. Karazin Kharkiv National University, 4 Svobody Sq., Kharkiv, 61022, Ukraine*
[c] *Laboratoire de Spectroscopie pour les Interactions, la Réactivité et L'environnement (UMR CNRS A8516), Université de Lille, 59655, Villeneuve d'Ascq Cedex, France.*

Recently, we proposed a new approach to study the crystal structure deformability based on knowledge of the special distribution of interaction energies between molecules and modeling of a shear deformation between strongly bound fragments of a crystal packing [1]. Aspirin polymorphic modifications were chosen as the most suitable object to verify the proposed method taking into account numerous experimental data on the crystal structures of this extremely popular drug. Our modeling allowed to recognize unambiguously the crystallographic plane in which the shear deformation is the easiest. Unfortunately, the aspirin crystal structure after polymorphic transition remains unknown.

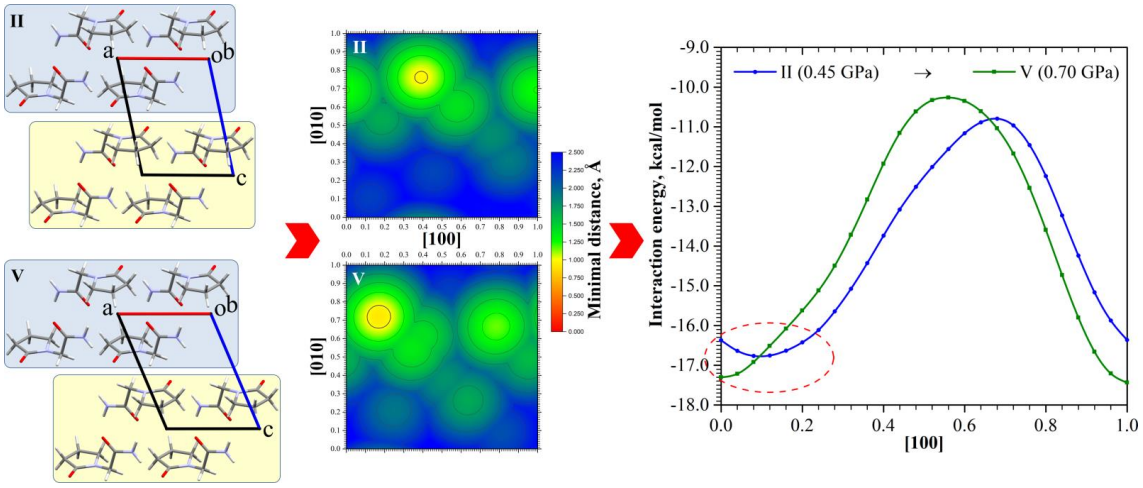

Fig. 1. Polymorphic transition of piracetam Form **II** to Form **V** under pressure.

The nootropic drug piracetam also undergoes a polymorphic transition under pressure. Both crystal structures, Form II before the transition and Form V after it, were determined using X-ray diffraction. Pressure has been described as the dominant and only factor necessary for this transformation without the need for a solvent. Moreover, Form **V** has been studied at various pressures.

The crystal structure of the polymorphic Form **II** at ambient pressure was classified as columnar-layered packing of complex dimeric building units based on the study of pairwise interaction energies between molecules. The preliminary assessment of a shear deformation along three crystallographic layers divided as possible BSM_2s has shown that the most probable way for deformation is the displacement in the [100]

crystallographic direction along the (001) crystallographic plane. The modeling of such a displacement has revealed some features of the shift energy profile that can prove to be pre-conditions of a polymorphic transition due to pressure influence. These are a small local minimum near the starting point, negative interaction energies between the mobile and fixed parts of the model system during the entire displacement, and a low energy barrier of the displacement.

The comparison of the crystal structures of Form **II** and Form **V** at different pressures has demonstrated that the pressure affects mainly the energy ratio between basic structural motifs (BSM_1 and BSM_2) while the interaction energy within the DBU and columns as the BSM_1 remains almost unchanged. The change in the piracetam crystal structure under pressure occurs in two stages. At the first stage, small pressure of 0.45 GPa leads to some increase in the interaction energies between all three types of layers. Further increase in pressure causes a shift of the layers parallel to the (001) crystallographic plane to each other. The crystal structure has a columnar-layered type from the energetic viewpoint before and after the polymorphic transition from Form **II** to Form **V**. At the second stage, the redistribution of interaction energies between columns (BSM_1) inside the layers and between layers (BSM_2) leads to the change of the energetic crystal structure type from columnar-layered to columnar without the change of polymorphic form. The pressure increase also causes also an increase in the shift energy barrier for the displacement in the [100] crystallographic direction along the (001) crystallographic plane.

The dimer bound by the C–H…O interaction in the polymorphic Form **II** proved to be the least rigid, despite the high interaction energy, due to the small contribution of the hydrogen bonding to the total interaction energy. As a result, this interaction can be easily disrupted which promotes a shift of neighboring layers and a polymorphic transition without a crystal structure destruction.

The proposed approach of shear deformation modeling using quantum chemical methods proved to be effective for the prediction of a polymorphic transition from piracetam Form **II** to Form **V** under pressure that is confirmed by the experimental data.

Literature

[1] Ye. Vaksler, A. Idrissi, V. Urzhuntseva, S. Shishkina, *Cryst. Growth Des.*, **21** (2021) 2176.
[2] Ye. Vaksler, A. Idrissi, S. Shishkina, *Cryst. Growth Des.*, submitted.

O-19

COMPUTATIONAL ANALYSIS OF PRESSURE-INDUCED SHEAR IN R,S-IBUPROFEN

Yevhenii A. Vaksler[a,b], Abdenacer Idrissi[c], Svitlana V. Shishkina[a,b]

[a] SSI "Institute for Single Crystals" NAS of Ukraine, 60 Nauky ave., Kharkiv, 61001, Ukraine
b. V.N. Karazin Kharkiv National University, 4 Svobody Sq., Kharkiv, 61022, Ukraine
c. LaSIRE (UMR CNRS A8516), Université de Lille, 59655, Villeneuve d'Ascq Cedex, France

Molecular crystals are one of the most used forms of active pharmaceutical ingredients (APIs) in the industry due to the constancy of their properties [1]. However, crystals are affected by polymorphism. Polymorphism is the ability of substances to form more than one crystalline phase with different arrangements of the molecules of that compound in the solid phase. The changes of crystalline structure may occur during the synthesis or processing (compression, heating, etc.) and cause significant deviations in properties of drugs [2]. Indeed, the study of the prerequisites for polymorphic transformations is important for the complete control of APIs production.

In the current report the influence of compression and grinding on ibuprofen will be analyzed. This well-known API behaves ambiguously under mechanical treatment. Its structure did not change under the pressure up to 4.00 GPa [3], while the grinding with mesoporous silica led to the amorphization of ibuprofen [4]. The solubility of ibuprofen is extremely low [5] and the amorphous drugs are often more soluble [2], so this transformation should be strictly controlled during the manufacturing.

For this, our new computational approach [6] was applied to the most stable polymorphic form I of ibuprofen to analyze the energetic structure of crystals and to model the shear of their most strongly bound fragments. At the first step, the pairwise interaction energies between the molecules in the experimental crystalline structures determined at various pressure values [3] were calculated using quantum chemical methods and the hydrogen bonded dimer was defined as a building unit (Fig. 1a). The second step consists of the computation of the pairwise interaction energies between the building units. The layers (100) were defined as the most probable structural motives (Fig. 1b). Thirdly, the model system was created to simulate the shear of a dimer from a layer (100), called a mobile part, and the set of dimers from an adjacent layer, which are neighboring to the mobile one during all its movements. The mobile part was shifted in the main crystallographic directions [010] and [001] and the minimal topological parameter δ was calculated to include the nature of atoms inside the building units as follows:

$$\delta_{ij} = d_{ij} - vdW_i - vdW_j \quad (1.1)$$

where: d_{ij}, vdW_i, vdW_j are the distance between the atoms i in mobile part and j in the fixed part and their van der Waals radii respectively.

The topological 2d maps of layers shear were built and treated in different manners to simulate the different types of displacements in crystals (Fig. 2a). The most probable direction of the shift was supposed from them as [001]. For this direction, the quantum chemical calculations were performed to estimate the shear energy profiles and

barriers occurring for the mutual displacement of layers in crystals of ibuprofen (Fig. 2b). The local minima were found at 0.40 of a translation for all the studied pressure values. They can be defined as the prerequisite of the polymorphic transformation. The shear energy barrier between the original position of the building units in structure and the local minima showed the gradual increase on compression. The shear of layers is possible till 0.23 GPa without their repulsion. Thus, the transformation of crystal structure of the polymorph I of ibuprofen is possible in this diapason and it becomes the easier, the lower pressure is.

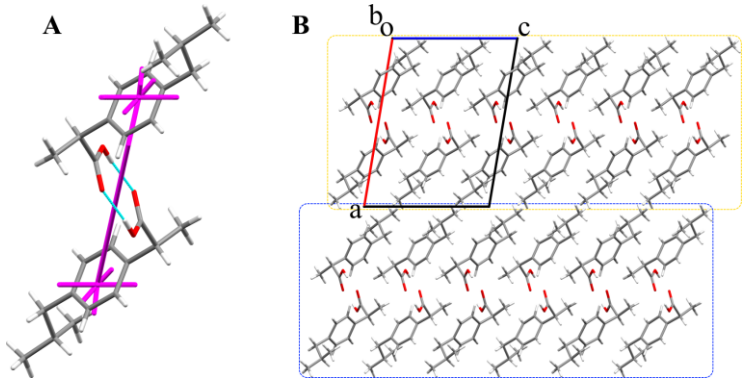

Fig. 1. The building unit in the crystal ibuprofen with the energy vector diagrams used for its determination (A) and the most probable layers (100), where the neighboring ones are marked with yellow and blue colors.

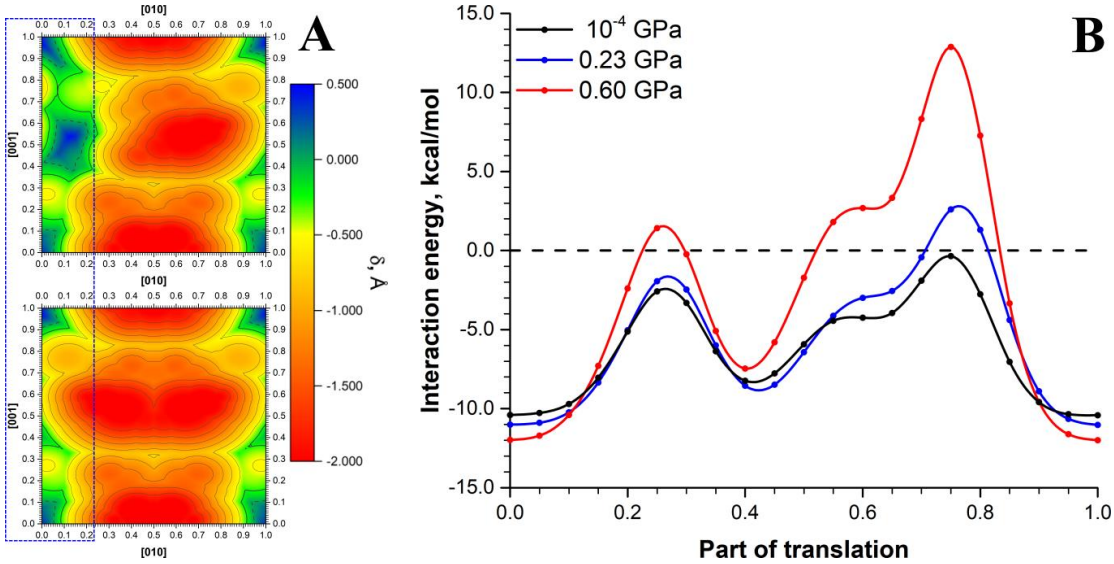

Fig. 2. The topological 2d maps of parameter δ for the displacements (A): a building unit to a neighboring (100) layer (at the top) and layer to layer (in the bottom). The shear energy profile of the (100) layers displacement in the direction [001] (marked with blue at A) at different pressures (B).

Literature

[1] E. Yonemochi, H. Uekusa, *Crystals*, **10**, 2 (2020) 89.
[2] Y.A. Abramov, *Computational pharmaceutical solid state chemistry*, John Wiley & Sons: Hoboken, New Jersey (2016) 1-13.
[3] K. Ostrowska, M. Kropidłowska, A. Katrusiak, *Crystal Growth & Design*, **15**, 3 (2015) 1512-1517.
[4] B. Malfait, et al., *The Journal of Chemical Physics*, **153** (2020) 154506.
[5] J. Manrique, F. Martínez, *Latin American Journal of Pharmacy*, **26**, 3 (2007) 344-354.
[6] Y. Vaksler, A. Idrissi, V.V. Urzhuntseva, S.V. Shishkina, *Crystal Growth & Design*, **21**, 4 (2021) 2176-2186.

O-20

NON-LINEAR OPTICAL PROPERTIES AND NEGATIVE AREA COMPRESSIBILITY OF (*S*)-2-AMINO-3-GUANIDINOPROPANOIC ACID MONOCHLORIDE

Piotr Rejnhardt[1], Jan K. Zaręba[2], Ida Moszczyńska[3], Marek Daszkiewicz[1]

[1] Institute of Low Temperature and Structure Research, Polish Academy of Sciences, P. O. Box 1410, 50-950 Wrocław, Poland,
[2]Advanced Materials Engineering and Modelling Group, Faculty of Chemistry, Wrocław University of Science and Technology, Wybrzeże Wyspiańskiego 27, 50-370 Wrocław, Poland
[3]Faculty of Chemistry, Adam Mickiewicz University, Umultowska 89b, 61-614 Poznań, Poland

Second harmonic generation (SHG) in organic crystals is a subject of extensive investigation for years [1]. The absence of an inversion centre in crystal is mandatory in order to obtain SHG response, although many other features play an important role and must be taken into account for synthesis of non-linear materials [2]. For example, an occurrence of delocalized π electrons and intramolecular donor-acceptor charge transfer between two molecular subparts (functional groups) is welcomed [3]. It leads to large hyper-polarizability β and this kind of materials are good candidates for second harmonic generation.

Negative area compressibility (NAC) is extremely rare phenomenon occurring under pressure and it is characterized by two-dimensional expansion of material. Most materials shrink in all directions under pressure, some of them expand in one direction (negative linear compressibility) and only few structures are capable of expanding in two directions [4]. The NAC is highly desirable for application such as pressure sensors and actuators [5].

Here we present crystal and molecular structure of a new salt of the homologue of L-arginine, (*S*)-2-amino-3-guanidinopropanoic acid monochloride (AGPA) and its deuterated analogue (DAGPA). Crystal structure were determined by X-ray diffraction at room temperature and over a dozen low-temperature conditions (down to 100 K) for both analogues. The crystals were also measured at 21 pressure points for AGPA and 10 pressure points for DAGPA. The temperature-dependent measurements showed no structural phase transition, but anomalous increase of the *c* lattice parameter upon cooling the sample. Contrary to this, the phase transition was observed by high-pressure diffraction. The isosymmetric phase transition ($P2_1$ space group) was noticed at 0.91 GPa for AGPA and 0.96 GPa for DAGPA (Figure 1 a and b). Calculations of median compressibility for the high-pressure phase of both compounds showed slight anomalous increase of *a* and *b* lattice parameters indicating the rare NAC phenomenon in the studied compounds.

Since earlier studies have shown that external pressure can tune SHG signal, diamond anvil cell (DAC) was used to investigate the pressure dependence of SHG response. The result of SHG measurements revealed that monochloride salt of (*S*)-2-amino-3-guanidinopropanoic acid and deuterated analogue have better optical non-linear properties than L-arginine chloride, $3 \cdot I_{KDP}$ *vs.* $0.3 \cdot I_{KDP}$. This fact can be associated with

shorter carbon chain (*S*)-2-amino-3-guanidinopropanoic acid and thus closer intramolecular distance between carboxyl and guanidinium groups than in L-arginine. The phase transition was also detected during the SHG measurements in the DAC. Dependence of SHG response on pressure revealed extreme decrease of the recorded SHG signal during squeezing the sample in the low region of high pressure conditions and the minimum at approximately 0.7-0.9 GPa associated with the structural phase transition (Figure 1c).

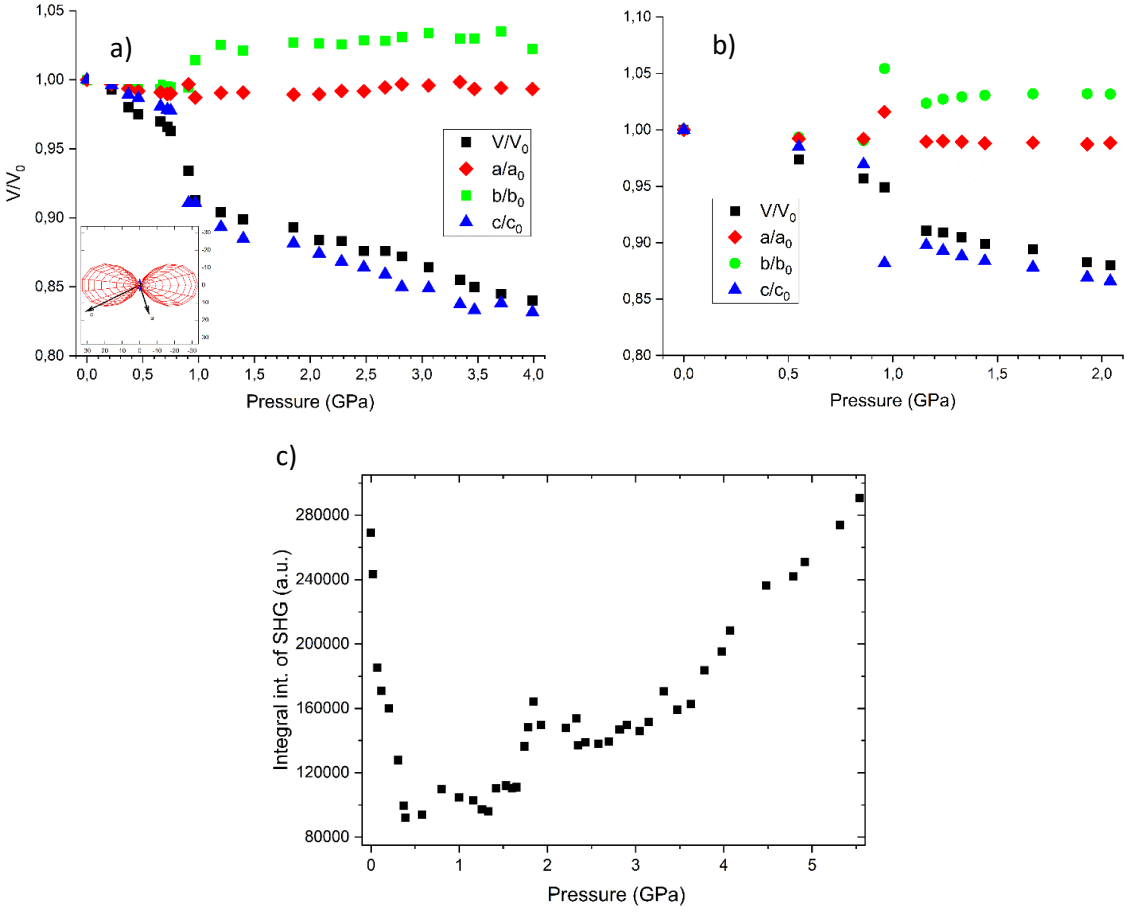

Figure 1. a) Normalized unit cell parameters and compressibility indicatrix for AGPA, b) and for DAGPA, c) dependence of the intensity of SHG response on pressure.

References

[1] Materials for Nonlinear Optics (Chemical Prospectives). Eds. S.R. Marder, J.E. Sohn, G.D. Stucky, ACS Symposium Series 455 (ACS Press Washington, DC, 1983).

[2] Elena Marelli, Nicola Casati, Fabia Gozzo, Piero Macchi, Petra Simonciccd and Angelo Sironie High pressure modification of organic NLO materials: Large conformational re-arrangement of 4-aminobenzophenone November 2011*CrystEngComm* **13(22)** (2011) 6845-6849.

[3] P.N. Prasad, D.J. Williams, Wiley, New York (1991).

[4] Cai, W., Gładysiak, A., Anioła, M., Smith, V. J., Barbour, L. J. & Katrusiak, A. *Journal of the American Chemical Society*. **137** (2015) 9296–9301.

[5] *Chem. Sci*., **10** (2019) 1309-1315.

O-21

SYNTEZA I BADANIA STRUKTURALNE POŁĄCZEŃ BROMKU KADMU Z DIAMINAMI ALIFATYCZNYMI Z WYKORZYSTANIEM TECHNIKI RENTGENOWSKIEJ DYFRAKTOMETRII PROSZKOWEJ

Michał Duda[1], Marta Grzesiak-Nowak[1], Marcin Oszajca[1], Wiesław Łasocha[1,2]

[1]Wydział Chemii Uniwersytetu Jagiellońskiego, ul. Gronostajowa 2, 30-387 Kraków
[2]Instytut Katalizy i Fizykochemii Powierzchni im. Jerzego Habera PAN, ul. Niezapominajek 8, 30-239 Kraków

Połączenia soli metali z aminami stanowią intensywnie badaną grupę połączeń nieorganiczno-organicznych; od lat są też przedmiotem badań Zespołu Strukturalnej Dyfraktometrii Proszkowej (Wydział Chemii UJ). Związki te są tym bardziej interesujące w kontekście badań prowadzonych przy użyciu techniki XRPD, że wiele tego typu materiałów otrzymywanych jest w formie proszku (polikrystalicznej). Celem prezentowanych badań była synteza – w możliwie czystej postaci, oraz analiza pod kątem krystalograficznym serii połączeń bromku kadmu z diaminami alifatycznymi, o liczbie atomów węgla w cząsteczce z zakresu 3 – 12. Informacje literaturowe dotyczące struktur samych diamin alifatycznych [1] wskazują na możliwość występowania zależności między symetrią struktury i wartościami parametrów sieciowych a liczbą atomów węgla w cząsteczce. Stąd, dodatkowym zamierzeniem przeprowadzonych prac było poszukiwanie takich prawidłowości.

Badane preparaty otrzymano poprzez zmieszanie roztworów substratów w temperaturze pokojowej. Wszystkie zsyntezowane materiały miały postać białego proszku. Wstępne pomiary dyfrakcyjne przeprowadzone w geometrii Bragga–Brentano (z wykorzystaniem uchwytu płaskiego) pozwoliły określić czystość produktów syntez. Natomiast dyfraktogramy służące do badań strukturalnych zarejestrowano w geometrii Debye'a–Scherrera, gdzie próbki umieszczone były w cienkościennych kapilarach szklanych. Modele struktur wyznaczono przy użyciu metod bezpośrednich oraz metod przestrzeni rzeczywistej (*direct space methods*) [2-4]. Struktury uściślono metodą Rietvelda z użyciem programu Jana2006 [5].

Uzyskane związki są polimerami koordynacyjnymi (mieszane warstwy nieorganiczno-organiczne [6]), gdzie każda cząsteczka liganda organicznego łączy dwa centra metaliczne (przykładową strukturę, z 1,8-diaminooktanem, przedstawiono na Rys. 1). Związki z diaminami o parzystej liczbie atomów węgla w cząsteczkach krystalizują w centrosymetrycznych grupach przestrzennych, a związki z diaminami o nieparzystej liczbie atomów węgla – w grupach bez środka symetrii. Dodatkowo, zauważono, że symetria struktur z ligandami o parzystej liczbie atomów węgla ulega obniżeniu z jednoskośnej do trójskośnej wraz z wydłużaniem cząsteczki diaminy. Zaobserwowano również występowanie liniowej zależności między wartością parametru sieciowego *a* i liczbą atomów węgla w cząsteczce liganda organicznego (zarówno w serii połączeń z diaminami o parzystej jak i nieparzystej liczbie atomów węgla). Wartości parametrów *b* i *c* zmieniają się tylko w niewielkim stopniu wraz ze wzrostem długości cząsteczki alifatycznej diaminy.

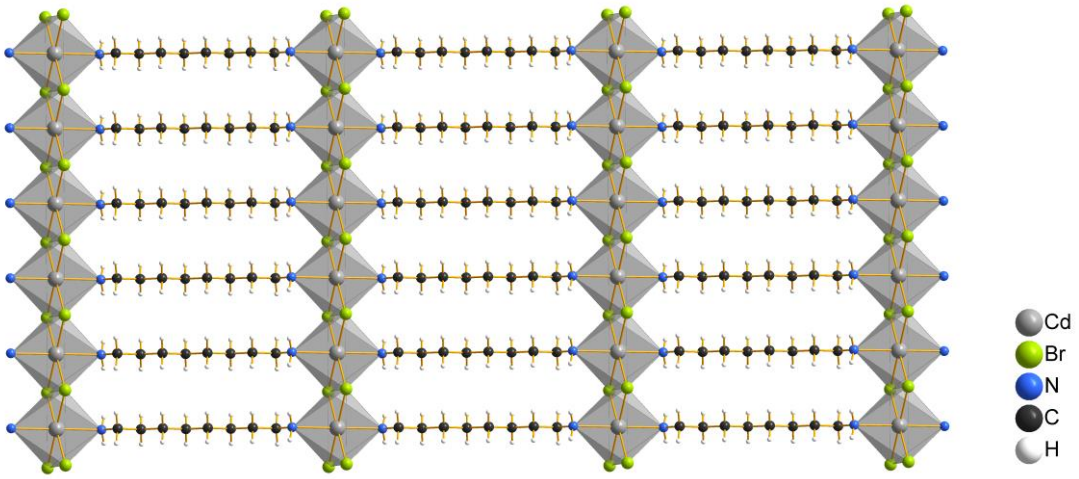

Rys. 1. Warstwy organiczno-nieorganiczne w strukturze związku bromku kadmu z 1,8-diaminooktanem

Prezentowane rezultaty badań stanowią kompilację i uzupełnienie wyników zamieszczonych w dwóch pracach doktorskich [7,8] przygotowanych w Zespole Strukturalnej Dyfraktometrii Proszkowej; w badaniach stosowano zarówno laboratoryjne, jak i synchrotronowe źródła promieniowania rentgenowskiego.

Literatura

[1] V.R. Thalladi, R. Boese, H.-Ch. Weiss, *Angew. Chem. Int. Ed.*, **39** (2000) 918.
[2] A. Altomare, M. Camalli, C. Cuocci, C. Giacovazzo, A. Moliterni, R. Rizzi, *J. Appl. Cryst.*, **42** (2009) 1197.
[3] A. Altomare, C. Cuocci, C. Giacovazzo, A. Moliterni, R. Rizzi, N. Corriero, A. Falcicchio, *J. Appl. Cryst.*, **46** (2013) 1231.
[4] V. Favre-Nicolin, R. Černý, *J. Appl. Cryst.*, **35** (2002) 734.
[5] V. Petricek, M. Dusek, L. Palatinus, *Z. Kristallogr.*, **229** (2014) 345.
[6] A.K. Cheetham, C.N.R. Rao, R.K. Feller, *ChemComm*, **46** (2006) 4780.
[7] M. Grzesiak-Nowak, *Rozprawa doktorska* (2014).
[8] M. Duda, *Rozprawa doktorska* (2021).

O-22

APPLICATION OF CRYSTALLOGRAPHY IN STUDIES OF SOFT MATERIALS

Henryk Drozdowski, Małgorzata Śliwińska-Bartkowiak, Stefan Jurga

Faculty of Physics, Adam Mickiewicz University,
ul. Uniwersytetu Poznańskiego 2, 61-614 Poznań, Poland

X-ray diffraction is a very efficient method of studying the structure of matter in both solid and liquid phase [1]. WAXS research, apart from spectroscopic methods, is one of the most important ways to learn about the mutual arrangement of molecules in the liquid phase. Recently [2–4] it has been shown that the X-ray diffraction method on liquid media allows not only determination of interatomic distances in a molecule but also brings information on the kind of interaction among the molecules and degree of their ordering.

Determination of the packing coefficient is of great practical importance as it helps to find the right molecular liquid structure. The packing coefficient of molecules in liquid due to its physical sense plays an important role in determining the structure of short-range molecular arrangement. As to the liquids and liquid solutions diffractions patterns provide only the information on the so called short-range arrangement of atoms and molecules.

By analogy with the packing coefficient defined for crystals [5] we can define the corresponding packing coefficient of molecules in liquids:

$$\bar{k} = \frac{\bar{V}^{incr}}{\frac{\bar{V}}{N}}, \tag{1}$$

where $\bar{V}^{incr}$ is the specific volume of the molecule and $\frac{\bar{V}}{N}$ is the volume available for one molecule in a pseudocell. The specific volume of a molecule may be found from its chemical structure, the length of bonds and van der Waals radii of atoms and functional groups. The specific volume of a molecule may be found from its chemical structure, the length of bonds and van der Waals radii of atoms and functional groups.

The packing coefficient is defined by Kitaigorodsky [6,7] as the ratio of the specific volume of the molecule to the volume per a molecule in a given liquid. The mean volume per one molecule of the liquid is calculated from the known macroscopic density, molecular mass and the Avogadro number according to the formula [8]:

$$\bar{V}_0^{\max} = \frac{M}{10^{-24} \cdot N_A \cdot d}, \tag{2}$$

where M is the molecular mass of the liquid [$g \cdot mol^{-1}$], d – the liquid density at a certain temperature and N_A – the Avogadro constant [mol^{-1}]. The volume $\bar{V}_0^{\max}$ is the

maximum because the liquid density d in formula (2) concerns the vhole volume of the liquid, including microvoids characteristic of the liquid phase [9].

Structural informations inferred from X-ray diffraction patterns for liquids and liquid solutions were based on the model-theoretical interpretations. Assuming the most probable model of intermolecular interactions for which the calculated scattering pattern agrees best with experimental one, we can estimate the number of molecules $\overline{N}$ per an elementary pseudocell. The right coefficient value is, however, obtained only when the assumed model of intermolecular liquid structure in a given liquid is correct.

The most probable simple configurations of neighboring molecules in the liquid in question can be examined by fitting positions of the maxima of the RDF to the distances between the centers of neighbors resulting from their van der Waals models. Figure 1 shows the packing of molecules of 1,3,5–triphenylbenzene in the liquid phase determined on the basis of the RDF analysis [10].

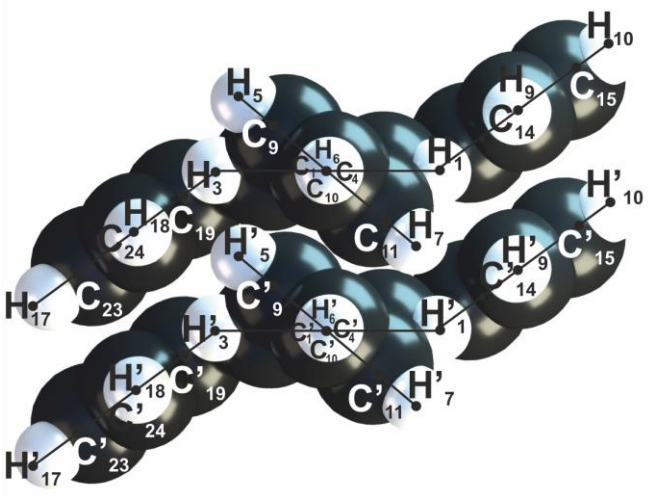

Fig. 1. Model of probable intermolecular interactions in liquid 1,3,5–triphenylbenzene.

Literature

[1] H. Ohno, K. Igarashi, N. Umesaki, K. Furukawa, *X-Ray Diffraction Analysis of Ionic Liquids*, Trans. Tech. Publications Ltd., Switzerland-Germany-UK-USA 1994.
[2] H. Drozdowski, M. Śliwińska-Bartkowiak, S. Jurga, *Acta Phys. Pol. B*, **13 (4)** (2020) 709.
[3] H. Drozdowski, T. Hałas, M. Śliwińska-Bartkowiak, *J. Mol. Struct*., **1148** (2017) 322.
[4] M. Śliwińska-Bartkowiak, H. Drozdowski, M. Kempiński, M. Jażdżewska, Y. Long, J.C. Palmer, K.E. Gubbins, *Phys. Chem. Chem. Phys*., **14 (19)** (2012) 7145.
[5] M. Van Meerssché, J. Feneau-Dupont, *Introduction à la Cristallographie et la Chimie Structural*, fourth ed., OYEZ, Leuven 1986.
[6] A.I. Kitaigorodsky, *Molecular Crystals and Molecules*, Academic Press, New York, London 1973.
[7] A.I. Kitaigorodsky, *The Theory of Crystal Structure of Organic Molecules*, Cornell University Press, Ithaca-New York 1979.
[8] H.P. Klug, L.E. Alexander, *X-Ray Diffraction Procedures for Pollycrystalline and Amorphous Materials*, John Wiley & Sons, New York 1966; 2nd ed., John Wiley, New York-London 1974.
[9] H.N.V. Temperley, D.H. Trevena, *Liquids and their Properties*, Ed. Ellis Horwood Limited, Chichester 1978.
[10] H. Drozdowski, M. Śliwińska-Bartkowiak, arXiv: 1908.02165

O-23

THEORETICALLY DERIVED THERMODYNAMIC PROPERTIES CAN BE IMPROVED BY THE REFINEMENT OF LOW-FREQUENCY MODES AGAINST X-RAY DIFFRACTION DATA

Anna A. Hoser[1]*, Marcin Sztylko[1], Anders Ø. Madsen[2]

1. Biological and Chemical Research Centre, Faculty of Chemistry, University of Warsaw, Żwirki i Wigury 101, 02-089 Warszawa, Poland
2. Department of Pharmacy, University of Copenhagen, Universitetsparken 2, Copenhagen 2100, Denmark

Accurate thermodynamic properties (heat capacity, entropy) for molecular crystals are still difficult to obtain for molecular crystals purely from theoretical calculations. From a computational point of view, the task is difficult because to compute thermodynamic properties one needs to calculate accurately frequencies of lattice vibrations, which require the high-level DFT calculations including empirical estimates of dispersion forces along with a thorough sampling of the Brillouin zone.

Recently, we have developed a new method, which allows estimating thermodynamic properties from frequencies, which are obtained from periodic *ab-initio* calculations and refined against single-crystal X-ray diffraction data. We called such refinement Normal Mode Refinement (NoMoRe) [1]. In this approach instead of refining ADPs, we are refining only a few frequencies related to low-frequency modes, which corresponds to the external vibrations of the molecule. The frequencies, which are obtained after the refinement, enable the calculation of thermodynamic properties. As opposed to previous efforts of extracting thermodynamic properties from X-ray diffraction data, our approach is not based on analysis of ADPs, but rather on a direct model refinement against the data. Thermodynamic properties, which we are obtaining after NoMoRe refinements are in good agreement with calorimetric results (especially heat capacity [2-4]). Moreover, after NoMoRe refinement, one can obtain ADPs for hydrogen atoms which are in very good agreement with those obtained from neutron diffraction measurements[1-3]. To enable other scientists to reproduce our work and use methods proposed by us for their systems we set up a user-friendly server through which NoMoRe refinement can be conducted.

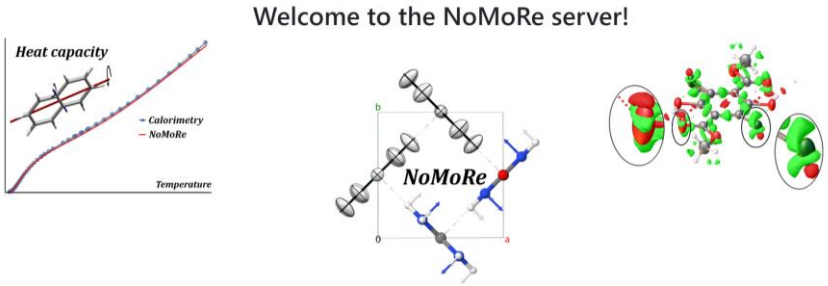

Fig 1. Screenshot from NoMoRe server.

References

[1] A. A. Hoser, A. Ø. Madsen, *Acta Cryst A*, **72** (2016) 206.
[2] A. A. Hoser, A. Ø. Madsen, *Acta Cryst A*, **73** (2017) 102.
[3] P. M. Kofoed, , A. A. Hoser, F.Diness, S. C. Capelli, A. Ø.Madsen, *IUCrJ*, **6** (2019) 558.
[4] A. A. Hoser, M. Sztylko, D. Trzybiński, A. Ø.Madsen, in press.

O-24

PHASE TRANSITIONS IN A $PbZr_{0.87}Ti_{0.13}O_3$ SINGLE CRYSTAL

[1]Iwona Lazar, [2]Andrzej Majchrowski, and [1]Krystian Roleder

[1]Institute of Physics, University of Silesia, ul. Uniwersytecka 4, 40-007 Katowice, Poland
[2]Institute of Applied Physics, Military University of Technology, ul. Kaliskiego 2, 00-908 Warsaw, Poland

$PbZr_{1-x}Ti_xO_3$ perovskite materials, known as PZT, are highly applicable, mainly due to their extraordinary piezoelectric properties. They are widely used in electronics, medical imaging, sports, piezoelectric clothing, the automotive industry, or research devices. Although these materials have been studied for many years, there are still many questions concerning their phase diagram. According to the phase diagram by Zhang [1], the structures of PZT solid solutions are complex, and local monoclinic phases exist for all Ti content levels in the range of $0.08<x<0.5$. However, most earlier research has focused on ceramics due to the difficulties in obtaining good quality PZT single crystals.

We succeeded in obtaining a transparent and homogenous PZT single crystal with x=0.13 through the top-seeded solution growth technique [2]. In $PbZr_{0.87}Ti_{0.13}O_3$ single crystal, the elastic, piezoelectric, and optical properties confirm an additional phase transition point at around 180°C. Cordero et *al*. [3] reported this phase characterized by the instability in octahedral sublattice. It appeared that such instability in the PZT single crystal leads to the high piezoelectric efficiency.

References

[1] N. Zhang, H. Yokota, A. M. Glazer, Z. Ren, D. A. Keen, D. S. Keeble, P. A. Thomas, Z.-G. Ye, *Nature Com.*, **5** (2014) 5231.
[2] I. Lazar, D. Kajewski, A. Majchrowski, A. Soszyński, J. Koperski, K. Roleder, *Ferroelectrics*, **500** (2016) 67.
[3] F. Cordero, F. Trequattrini, F. Craciun, C. Galassi, *J. Phys.: Condens. Matter*, **23** (2011) 415901.

O-25

MODULATED STRUCTURES IN $Pb(Hf_{1-x}Sn_x)O_3$ SINGLE CRYSTALS BY X-RAY DIFFRACTION

Irena Jankowska-Sumara[1], Marek Paściak[2], Andrzej Majchrowski[3]

1. *Institute of Physics, Pedagogical University of Cracow, Kraków, Poland*
2. *Institute of Physics of the Czech Academy of Sciences, Prague, Czech Republic*
3. *Institute of Applied Physics, Military University of Technology, Warsaw, Poland*

Antiferroelectric perovskite crystals such as $PbZrO_3$ and $PbHfO_3$ are technologically important materials with complex picture of phase transitions. Among the parameters that affect strongly the stability of particular phases are temperature, pressure and chemical doping. We report on our recent X-ray diffraction experiments, aiming at pinpointing the similarities and differences between the effects of hydrostatic pressure and doping by Sn^{4+} ions of $PbHfO_3$. The latter can be understood as chemical pressure, since Sn^{4+} ions have slightly smaller ionic radii that Hf^{4+} ion.

For this purpose the solid solution $Pb(Hf_{1-x}Sn_x)O_3$ – (PHS-x) were characterized using single-crystal X-ray diffraction in the wide temperature range. The information on the structure of two intermediate phases, situated between low-temperature antiferroelectric A1 and high temperature paraelectric (PE) phases has been obtained. The lower-temperature intermediate A2 phase is characterized by incommensurate displacive modulations in the Pb sublattice. The higher temperature intermediate IM phase is characterized by distortion of oxygen octahedra, and large disorder coming from lead ions represented by X-ray diffuse scattering. It can be expected that the IM phase is of AFD (antiferrodistorsive) character mainly related to an antiphase octahedral tilts. This implies that the resulting IM phase has a long-range order of oxygen octahedral rotations, and Pb atomic displacements are still correlated only on a short range with some signatures of local modulation.

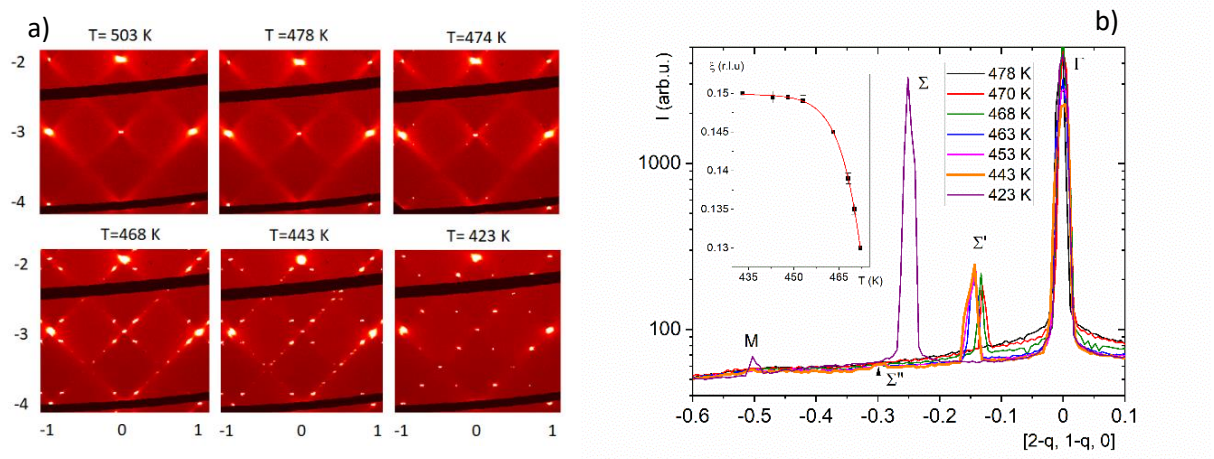

Figure 1. a) Reciprocal space map of PHS-0.08 in the (*H*,0,*L*) plane at temperatures which correspond to different phases on cooling: 508 K – PE phase, 478 K near T_C, 474 K just before IM-A2 phase transition, 468 K and 443 K – A2 phase, 423 K – A1 phase. b) Profiles of signal intensity along the Γ-M direction, in which the subsequent superstructures develop. The temperatures correspond to different phases (PE – IM – A2 – A1). An inset presents the temperature dependence of the component ξ_o of the modulation wave vector **q** =(ξ_o, ξ_o, 0).

O-26

INTERPLAY BETWEEN THE CRYSTAL STABILITY AND THE ENERGY OF THE MOLECULAR CONFORMATION

Konrad Dyk[1], Łukasz Baran[2], Wojciech Rżysko[2], Marek Stankevič[3] i Daniel Kamiński[1]

[1]Department of General, and Coordination Chemistry and Crystallography, Institute of Chemical Sciences, Faculty of Chemistry, Maria Curie-Skłodowska University in Lublin, Poland
[2]Department of Theoretical Chemistry, Institute of Chemical Sciences, Faculty of Chemistry, Maria Curie-Skłodowska University in Lublin, Poland
[3]Department of Organic Chemistry, Institute of Chemical Sciences, Faculty of Chemistry, Maria Curie-Skłodowska University in Lublin, Poland

The specially designed new compound of 5,5'-bis(4-hydroxyphenyl)-2,2'-dihydroxy-1,1'-biphenyl (**BHDB**) Figure 1, can crystallize in different crystallographic systems. The molecule adopts the C–conformation for the torsion angle around 60° and the T–conformation for the angle around 130°, which differ in energy by ~0.8 kJ/mol, see Figure 2. The theoretical studies for the gaseous phase show that the C-conformer has the lower energy [1].

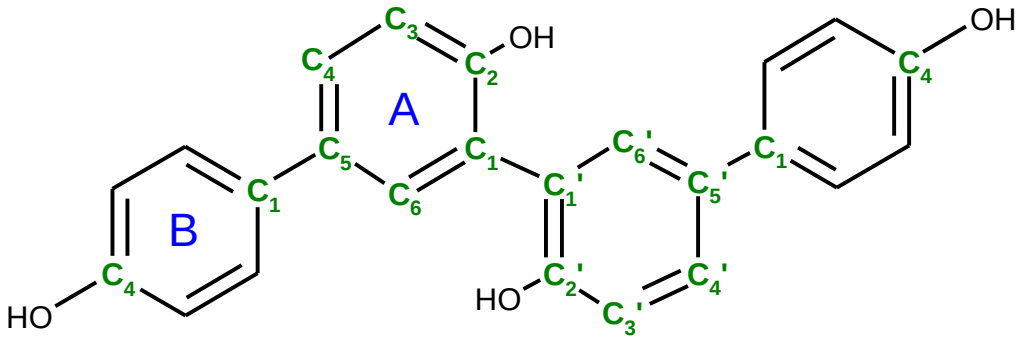

Figure 1. The scheme of the **BHDB** molecule with atom numbering.

However, crystallization experiments show that the most stable crystal structure consists of only the energetically less stable T–conformer. On the other hand, fast crystal growth at low temperature and crystal growth after milling both leads to the formation of metastable crystals in which the studied molecule adopts the C–conformation. Our study shows that the total crystal net energy is the main factor determining the molecular conformations even if the molecular conformation has higher energy in the gaseous phase [1].

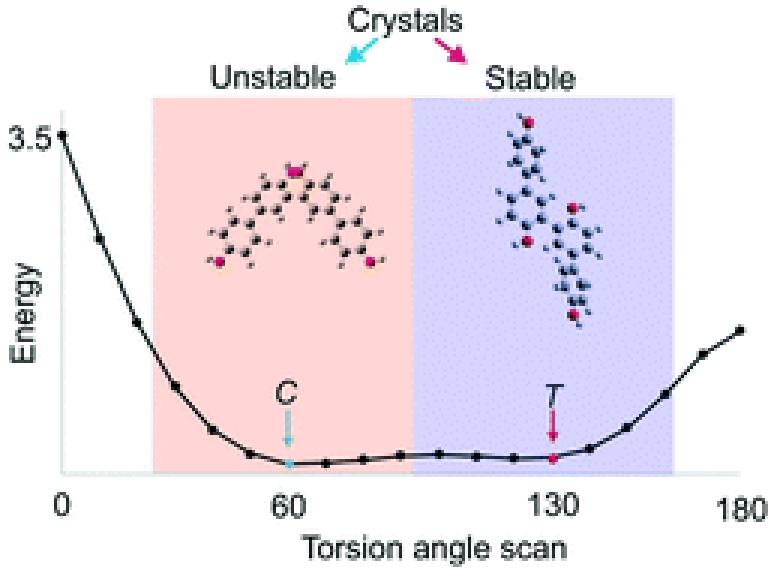

Figure 2. Gaussian16 calculations for the gaseous phase of **BHDB**. The geometry of the molecule was optimized at each step of calculations.

References

[1] K. Dyk, Ł. Baran, W. Rżysko, M. Stankevič, D. Kamiński, *CrystEngComm*, **23** (2021) 2683.

PLAKATY – SESJA A
POSTERS – SESSION A

A-01

THE FIRST INSIGHT INTO THE SUPRAMOLECULAR SYSTEM of *D,L*-*α*-DIFLUOROMETHYLORNITHINE: A NEW ANTIVIRAL PERSPECTIVE

Joanna Bojarska[1], Roger New[2], Paweł Borowiecki[3], Milan Remko[4], Martin Breza[5], Izabela D. Madura[6], Andrzej Fruziński[1], Anna Pietrzak[1] & Wojciech M. Wolf [1]

[1]Chemistry Department, Institute of Ecological and Inorganic Chemistry, Technical University of Łódź, Poland,
[2]Faculty of Science & Technology, Middlesex University, London, United Kingdom,
[3]Faculty of Chemistry, Department of Drugs Technology and Biotechnology, Laboratory of Biocatalysis and Biotransformation, Warsaw University of Technology, Warsaw, Poland,
[4]Remedika, Bratislava, Slovakia,
[5]Department of Physical Chemistry, Slovak Technical University, Bratislava, Slovakia,
[6]Faculty of Chemistry, Warsaw University of Technology, Poland

Targeting the polyamine biosynthetic pathway by inhibiting ornithine decarboxylase (ODC) is a powerful approach in the fight against diverse viruses, including SARS-CoV-2. Difluoromethylornithine (DFMO, eflornithine) is the best-known inhibitor of ODC and a broad spectrum, unique therapeutical agent. Nevertheless, its pharmacokinetic profile is not perfect, especially when large doses are required in antiviral treatment. Here, we will present a holistic study focusing on the molecular and supramolecular structure of DFMO and the design of its analogues toward the development of safer and more effective formulations. In this context, we will provide the first deep insight into the supramolecular system of DFMO supplemented by a comprehensive, qualitative and quantitative survey of non-covalent interactions *via* Hirshfeld surface, molecular electrostatic potential, enrichment ratio and energy frameworks analysis visualizing 3-D topology of interactions in order to understand the differences in the cooperativity of interactions involved in the formation of either basic or large synthons (Long-range Synthon Aufbau Modules, LSAM) at the subsequent levels of well-organized supramolecular self-assembly, in comparison with the ornithine structure. In the light of the drug discovery, supramolecular studies of amino acids, essential constituents of proteins, are of prime importance. In brief, the same amino-carboxy synthons are observed in the bio-system containing DFMO (Fig. 1). DFT calculations revealed that the biological environment changes themolecular structure of DFMO only slightly. The ADMET profile of structural modifications of DFMO and optimization of its analogue as a new promising drug *via* molecular docking will be discussed in detail.

A-01

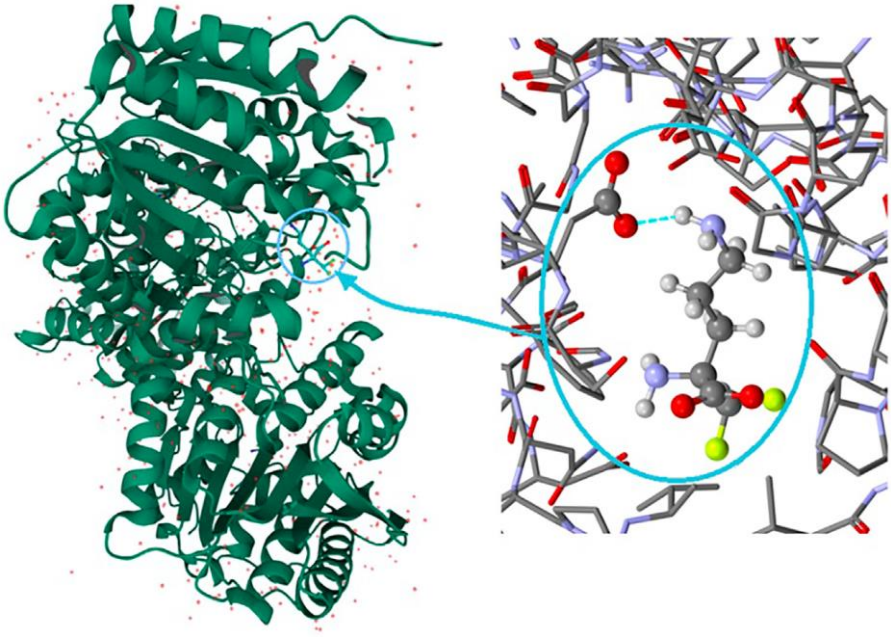

Fig. 1. On the left: the bio-complex of arginase with the DFMO ligand. On the right: the supramolecular synthon *D*(2) builded by amino and carboxy groups (PDB code: 3GN0).

A-02

BINDING OF CEFACLOR AND HYDROCORTISONE BY SERUM ALBUMINS

Kajetan Duszyński[1], Julita Tałaj[2], Kamil Zieliński[3], Anna Bujacz[1]

[1]*Institute of Molecular and Industrial Biotechnology, Łódź University of Technology, Stefanowskiego 2/22, 90-537 Łódź;*
[2]*Department of Molecular Biology of Cancer, Medical University of Łódź, 6/8 Mazowiecka Street, 92-215, Łódź, Poland.*
[3]*Department of Hematology, Comprehensive Cancer Center and Traumatology, Copernicus Memorial Hospital, Pabianicka 62, 93-513 Łódź, Poland.*

Serum albumins (SA) are the most abundant protein in vertebrate's plasma. These non-glycosylated proteins have an anionic character and are well soluble in water. Besides the SA function of maintaining colloid osmotic pressure SA have a vital role in transporting various molecules in the circulatory system. A significant part of the transported substances is pharmacologically active ligands. Determining the interactions in the SA-drug complex will allow for a better understanding of the drug distribution phenomena and in consequence, allow for reasonable drug design.

At the beginning of the SA structural investigation, the studies were concentrated on Human Serum Albumin (HSA). However, understanding the complexities of various species' albumin with therapeutic ligands would allow for a better understanding of the underlying principles of high binding sites affinity towards ligands. Additionally, determining the structures of different organisms will help investigate the evolution of SA. In our previous study, the structures of Equine Serum Albumin (ESA) and Leporine Serum Albumins (LSA) in complex with antiinflammatory drugs were determined [1,2].

Currently, medicine could not be such effective without the application of antibiotics and steroid hormones. The growing number of antibiotic-resistant infections force scientists to design novel antibiotics. However, despite the high scientific interest in albumin studies, there is a lack of structural data of SA in complexes with antibiotics, which could be crucial in antibiotic design. Also, SA structures with hormones are not investigated. Besides one structure of ESA with testosterone, which was determined recently (PDB ID: 6MDQ) [3].

We present crystal structures of Equine (ESA), Ovine (OSA), and Leporine (LSA) Serum Albumin, isolated from a horse, sheep, and rabbit blood, in a complex with cefaclor and hydrocortisone. Determined crystal structures show different binding sites of these steroid hormones.

References

[1] Sekula, B., Bujacz, A. *J Med Chem* **59** (2016) 82-89.
[2] K. Zieliński, B. Sekuła, A. Bujacz, I. Szymczak, *Chirality* **32** (2021) 334-344.
[3] Czub, M.P., Venkataramany, B.S., Majorek, K.A., Handing, K.B., Porebski, P.J., Beeram, S.R., Suh, K., Woolfork, A.G., Hage, D.S., Shabalin, I.G., Minor, W. *Chem Sci* **10** (2019) 1607-1618.

A-03

MACROMOLECULAR XTALLOGRAPHY RAW DATA REPOSITORY MX-RDR

M. Gilski[*1,2], P. Poniatowska[1], A. Rynkiewicz[1]

[1]Department of Crystallography, Faculty of Chemistry, A. Mickiewicz University, Uniwersytetu Poznańskiego 8, 61-614 Poznań, Poland
[2]Center for Biocrystallographic Research, Institute of Bioorganic Chemistry, Polish Academy of Sciences, Noskowskiego 12/14, 61-704 Poznań, Poland

The rapid development of computer technology in the past decades has opened new opportunities and challenges for researchers. Storing, handling and analysis of huge amounts of raw data has become possible and has created a new platform for research.

The crystallographic community has taken significant steps towards making experimental data available. The Protein Data Bank (PDB), established in 1971 with only seven X-ray crystallographic structures of proteins, experienced an almost exponential growth up to almost 180,000 currently stored structures and became the first open access digital data resource in biological sciences. Unfortunately, the vast majority of raw experimental data are only stored on local archive systems and, due to disk-space limitations, often are discarded or irreversibly lost for other reasons.

The Macromolecular Xtallography Raw Data Repository (MX-RDR) was developed as a part of an EU funded project, coordinated by ICM UW, which aimed to create three open access discipline dedicated raw data repositories.

The MX-RDR repository, which is accessible via the web portal at https://mxrdr.icm.edu.pl, was designed to archive and provide access to raw diffraction data collected for macromolecular crystals. It includes tools for creating sets of crystallographic metadata by combining information extracted directly from diffraction images and obtained from a PDB deposit and/or user input. Each data set is characterized by rich metadata, both to facilitate their management and long-term curation, and to allow effective scientific reuse. The resource can be searched using various criteria and all data are available for unrestricted access and download.

The research experimental data deposited in the repository, in the form of raw diffraction data and metadata, are stored on ICM UW servers with the highest standards of protection against their loss.

Other key features of the MX-RDR repository include: (1) Persistent identifiers. All data sets receive a persistent and unique DOI (Digital Object Identifier) that makes it easy to find and cite data. (2) Versioning. Possibility of placing the next, corrected or supplemented version of the data set. (3) Embargo. Possibility to set a period during which research data will not be made available to the public. (4) API (Application Programming Interface). Ability to prepare scripts that use internal API functions.

Acknowledgments: This work was supported by Operational Programme Digital Poland, OPC.02.03.01-00-0036/18-00

A-04

STRUCTURAL AND FUNCIONAL STUDIES OF PLANT-TYPE L-ASPARAGINASES WITH RANDOM MUTATIONS IN THE ACTIVE SITE

Agnieszka Klonecka[1], Piotr Bonarek[2], Jakub Barciszewski[3], Krzysztof Lewiński[1], Mariusz Jaskolski[3,4], Joanna Loch[1]

[1]Jagiellonian University, Faculty of Chemistry, Krakow, Poland
[2]Jagiellonian University, Faculty of Biochemistry, Biophysics and Biotechnology, Krakow, Poland
[3]Polish Academy of Sciences, Institute of Bioorganic Chemistry, Poznan, Poland
[4]A. Mickiewicz University, Faculty of Chemistry, Poznan, Poland

Acute lymphoblastic leukemia (ALL) is the most common childhood cancer. One of the chemotherapeutic agents used to treat ALL is Class 1 *E. coli* L-asparaginase (EcAII). However, EcAII exhibits a lot of undesired side effects. Therefore, novel therapeutic enzymes are highly required. Promising candidates could be found among plant-type (Class 2) asparaginases, e.g. EcAIII, belonging to the family of Ntn-hydrolases. Ntn-hydrolases are produced as inactive precursors and develop catalytic activity in an autoproteolytic maturation process. Unfortunately, natural EcAIII has too low substrate affinity to be considered as a potential therapeutic enzyme for ALL treatments.

Random mutagenesis is a common approach used in designing enzymes with novel properties. This strategy was used in this project to create new variants of EcAIII. We prepared a library of EcAIII variants possessing multiple substitutions in the active site (Fig. 1).

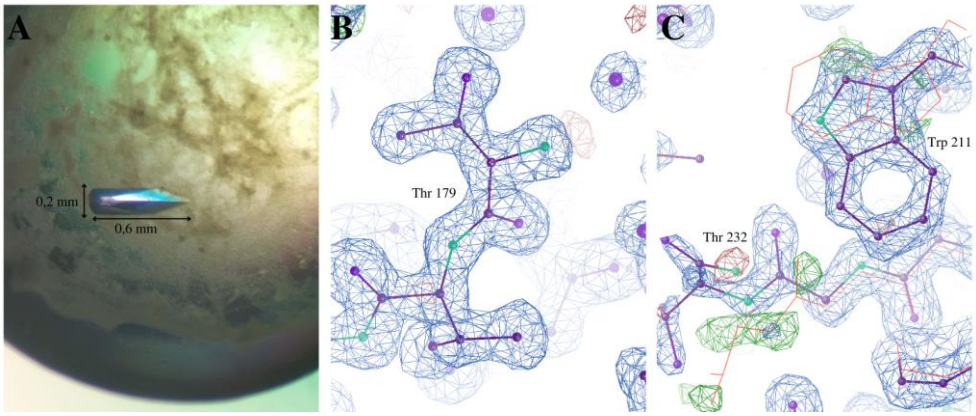

Fig. 1. (A) Crystal of EcAIII variant "18" (B) 2Fo Fc (1.50 σ) electron density of the variant "18" in the active site region. (C) 2Fo Fc (1.50 σ) electron density of variant "18" around the mutations sites reveals different conformations of Trp211 in chain A (violet) and chain B (orange).

The new variants were characterized by biophysical and crystallographic methods. The results reveal that the new EcAIII variants, depending on their susceptibility to autoproteolysis, can be divided into two groups: processing and non-processing for subunits α and β. The non-processing variants have reduced T_m

compared to the WT protein and some of them carry out structural distortions, as indicated by CD spectra. It was not possible to crystallize these variants despite extensive screening experiments. In contrast, the mutants carved for subunits can be easily crystallized (Fig. 1), although the quality of the crystals depends on the mutations present in the active site region.

The crystal structure (1,5 Å) of variant "18" (with increased T_m and ability to autoprocess), revealed different conformations of Trp211 in the two β subunits and additional small shifts of residues (e.g. Thr 232) in the region of the mutations. Analysis of the changes induced by the mutations help to understand the relationship between the increased thermal stability and molecular interactions in the crystal structure.

Work supported by NCN grants 2020/38/E/NZ1/00035 and 2019/03/X/NZ1/00584

A-05

STRUKTURA SOLI KWASU NIFLUMOWEGO Z AMANTADYNĄ

Marta S. Krawczyk, Irena Majerz

Wydział Farmaceutyczny, Uniwersytet Medyczny im. Piastów Śląskich we Wrocławiu, ul. Borowska 211, 50-556 Wrocław

Otrzymywanie soli i kompleksów substancji leczniczych wpływa na zmianę właściwości fizykochemicznych, a tym samym stanowi metodę poprawy właściwości farmakodynamicznych aktywnych substancji farmaceutycznych (API). Przedstawione badania stanowią kontynuację projektu dotyczącego struktury i analizy słabych oddziaływań w kryształach soli metali i kompleksów kwasu niflumowego oraz kwasów fenamowych. Kwas niflumowy należy do grupy niesteroidowych leków przeciwzapalnych (NLPZ) i stosowany jest głównie w leczeniu reumatoidalnego zapalenia stawów i ostrego bólu [1]. Amantadyna jest substancją stosowaną w leczeniu choroby Parkinsona oraz zespołach parkinsonowskich, a także jako lek przeciwko wirusowi grypy typu A [2,3].

Kryształy soli kwasu niflumowego z amantadyną otrzymano w wyniku krystalizacji z metanolu. W krysztale kationy uprotonowanej amantadyny oddziałują z anionami kwasu niflumowego poprzez wiązania wodorowe N-H···O, w które zaangażowana jest grupa NH_3^+ i grupa karboksylanowa. W anionach kwasu obserwowane są wewnątrzcząsteczkowe wiązania wodorowe: N1-H1N···O2 oraz C9-H9···N4. W badanym krysztale nie występują cząsteczki rozpuszczalnika – metanolu, dzięki czemu analizowana sól jest obiecującym układem do badań aktywności biologicznej i stanowi istotne osiągnięcie z punktu widzenia potencjalnego zastosowania farmakologicznego.

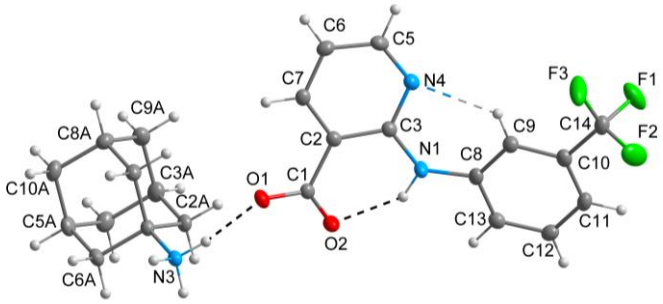

Rys. 1. Struktura soli kwasu niflumowego z amantadyną.

Źródło finansowania: Uniwersytet Medyczny we Wrocławiu, grant SUB.D050.21.034.

Literatura

[1] S. Mittapalli, M. K. Ch. Mannava, R. Sahoo, A. Nangia, *Cryst. Growth Des.*, **19**(1) (2019) 219.
[2] G. Hubsher, M. Haider, M.S. Okun, *Neurology*, **78**(14) (2012) 1096.
[3] B. Kumar, K. Asha, M. Khanna, L. Ronsard, CA. Meseko, M. Sanicas, *Archives of Virology*, **163**(4) (2018) 831.

A-06

FROM ELECTRON DENSITY MAPS TO ELECTROSTATIC POTENTIAL DENSITY MAPS OF MACROMOLECULES WITH MATTS DATABANK

Marta Kulik, Michał L. Chodkiewicz i Paulina M. Dominiak

Centrum Nauk Biologiczno-Chemicznych Uniwersytetu Warszawskiego, Wydział Chemii, Uniwersytet Warszawski, ul. Żwirki i Wigury 101, 02-089 Warszawa

Structure factors in the X-ray diffraction experiment enable the calculation of the density of the core and valence electrons in the studied crystal. In the electron diffraction experiment, the structure factors convey the information about the electrostatic potential density map. Such density maps are being obtained in micro-electron diffraction at atomic resolution. An important difference between the atomic scattering factors for X-rays and electrons is that the latter are strongly dependent on scattering angle and at low scattering angle may become negative. Modeling of the structure factors can be done in a spherical way, using Independent Atom Model (IAM) and in aspherical way with the Multipolar Atom Types from Theory and Statistical clustering (MATTS) databank (successor of UBDB2018 [1]), which gathers atom types, useful for deriving the multipolar electron scattering factors. MATTS is a database universal for various macromolecules as the atom types are transferable between similar chemical environments. Using MATTS it is possible to recreate the electron density distribution of macromolecules via structure factors [2] or to calculate the accurate electrostatic potential maps for small molecules [3]. MATTS is able to reproduce the molecular electrostatic potential of molecules within their entire volume better than the simple point charge models used in molecular mechanics or neutral spherical models used in electron crystallography.

Here, we calculate both the electron density maps and the electrostatic potential maps for two model proteins and compare the latter with experimental maps from micro-electron diffraction. We apply the multipolar electron scattering factors and advance the knowledge how the theoretically-obtained potential maps of proteins should look like. We also consider the influence of atomic displacement parameters on the theoretical maps as their physical meaning in cryo-electron microscopy is not as well established as in X-ray crystallography.

The authors acknowledge NCN UMO-2017/27/B/ST4/02721 grant.

References

[1] Kumar *et al*., *Acta Cryst*., A**75** (2019) 398-408.
[2] Chodkiewicz *et al*., *J. Appl. Cryst*., **51** (2018) 193-199.
[3] Gruza *et al*., *Acta Cryst*., A**76** (2019) 92-109.

A-07

THE ATOMIC STRUCUTRE OF DECAGONITE, THE EXTRATERRESTRIAL QUASICRYSTAL

Ireneusz Bugański[1], Luca Bindi[2]

[1]AGH University of Science and Technology,
Faculty of Physics and Applied Computer Science
[2]Dipartimento di Scienze della Terra, Università degli Studi di Firenze,
Via La Pira 4, Firenze I-50121, Italy

Quasicrystalline long-range order was known to be formed synthetically in a laboratory environment. It was manifested both in intermetallic compounds and soft matter. We know how to create them, with a quality rivalling these of the periodic crystals. We only wondered if quasicrystals as minerals could be found somewhere in nature. Only recently, in 2009, it was confirmed that the first natural quasicrystal was found in Koryak Mountains in Russia [1]. It was more special than we originally thought. Its origins are extraterrestrial. Unfortunately, the atomic structure of icosahedrite, that is the name of the mineral, could not be solved quantitatively.

In 2015, after the expedition to the same region a new mineral was found, decagonite – natural quasicrystal with decagonal symmetry. The X-ray diffraction experiment provided enough information to solve its atomic structure and compare its quality with its synthetic counterpart. This presentation focuses on the work [2], dedicated to describing the atomic structure of this natural quasicrystal, especially focusing on the nature of its disorder. We can conclude, the quality of the long-range order does not depart from crystal of laboratory origin. Especially the phasonic disorder, the type of disorder peculiar only to aperiodic systems, in magnitude is standard. It proves the conditions for the natural growth of quasicrystals, even though extraterrestrial, are suitable and we can expect more occurrences of this phase in nature.

References

[1] L. Bindi, P. J. Steinhardt, N. Yao, P. Lu, *Science* **324**, (2009) 1306.
[2] I. Buganski, L. Bindi, *IUCrJ* **8**, (2021) 87.

A-08

BADANIA STRUKTURALNE FAZ KRYSTALICZNYCH I CIEKŁOKRYSTALICZNYCH TIOESTRU 7OS5

Aleksandra Deptuch[1,2,*], Teresa Jaworska-Gołąb[2], Joachim Kusz[3], Maria Książek[3], Keigo Nagao[4], Takashi Matsumoto[4], Akihito Yamano[4], Mirosława D. Ossowska-Chruściel[5], Janusz Chruściel[5], Monika Marzec[2]

[1] Instytut Fizyki Jądrowej im. Henryka Niewodniczańskiego PAN, 31-342 Kraków
[2] Instytut Fizyki im. Mariana Smoluchowskiego UJ, 30-348 Kraków
[3] Instytut Fizyki im. Augusta Chełkowskiego UŚ, 41-500 Chorzów
[4] Laboratorium Aplikacyjne Rigaku, Tokio, Japonia
[5] Wydział Chemii UPH, 08-110 Siedlce
[*] aleksandra.deptuch@ifj.edu.pl

Szereg homologiczny 4-n-alkoksybenzenotiokarboksylanów S-4-pentylofenylu (wzór chemiczny $H_{2n+1}C_nO–C_6H_4–COS–C_6H_4–C_5H_{11}$; akronim nOS5; n = 4-12) stanowi przykład achiralnych związków wykazujących silną zależność między długością łańcucha węglowego -C_nH_{2n+1} a polimorfizmem faz ciekłokrystalicznych [1]. Badania strukturalne tych związków w fazach ciekłokrystalicznych i w fazie krystalicznej [2] stwarzają możliwość powiązania struktury krystalicznej z mezofazami obserwowanymi w sekwencjach fazowych poszczególnych homologów. Właściwości fizyczne ciekłych kryształów zależą nie tylko od temperatury, w jakiej prowadzony jest pomiar, ale również od szybkości i kierunku zmian temperatury oraz od historii termicznej próbki. Dlatego jest to również wyzwanie badawcze od strony aparaturowej. W przedstawionych badaniach tioestru 7OS5, oprócz dyfrakcji rentgenowskiej na monokrysztale i na próbkach polikrystalicznych, wykonany został jednoczesny pomiar metodą dyfrakcji rentgenowskiej i różnicowej kalorymetrii skaningowej (XRD-DSC).

Pomiary dyfrakcyjne na bardzo małym monokrysztale (ochłodzonym z szybkością 6°C/min z temperatury pokojowej do -183°C) przeprowadzone na dyfraktometrze SuperNova umożliwiły rozwiązanie przechłodzonej, wysokotemperaturowej, rombowej fazy krystalicznej (grupa przestrzenna $Pca2_1$; a = 54.285 (5) Å, b = 5.5843 (3) Å, c = 14.841 (1) Å, Z = 8). W fazie tej stwierdzono obecność wiązań wodorowych C-H…O i C-H…S. Pomiary przeprowadzone dla tego samego monokryształu po ogrzaniu do temperatury pokojowej i ponownym ochłodzeniu z szybkością 2°C/min wykazały istnienie dwóch faz krystalicznych: jednoskośnej i rombowej, z temperaturą przejścia fazowego ok. -40°C. Z temperaturowej zależności parametrów komórki elementarnej wynika, że przejście fazowe charakteryzuje się nagłą zmianą wartości kąta β, natomiast pozostałe parametry nie wykazują nieciągłości (Rys. 1a). Co ciekawe liniowe współczynniki rozszerzalności termicznej są silnie anizotropowe (Rys. 1b) w obu fazach krystalicznych, natomiast kierunki główne tensora odkształceń termicznych są zgodne z kierunkami krystalograficznymi tylko w fazie rombowej [3].

Wyniki pomiarów metodą XRD-DSC na polikrystalicznej próbce 7OS5 potwierdziły sekwencję fazową, ale przede wszystkim umożliwiły wyznaczenie temperaturowej zależności parametrów strukturalnych faz ciekłokrystalicznych: długości korelacji i średnich odległości między molekułami dla porządku krótkiego zasięgu oraz grubości warstw smektycznych. Wykorzystując długość molekuły

określoną z pomiarów dla monokryształu, wyznaczono kąt pochylenia molekuł w fazie smektycznej C, obserwowanej przy chłodzeniu [3]. Pomiary XRD przeprowadzone dla próbek polikrystalicznych wykazały dużą wrażliwość polimorfizmu faz krystalicznych 7OS5 na historię termiczną próbki. Z analizy dyfraktogramów proszkowych metodą Le Baila wynika, że przejście do fazy ciekłokrystalicznej następuje, podobnie jak w przypadku próbki monokrystalicznej, z wysokotemperaturowej fazy krystalicznej o strukturze rombowej (grupa przestrzenna $Pca2_1$).

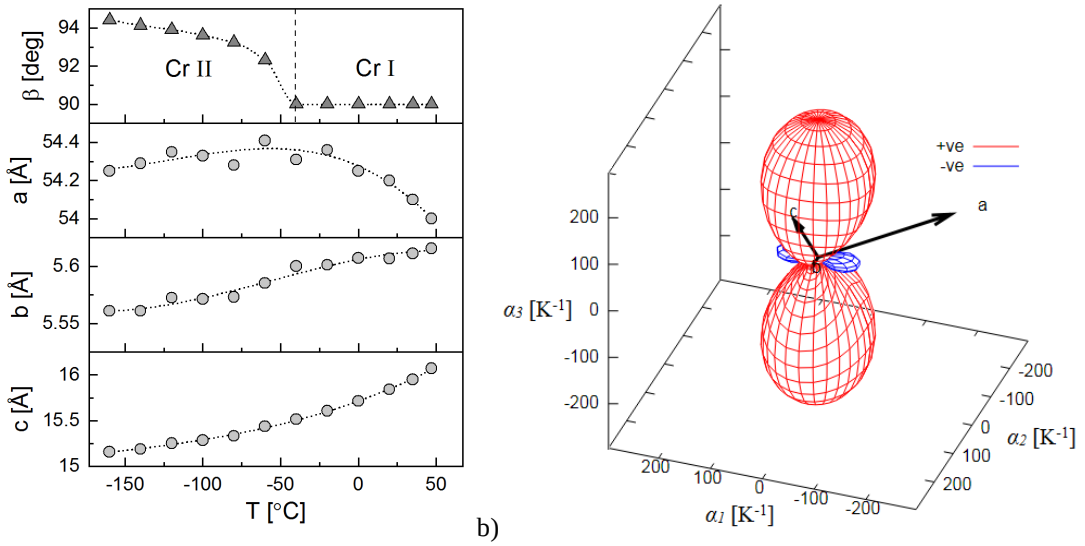

a) b)

Rys. 1. Parametry komórki elementarnej faz krystalicznych 7OS5 otrzymane podczas ogrzewania dla wolno schłodzonego monokryształu (a) oraz indykatrysa współczynników rozszerzalności termicznej dla fazy Cr II (wygenerowana w programie PASCal [4]) (b).

Literatura

[1] M. D. Ossowska-Chruściel, *Otrzymywanie i badania ciekłokrystalicznych tioestrów*, praca habilitacyjna, Wydawnictwo Akademii Podlaskiej, Siedlce 2008.

[2] A. Deptuch, *Badania struktury faz krystalicznych i ciekłokrystalicznych związków z szeregu homologicznego nOS5 metodami komplementarnymi*, praca magisterska, Uniwersytet Jagielloński 2015, https://fais.uj.edu.pl/documents/41628/0105a397-2f6e-472f-856f-35e43fcf38ac.

[3] A. Deptuch, T. Jaworska-Gołąb, J. Kusz, M. Książek, K. Nagao, T. Matsumoto, A. Yamano, M. D. Ossowska-Chruściel, J. Chruściel, M. Marzec, *Acta Cryst. B*, **76** (2020) 1128-1135.

[4] M. J. Cliffe, A. L. Goodwin, *J. Appl. Cryst.*, **45** (2012) 1321-1329.

A-09

INTERMOLECULAR INTERACTIONS IN PURINE HYPODIPHOSPHATE SALTS

Marta Otręba, Katarzyna Ślepokura

University of Wroclaw, Faculty of Chemistry, F. Joliot - Curie 14 St., 50-383 Wroclaw

Adeninium salts of hypodiphosphoric acid have been found as an interesting model system for study of intermolecular interactions in the crystals of hypodiphosphate nucleoside esters.[1] Continuing studies over structural behaviour of hypodphosphoric acid ($H_4P_2O_6$) in its organic compositions we decided to synthesise a series of salts with purinium cations, such as xanthinium and its methyl derivatives (theophyllinium, theobrominium and caffeinium, Fig 1). Purine alkaloids (methylxanthine derivatives) can act as antagonists of adenosine receptors thus they are potential therapeutic agents against asthma or intestinal disorders.[2] Differentiation of substituent groups in purine core allows to analyse how they affect intermolecular interactions with hypodiphosphate ions.

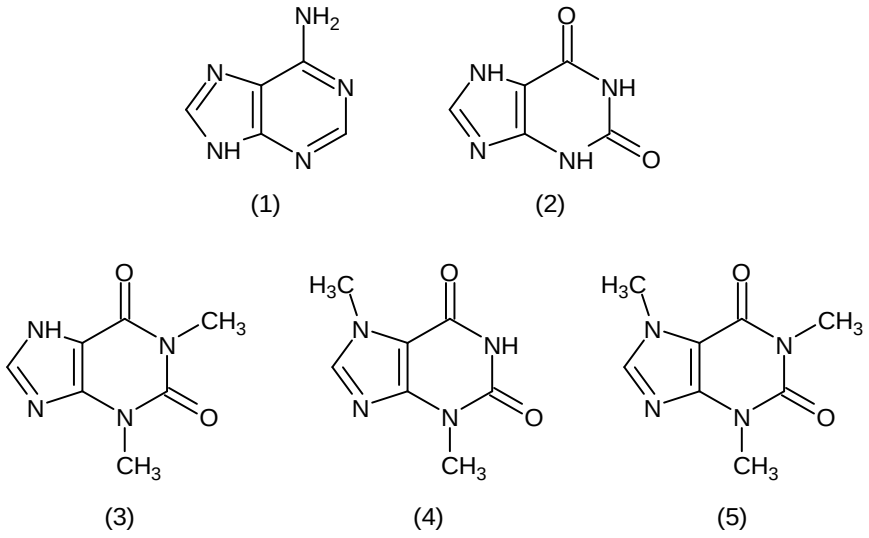

Figure 1. Structural formulae of adenine (1, Ade), xanthine (2, Xan), theophylline (3, Teof), theobromine (4, Teob) and caffeine (5, Caff).

Six new purinium hypodiphosphate salts were synthesized and characterized in the crystalline form: $(XanH)_2(H_2P_2O_6)$, $(TeofH)_2(H_2P_2O_6)\cdot H_4P_2O_6\cdot 2H_2O$, $(TeofH)(H_3P_2O_6)\cdot 0.5H_2O$, $(TeofH)(H_3P_2O_6)$, $(TeobH)(H_3P_2O_6)\cdot H_2O$ and $(TeobH)_2(H_2P_2O_6)\cdot 2H_2O$. The related compounds, $(AdeH_2)(H_2P_2O_6)$, $(TeofH)_2(H_2P_2O_6)$ and $(CaffH)(H_3P_2O_6)$ have been recently presented and will be further compared.[3,4]

In all crystals, base–hypodiphosphate hydrogen bonds seem to play important role. Despite of differences in substituents (–H or $–CH_3$ groups) and their position, purinium cations seek to be involved into structural ring motif by participation in two hydrogen bonds with hypodiphosphate anion. Four types of rings can be distinguished: $R^1_2(7)$, $R^2_2(7)$, $R^2_2(8)$ and $R^2_2(9)$ where cations are engaging Hoogsteen or sugar edge or both of them. Direct base–base interactions are not observed in any of the crystals, in

some of them cations are bridged by hypodiphosphate anions or water molecules. In several crystals there are $\pi\cdots\pi$ stacking interactions between base rings or lone pair–π (lp–π) interactions that additionally stabilize crystal packing.

References

[1] M. Otręba, D. Budzikur, Ł. Górecki & K. A. Ślepokura, *Acta Crystallogr. C.*, **74** (2018) 571.
[2] S. A. Kim, M. A. Marshall, N. Melman, H. S. Kim, C. E. Müller, J. Linden, K. A. Jacobson, *J. Med. Chem.* **45** (2002) 2131.
[3] D. Budzikur, A. Nowak, M. Otręba, K. Ślepokura, Poster: Wpływ podstawnika w pozycji 6 pierścienia purynowego na schemat wiązań wodorowych w kryształach hipodifosforanów adeniny, hipoksantyny oraz 6-merkaptopuryny. 61 Konwersatorium Krystalograficzne (61st Polish Crystallographic Meeting), Warsztaty Naukowe PTKryst, Wrocław, 26–28 VI 2019, str. 69–70.
[4] M. Otręba, K. Ślepokura, Poster: Intermolecular interactions in hypodiphosphate salts of caffeine and theophylline. Wspólna Polsko-Niemiecka Konferencja Krystalograficzna (Joint Polish-German Crystallographic Conference 2020), Wrocław, 23–27 II 2020, P86, str. 99.

A-10

PRZEJŚCIA FAZOWE W DWÓCH IZOSTRUKTURALNYCH KOMPLEKSACH BIZMUTU (III)

Anita M. Grześkiewicz[1], Ibrahim I. Ozturk[2], Maciej Kubicki[1]

[1]Wydział Chemii, Uniwersytet im. Adama Mickiewicza w Poznaniu,
[2]Section of Inorganic Chemistry, Department of Chemistry, Tekirdag Namık Kemal University, 59030, Tekirdag, Turkey

Kompleksy bizmutu ze względu na swoje właściwości biologiczne, dużą różnorodność strukturalną jak i niską toksyczność zyskują ostatnio na popularności. Zwłaszcza interesujące, ze względu na ich właściwości antynowotworowe i bakteriobójcze, są kompleksy Bi(III) z tioamidami.. Rosnący problem antybiotyko-oporności skutkuje więc także poszukiwaniem nowych związków kompleksowych tego metaloidu.

W toku prowadzonych badań scharakteryzowano dwa nowe izostrukturalne (w temperaturze pokojowej) związki kompleksowe bizmutu (III): {[($BiCl_2$(μ_2-Cl(Pheetsc)$_2$)$_2$]} (**1**) oraz {[($BiBr_2$(μ_2-Br(Pheetsc)$_2$)$_2$]} (**2**) (Pheetsc: 1-fenyloetylo-N-etylotiosemikarbazon) .

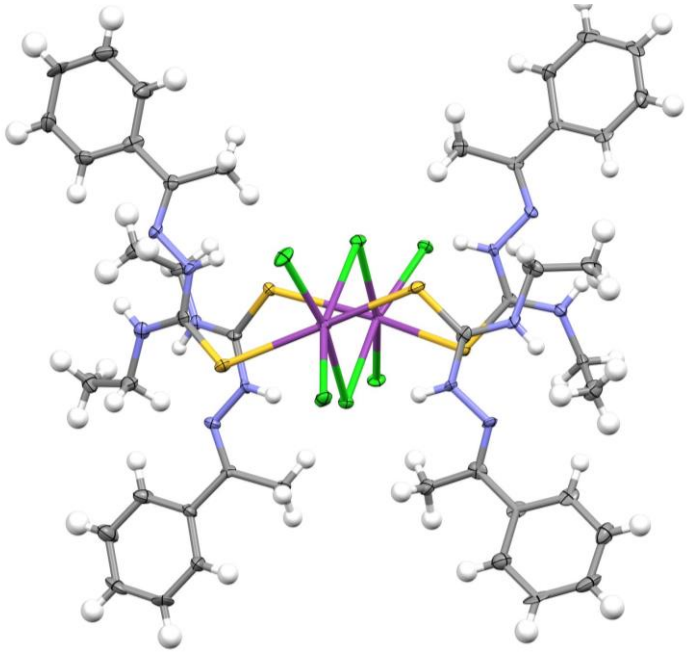

Rys. 1. Cząsteczka kompleksu **(1)**

Związki te przechodzą w nową zbliźniaczoną fazę krystaliczną w temperaturze ok. 235 K **(1)** i 175 K **(2)**. W obu przypadkach przemiana ta jest odwracalna. Niemniej jednak badania przy użyciu dyfraktometrii proszkowej, skaningowej kalorymetrii różnicowej oraz rentgenowskiej analizy monokrystalicznej umożliwiły znalezienie szeregu innych efektów strukturalnych zależnych od temperatury, które dość istotnie różnią te dwie pochodne.

A-11

NIETYPOWE PRZEJŚCIE FAZOWE W KRYSZTALE $SiPh_3OH$

Monika K. Krawczyk

Instytut Fizyki Doświadczalnej, Uniwersytet Wrocławski, Pl. M. Borna 9, 50-204 Wrocław

W poszukiwaniu materiałów wykazujących przejścia fazowe podjęto badania kryształu trifenylosilanolu, $SiPh_3OH$. Z doniesień literaturowych wiadomo, że struktura krystaliczna tego związku zbadana została w temperaturze pokojowej oraz w temperaturach: 120, 123 i 173 K [1-4]. W każdym ze wspomnianych pomiarów uzyskano rozwiązania struktury w typie grup przestrzennych $P\bar{1}$ dla tej samej fazy kryształu, w której stałe sieciowe wynosiły: a = 15.07, b = 19.57, c = 23.10 Å, α = 108.0, β = 102.8, γ = 101.3°, V = 6051.8 Å^3 (w temperaturze 123 K [3]). Tymczasem badając właściwości kryształu trifenylosilanolu zaobserwowano, że w wyniku gwałtownego schłodzenia z temperatury pokojowej do temperatury 100 K, kryształ ten wykazuje przejście fazowe prowadzące do zwiększenia rozmiarów komórki sieciowej. Satysfakcjonujące rozwiązania uzyskano zarówno w grupie przestrzennej $P\bar{1}$ jak i $P1$. W temperaturze T = 100(2) K w grupie przestrzennej $P1$ stałe sieciowe są następujące: a = 22.178(2), b = 24.504(2), c = 25.106(2) Å, α = 114.21(2), β = 101.16 (2), γ = 95.37(2)°, V = 11978.30 Å^3. Istotny jest fakt, że wspomniana przemiana fazowa nie następuje, gdy kryształ $SiPh_3OH$ schładzany jest stopniowo do temperatury 100 K. Natomiast powolne ogrzewanie kryształu powoduje przejście fazowe w temperaturze około 120 K, w którym kryształ powraca do pierwotnej fazy o zmniejszonej komórce elementarnej.

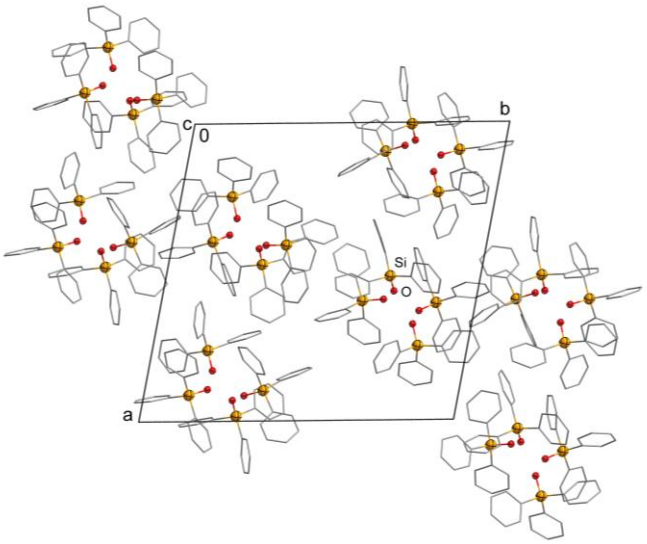

Rysunek. Struktura $SiPh_3OH$ uzyskana w wyniku gwałtownego schłodzenia kryształu do 100 K.

Literatura

[1] H. Puff, K. Braun, H. Reuter, *J. Organomet. Chem.*, **409** (1991) 119.
[2] K. F. Bowes, C. Glidewell, J. N. Low, *Acta Cryst. C.*, **58** (2002) o409.
[3] M. Nieger, informacja prywatna (1999).
[4] M. Bolte, S. Nordschild, informacja prywatna (2006).

A-12

DWUETAPOWE, JEDNOSTOPNIOWE PRZEJŚCIE SPINOWE W ZWIĄZKU KOMPLEKSOWYM $[Fe(bbtr)_3](CF_3SO_3)_2$

Maria Książek[1], Marek Weselski[2], Joachim Kusz[1] i Robert Bronisz[2]

[1]Instytut Fizyki, Uniwersytet Śląski, ul. 75 Pułku Piechoty 1, 41 – 500 Chorzów
[2]Wydział Chemii, Uniwersytet Wrocławski, ul. F. Joliot – Curie 14, 50 – 383 Wrocław

Zjawisko przejścia spinowego występuje w oktaedrycznych kompleksach metali o konfiguracjach elektronowych $3d^4$-$3d^7$. W przypadku kompleksów Fe(II) zmiana stanu spinowego podczas przejścia HS→LS (HS – wysoki stan spinowy, LS – niski stan spinowy) jest związana ze skróceniem odległości Fe-N o około 0.2 Å. Należy podkreślić, że budowa pierwszej sfery koordynacyjnej jonu metalu, jak również upakowanie cząsteczek w sieci krystalicznej ma istotny wpływ na przebieg przejścia spinowego, co znajduje odzwierciedlenie w zależności γ_{HS} od temperatury (γ_{HS} – ułamek molowy formy wysokospinowej).

Badania przeprowadzone dla polimerów koordynacyjnych Fe(II) uzyskanych na bazie ligandu 1,4-di(1,2,3-triazol-1-ylo)butanu (bbtr) i jego pochodnych wykazały różnorodność przebiegów przejść spinowych. W przypadku kompleksu $[Fe(bbtr)_3](ClO_4)_2$ przejście spinowe jest gwałtowne, z towarzyszącą mu histerezą ($T_{1/2}^{\downarrow}$ = 112 K, $T_{1/2}^{\uparrow}$ =141 K)[1]. Co więcej, zjawisko to jest stowarzyszone z przejściem fazowym P-3→P-1. W kompleksie $[Fe(bbtr)_3](BF_4)_2$ nie występuje analogiczne przejście fazowe, a kompleks pozostaje w stanie HS w zakresie temperatur 10 – 300K[2]. Wykorzystanie 1,4-di(5-etylo-1,2,3-triazol-1-ylo)butanu (ebbtr) prowadzi do uzyskania dwuwymiarowego polimeru koordynacyjnego, który wykazuje niezwykle wyjątkowe przejścia spinowe: „podwójne" [3] oraz „normalne i odwrócone" [4]. Tak nietypowe przejścia spinowe w tym kompleksie są związane z istotnymi zmianami strukturalnymi. Natomiast w wyniku zastosowania regioizomerycznego liganda bbtre (rys. 1) otrzymuje się trójwymiarowy polimer koordynacyjny, gdzie wieloetapowe przejście spinowe jest uzależnione od zmian konformacyjnych ligandów.[5]

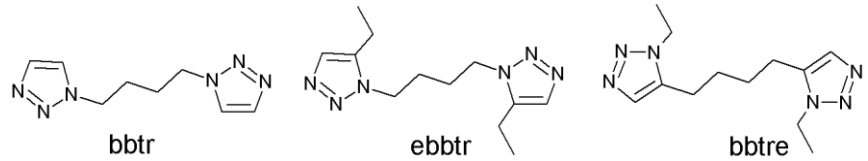

Rys. 1. Struktury ligandów bbtr, ebbtr oraz bbtre.

Niemniej istotnym czynnikiem wpływającym na przebieg przemian spinowych, oprócz zastosowanego liganda, jest także wybór cząsteczki stanowiącej część anionową kompleksu. Zastosowanie $Fe(CF_3SO_3)_2 \cdot 6H_2O$ i liganda bbtr pozwoliło otrzymać dwuwymiarowy polimer koordynacyjny $[Fe(bbtr)_3](CF_3SO_3)_2$. Związek kompleksowy krystalizuje w grupie przestrzennej R-3. Cechą charakterystyczną tego kompleksu jest uporządkowanie połowy cząsteczek ligandów mostkujących bbtr oraz obecność dwóch, niezależnych jonów Fe(II). Przejście spinowe dla tego związku jest łagodne i kompletne. Dokładniejsza analiza zmian długości wiązań Fe-N wykazała, że oba niezależne krystalograficznie jony Fe(II) zmieniają swój stan spinowy w różnych

zakresach temperatur. Co więcej, zaobserwowano występowanie bardzo wolnego przejścia strukturalnego R-3→P6_3. Jest ono stowarzyszone z porządkowaniem się cząsteczek liganda. Na posterze zostaną przedstawione szczegóły dotyczące struktur krystalicznych przed i po przejściu fazowym.

Literatura

[1] R. Bronisz, *Inorg. Chem*., **44** (2005) 4463.
[2] J. Kusz, R. Bronisz, M. Zubko, G. Bednarek, *Chem. Eur. J*., **17** (2011) 6807.
[3] M. Weselski, M. Książek, D. Rokosz, A. Dreczko, J. Kusz, R. Bronisz, *Chem. Commun*., **54** (2018) 3895.
[4] M. Weselski, M. Książek, P. Mess, A. Dreczko, J. Kusz, R. Bronisz, *Chem. Commun*., **55** (2019) 7033.
[5] M. Książek, M. Weselski, A. Dreczko, V. Maliuzhenko, M. Kaźmierczak, A. Tołoczko, J. Kusz, R. Bronisz, *Dalton Trans*., **49** (2020) 9811.

A-13

THE INFLUENCE OF PRESSURE ON THE COURSE OF PHOTODIMERIZATION IN CRYSTALS OF 9-METHYLANTHRACENE

Julia Bąkowicz and Ilona Turowska-Tyrk

Faculty of Chemistry, Wrocław University of Science and Technology, Wybrzeże Wyspiańskiego 27, 50-370 Wrocław

The results of monitoring structural changes in crystals of 9-methylanthracene during the photochemical reaction at high pressure will be presented. The studies were performed at 0.1 GPa and 0.4 GPa. The analogous experiments at ambient pressure were carried in the past [1].

The compound under the influence of UV-vis radiation undergoes the [4+4] photodimerization in a crystalline state both in ambient and high pressure conditions, see Scheme 1:

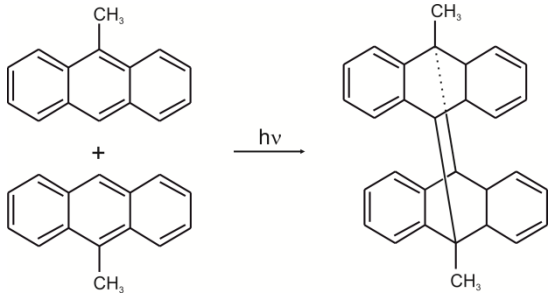

The variations in the cell constants and in the geometry of the reaction centre brought about the photochemical reaction at high pressure and also the behavior of molecules during the reaction were monitored and analyzed. In ambient conditions, the cell volume increases at the initial stage of the reaction (to *ca*. 15 % of the product content) and afterwards decreases [1]. The high pressure counteracts this growth: the volume of the unit cell is constant until *ca*. 20 % of the reaction progress (at 0.1 GPa) or even decreases from the beginning of the reaction (at 0.4 GPa) (Fig. 1).

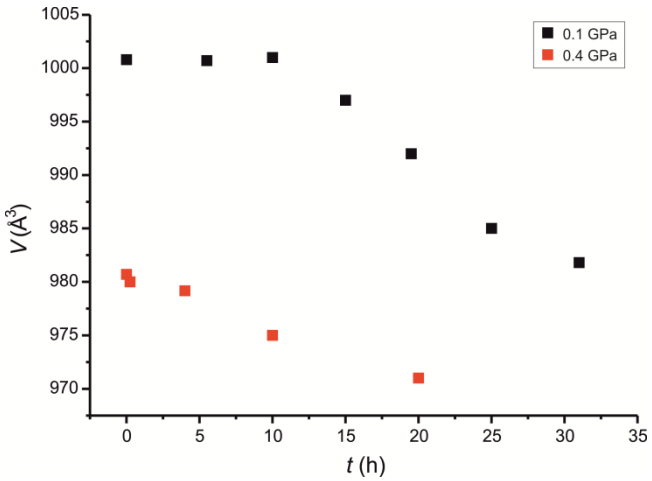

Fig. 1. The variations in the unit cell volume of 9-methylanthracene with the irradiation time.

The X-ray structure analysis revealed the crystal of the pure dimer after 30 h and 20 h of irradiation at 0.1 GPa and 0.4 GPa, respectively. In contrast, at ambient pressure after similar irradiation time, the progress of the reaction was only *ca*. 30 % and the pure product crystal was obtained after crystallization of irradiated powder.

The above-mentioned facts show that the [4+4] photodimerization in crystals of 9-methylanthracene is faster at higher pressures. This indicates that the decrease in the distance between reactant molecules at high pressure (which makes the reaction easier) dominates over the decrease in free space (which makes the reaction more difficult).

References

[1] I. Turowska-Tyrk, E. Trzop, *Acta Cryst. B.*, **59** (2003) 779.

A-14

STRUCTURAL AND COMPUTATIONAL STUDIES OF A NEW DIASTEREOMERIC TYPE OF *N*-MORPHOLINO-SPIRO DERIVATIVE

Mateusz Gołdyn, Weronika Nowak, Elżbieta Bartoszak-Adamska, Anna Komasa, Zofia Dega-Szafran

Wydział Chemii UAM, ul. Uniwersytetu Poznańskiego 8, 61-614 Poznań

Spiranes belong to the group of organic compounds characterized by two cyclic rings sharing a common atom [1]. The investigated spirane derivative, *N*-morpholinyl-spiro-*β*-hydroxy-*β*-methylmorpholinyl chloride, was obtained in the reaction between chloroacetone and *N*-(2-hydroxyethyl)morpholine [2].

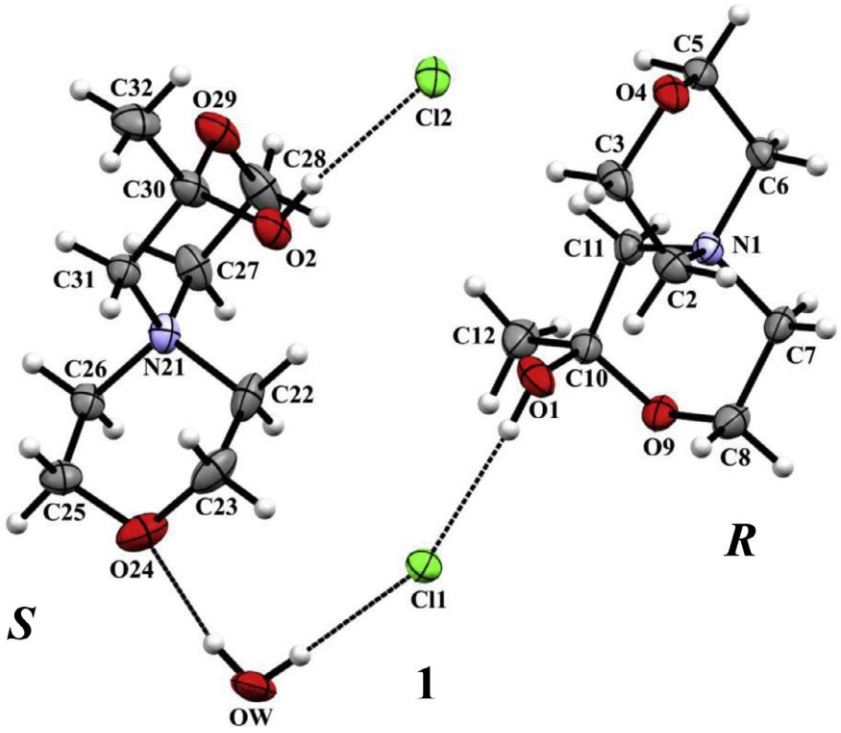

Fig. 1. ORTEP representation of (*R*/*S*)-di-(*N*-morpholinyl-spiro-*β*-hydroxy-*β*-methylmorpholinyl chloride) hydrate.

The structure of (*R*/*S*)-di-(*N*-morpholinyl-spiro-*β*-hydroxy-*β*-methylmorpholinyl chloride) hydrate was characterized by a single-crystal X-ray diffraction and DFT calculations. This compound crystallizes in monoclinic space group $P2_1/c$ as a racemate. Asymmetric part of the unit cell consists of two (*R* and *S*) non-equivalent spiro units (Fig. 1). Each unit is built of two morpholine rings joined at the *N*(1) spiro center. The spiro units are linked through the O(W)-H(WA)···Cl(1) hydrogen bond by a water molecule of 3.141(7) Å with *R*-isomer and by an unusual interaction of water with the electron pair of morpholine oxygen atom of the other *S*-isomer. The solvent molecule was refined as a rigid body with partial (20%) occupancy. The total energy, geometry

and natural atomic charges, calculated at the B3LYP/6-311++G(d,p) level of theory, for the studied compound and for *R* and *S* isomers were analyzed.

The low-temperature data collection was performed with an Oxford Diffraction SuperNova single-crystal diffractometer with CuKα radiation. The monoclinic crystal used for the measurements was identified as a non-merohedral twin with the [−1 0 0 0 −1 0 0.233 0 1] twin matrix corresponding to 180° rotation about the [001] reciprocal lattice direction. The Olex2 program was used as an interface for the structure solution (SHELXT), refinement (SHELXL) and for structural analysis [3,4,5]. The crystal structure was refined using the diffraction intensity data written in the HKLF 5 format. The reflections originating from a smaller twin component that did not overlap with those from the larger component were excluded in the refinement process. The component ratio was refined at 0.256(2)/0.744(2).

References

[1] G. P. Moss, *Pure Appl. Chem*., **70** (1998) pp. 143-216.
[2] A. Komasa, E. Bartoszak-Adamska, Z. Dega-Szafran, M. Gołdyn, M. Szafran, *J. Mol. Struct*., **1232** (2021) 130018.
[3] O. V. Dolomanov, L. J. Bourhis, R. J. Gildea, J. A. K. Howard, H. Puschmann, *J. Appl. Cryst*., **42** (2009), pp. 339-341.
[4] G. M. Sheldrick, *Acta Crystallogr. C*, **71** (2015), pp. 3-8.
[5] G. M. Sheldrick, *Acta Crystallogr. A*, **71** (2015), pp. 3-8.

A-15

STRUKTURA KRYSTALICZNA NOWYCH SIARCZANÓW 2,4,6-TRIMETYLOPIRYDYNIOWYCH

Tamara J. Bednarchuk, V. Kinzhybalo, A. Pietraszko

Instytut Niskich Temperatur i Badań Strukturalnych, Polska Akademia Nauk, ul. Okólna 2, 50-422 Wrocław

Kontynuując badania nad kompleksami amin z anionem siarczanowym(VI) [1-3] zostały otrzymane trzy nowe organiczne kompleksy jonowe w postaci monokrystalicznej. Na posterze zostaną zaprezentowane wyniki badań strukturalnych dla nowych związków, otrzymanych na drodze reakcji 2,4,6-trimetylopirydyny z kwasem siarkowym(VI):

- wodorosiarczan 2,4,6-trimetylopirydyniowy ($C_8H_{12}N^+ \cdot HSO_4^-$) krystalizuje w układzie rombowym w typie grup przestrzennych $Pna2_1$, a jednostka asymetryczna (Rys.1a) złożona jest z jednego kationu organicznego i jednego anionu HSO_4^-;
- siarczan 2,4,6-trimetylopirydyniowy ($2C_8H_{12}N^+ \cdot SO_4^{2-} \cdot 3H_2O$) otrzymano w postaci trihydratu. Krystalizuje on w typie grup przestrzennych $P\bar{1}$ układu trójskośnego, a niezależną część komórki elementarnej (Rys.1b) stanowią dwa kationy sprotonowanej aminy, jeden nieuporządkowany anion SO_4^{2-} oraz trzy nieuporządkowane molekuły wody krystalizacyjnej;
- wodorosiarczan siarczan 2,4,6-trimetylopirydyniowy ($4C_8H_{12}N^+ \cdot 2HSO_4^- \cdot SO_4^{2-}$) krystalizuje w układzie jednoskośnym w typie grup przestrzennych *Cc*, a część asymetryczna komórki elementarnej (Rys.1c) zawiera cztery kationy organiczne, jeden anion SO_4^{2-} oraz dwa aniony HSO_4^-.

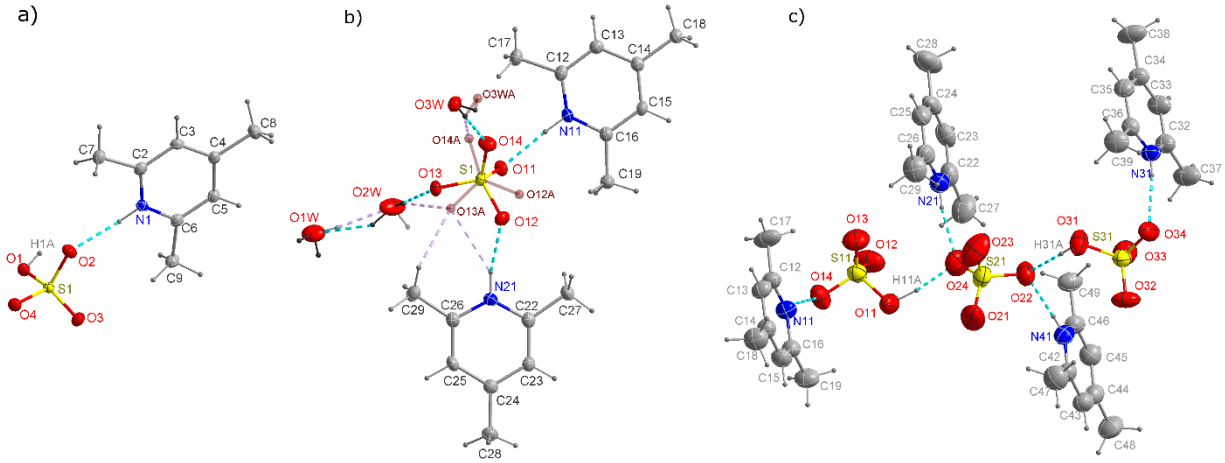

Rysunek 1. Wizualizacja części niezależnej w komórce elementarnej siarczanów 2,4,6-trimetylopirydyniowych.

Literatura

[1] T.J. Bednarchuk, V. Kinzhybalo, E. Markiewicz, B. Hilczer & A. Pietraszko. *J. Solid State Chem*. **258** (2018) 753–761.
[2] T.J. Bednarchuk, D. Kowalska, V. Kinzhybalo & M. Wołcyrz. *Acta Cryst*. **B73** (2017) 337–346.
[3] T.J. Bednarchuk, V. Kinzhybalo & A. Pietraszko. *Acta Cryst*. **C72** (2016) 882–889.

A-16

INFLUENCE ON THE STRUCTURE AND CYTOTOXIC ACTIVITY OF MONO- AND DI-SUBSTITUTED ETHYL ACETATE OF 1-HYDROXY-5-METHYL-7-PHENYLPYRIDO[3,4-*d*]PYRIDAZIN-4(3*H*)-ONE

Anna Wojcicka[1], Lilianna Becan[1], Anna Pyra[2], Nina Rembiałkowska[3], Iwona Bryndal[1]

[1]Department of Pharmaceutical Technology, Faculty of Pharmacy, Wroclaw Medical University, Borowska 211A, 50-556 Wrocław
[2]Faculty of Chemistry, University of Wroclaw, Joliot-Curie Street 14, 50-383 Wrocław
[3]Department of Molecular and Cellular Biology, Faculty of Pharmacy, Wroclaw Medical University, Borowska 211A, 50-556 Wrocław

Considerable attention has been focused on the study on design and synthesis of pyridopyridazines derived from phthalazines which contain a nitrogen atom in the benzene ring. There are eight structural isomers of the bicyclic ring system containing a pyridine moiety condensed with a pyridazine nucleus. Biological investigations have shown a broad spectrum of activity, especially for [3,4-*d*] and [2,3-*d*]pyridopyridazine isomers [1]. Pyrido[3,4-*d*]pyridazine derivatives have been evaluated as antitumor and analgesic agents [2,3]. Antibacterial [4] and antiviral [5] activities of these compounds have been also found. In addition, 7-phenylpyrido[3,4-*d*]pyridazine derivatives exhibit a diuretic activity [6].

The various biological properties of pyrido[3,4-*d*]pyridazines are the main reason for the preparation of new compounds containing this scaffold. On the other hand, a search of the Cambridge Structural Database [7] for the combined pyrido [3,4-*d*]pyridazine-1,4-dione skeleton showed that only two related structures had been structurally determined previously, catena-(bis(μ^3-pyridine-3,4-dicarboxylhydrazidato-N,O,O)-lead(II)) (WUFFUZ) [8] and catena-[(μ-pyrido[3,4-*d*]pyridazine-1,4-diolato)-zinc] (MUJNUD) [9].

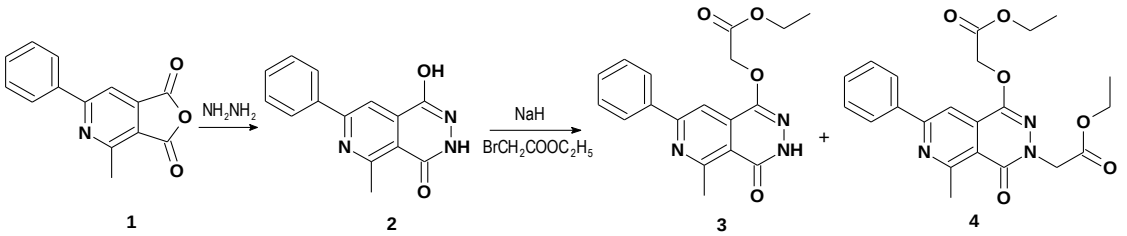

Scheme 1. The synthetic routes to compounds **2**-**4**.

The aim of this work was to synthesize and structural characterized the new pyrido[3,4-*d*]pyridazine derivatives with potential biological activity. Condensation of previously prepared [10] 4-methyl-6-phenyl-1*H*-pyrrolo[3,4-*c*]pyridine-1,3-dione (**1**) with hydrazine monohydrate resulted in rearrangement to 5-methyl-7-phenyl-pyrido[3,4-*d*]pyridazine derivative **2** which may exist in four tautomeric forms. The obtained compound **2** was alkylated with ethyl bromoacetate according to the method described in our previous article [10]. To obtain mono- (**3**) and di-substituted 5-methyl-7-

phenylpyridine[3,4-*d*]pyridazine derivatives (**4**), compound **2** was converted to the sodium salt by reaction with sodium hydride in anhydrous DMF and then reacted with ethyl bromoacetate (Scheme 1). Thus, an N- or O-substituted derivative may result from an alkylation reaction with the compound **2**. Crystals of compounds **2**, **3** and **4** suitable for single-crystal X-ray diffraction analysis were grown by slow evaporation of solutions in DMF or DMSO, at ambient temperature and in the presence of air. The collected X-ray data revealed that the molecule of **2** existed in 1-hydroxy-4-keto form (Fig. 1) and O-alkylation occurred before N-alkylation.

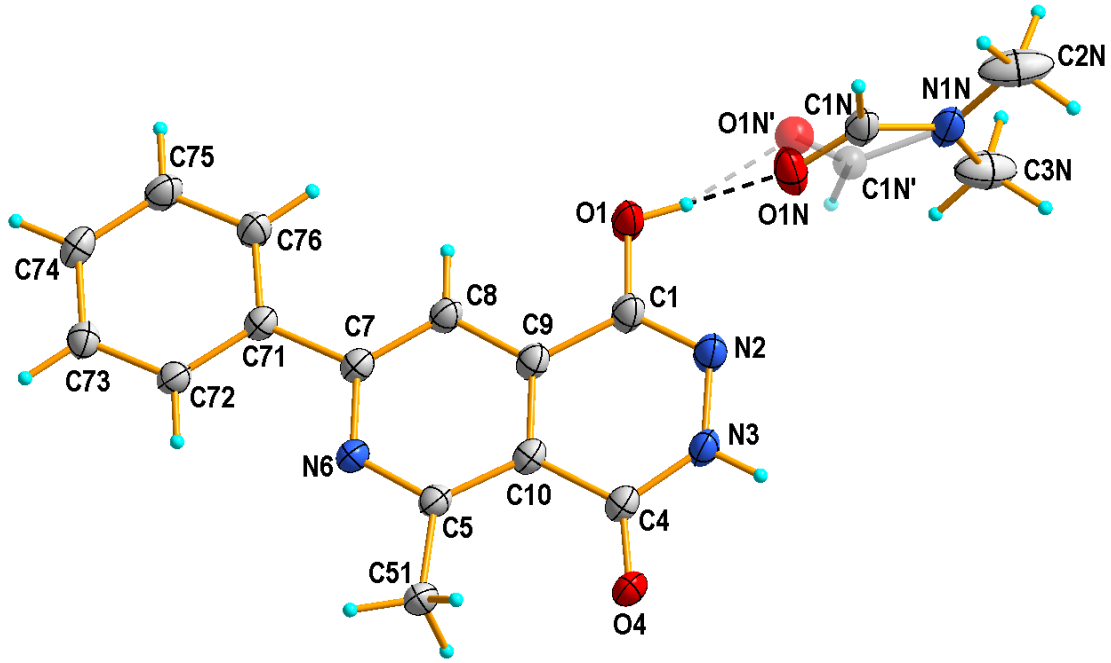

Fig. 1. View of the asymmetric unit of **2**, showing the atom-numbering scheme and displacement ellipsoids drawn at the 50% probability level. Dashed lines represent hydrogen bonds. Transparent spheres and light grey bonds represent the disordered part of solvent with lower site-occupation factors.

References

[1] A. Wojcicka, A. Nowicka-Zuchowska, *Mini-Rev. Org. Chem.*, **16** (2019) 3.
[2] K.A. El-Sharkawy, R.A. Ibrahim, *Eur. Chem. Bull.*, **2** (2013) 530.
[3] H. Śladowska, J. Stanasiuk, M. Sieklucka-Dziuba, T. Saran, Z. Kleinrok, *Il Farmaco*, **53** (1998) 475.
[4] A-Z. Elassar, *Indian J. Chem*., **43B** (2004) 1314.
[5] J.G. Cumming, X. Lin, H. Liu, I. Najera, Z. Qiu, V. Sandrin, G. Tang, G. Wu, (2018) US WO 2018/001948 Al.
[6] K. Omura, N. Tada, M. Tomimoto, Y. Usui, Y. Oka, S. Yurugi, *Chem. Pharm. Bull.*, (1976) 24 (11), 2699-2710.
[7] C.R. Groom, I.J. Bruno, M.P. Lightfoot, S.C. Ward, *Acta Cryst.* **B72** (2016) 171.
[8] J.-H. Yu, Y.-C. Zhu, D Wu, Y. Yu, Q. Hou, J.-Q. Xu, *Dalton Trans.*, (2009) 8248.
[9] Y. Wu, Y.-H. Lu, S.-F. Ping, Z.-Y. Jiang, *Spectrochim.Acta*, Part A, **233** (2020) 118232.
[10] E. Wagner, A. Wójcicka, I. Bryndal, T. Lis, *Pol. J. Chem*., (2009), 83, 207-215.

A-17

STRUCTURAL CHANGES DURING DEHYDRATION OF AMINOPYRIDINIUM HYPODIPHOSPHATES

Daria Budzikur[1], Katarzyna Ślepokura[1] and Vasyl Kinzhybalo[2]

[1]Uniwersity of Wrocław, Faculty of Chemistry, 14. F. Joliot-Curie, 50-383 Wrocław
[2]Institute of Low Temperature and Structure Research, Polish Academy of Sciences, 2 Okólna, 50-422 Wrocław, Poland

In recent years, there has been an increasing amount of research on organic-inorganic hybrids, e.g. salts of organic hypodiphosphates [1-3]. Hypodiphosphate anions and acid molecules (containing six oxygen atoms acting as hydrogen bond donor and/or acceptor) tend to form different types of inorganic substructures stabilized by hydrogen bonding. It has been noted that there are several types of multidimensional inorganic substructures typical for hypodiphosphates (e.g. chains, layers or 3D networks) [4].

Dehydration processes are particularly important in the material chemistry and pharmaceutical industry. The state of knowledge on dehydration for organic-inorganic hybrids is still scarce. In particular, the structural changes during these processes for hydrated organic hypodiphosphates are not yet understood in detail. In 2018 it was observed that while dehydration of a tetra-*n*-butylammonium hypodiphosphate a change in the conformation of the anion occurs which is accompanied by rearrangement of hydrogen bonding network [2]. Therefore, the aim of our work was to obtain aminopyridinium hypodiphosphate hydrates and to analyze the structural changes in dehydration of the compounds.

Three hydrated hypodiphosphate salts containing 2-, 3- and 4-aminopirydinium cations will be presented (Fig. 1). Variable temperature microscopy studies have been performed during which destructive dehydrations were observed. Anhydrous aminopyridinium hypodiphosphates with rearranged crystal structures were obtained. Structural changes that took place during the dehydration were analyzed.

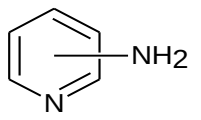

2-, 3-, 4-aminopyridine

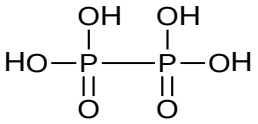

hypodiphosphoric acid

1 – $(2\text{-apH})_2(H_2P_2O_6)\cdot 2H_2O$
2 – $(2\text{-apH})_2(H_2P_2O_6)$
3 – $(3\text{-apH})_2(H_2P_2O_6)\cdot(3\text{-ap})\cdot 2H_2O$
4 – $(3\text{-apH})_2(H_2P_2O_6)\cdot(3\text{-ap})$
5 – $(4\text{-apH})_2(H_2P_2O_6)\cdot(H_4P_2O_6)\cdot 2H_2O$
6 – $(4\text{-apH})(H_3P_2O_6)$

Fig. 1. 2-, 3-, 4-Aminopyridines (ap) and hypodiphosphoric acid (neutral forms) used for preparation of (**1**)–(**6**).

Loss of water from (**1**) takes place above 100 °C. The structure is significantly changed by dehydration, however, the inorganic fragment remains one dimensional, although some anions reorient.

Dehydration of (**3**) does not lead to a substantial reorganization of the structure packing but is followed by a rearrangement of crystal system from monoclinic to orthorhombic and, interestingly, from centrosymmetric structure to polar.

Dehydration of (**5**) is observed at a relatively low temperature (64 °C) and gives rise to a significant reorganization of the structure (Fig. 2). Anionic network changes from one-dimensional to three-dimensional.

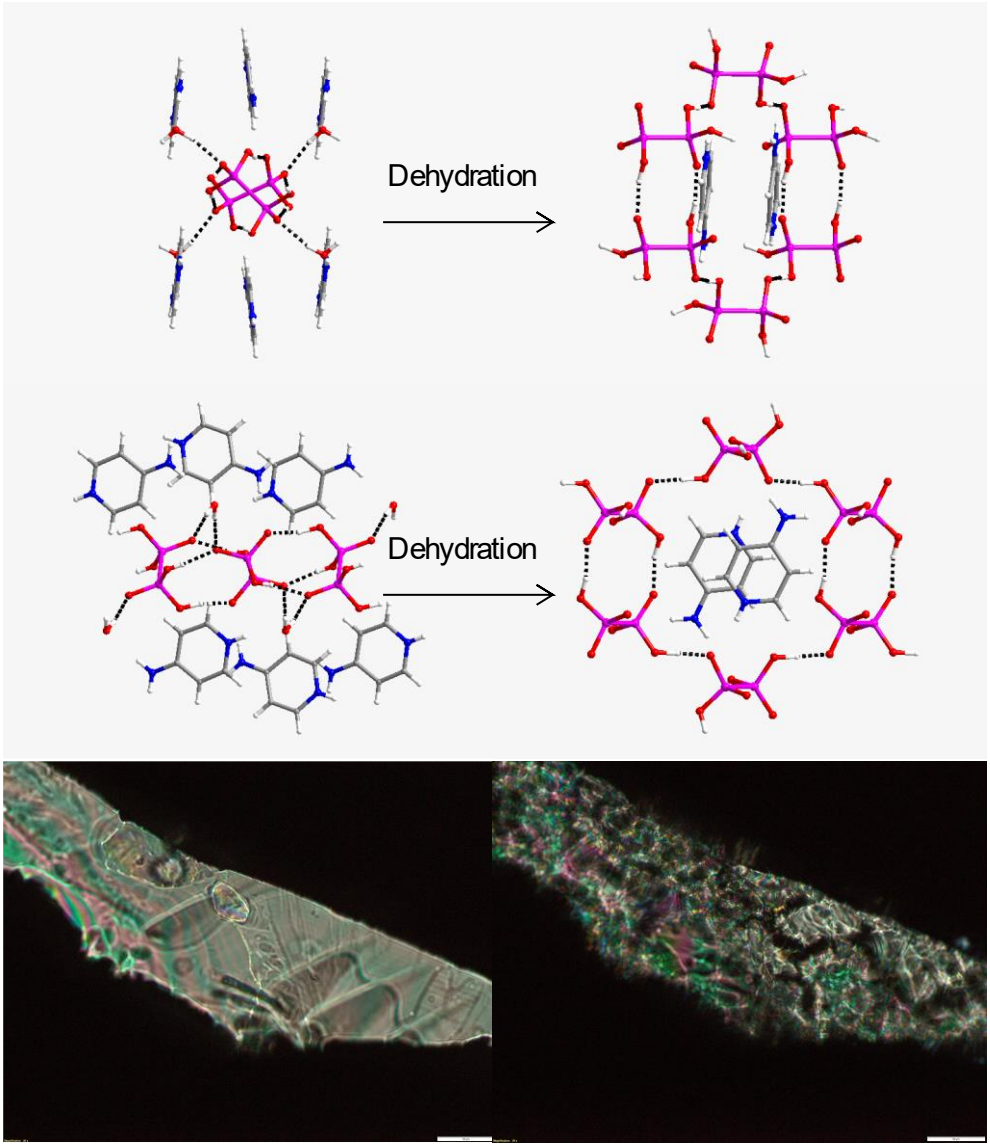

Fig. 2. Structural changes in the dehydration process of (**5**) observed by X-ray analyses (different views) and variable temperature microscopy.

Literature

[1] M. Otręba, D. Budzikur, Ł. Górecki, K. Ślepokura, *Acta Cryst.*, **C74** (2018) 571–583.
[2] M. Emami, K. Ślepokura, M. Trzebiatowska, N. Noshiranzadeh, V. Kinzhybalo, *CrystEngComm*, **20** (2018) 5209–5219.
[3] D. Budzikur, P. Szklarz, V. Kinzhybalo, K. Ślepokura, *Acta Cryst.*, **B76** (2020) 939-947.
[4] V. Kinzhybalo, M. Otręba, K. Ślepokura, T. Lis, *Wiad. Chem.*, **75** (2021) 423-466.

A-18

DISTORTIONS OF INORGANIC POLYHEDRA IN CHLORIDOBISMUTHATES(III)

Maciej Bujak

Faculty of Chemistry, University of Opole, Oleska 48, 45-052 Opole, Poland
e-mail: mbujak@uni.opole.pl

The inorganic substructures of hybrid inorganic-organic chloridobismuthates(III) with organic cations are mainly based on relatively simple $[BiCl_6]^{3-}$ octahedra. These polyhedra can exist as isolated units, but very often they are joined together by corners, edges or faces, and, as a consequence, form more complicated isolated and polymeric architectures. Such a behavior, *i.e.* formation of various inorganic substructures, is associated with the other relevant structural issue related to this group of hybrids - distortions of inorganic polyhedra.

The poster will present the results on crystallization and single crystal X-ray diffraction studies of four chloridobismuthates(III) showing different inorganic substructures (Fig. 1), but at the same time possessing, in pairs, the same: doubly-*N*,*N*-dimethylethane-1,2-diammonium (DMED) and singly-protonated *N*,*N*,*N*',*N*'-tetramethylguanidinium (TMG) organic cations: $DMED_3[BiCl_6]_2$, $DMED[BiCl_5]$, $TMG_3[Bi_2Cl_9]$ and $TMG[BiCl_4]$. The crystals have been studied in the context of the particular inorganic substructure formation as well as main factors that cause the distortions of single inorganic $[BiCl_6]^{3-}$ units from the ideal octahedral geometry [1]. Additionally, the experimental studies have been supported by the analysis of the data retrieved from the Cambridge Structural Database [2,3].

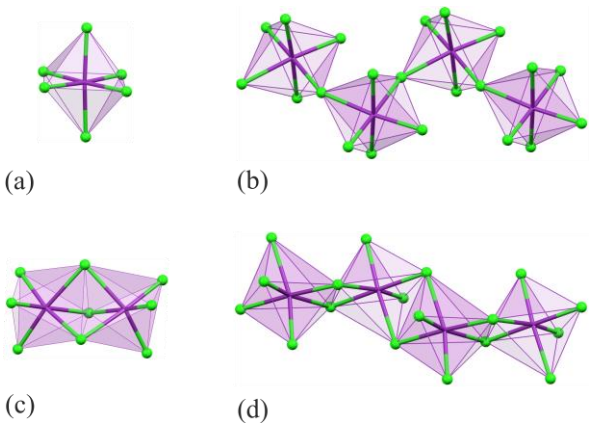

Fig. 1. The inorganic substructures, in a polyhedral representation, composed of: (a) isolated $[BiCl_6]^{3-}$ octahedra in $DMED_3[BiCl_6]_2$, (b) chains $[\{BiCl_5\}_n]^{2n-}$ in $DMED[BiCl_5]$, (c) bioctahedral $[Bi_2Cl_9]^{3-}$ units in $TMG_3[Bi_2Cl_9]$ and (d) chains $[\{BiCl_4\}_n]^{n-}$ in $TMG[BiCl_4]$ [1,4].

References

[1] M. Bujak, *Acta Cryst. B.*, accepted.
[2] C. R. Groom, I. J. Bruno, M. P. Lightfoot, S. C. Ward, *Acta Cryst. B.*, **72** (2016) 171.
[3] I. J. Bruno, J. C. Cole, P. R. Edgington, M. Kessler, C. F. Macrae, P. McCabe, J. Pearson, R. Taylor, *Acta Cryst. B.*, **58** (2002) 389.
[4] C. F. Macrae, I. Sovago, S. J. Cottrell, P. T. A. Galek, P. McCabe, E. Pidcock, M. Platings, G. P. Shields, J. S. Stevens, M. Towler, P. A. Wood, *J. Appl. Cryst.*, **53** (2020) 226.

A-19

HOST-GUEST COMPLEXES OF CARBOXYLATED PILLAR[5]ARENE WITH ANTIMICROBIAL DRUG PENTAMIDINE

Helena Butkiewicz, Sandra Kosiorek, Volodymyr Sashuk, Oksana Danylyuk

Institute of Physical Chemistry Polish Academy of Sciences, Kasprzaka 44/52, 01-224 Warsaw, Poland

Pillar[5]arenes (PA5), first reported by Ogoshi in 2008 [1], are highly symmetrical pillar-shaped compounds, composed of hydroquinone units linked by methylene bridges at the para-positions. Their rigid hydrophobic, electron-rich cavity makes them great candidates as host molecules for various electron-deficient guest or other neutral molecules. The introduction of functional groups at both rims can improve the solubility of these macrocycles in water, which is an environmentally friendly solvent [2].

Water-soluble pillar[5]arene substitued by carboxylic acid groups (CPA5) is in the centre of interest in the studies of its ability to complex different biologically important molecules. Under basic conditions it acts as receptors for cations in water. Moreover, these carboxyl groups are located at the terminal positions of flexible aliphatic chains, so they can adjust to the size and shape of guest molecules.

Here we want to present X-ray structures of the carboxylic acid substituted pillar[5]arene in the form of its host–guest complexes with pentamidine. Chosen guest molecule is biologically important compound used in the management and treatment of African trypanosomiasis, leishmaniasis and Pneumocystis carnini pneumonia [3]. Under physiological conditions pentamidine is protonated to form stable cations. The formation of supramolecular complexes between CPA5 and pentamidine drug may prevent side effects and potentially enable the obtaining of new transport and drug release systems under different conditions.

References

[1] T Ogoshi, S. Kanai, S. Fujinami, T. Yamagishi, Y. Nakamoto; *J. Am. Chem. Soc*., **130** (2008) 5022.
[2] T Ogoshi, M Hashizume, T Yamagishi, Y Nakamoto, *ChemComm* **21** (2010) 3708.
[3] T Srikrishnan, N.C. De, A.S. Alam, *J Chem Crystallogr* **34** (2004) 813.

A-20

WEAK INTERMOLECULAR INTERACTIONS IN THE COMPLEXES OF HALOFORMS WITH FLUORENONOPHANE

V. V. Dyakonenko[a], S. V. Shishkina[a], A. Yu. Lyapunov[b], T.Yu. Bogashchenko[b], T.I. Kirichenko[b]

[a] SSI "Institute for Single Crystals" National Academy of Sciences of Ukraine, Nauki Ave 60, Kharkiv 61001, Ukraine
[b] A. V. Bogatsky Physico-Chemical Institute, National Academy of Science of Ukraine, 86 Lustdorfskaya doroga, Odessa, Ukraine
E-mail: vika@xray.isc.kharkov.com

It was recognized that weak intermolecular interactions influence a crystal structure of many biomolecules and molecular complexes. This especially concerns non-conventional hydrogen bonds like C-H…O or C-H…π, stacking interactions etc. Recently, great attention was paid to halogen bonding as an important contributor to the stability of supramolecular structures, crystals, protein-ligand complexes, as well as other chemical and biomolecular structures. The importance of C–Halogen…π interactions is now recognized, and many properties (magnitude directionality and origin of the C–Halogen…π interaction) have been clarified with high level computational methods based on theoretical chemistry. Despite the progress, additional experimental data on C–Halogen…π interactions are necessary because halogen bonding competes with stronger noncovalent interactions, including the hydrophobic interaction, hydrogen bond, and electrostatic interactions.

In this work we have studied the molecular and crystal structures of complexes of the fluorenonophane with the chloroform (3Cl) and bromoform (3Br). The fluorenonophane (2,6,8,12-tetraoxa-4,10(1,4)-dibenza-1,7(2,7)-diflurenacyldo-decaphane-1,7-dione) is representing a new macrocyclic receptor for polar organic molecules. It was demonstrated that such types of hosts have the hollow intramolecular cavity, limited by two fluorenone and two phenylene fragments. Different organic molecules of both aromatic and heteroaromatic type can easily come into this cavity forming stable molecular complexes.

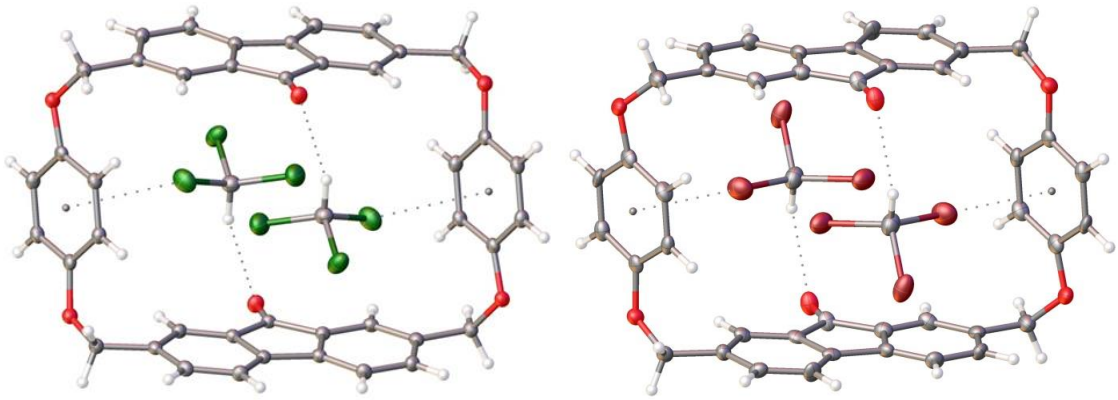

3Cl 3Br

A-20

In these complexes the molecules of chloroform/bromoform occupy boundary part of macrocyclic cavity and located over fluorenone fragments. This mutual arrangement of molecules is stabilized by weak halogen-π and C-H…O interactions. Using quantum chemical calculations we evaluated the energy of the true halogen bonds in these complexes, and it was -3.87 kcal/mol and -4.94 kcal/mol for 3Cl and 3Br respectively.

A-21

PHOTOREACTIVE CRYSTAL OF COPPER(I) COMPLEX SALT WITH CINNAMALDEHYDE DERIVATIVE

Emilia Ganczar[a], Vasyl Kinzhybalo[b], Agata Białońska[a]

[a] *Department of Chemistry, University of Wrocław, 14. F. Joliot-Curie, 50-383 Wrocław, Poland*
[b] *Institute of Low Temperature and Structure Research, Polish Academy of Sciences, 50-422 Wrocław, Poland*

Design of photoactive systems and control of the reactions in the solid state are one of the main goals of crystal engineering.[1] The solid state [2+2] reaction is a well-studied reaction in both organic and metalorganic chemistry. Various approaches related to formation of intermolecular interactions like halogen or hydrogen bonds, π···π stacking and coordination bonds are applied to control the packing of C=C bonds, so they are suitable for the reaction in the solid state.[2] Schmidt and Cohen postulated geometrical conditions that must be fulfilled to carry out the [2+2] photoreaction, namely reactive centers have to be aligned parallel to each other and separated by less than 4.2 Å.[3-4] Other factors that can decide about the success of the reaction are: the geometric parameters (the C=C···C angle formed by the two C=C bonds, the torsion C=C···C=C angle, the angle between planes of >C=C< fragments, the angle between a plane of C atoms of the two C=C bonds and the >C=C< fragment), available free surrounding space around the reactive center which enables the move in the crystal lattice, type of intermolecular interactions and structure of the molecule (types and positions of substituents). [6-7] Cinnamic acid and its derivatives are one of the most frequently examined compounds in the photochemical [2+2] dimerization reaction. Inspired by the ability of derivatives of cinnamic acid to undergo reaction induced by light we extended the studies on cinnamaldehyde derivative in photochemical reaction.

On the poster, structural studies of the copper(I) coordination compound with *N*-[3-(4-(chlorophenyl)-2-propen-1-ylidene]-4*H*-1,2,4-triazol-4-amine (pClcinatrz) (Fig.1) will be presented. The x-shaped binuclear cationic units in the obtained compound are preserved, and directional interactions orient the aliphatic chain for the regiospecific photoinduced reaction. The distance between the nearest C=C centers of neighboring ligands was found to be smaller than 4.0 Å which meets the geometric criteria described by Schmidt's and Cohen. Photo-induced changes in the crystal were observed by X-ray methods.

A-21

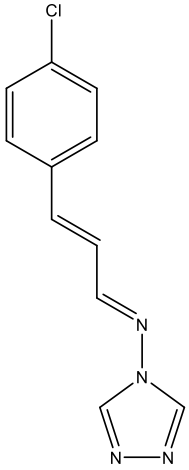

Fig.1. *N*-[3-(4-(chlorophenyl)-2-propen-1-ylidene]-4*H*-1,2,4-triazol-4-amine (pClcinatrz).

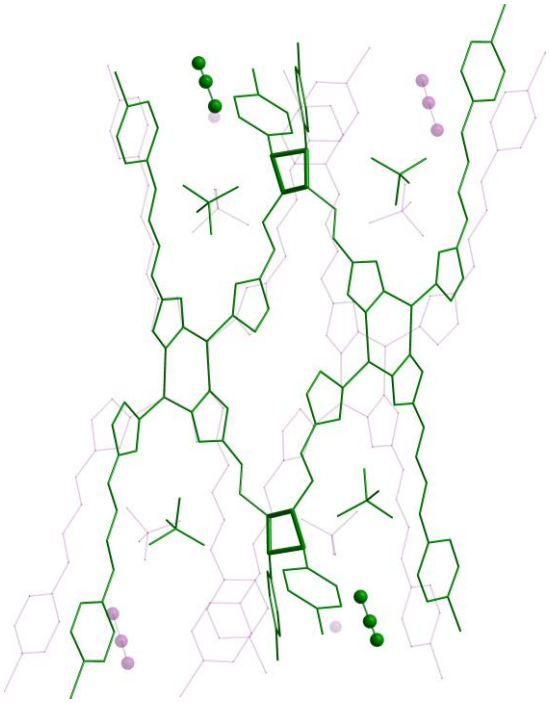

Fig.2. The imposition of the structure before (purple color) and after (green color) radiation of the crystal. The hydrogen atoms are omitted for the clarity of the figure.

Literature

[1] G. R. Desiraju, *Crystal Engineering*, Elsevier, Amsterdam, **54** (1989) 85.
[2] K. Biradha, R. Santra, *Chem. Soc. Rev.*, **42** (2013) 950.
[3] M. D. Cohen, G. M. J. Schmidt, *J. Chem. Soc.*, (1964) 1996.
[4] G. M. J. Schmidt, *Pure Appl. Chem.*, **27(4)** (1971), 647.
[5] K. Saigo, M. Hasegawa, *Reactivity in Molecular Crystals*, VCH, Tokyo (1993) 203.
[6] E. Boldyreva, *Solid State Ion.*, **101–103** (1997) 843.
[7] I. Turowska-Tyrk, J. Bąkowicz, *Wiadomości chemiczne*, **68(5-6)** (2014) 382.

A-22

COMPLEXES OF SILVER(I) NITRITE WITH 3-CYANOPYRIDINE

Karolina Gutmańska*, Anna Ciborska and Anna Dołęga

Department of Inorganic Chemistry, Faculty of Chemistry, Gdansk University of Technology, G. Narutowicza 11/12, 80-233 Gdańsk,
e-mail: s171467@student.pg.edu.pl

Cyanopyridines are pyridine derivatives consisting of a pyridine ring with a nitrile group attached to it. There are three isomers with the -CN group located in the 2, 3 and 4 positions. The molecules are flat with a characteristic ring deformation resulting from the presence of a lone pair on the nitrogen atom within the ring. Due to the very weak basicity, the ability of the nitrile group to donate an electron pair is less than that of the pyridine nitrogen atom. [1] Therefore in most complexes with metal ions cyanopyridines act as monodentate ligands that coordinate metal ions through the ring nitrogen atom. Structures with bridging cyanopyridine molecules are very rare, as far as we know there are approximately ten complexes characterized structurally including three cyanopyridine isomers and all metal ions. [1-7]

Here we report the crystal and molecular structures of two different complexes obtained as a result of the reaction of silver(I) nitrite with 3-cyanopyridine: molecular complex **1** and polymeric complex **2 (**Scheme I). The complexes crystallize in pure form from the reaction solutions featuring different molar ratio of silver nitrite and 3-cyanopyridine.

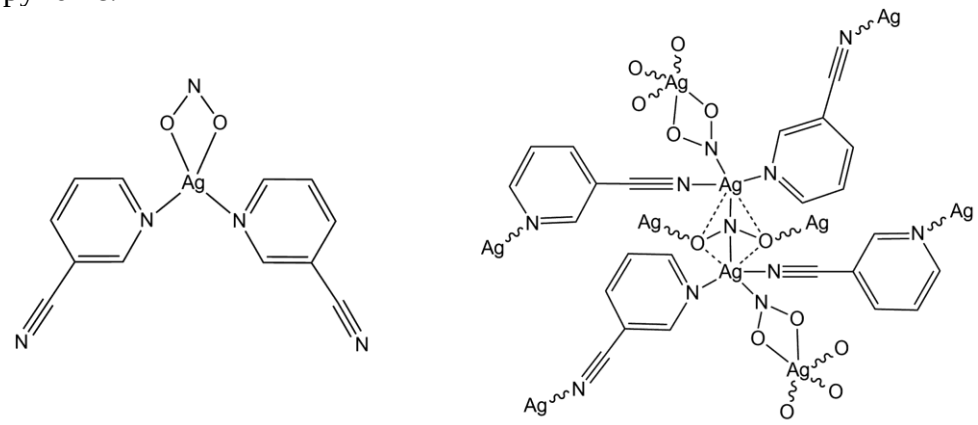

Scheme. I. Formulas of complexes **1** and **2**.

The molecular complex **1** (Fig. 1, left side) crystallizes in a $P2_1/n$ space group of a monoclinic system with a = 3.76176(12) Å, b = 23.6955(6) Å, c = 14.2655(4) Å, β = 96,174°. The silver atom is characterized by a coordination number equal to 4. The geometric parameter τ_4 characterizing the geometry of complex compounds with the coordination number, C.N. = 4 is 0.48 [8], which indicates coordination geometry of silver(I) intermediate between tetrahedral and planar square. The central Ag1 atom is bonded to two nitrogen atoms of two 3-cyanopyridine rings with slightly different bond lengths Ag1-N2 2.302Å and Ag1-N4 2.294Å and the angle N4-Ag1-N2112.87°. The

nitrite anion in complex **1** chelates the silver ion but the coordination is asymmetric: the Ag1–O1 and Ag1–O2 bond lengths are 2.343 Å and 2.628 Å, respectively, and form the narrow angle O1-Ag1-O2 of 49.93°. Molecules of complex **1** aggregate via π-stacking interactions with the formation of piles of molecules parallel to crystallographic *a* axis; these intermolecular forces and the resulting crystal packing will be further discussed in a poster.

The rare three-dimensional coordination polymer **2**, in which cyanopyridine serves as bridging ligand (Fig. 1, right side of the figure) crystallizes in a triclinic system, space group *P*-1 with a = 7.2751(9) Å, b = 8.0268(9) Å, c = 8.5796(8) Å, α = 103.035(8)°, β = 90.919(9)°, γ = 113.904(8)°. It features two silver atoms Ag1 and Ag2 with a different coordination numbers and obviously different coordination geometries. Atom Ag1 is characterized by coordination number equal 4 (C.N. = 4); it is coordinated by atoms N1, N2 derived from the nitrite and by N3, N4 derived from the 3-cyanopyridine with N3 being a pyridine nitrogen and N4 belonging to nitrile group. Ag2 atom, which is surrounded exclusively by oxygen atoms of nitrite anions is disordered over two positions with lengths: Ag2 - O1 2,460/2,520Å, Ag2 - O2 2.324/2.474 Å and Ag2 - O3 2.661 Å (C.N. = 5). The O3 atom is further disordered between two equally occupied positions. The details of these complex structure will be discussed in a poster.

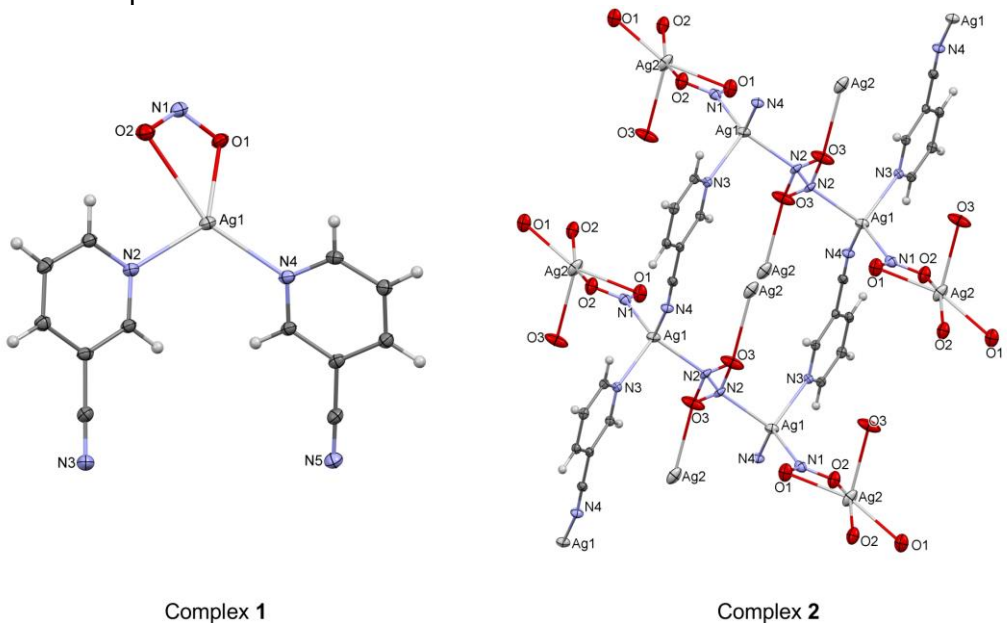

Fig. 1. Molecular structures of the complexes **1** and **2**.

References

[1] M. K. Broderick, C. Yang, R. D. Pike, A. Nicholas, D. May, H. H. Patterson,. *Polyhedron*, **114** (2016) 333.
[2] H. Leung, W. Lai, I. D. Williams, *J. Organomet. Chem*. **604** (2000) 197.
[3] A. J. Blake, N. R. Champness, J. E. B.Nicolson, C. Wilson, *Acta Crystallogr., Sect.C: Cryst. Struct. Commun*. **C57** (2001) 1290.
[4] X.-L. Zhao, T. C. W. Mak, *Dalton Trans.* (2004) 3212.
[5] A. Bacchi, G. Cantoni, P. Pelagatti, S. Rizzato, *J. Organomet. Chem*. **714** (2012) 81.
[6] T. Hu, L. Zhao, T. C. W. Mak, *Organometallics* **31** (2012) 7539.
[7] A. Jochim, I. Jess, C. Näther, *Z. Naturforsch., B: Chem. Sci.* **75** (2020) 163.
[8] W. Addison, N. T. Rao, J. Reedijk, J. van Rijn, G. C. Verschoor, *J. Chem. Soc. Dalton Trans*. (1984) 1349.

A-23

X-RAY CRYSTAL STRUCTURE OF TRIETHYLAMMONIUM 3-[(R,Ar,Het)(1-ETHYL-4-HYDROXY-2,2-DIOXIDO-1*H*-2,1-BENZOTHIAZIN-3-YL)METHYL]-1-ETHYL-1*H*-2,1-BENZO-THIAZIN-5-OLATE AND 3-((4-HYDROXY-2,2-DIOXIDO-BENZO[e][1,2]OXATHIIN-3-YL)(R,Ar,Het)METHYL) BENZO[e][1,2]OXATHIIN-4-OLATE 2,2-DIOXIDES

Ewa Wieczorek-Dziurla,[1] Leonid A. Shemchuk,[2] Dmitry A. Lega,[2]
Andrzej Gzella[1]

[1] Department of Organic Chemistry, Poznan University of Medical Sciences, 6 Grunwaldzka St., Poznań 60-780, Poland; e-mail: akgzella@ump.edu.pl
[2] National University of Pharmacy, 53 Pushkinska St., Kharkiv 61002, Ukraine; e-mail: leonid.shemchuk@gmail.com

Stable triethylammonium salts of 3-[(4-hydroxy-1-ethyl-2,2-dioxido-1*H*-2,1-benzothiazin-3-yl)(aryl)methyl]-1-ethyl-1*H*-2,1-benzothiazin-5-olate 2,2-dioxides and 3-((4-hydroxy-2,2-dioxidobenzo[*e*][1,2]oxathiin-3-yl)(aryl)methyl)benzo[e][1,2]oxa-thiin-4-olate 2,2-dioxides have been appeared to be a new result of interaction between benzaldehydes, ethyl cyanoacetate and sulfoketones, namely 1-ethyl-1*H*-benzo[*c*]-[1,2]thiazin-4(3H)-one 2,2-dioxide/benzo[*e*][1,2]oxathiin-4(3*H*)-one 2,2-dioxide, respectively. Subsequently, we have found the way of their purposeful synthesis by interaction of above mentioned sulfoketones with aldehydes in the presence of triethylamine. Thus, a series of corresponding (het)arylmethyl derivatives was obtained. The present study was focused on the elucidation of the mutual arrangement of cation and anion molecules of triethylammonium salts of 3-[(R,Ar,Het))(1-ethyl-4-hydroxy-2,2-dioxido-1*H*-2,1-benzothiazin-3-yl)methyl]-1-ethyl-1*H*-2,1-benzothiazin-4-olate and 3-((4-hydroxy-2,2-dioxidobenzo[e][1,2]oxathiin-3-yl)(R,Ar,Het)ethyl)benzo[e][1,2]oxathiin-4-olate 2,2-dioxides in the crystalline phase.

The performed structural studies reveal that in the crystalline state cation and anion of triethylammonium 3-[(R,Ar,Het[1]))(1-ethyl-4-hydroxy-2,2-dioxido-1*H*-2,1-benzo-thiazin-3-yl)methyl]-1-ethyl-1*H*-2,1-benzothiazin-4-olate 2,2-dioxide salt crystals are connected by hydrogen bonds of the N–H··· O type with ammonium nitrogen atom and oxygen atom belonging to one of two sulfonyl groups (Fig. 1, a). In the case of triethylammonium 3-((4-hydroxy-2,2-dioxidobenzo[e][1,2]oxathiin-3-yl)(R,Ar,Het[2])-methyl)benzo[e][1,2]oxathiin-4-olate 2,2-dioxide salt crystals the opposite arrangement is observed. The cation and anion pair is connected by N–H···O hydrogen bond with ammonium nitrogen atom and the oxygen atom of alkoxide group (Fig. 1, b). The formation of two alternative hydrogen bonds is supported by the resonance effect in the group of atoms depicted in Fig. 1, a.

[1] R = isobutyl; Ar = phenyl, p-chlorophenyl, p-nitrophenyl; Het = furan-2-yl, thiol-2-yl
[2] R = isopropyl; Ar = m-chlorophenyl, p-dimethylaminophenyl, p-methoxyphenyl; Het = furan-2-yl

A-23

a) 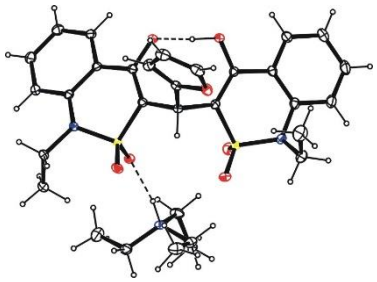	***b)*** 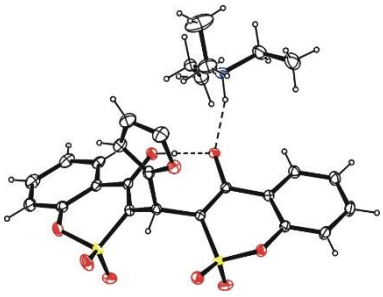
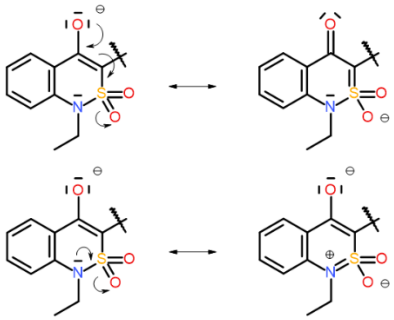	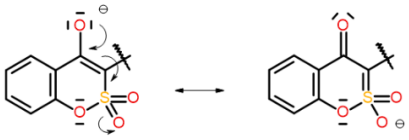
Triethylammonium 3-[(furan-2-yl))(1-ethyl-4-hydroxy- 2,2-dioxido-1*H*-2,1-benzothiazin-3-yl) methyl]-1-ethyl-1*H*-2,1-benzothiazin-5-olate 2,2-dioxide	Triethylammonium 3-((4-hydroxy-2,2-dioxido-benzo[e][1,2]oxathiin-3-yl)(furan-2-yl) methyl) benzo[e][1,2] oxathiin-4-olate 2,2-dioxide

Figure 1. *ORTEP view and mesomerism of two exemplary salts.*

A-24

STRUCTURAL AND SPECTROSCOPIC STUDIES OF NEW MACROCYCLIC ZINC(II) COMPLEXES DIFFERING IN COUNTER ION

Dominika Jankowska[a], Tadeusz M. Muzioł[a], Sławomir Wojtulewski[b] and Magdalena Barwiołek[a]

[a] Faculty of Chemistry, Nicolaus Copernicus University in Toruń, ul. Gagarina 7, 87-100 Toruń, Poland
[b] Faculty of Chemistry, University of Białystok, Ciolkowskiego 1K, 15-245 Białystok, Poland

Zn (II) and Cu (II) complexes with Schiff bases constitute an exciting class of compounds showing luminescence, magnetic and non-linear properties [1]. To obtain thin films of metal complexes, a wet method of spin coating application is used. This allows for obtaining materials with specific and controlled physical properties, such as photochromism, luminescence, electrical conductivity, and magnetic properties. Thin light-emitting films have potential applications in organic OLEDs, televisions, smartphones, displays, or satellite navigation systems [2].

We synthesized zinc complexes with the same Schiff base (H_2L = C_{36} H_{36} N_4 O_2) differing in counter ion. We aimed to elucidate the influence of anion on the structure and optical properties of the complex. This macrocycle offers two binding sites for metal ions. Crystals were grown by slow evaporation of the solvent. The data collection was performed using Oxford Diffraction SuperNova DualSource diffractometer with monochromated Cu Kα X-ray source (λ = 1.54184 Å) for **(1)** and XtaLAB Synergy, Dualflex with HyPix detector, CuKα radiation λ = 1.54184 Å. We obtained two complexes given by the formulae: {$[Zn_2L(CH_3COO)_2)]$·2EtOH **(1)** and $[Zn_2L(NO_3)_2]$·$0.25H_2O$ **(2)**. For these complexes, structural and spectroscopic studies were performed.

First, crystals of $[Zn_2(L)(CH_3COO)_2]$ **(1)** were grown forms a mixture of methanol and chloroform. However, they turned out to be fragile and diffracted poorly. Recrystallization from ethanol resulted in **(1)** changed cell parameters and crystals suitable for diffraction experiments. The structure was solved in the monoclinic P 21/n space group. It showed both coordination sites occupied by zinc(II) cations in a pentacoordinate environment with τ_5 = 0.037 and 0.085 indicating a slightly distorted square pyramid. Its coordination sphere consists of two nitrogen atoms and two oxygen atoms from the macrocycle and one oxygen atoms from the monodentate coordinated acetate anion in the apical position. Both zinc(II) ions are shifted from the basal planes toward the apical oxygen atom, and their basal planes share the common edge. Still, apical vertices point in the opposite directions.

In **(2)** crystallizing in the monoclinic P $2_1/c$ space group, two halves of the macrocycle and two zinc(II) ions in the asymmetric unit are completed by two nitrate anions and partially occupied water molecules. The counter ions are positionally disordered in the Zn2 molecule (0.6:0.4). In the major population, it is monodentate coordinated similarly to the Zn1 molecule. In contrast, in the minority population, bidentate coordination was detected, resulting in a strongly distorted hexacoordinated

environment. τ_5 parameter was 0.010 for Zn1. In contrast, the Zn2 environment is much more distorted due to positional disorder found not only for nitrate anion but also for O34 oxygen atom.

We obtained two Schiff base complexes with zinc(II) *via* different synthetic procedures. They can affect the symmetry and cell parameters as well as the experimental data quality, which are sensitive to the synthesis conditions and used counter ions and solvents. These factors allow for the tailoring of crystal structure and can also influence the properties of the obtained compounds.

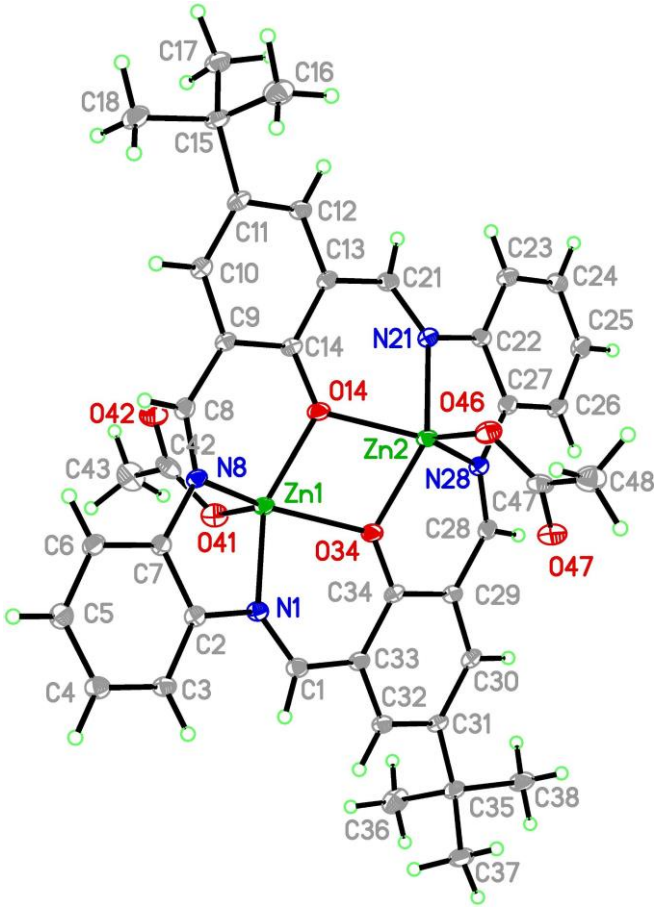

Figure 1. Structure of $[Zn_2(CH_3COO)_2(L)]\cdot 2EtOH$ **(1)** with a numbering scheme and thermal ellipsoids at 30% probability.

References

[1] U. C. Saha, B. Chattopadhyay, K. Dhara, S. K. Mandal, S. Sarkar, A. R. Khuda-Bukhsh, M. Mukherjee, M. Helliwell, P. Chattopadhyay, *Inorg. Chem*., **50** (2011) 1213–1219.
[2] H. Xu, R. Chen, Q. Sun, W. Lai, Q. Su, W. Huang, X. Liu, *Chem. Soc. Rev.*, **43** (2014) 3259.

A-25

ORGANOBORON COMPLEXES WITH (N,O) LIGANDS EXHIBITING *SPIRO* ARCHITECTURE AS POTENTIAL PHOTOSENSITIZERS

Grzegorz Jędrzejczyk[a], Paulina H. Marek[a,b], Agata Blacha-Grzechnik[c], Krzysztof Woźniak[b], Krzysztof Durka[a]

[a] *Faculty of Chemistry, Warsaw University of Technology, Noakowskiego 3, 00-664 Warsaw, Poland*
[b] *Faculty of Chemistry, University of Warsaw, Pasteura 1, 02-093 Warsaw, Poland*
[c] *Faculty of Chemistry, Silesian University of Technology, Strzody 9, 44-100 Gliwice, Poland*

Nowadays, singlet oxygen ($^1O_2$), excited state of naturally occurring triplet oxygen ($^3O_2$), is attracting more attention due its very strong oxidizing properties and therefore has a wide range of potential applications – from the synthesis of fine chemicals, air and water purification to medicine, where its principal application is directed toward photodynamic cancer therapy (PDT). [1, 2] $^1O_2$ can be produced with use of triplet photosensitizers, usually based on heavy atoms e.g. iridium complexes, which upon irradiation can excite to triplet state and interact with $^3O_2$. Due to the cost of aforementioned compounds and relatively high toxicity, their applications are limited. However, heavy atom-free photosensitizers must facilitate different mechanism of triplet state generation, which is not fully investigated and may differ depending on the structure of the molecule. [3]

Our attention was drawn to the *spiro*-type organoboron complexes with (N,O) ligands which, according to our initial studies, exhibit previously overlooked photocatalytic properties and can generate singlet oxygen with satisfactory yields. In my research I have focused on complexes encompassing SO_2 and P(O)Ph groups in boracyclic moiety and various (N,O) ligands. [4] Herein, I present structural analysis of selected complexes complemented by theoretical calculations (TD-DFT) aimed at understanding of role of ligand and type of organoboron moiety in generation of triplet excited states. Understanding structure-properties relationship is crucial in rational design of future photosensitizers.

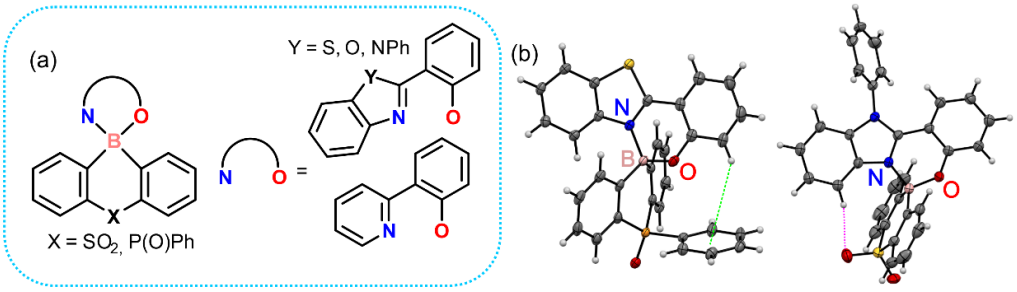

Fig 1. Scheme of analyzed complexes (a) and examples of analyzed structures (b).

References

[1] B. Carpenter, *et al.*, *Molecules*, **20** (2015) 10604–10621.
[2] P. Agostinis, *et al.*, *CA: A Cancer J. Clin.*, **61** (2011) 250–281.
[3] T. N. Singh-Rachford, *et al.*, *J. Am. Chem. Soc.*, **130** (2008) 16164–16165.
[4] M. Urban, K. Durka, P. Górka, G. Wiosna-Sałyga, K. Nawara, P. Jankowski, S. Luliński, *Dalton Trans.*, **48** (2019) 8642–8663.

A-26

STRUCTURAL STUDIES OF Fe (III) COMPLEXES OF N_2O_2 LIGANDS MIMICKING CATECHOL DIOXYGENASE

Karolina Kałduńska, Magdalena Barwiołek, Anna Kozakiewicz i Andrzej Wojtczak

Faculty of Chemistry, Nicolaus Copernicus University in Toruń, 87-100 Toruń, Poland

1. Introduction.

The amount of artificially produced hydrocarbon compounds, especially arenes, released into the environment is highly increased with the development of the industry. One group of aromatic hydrocarbons with a wide range of applications are polyphenols, including catechols, which produce many substances, e.g., pesticides, photographic developers. Catechol is easily absorbed through the skin and gastrointestinal of humans and animals, and a threshold limit value is five ppm. Oxidative cleavage of polyphenols by enzymes, including catechol dioxygenases (CDs), is an integral part of the natural carbon cycle [1]. In nature, non-heme CDs occur in soil bacterias, and they are metalloenzymes containing iron cations or, in some cases, manganese ions [2]. Depending on products, CDs are divided into intradiol (catechol 1,2-dioxygenase (EC 1.13.11.1) and protocatechuate 3,4-dioxygenase (EC 1.13.11.3)) and extradiol dioxygenases (2,3-dioxygenases (EC 1.13.11.2)). The main product of the catechol cleavage *via* the intradiol mechanism is *cis,cis*-muconic acid [3,4], while the extradiol CDs convert catechol to 2-hydroxymuconate semialdehyde [2]. Therefore, a continuous increase in interest in compounds that mimic the action of these enzymes is observed. Many biomimetic Fe complexes acting like CDs were described in the literature [3].

2. Objectives

The aim was to synthesize and determine the structure of mononuclear and dinuclear Fe(III) complexes with $\mathbf{N_2O_2}$ ligands based on ethylenediamine (**L1**) (**Figure 1**) and 1,2-diaminocyclohexane (**L2**).

3. "Materials & methods"

The X-ray data for the complexes were collected using XtaLAB Synergy-S (Rigaku - Oxford Diffraction) diffractometer. The obtained data sets were processed with CrysAlisPro software [4]. The structures were solved by direct methods and refined using SHELX-2017 program packages [5].

4. Results

Two dimers and two mononuclear complexes with $\mathbf{N_2O_2}$ ligands were synthesized using the standard procedure. We found that the addition of deprotonating base Et_3N induced the formation of dinuclear complexes. Otherwise, the mononuclear complexes were obtained. Structural studies were performed for complexes **[FeL1Cl(OCH$_3$)]**, **[FeL2Cl]**, and dimers **[(FeL1)$_2$O]**, **[(FeL2)$_2$O].**

In the complex **[FeL2Cl]**, and dimers **[(FeL1)$_2$O]**, **[(FeL2)$_2$O]**, central iron (III) ions have a deformed square pyramid environment where the fifth site in the first coordination sphere is occupied by monodentate ligand as chloride ion or bridged O^{2-}

ion, respectively. Only **[FeL1Cl(OCH$_3$)]** complex has an octahedral coordination sphere formed by **L1**, chloride ion, and methanol.

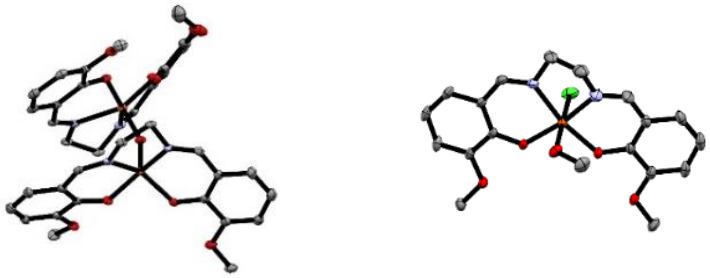

a **b**

Figure 1. Structure of Fe(III) dimer with the **L1** ligand based on ethylenediamine (**a**) and mononuclear Fe(III) complex with this ligand (**b**). For clarity, hydrogen atoms and solvent molecules have been omitted.

In dimers **[(FeL1)2O]**, **[(FeL2)2O]**, and **[FeL2Cl]**, the iron atoms displacement from the **N2O2** plane is approximately 0,56 Å for iron atoms, but in **[FeL1Cl(OCH3)]** central ion is placed almost in the **L1** plane. In each complex, the architecture of the ligand is similar, and the dihedral angles between aromatic rings are in the range of 12-28˚.

5. Conclusion

Based on literature reports, we expect that dimers will have greater catalytic activity than mononuclear complexes with identical ligands. It is related to better access of substrate and molecular oxygen to the iron (III) center. We expect that complexes with **L1** will be more efficient than compounds with **L2** because the steric hindrance plays an essential role in catechol conversion. Tests of the catalytic activity and assessment of the reaction mechanism for obtained complexes are in progress.

References

[1] Fiege, H.; Voges, H.-W.; Hamamoto, T.; Umemura, S.; Iwata, T.; Miki, H.; Fujita, Y.; Buysch, H.-J.;Garbe, D.; Paulus, W. Phenol Derivatives. In Ullmann's Encyclopedia of Industrial Chemistry; Wiley-VCH Verlag GmbH & Co. KGaA: Weinheim, Germany, 2000.
[2] Lipscomb, J.D. Mechanism of extradiol aromatic ring-cleaving dioxygenases. *Curr. Opin. Struct. Biol.* **18** (2008) 644–649
[3] Safaei, E.; Heidari, S.; Wojtczak, A.; Cotič, P.; Kozakiewicz, A. 4-Nitrocatecholato iron(III) complexes of 2-aminomethyl pyridine-based bis(phenol) amine as structural models for catechol-bound 3,4-PCD. *J. Mol. Struct*., **1106** (2016) 30–36
[4] Oxford Diffraction Ltd. CrysAlisPro. CrysAlisPro 2010.
[5] G. M. Sheldrick, *Acta Cryst.*, **C71** (2015) 3-8.

A-27

NON-COVALENT BONDS IN CRYSTALS OF NEW SULFUR DERIVATIVE OF URACIL

Michał Dominik Kamiński[1], Kunal Kumar Jha[1], Damian Trzybiński[1], Adam Mieczkowski[1] and Paulina Maria Dominiak[1]

[1]Biological and Chemical Research Centre, Department of Chemistry, University of Warsaw, Żwirki i Wigury 101, 02-089 Warszawa,
[2]Institute of biochemistry and biophysics Polish Academy of Sciences, Pawińskiego 5A, 02-106 Warszawa

The pyrimidine bases derivatives, such as fluorouracil, barbituric acid or orotic acid are commonly used as medicaments in pharmacological therapy. One of the new derivatives is untypical in its structure sulfur derivative of uracil - the F-10 molecule. The F-10 occurs in a solid-state in two forms - as a core itself and as a co-crystal with the 5-iodouracil [Fig.1]. The mechanism of its forming is not yet known. Therefore, structural crystallographic studies play a key in its understanding.

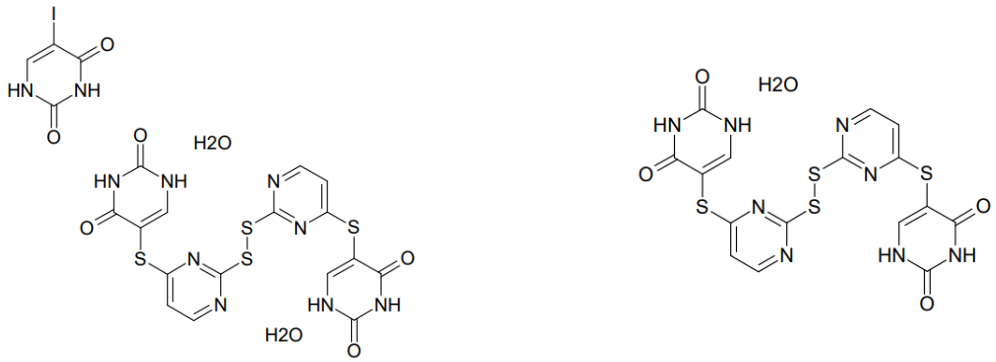

Fig. 1 Chemical formulas of molecules in both types of F-10 crystals.

In this work, we focused on determining the exact crystallographic structure of both F-10 crystal types with particular emphasis on non-covalent bonds occurring in these molecules - hydrogen bonds, halogen bonds and chalcogen bonds [1]. For this purpose, we made an XRD measurements of both crystal types and solved and refined them using the ShelXT and ShelXL programs. To describe the molecules packing in crystals we made geometrical studies of the non-covalent interactions. Also, to determine the effect of the bonds on the electron density surfaces of the molecules we made the Hirshfeld surface analysis [2] with the d_{norm} parameter.

References

[1] Alkorta, I., Elguero, J., Frontera, A., *Crystals*, **10,** 3 (2020) 180.
[2] Tan, S. L., Jotani, M. M., Tiekink, R. T., *Acta Crystallogr. E*, **75**, 3 (2019) pp. 308-318.

A-28

SYNTHESIS AND STRUCTURE OF THREE NEW PYRIDINE-CONTAINING OXAZOLINE LIGANDS OF COMPLEXES FOR ASYMMETRIC CATALYSIS

Ewa Wolińska, Waldemar Wysocki and Zbigniew Karczmarzyk

Faculty of Science, Siedlce University of Natural Sciences and Humanities, 3 Maja 54, PL-08110 Siedlce.

Chiral oxazoline derivatives constitute a huge class of versatile chiral ligands that utility was proved in diverse metal catalysed asymmetric reactions including cyclopropanations, hydrosilylations, hydrogenations, allylic alkylations, diethylzinc additions to aldehydes, Diels-Alder reactions, nitroaldol reaction, and many others [1-4]. During our research, we developed ligands bearing six-membered azaheteroaromatic ring including pyridine linked with the chiral oxazoline by an *N*-phenylamine unit. The enantiocontrolling activity of the ligands was evaluated in the asymmetric nitroaldol reaction of nitromethane with a variety of aromatic and aliphatic aldehydes catalysed by copper ions [5-8].

Taking into account, that oxazoline-pyridine type chiral ligands have been recently successfully applied in many new asymmetric processes [4], we synthesised and determined crystal structures of three new pyridine-containing oxazoline ligands with fluorine and perfluoromethyl group in the structures, namely: (*S*)-*N*-[2-(4-phenyl-4,5-dihydrooxazol-2-yl)phenyl]-5-(trifluoromethyl)pyridin-2-amine (**5a**), (*S*)-*N*-[4-fluoro-2-(4-isopropyl-4,5-dihydro-oxazol-2-yl)phenyl]-5-(trifluoromethyl)pyridin-2-amine (**5b**), and *N*-{2-[(3a*R*,8a*S*)-3a,8a-dihydro-8*H*-indeno[1,2-d]oxazol-2-yl]phenyl}-5-(trifluoromethyl)pyridin-2-amine (**5c**). The synthetic rout towards compounds (**5a**), (**5b**), and (**5c**) is depicted in Fig. 1.

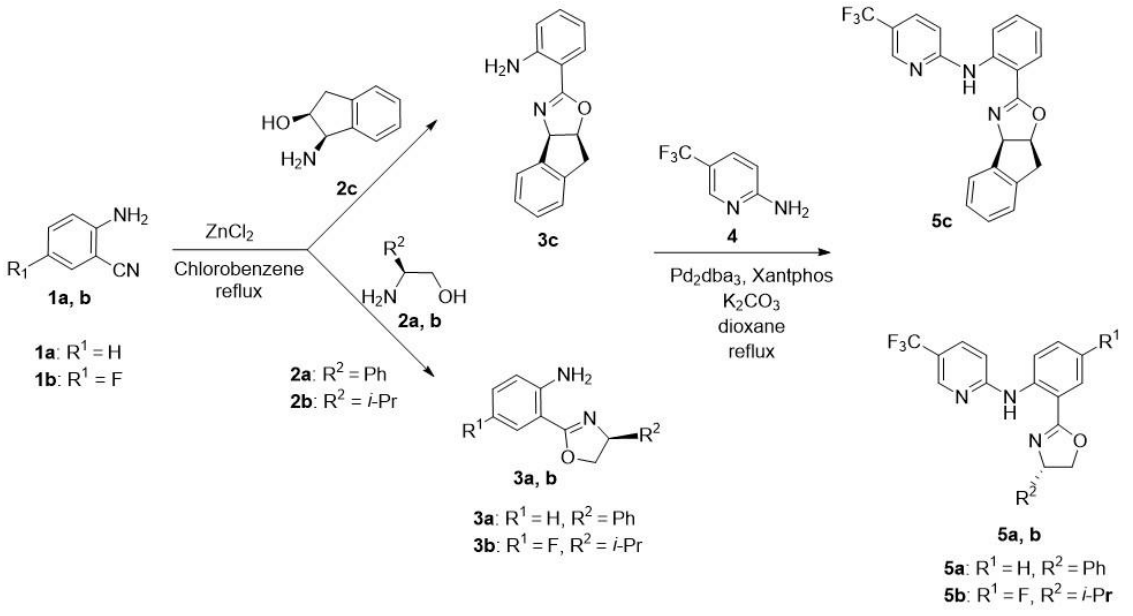

Fig. 1. The synthetic rout towards compounds (**5a**), (**5b**), and (**5c**).

A-28

The theoretical calculations using DFT method were undertaken to investigate the energetic, electronic and conformational preferences of searched derivatives.

References

[1] S. O'Reilly, P. J. Guiry, *Synthesis*, **46** (2014) 722.
[2] G. C. Hargaden, P. J. Guiry, *Chem. Rev.,* **109** (2009) 2505.
[3] G. Desimoni, G. Faita, K. A. Jørgensen, *Chem. Rev.,* **111** (2011) PR284.
[4] G. Yang, W. Zhang, *Chem. Soc. Rev*., **47** (2018) 1783.
[5] E. Wolińska, *Tetrahedron***, 69** (2013) 7269.
[6] E. Wolińska, *Tetrahedron:Asymmetry*, **25** (2014) 1122.
[7] E. Wolińska, *Tetrahedron:Asymmetry*, **25** (2014) 1478.
[8] E. Wolińska, *Heterocyclic Commun*., **22** (2016) 85.

A-29

CRYSTAL STRUCTURES OF ADENOSINE 5′-DIPHOSPHATE POTASSIUM SALTS

Oskar Kaszubowski, Katarzyna Ślepokura

Department of Chemistry, University of Wrocław,
Joliot-Curie 14, 50-383 Wrocław, Poland

Adenosine 5′-phosphates are ribonucleotides that play a main role in cellular metabolism [1]. They regulate, among others, AMPK kinase activity, which is one of the most important factors responsible for maintaining energy homeostasis in mammals cells [2]. The basis for understanding these processes is to understand the interactions of adenyl nucleotides with other cell components, including metal ions [3].

Both salts were obtained from commercially available K(ADP)·2H_2O (Sigma). The crystals of K(ADP)·4H_2O salt were obtained by diffusing methanol into a water/ethanol solution. Crystalline K(H_5O_2)(ADP)$_2$·4.3H_2O was grown from an aqueous solution with the addition of 1,4-dioxane. Both salts crystallize in the orthorhombic system, in the $P2_12_12_1$ space group.

One of the most important differences in the crystal structures of both salts is the coordination of potassium ions. In the case of the K(ADP)·4H_2O salt, the potassium ion is coordinated by four oxygen atoms of the diphosphate groups of adjacent nucleotides, two oxygen atoms of water molecules and one nitrogen atom of nucleobase (Fig. 1). In K(H_5O_2)(ADP)$_2$·4.3H_2O, the potassium ion is coordinated also by seven atoms, but different from the previous salt: two oxygen atoms of the diphosphate groups, one oxygen atom of sugar ring, three oxygen atoms of water molecules and one nitrogen atom of adenine base (Fig. 2).

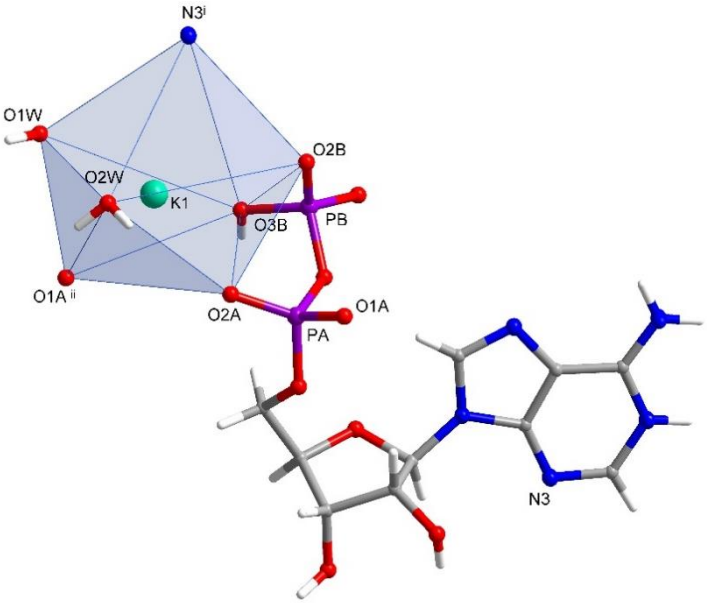

Fig. 1. Structural unit with coordination sphere of potassium ion in K(ADP)·4H_2O salt. Some water molecules are omitted for clarity; [i] (x+1,y-1,z), [ii](x+1,y,z).

A-29

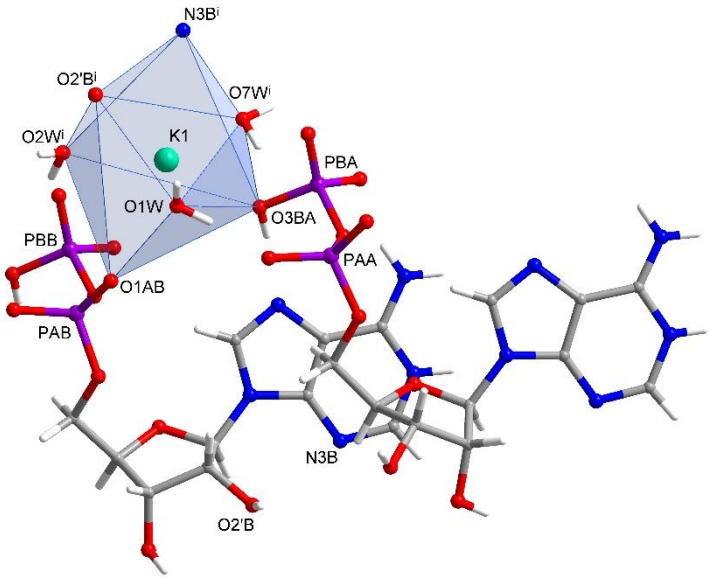

Fig. 2. Structural unit cells with coordination sphere of potassium ion in $K(H_5O_2)(ADP)_2 \cdot 4.3H_2O$ salt. Some water molecules are omitted for clarity; ^{i}(x-1,y,z).

References

[1] R. L. Veech, J .W. Lawson, N. W. Cornell, H. A. Krebs, *J. Biol. Chem.* **254** (1979) 6538-6547.
[2] B. Xiao, M. Sanders, E. Underwood, et al., *Nature* **472** (2011) 230-233.
[3] R. A. Alberty, *J. Biol. Chem*. **243** (1968) 1337-1343.

A-30

NOVEL POLINITRILE, AZOLE BASED LIGANDS DESIGNED FOR PREPARATION OF COORDIANTION POLYMERS

Marcin Kaźmierczak, Maciej Witwicki, Agnieszka Lewińska, Robert Bronisz

Wydział Chemii, Uniwersytet Wrocławski, ul. F. Joliot-Curie 14, 50-383 Wrocław

1-substituted 1,2,3-triazoles and 2-substituted tetrazoles can form two types of complexes. The first group is consisted of coordination compounds in which metal ions (M) are surrounded by six azole rings, thus, forming [M(azolyl)$_6$]-type cores (azolyl = 1,2,3-triazol-1-yl, tetrazol-2-yl) [1]. Exploiting 1,ω-di(azolyl)alkanes we have also prepared second type of coordination compounds in which the first coordination sphere is composed of four azole rings and two axially coordinated coligand molecules (nitriles or alcohols) [2,3]. 1,ω-di(azolyl)alkanes join neighboring metal ions through *exo*-positioned nitrogen atoms of azole rings and it results in formation of coordination polymers. The characteristic feature of our ligands is the presence of conformationally labile alkyl spacers tethering azole rings. Hence, resulting structural lability is an origin of uncommon spin crossover transitions [4].

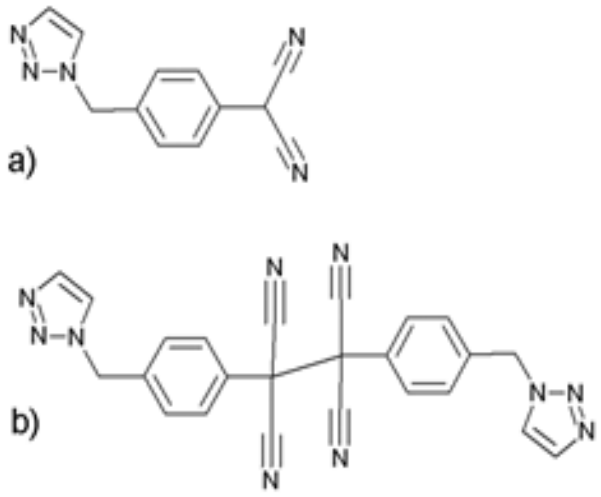

Fig 1. Molecular structures of **L1** (a), **L2** (b).

Considering that presence in both types of complexes of [FeN$_6$] chromophore creates conditions for occurrence of spin crossover phenomenon, we have designed novel flexible ligands containing azole and nitrile donors in the bridging molecule. In bitopic [4-(1*H*-1,2,3-triazol-1-ylmethyl) phenyl]propanedinitrile (**L1**, Fig. 1a) 1,2,3-triazole ring is linked with fragment containing nitrile donors through methylene spacer. Ligand **L1** crystallizes in I2/a space group (a = 18.589, b = 5.622, c = 20.723, α = 90.0, β = 101.27, γ = 90.0). We have exploited **L1** as precursor for preparation of dimeric 1,2-bis[4-(1H-1,2,3-triazol-1-ylmethyl)phenyl]ethane-1,1,2,2-tetracarbonitrile (**L2**). The compound **L2** crystallizes in P2$_1$/c space group (a = 11.967, b = 10.907, c = 8.386, α = 90.0, β = 102.35, γ = 90.0). The characteristic feature of **L2** is the presence of C-C linkage, joining the starting fragments (Fig. 1b). C-C bond adopts uncommon length of 1.63 Å. There will be details presented on the poster concerning crystal structures of **L1** and **L2**.

A-30

References

[1] a) R. Bronisz, *Inorg. Chem*. **44** (2005) 4463-4465; b) J. Kusz, R. Bronisz, M. Zubko, G. Bednarek,. *Chem. Eur. J*. **17** (2011) 6807-6820; c) A. Białońska, R. Bronisz, J. Kusz, M. Weselski, M. Zubko, *Eur. J. Inorg. Chem*. **5-6** (2013) 875-883.

[2] a) M. Książek, M. Weselski, M. Kaźmierczak, A. Tołoczko, M. Siczek, P. Durlak, J. A. Wolny, V. Schünemann, J. Kusz, R. Bronisz, *Chem. Eur. J*. **26** (2020) 14419-14434; b) A. Białońska, R. Bronisz, Ł. Baranowski, *Eur. J. Inorg. Chem*. **5-**6 (2013) 720–724; c) A. Białońska, R. Bronisz, *Inorg. Chem*. **51** (2012) 12630-12637; d) M. Książek, J. Kusz, A. Białońska, R. Bronisz, M. Weselski, *Dalton Trans*. **44** (2015) 18563-18575.

[3] a) A. Białońska, R. Bronisz, *Inorg. Chem.* **49** (2010) 4534-4542; b) R. Bronisz *Inorg. Chim. Acta*, **357** (2004) 396-404.

[4] a) M. Weselski, M. Książek, D. Rokosz, A. Dreczko, J. Kusz, R. Bronisz, *Chem. Commun*., **54** (2018) 54, 3895-3898; b) M. Weselski, M. Książek, P. Mess, A. Dreczko, J. Kusz, R. Bronisz, *Chem. Commun*., 55 (2018) 7033-7036; c) M. Książek, M. Weselski, A. Dreczko, V. Maliuzhenko, M. Kaźmierczak, A. Tołoczko, J. Kusz, R. Bronisz, *Dalton Trans*., 49 (2020) 9811-9819.

A-31

MAGNESIUM HYPODIPHOSPHATES

Vasyl Kinzhybalo

Institute of Low Temperature and Structure Research, 50-422 Wrocław

Recent review about inorganic hypodiphosphates summarizes current knowledge on the topic [1]. Alkali and alkaline earth metal hypodiphosphate salts are one of the most extensively studied up-to-date, though some of them still require further structural investigation. For example, there is only one magnesium hypodiphosphate crystal structure reported – magnesium dihydrogen hypodiphosphate tetrahydrate [2].

The structural study of two new magnesium hypodiphosphate crystals will be presented. One of them is another polymorphic modification of upper-mentioned magnesium dihydrogen hypodiphosphate tetrahydrate, $MgH_2P_2O_6{\cdot}4H_2O$. It crystallizes in the monoclinic system (contrary to the known modification that is triclinic [2]) and is built of infinite chains, that are similar to the ones from triclinic modification (Fig. 1). The mutual arrangement of infinite $[Mg(H_2O)_4(H_2P_2O_6)]_\infty$ chains is different.

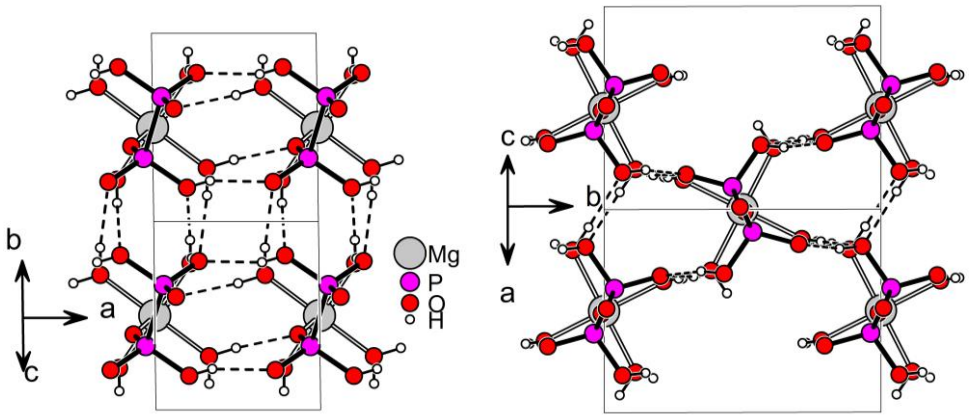

a) b)

Fig. 1. The arrangement of chains in triclinic (a) and monoclinic (b) modifications of $MgH_2P_2O_6{\cdot}4H_2O$.

The second compound is the normal magnesium salt of $Mg_2P_2O_6{\cdot}12H_2O$ composition. It crystallizes in trigonal *R*32 space group type and consists of isolated $[Mg(H_2O)_6]^{2+}$ octahedra and hydrogen-bonded to them $P_2O_6^{4-}$ anions packed in columns (Fig. 2). The anion adopts rarely-encountering intermediate conformation.

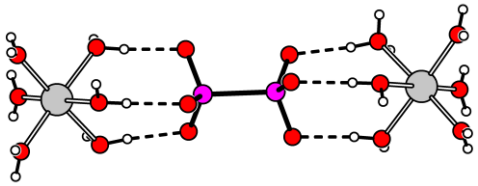

Fig. 2. The hydrogen-bonded motif in $MgH_2P_2O_6{\cdot}4H_2O$.

Literatura

[1] V. Kinzhybalo, M. Otręba, K. Ślepokura, T. Lis, *Wiadomości Chemiczne*, **75** (2021) 423.
[2] M. Gjikaj, M. Haase, *Acta Cryst. E*., **71** (2015) 867.

A-32

IMIDAZOLOKARBACHLORYNA I JEJ TRANSFORMACJA W KOMPLEKS N-HETEROCYKLICZNEGO KARBENU

Sebastian Koniarz*, **Piotr J. Chmielewski**

Wydział Chemii, Uniwersytet Wrocławski, ul. Joliot-Curie 14, 50-383 Wrocław, Polska

W szeroko pojętym obszarze chemii porfiryn istnieje bardzo duże zainteresowanie syntezą monomerycznych oraz oligomerycznych porfiryn lub porfirynoidów zawierających dodatkowe pierścienie na obrzeżach układu tetrapirolowego [1][2]. Szczególnie interesujące są pod tym względem pochodne porfiryny skondensowane z imidazolem ze względu na możliwość ich zastosowania w budowie układów multiporfirynowych albo połączonych ze sobą diad lub triad donor-akceptor. Mogą one być również łatwo przekształcone w N,N'-dialkilopochodne zawierające N-heterocykliczne ugrupowanie karbenowe (NHC) [3].

W wyniku naszych badań otrzymaliśmy pierwszą imidazolo[1,5]karbachlorynę. Powstaje ona w jednoetapowej syntezie wykorzystującej post-syntetyczną anulację pericykliczną, która zachodzi łatwo dla 2-aza-21-karbaporfiryny, znanej również jako N-odwrócona porfiryna [4][5]. Wprowadzenie jonu srebra(III) do wnęki imidazolokarbachloryny zapobiega alkilacji wewnętrznych atomów azotu, co powoduje, że metylacja takiego układu zachodzi selektywnie na atomie azotu skondensowanego imidazolu. W ten sposób zostaje wytworzony kationowy układ, który może być wykorzystany do otrzymania kompleksów metali z N-heterocyklicznym karbenem m.in. złota(I) [4].

Na posterze zostaną zaprezentowane struktury krystaliczne otrzymanych produktów – imidazolokarbachloryny oraz kompleksu złota(I) z N-heterocyklicznym karbenem wytworzonym z tego makrocykla, a także ścieżki syntetyczne otrzymanych produktów.

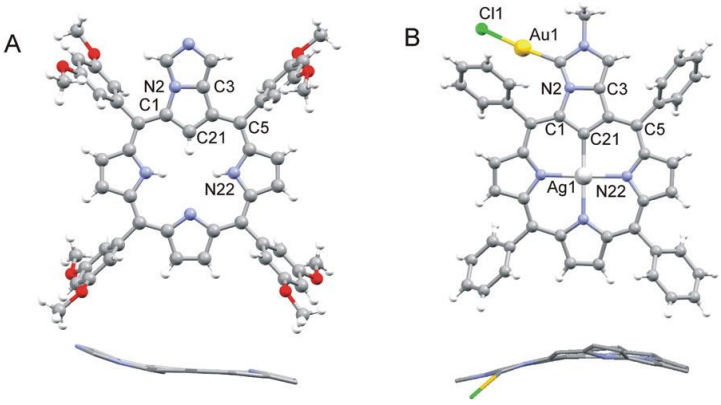

Rys. 1. Struktura molekularna A – imidazolokarbachloryny B – kompleksu karbenowego złota(I)

Literatura

[1] P. J. Chmielewski, Org. Lett., **7** (2005) 1789.
[2] A. Tsuda,A. Osuka, *Adv. Mater*., **4** (2002) 75.
[3] J.-F. Lefebvre, M. Lo, J.-P. Gisselbrecht, O. Coulembier, S. Clément ,S. Richeter, *Chem. – Eur. J.*, **19** (2013) 15652.
[4] D. Ren, S. Koniarz, X. Li, P. J. Chmielewski *Chem. Commun.*, **56** (2020) 4836.
[5] P. J. Chmielewski, L. Latos-Grażyński, K. Rachlewicz, T. Głowiak, *Angew. Chem., Int. Ed. Engl*., **33** (1994) 77.; H. Furuta, T. Asano, T. Ogawa, *J. Am. Chem. Soc*., **116** (1994) 767.

A-33

SUPRAMOLECULAR CHEMISTRY OF AMINOPIRYDINES

Irina Konovalova, Svitlana Shishkina

STC "Institute for Single Crystals", National Academy of Science of Ukraine, 60 Nauki ave., Kharkiv, 61001, Ukraine.

Aminopyridines are known to be key structural fragments of bioactive natural products, medicinal compounds and organic materials, as well as extremely valuable synthetic reagents. However, despite the popularity and seeming study of this type of compounds, the literature provides only data on their properties and methods of synthesis. There is no information on the ability of aminopyridines to form certain types of intermolecular interactions. However, these studies are extremely important in view of the fact that most pharmaceutical products containing biologically active molecules are used in the solid crystal state.

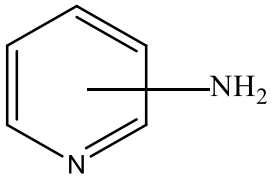

All modern approaches to the structure analysis of molecular crystals are based on the comparison of the geometric characteristics of intermolecular interactions. However, in many cases, these approaches are useless: the presence of a large number of weak interactions, the absence of specific directional interactions, and so on. N-H…N hydrogen bonds with the participation of the amino group as a proton acceptor are weak interactions, so it is almost impossible to determine their role in the formation of the crystal structure.

The amino group always exhibits donor properties, and the acceptor properties depend on the hybridization of the nitrogen atom and its basicity. We investigated a number of aminopyridines with one and two amino groups in *ortho*-, *meta*- and *para*-positions as model molecules. Hybridization of the nitrogen atom in these molecules is associated with the conjugation between the aromatic cycle and the lone pair of the nitrogen atom. In the case of aminopyridines, the presence of only three types of weak intermolecular interactions (N-H…N, N-H…π and C-H…π) complicates the analysis of crystal structures. It is difficult to determine the main structural motif in the solid state only on the basis of geometric considerations. It is not understand which interaction has an energetically dominant role in the crystal structure.

Analysis of packing from the energetic viewpoint provides more information about the supramolecular organization of these crystals.

A-34

DIFFUSE SCATTERING EFFECTS IN 1-AZIDO-4-NITROBENZENE

Dorota A. Kowalska[1], Yuriy O. Teslenko[2], Nazariy T. Pokhodylo[2], Mykola D. Obushak[2], Vasyl Kinzhybalo[1], Marek Wołcyrz[1]

[1]*Institute of Low Temperature and Structure Research, Polish Academy of Sciences, Okólna 2, 50-422 Wrocław, Poland*
[2]*Department of Organic Chemistry, Ivan Franko National University of Lviv, Kyryla i Mefodiya Str., 6, 79005,Ukraine*

The single crystals of 1-azido-4-nitrobenzene have been obtained from the ethanol solution [1]. The structure is monoclinic and accommodates *C*2/*c* space group with cell parameters: $a = 10.915(4)$ Å, $b = 10.324(4)$ Å, $c = 13.379(5)$ Å and $\beta = 95.64(3)°$; $Z = 8$. The asymmetric unit comprises of one 1-azido-4-nitrobenzene molecule in which two nitrogen atoms (N3 and N4) are disordered over two alternative positions (Fig. 1a) with the refined site occupancy factor close to 0.5. The N_3 groups are ordered in one direction and create atomic 'ribbons' along *c* axis. Therefore, two different types of ribbons can appear in the structure. Both possibilities belonging to one of *bc* layers are shown in Fig. 1b. But information about their relative position, whether they alternate or not, cannot be found from average structure.

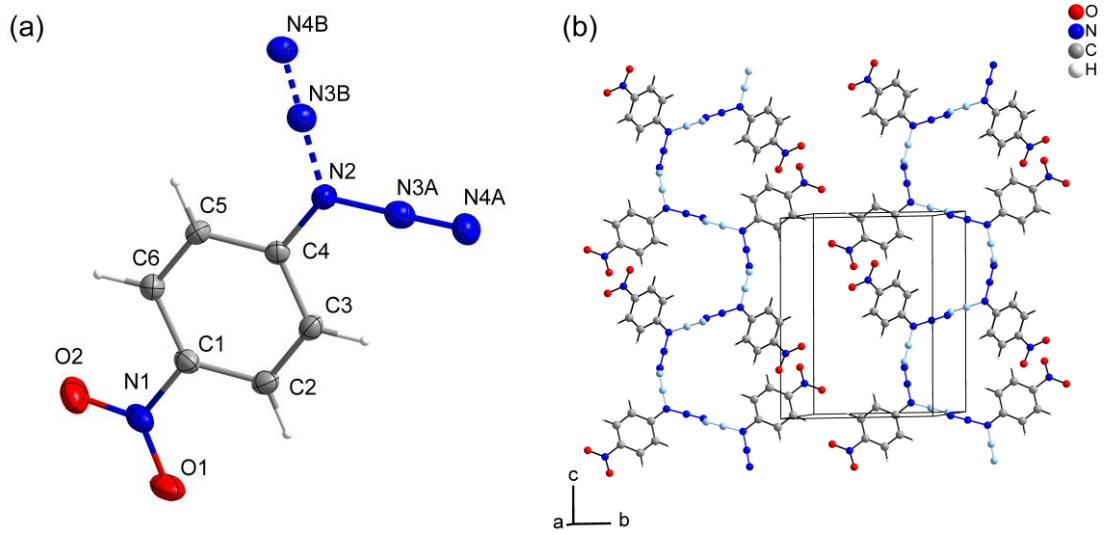

Figure 1. (a) The asymmetric unit of the compound showing atom numbering scheme. Atoms belonging to N3 group marked with letters A and B are disordered (SOF = 0.5). (b) Possible arrangement of N3 groups in two adjacent atomic ribbons arranged in the *cb* structure layer (marked with light and dark blue colour).

Three reciprocal space sections perpendicular to each of reciprocal space directions are presented in Fig. 2. Among Bragg intensities the X-ray diffuse scattering effects can be found. Diffuse scattering streaks arranged along a^* direction (Fig. 2a,b) are crossing b^*c^* reciprocal section (Fig. 2c) for $k = ½+n$ ($n = 0, 1, 2, \ldots$) and integer *l*.

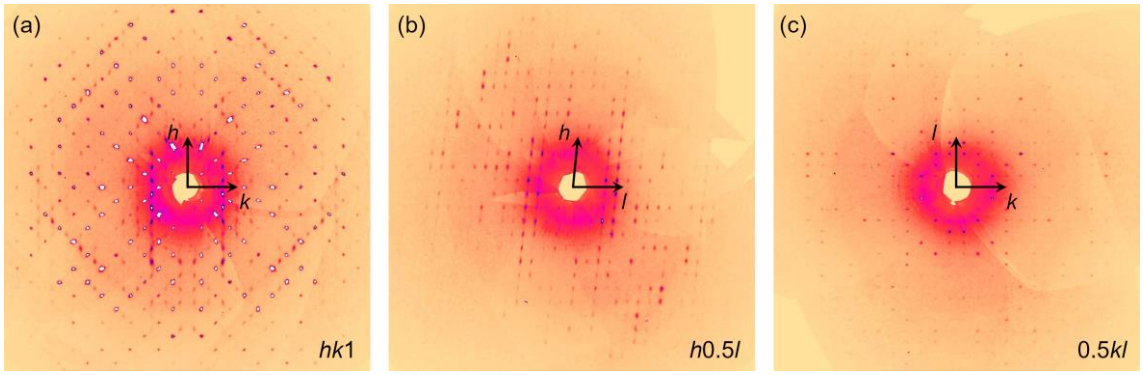

Figure 2. Reciprocal space sections showing streaks of X-ray diffuse scattering: (a) *hk*1 and (b) *h*0.5*l*. In the perpendicular 0.5*kl* direction there is no diffuse scattering visible (c).

Careful examination of the diffractions effects and comparison with some of already published works [2,3] may lead to a proposition of the local ordering of atomic 'ribbons' in the structure. The existing arrangement of diffuse scattering streaks indicates strong/infinite correlations in the crystal structure in the *c*-axis direction. In the *b*-axis strong (*ca.* several unit cells) correlations between different type of ribbons are expected to exist and in the *a*-axis direction much weaker correlations or even lack of them may be assumed. The planned Monte Carlo calculations will allow to confirm our suppositions about the local structure.

References

[1] N. T. Pokhodylo, O. Ya. Shyyka, V. S. Matiychuk, M. D. Obushak, V. V. Pavlyuk, *ChemistrySelect*., **2(21)** (2017) 5871–5876.
[2] D. Komornicka, M. Wołcyrz, A. Pietraszko, *J. Sol. State Chem.*, **192** (2012) 54–59.
[3] T. J. Bednarchuk, D. Komornicka, V. Kinzhybalo, M. Wołcyrz, *Acta Cryst. B*, **73** (2017) 337–346.

A-35

ANALIZA SKŁADU FAZOWEGO PROSZKOWYCH STAŁYCH NOŚNIKÓW TLENU W ASPEKCIE PRAKTYCZNEGO ZASTOSOWANIA W TECHNOLOGII SPALANIA PALIW W CHEMICZNEJ PĘTLI TLENKOWEJ

Ewelina Ksepko, Rafał Łysowski

Politechnika Wrocławska, Katedra Chemii i Technologii Paliw
ewelina.ksepko@pwr.edu.pl

Technologia chemicznej pętli tlenkowej w tym CLC (*Chemical looping combustion*) oraz jej odmiana CLOU *(Chemical looping with oxygen uncoupling)* umożliwia owocne spalanie paliw z dodatkowym efektem ograniczenia emisji gazów cieplarnianych w tym tlenków azotu i węgla do atmosfery. Zasada działania polega na uniknięciu bezpośredniego kontaktu paliwa z tlenem z powietrza. Można to zrealizować stosując odpowiednio zaprojektowany materiał tlenkowy tzw. stały nośniki tlenu. To on stanowi źródło tlenu niezbędnego dla przeprowadzenia energetycznego procesu spalania paliw, w tym biomasy czy węgla.

W pracy zsyntetyzowano nowe stałe nośniki tlenu w formule opartej na metodzie mechanicznego mieszania a następnie wysokotemperaturowej kalcynacji. Złożone nośniki tlenu otrzymano z wyjściowych surowców tj. wysokiej czystości MnO_2, Fe_2O_3 i ZrO_2. Dla celów porównawczych nowoopracowanych materiałów otrzymano również materiał odniesienia składający się jedynie z Fe_2O_3 i ZrO_2.

Badania składu fazowego otrzymanych złożonych materiałów tlenkowych przeprowadzono za pomocą proszkowego dyfraktometru rentgenowskiego (XRD) MiniFlex 600 marki Rigaku. Zaobserwowano wytworzenie się szeregu faz, oprócz mało skomplikowanych takich jak Fe_2O_3, ZrO_2 zidentyfikowano również struktury złożone tlenkowe np. o strukturze typu perowskitu. Ocenę zdolności przenoszenia tlenu (efekt CLOU-wydzielania tlenu pod wpływem działania wysokich temperatur), przeprowadzono w funkcji temperatury przy pomocy analizatora termograwimetrycznego (TGA) Luxx STA 449 F5 Jupiter marki Netzsch. Na podstawie wyników analiz reaktywności metodą TGA wnioskowano o znaczącym udziale w wydajności efektu CLOU struktur typu bixbyite $(Mn,Fe)_2O_3$ czy spinelu np. $FeMn_2O_4$.

Podziękowanie: Praca została częściowo sfinansowana w ramach projektu NCN nr 2020/37/B/ST5/01259.

A-36

FACTORS DETERMINING THE EFFICIENCY OF PHOTOISOMERISATION REACTION OCCURRING IN CRYSTALS OF SELECTED NICKEL(II) AND COPPER(II) NITRO COMPLEXES

Sylwia E. Kutniewska, Patryk Borowski, Radosław Kamiński and Katarzyna N. Jarzembska

Department of Chemistry, University of Warsaw, Żwirki i Wigury 101, 02-089 Warsaw, Poland

The design of solid-state materials exhibiting properties controllable by the use of light and/or dependent on temperature is an important goal of modern materials chemistry. Potential applications of such systems range from biosensors, data carriers, to optoelectronic materials.

In view of the above, transition-metal complexes that contain ambidentate ligands are currently attracting great interest. Upon UV-Vis light irradiation they can undergo isomerisation reaction in the solid state. During such process the ligand changes its binding mode, which can further significantly alter a number of material's properties, such as colour, reactivity etc. Therefore, in this work we present a detailed study of the photo-induced solid-state linkage isomerism in a series of new Ni/Cu nitro complexes containing ligands based on e.g. 8-aminoquinoline, N-piperidine and 2-picoclyamine derivatives. In order to characterize the synthesized materials' properties various techniques were applied, e.g. spectroscopic methods (e.g., UV-vis, solid-state IR), physicochemical analyses, computational studies and, most importantly, photocrystallographic approach.

All of studied nickel complexes exist as a nitro isomer or mixture nitro/nitrito forms in the ground state structures at 100 K, and all of them to some extent switch to another isomer upon LED light irradiation. So far, the most promising photoswitchable system is [**1**] (Figure 1). Photocrystallographic studies show that the metastable state is formed with a 100% conversion level at 160 K when they crystal sample is exposed to the 660 nm LED-light irradiation, and the induced *endo*-nitrito isomer is stable up to around 220 K. In turn, the same reaction conditions applied to a crystal of complex [**2**] lead to the formation of *endo*-nitrito and *exo*-nitrito isomers with populations 14% and 10% respectively. Complex [**3**] contains two molecules in ASU, among which one undergoes photoisomerisation with the 25% conversion level and the second molecule with only 5% efficiency.

As far as the copper systems are concern, it appears they work most efficiently at 10 K, while the metastable form is usually stable only up to 60 K, which hampered the photocrystallographic studies and, at the same time, makes these systems less attractive regarding potential applications.

In conclusion, we have determined that efficient switching between nitro and nitrito isomers in the solid state is highly dependent on crystal packing and intermolecular interactions, especially there involving the nitro fragment, as well as the temperature of the experiment. In the case of the studied series, the stronger basic character of the cyclic aliphatic amine ligand when compared to the aromatic 8-aminoquinoline fragment seems

to enhance the photoswitchable properties. Nevertheless, the last aspect should be further explored.

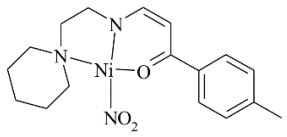	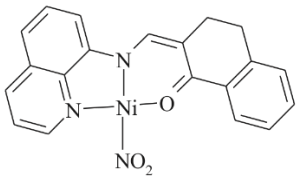	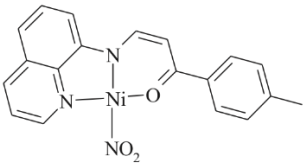
[**1**]	[**2**]	[**3**]

Figure 1. Some examples of the studied nickel complexes.

The authors thank the PRELUDIUM grant (2017/25/N/ST4/02440) of the National Science Centre in Poland and the Inter-Faculty of Individual Studies in Mathematics and Natural Sciences, University of Warsaw, for financial support. The Wrocław Centre for Networking and Supercomputing (grant No. 285) is gratefully acknowledged for providing computational facilities. The in-house X-ray diffraction experiments were carried out at the Department of Physics, University of Warsaw, on Rigaku Oxford Diffraction SuperNova diffractometer, which was co-financed by the European Union within the European Regional Development Fund (POIG.02.01.00-14.122/09).

A-37

STRUCTURAL STUDIES OF TWO OXALATO BASED COORDINATION POLYMERS

Tadeusz M. Muzioł i Maciej Lewandowski

Wydział Chemii Uniwersytetu Mikołaja Kopernika w Toruniu,
ul. Gagarina 7, 87-100 Toruń

New multifunctional compounds sharing several properties, *e.g*. magnetism with porosity, chirality, luminescent properties are challenging and very appealing field of chemistry [1]. Effective magnetic materials require paramagnetic centers connected *via* bridges efficiently transmitting magnetic couplings. Oxalate anion offers a variety of coordination modes resulting in different topologies allowing for tuning of magnetic properties. There are known 0D, 1 D, 2D and 3D oxalato complexes [2, 3]. A chirality control enables preparation of multifunctional materials exploiting magnetochiral effects in paramagnetic chiral systems.

We synthesized complexes with oxalate anions bridging paramagnetic centers. We aimed to obtain chiral magnets and the chirality was introduced by chiral ligand – (1R,2R)-(-)-cyclohexanediamine (dach). It creates stable complexes due to bidentate coordination to a variety of metal ions. Crystals were prepared by slow evaporation of the solvent. The data collection was performed using XtaLAB Synergy, Dualflex with HyPix detector, CuKα radiation λ = 1.54184 Å. We obtained two oxalate complexes given by the formulae: $\{[Cu(dach)_2][Cu(C_2O_4)_2(H_2O)_2]\}_n$ (**1**) and $\{[Cu(dach)_2][Fe^{II}_2(C_2O_4)_3]\cdot 4H_2O\}_n$ (**2**).

(**1**) forms chain polymer with copper(II) cations in both units found in strongly distorted octahedral environment. In $[Cu(C_2O_4)_2(H_2O)_2]^{2-}$ Cu2 coordination sphere is formed by six oxygen atoms – four coming from bidentately coordinated oxalate anions and two water molecules occupying *trans* positions. The latter create strongly elongated bonds with Cu2-O distances ranging from 2.582(7) – 2.685(7) Å. Cu1 in $[Cu(dach)_2]^{2+}$ moiety is coordinated by four nitrogen atoms from two dach molecules and the long Cu1-O (2.495(4) – 2.683(4) Å) bonds are formed by two oxygen atoms from two oxalate anions. Hence, the oxalate anion was found in bidentate/monodentate coordination mode with inner O21 and O33 atoms involved in bridging between units. These bonds assure propagation of the chain with the shortest intermetallic distances being 3.976 and 4.102 Å (Fig. 1).

In (**2**) 3D anionic network is observed composed of connected $[Fe^{II}(C_2O_4)_3]^{4-}$·units. The presence of iron(II) ions in the final product indicates that reduction process occurred during synthesis or crystallization step because $K_3[Fe^{III}(C_2O_4)_3]\cdot 3H_2O$ was used. It is proved by significantly elongated Fe-O bonds ranging from 2.096(9) – 2.161(8) Å, whereas for $[Fe^{III}(C_2O_4)_3]^{3-}$ units they are usually close to 2.0 Å (*e.g*. 1.9750(14) to 2.0383(14) Å [4]). All oxalate anions are found in bisbidentate coordination mode. In this sublattice there are formed decagonal (with 10 iron(II) ions as nodes connected by oxalate anions) non-planar rings composed of Λ and Δ isomers of $[Fe^{II}(C_2O_4)_3]^{4-}$ units. $[Cu(dach)_2]^{2+}$ moieties and crystallization water molecules are found in cavities of the oxalate sublattice (Fig. 2). Cu(II) coordination sphere is planar and composed of four nitrogen atoms from two dach molecules whereas Cu-O distances exceed 3.1 Å and fall out from the coordination range.

A-37

We obtained two oxalato complexes being coordination polymers – 1D (**1**) and 3D (**2**) with bridges formed between paramagnetic centers. Both compounds crystallized in chiral space groups and the chirality was imposed by chiral ligand used at the preparation step. These compounds showed different topologies due to different metal:oxalate ratio and also coordination modes affecting the obtained topologies. Currently we aim to start magnetic studies for these compounds.

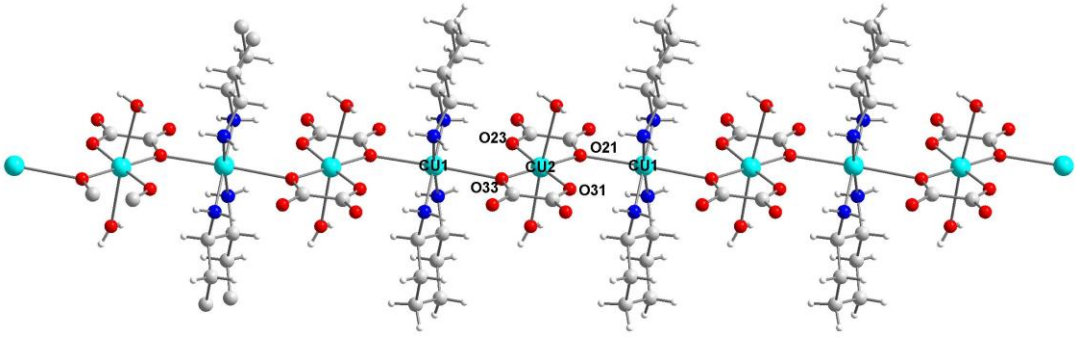

Fig. 1. Chain structure in $\{[Cu(dach)_2][Cu(C_2O_4)_2(H_2O)_2]\}_n$ (**1**)

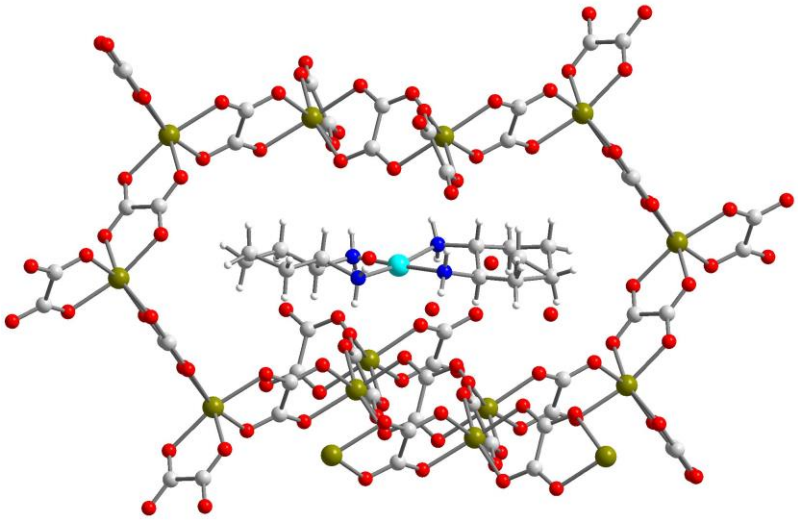

Fig. 2. The network structure of $\{[Cu(dach)_2][Fe^{II}_2(C_2O_4)_3]\cdot 4H_2O\}_n$ (**2**).

References

[1] M. Pilkington, S. Decurtins, in: *Comprehensive Coordination Chemistry II*, eds. J.A. McCleverty, T. J. Meyer, Elsevier, 2003, vol. 7, ch. 7.4 (High Nuclearity Clusters: Clusters and Aggregates With Paramagnetic Centers: Cyano and Oxalato Bridged Systems), pp. 177-229.

[2] M. Gruselle, C. Train, K. Boubekeur, P. Gredin, N, Ovanesyan, *Coord. Chem. Rev.*, **250** (2006) 2491-2500.

[3] T. M. Muzioł, G. Wrzeszcz, *Polyhedron*, **109** (2016) 138-146.

[4] T. M. Muzioł, N. Tereba, R. Podgajny, D. Kędziera and G. Wrzeszcz, *Dalt. Trans.*, **48** (2019) 11536–11546.

A-38

CRYSTAL STRUCTURES OF TWO NEW COORDINATION POLYMERS OF IRON(II) BASED ON 1-(3-(2-PYRIDYL)-1,2,4-TRIAZOL-1-YL)-3-(TETRAZOL-1-YL)PROPANE

Vladyslav Maliuzhenko,[2] Marek Weselski,[2] Maria Książek,[1] Joachim Kusz,[1] Robert Bronisz[2]

[1]Wydział Fizyki, Uniwersytet Śląski, ul. Uniwersytecka 4, 40-007 Katowice
[2]Wydział Chemii, Uniwersytet Wrocławski, ul. F. Joliot-Curie 14, 50-383 Wrocław

Pyridylazole-based ligands form a wide group of chelating molecules exploited in the coordination chemistry. They form mononuclear as well as oligomeric coordination compounds. The coordination chemistry of 1-R-3-(2-pyridyl)-1,2,4-triazole derivatives is less known. We have decided to exploit abovementioned chelating fragment in preparation of bitopic, bridging ligands in which pyridylazole fragment would be tethered with monodentately coordinating 1,2,3-triazole or tetrazole ring through flexible, alkyl linker.[1] Preliminary studies of 1-(3-(2-pyridyl)-1,2,4-triazol-1-yl)-4-(tetrazol-1-yl)butane (**L1**) in the reaction with iron(II) perchlorate afforded coordination compound $[Fe(\mathbf{L1})_2](ClO_4)_2$. Importantly it was established that the complex exhibits thermally induced spin crossover. Unfortunately, the crystal structure of the compound was not determined. Taking into account successful preparation of spin crossover system, further studies were carried out exploiting of 1-(3-(2-pyridyl)-1,2,4-triazol-1-yl)-3-(tetrazol-1-yl)propane (**L2**, Fig. 1) bridging ligand. Synthesis between **L2** and iron(II) tetrafluoroborate, performed in acetonitrile, led to formation the coordination compound $[Fe(\mathbf{L2})_2](BF_4)_2{\cdot}CH_3CN$. The complex crystallizes as yellow crystals and is stable during storage. Measurements of temperature dependence of magnetic susceptibility revealed an occurrence of abrupt and complete thermally induced spin crossover. Spin crossover is accompanied by hysteresis loop ($T_{1/2}^{\downarrow}$= 114 K, $T_{1/2}^{\uparrow}$=131 K). It was found that LS→HS switching triggered by light (520 nm) can be realized, too. The complex crystallizes in the form of one-dimensional coordination polymer. The first coordination sphere is formed by two pyridyl-1,2,4-triazole fragments and two *cis* positioned tetrazole rings coordinated through *exo* positioned nitrogen atoms N4. Such arrangement of donors causes that the polymeric chain takes a shape of *zig-zag*. At 250 K the Fe-N distances are in the range 2.15-2.21 Å, thus, they are characteristic for HS form of the complex. Lowering temperature to 100 K triggers HS→LS transition associated with shortening of Fe-N distances to values of 1.98-2.04 Å. Change of reaction medium on methanol led to formation of $[Fe(\mathbf{L2})_2](BF_4)_2{\cdot}CH_3OH$. Also in this complex the first coordination sphere is composed of two pyridyl-1,2,4-triazole fragments and two tetrazole rings. Unlike the first complex the tetrazole rings are axially coordinated. It results in formation of polymeric chains in which iron(II) ions are arranged collinearly. At 250 K the Fe-N distances are in adopt values 2.16-2.20 Å, however, in contrast to acetonitrile solvate in this case lowering of temperature to 90 K does not involve shortening of Fe-N distances, thus, the complex remains in the HS form. Results of magnetic studies confirmed an absence of spin crossover behavior. On the poster the details concerning

crystal structures of complexes $[Fe(\mathbf{L2})_2](BF_4)_2 \cdot CH_3CN$ and $[Fe(\mathbf{L2})_2](BF_4)_2 \cdot CH_3OH$ will be presented.

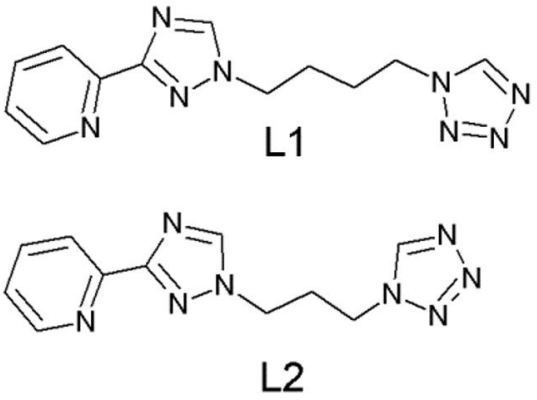

Fig 1. Molecular structures of **L1** and **L2** ligands.

References

[1] A. Białońska, R. Bronisz, *Tetrahedron*, **64** (2008) 9771.

A-39

STRUCTURAL AND TOPOLOGICAL ANALYSIS OF IONIC CO-CRYSTALS BULIT OF AMINOACIDS AND LITHIUM SALTS

Paulina H. Marek[a,b], Karolina A. Urbanowicz[a], Grzegorz Jędrzejczyk[a], Izabela Madura[a], Michał K. Cyrański[b], Arkadiusz Ciesielski[b]

[a]Faculty of Chemistry, Warsaw University of Technology, Noakowskiego 3, 00-664 Warsaw
[b]Faculty of Chemistry, Uniwersity of Warsaw, ul. Pasteura 1, 02-093 Warsaw
pmarek@ch.pw.edu.pl

Ionic co-crystals constitute a new class of substances composed of co-crystallizing: salts, usually inorganic, and an organic compound. Such systems may exhibit properties resulting from both components such as good water solubility and biological activity. Ionic co-crystals are therefore the subject of research in the pharmaceutical industry, as they create the possibility of creating new forms of drugs with new or improved properties. [1]

In the recent years, ionic co-crystals composed of alkali metal halides and biogenic aminoacids have been the subject of research on the phenomenon of spontaneous chiral separation. [2] A special role can be assigned to lithium halide co-crystals. These systems form polycationic coordination polymers exhibiting chain topology, built of Li^+ cations coordinated with the zwitterionic form of amino acids. [3] It has been postulated that the possibility of separation is determined by the tetrahedral environment of the lithium coordination sphere, which cannot be centrosymmetric and therefore the formation of chiral motifs in the structure is preferred. Most of formed coordination polymers are built of chiral subunits – six-membered LiOLiOCO rings. The role of this motif in chiral separation was not discussed in the literature, so far.

Herein, I present structural and topological analysis of newly obtained ioinc co-crystals and records from CCDC database with special attention devoted to observed levels of chirality present in the crystal structure.

Work implemented as a part of Operational Project Knowledge Education Development 2014-2020 cofinanced by European Social Fund. This work was financed by a grant from the National Science Centre (2018/29/N/ST4/00451).

References

[1] D. Braga, *Cryst. Growth Des.*, **12** (2011) 5621-5627.
[2] O. Schemchuk, *CrystEngComm* **19** (2017) 6267-6273.
[3] O. Schemchuk, *Chem. Eur. J.*, **24**(48) (2018) 12564-12573.

A-40

INFLUENCE OF WEAK INTERACTIONS OF THE NITRO GROUP ON BAND SHIFT IN THE IR AND RAMAN SPECTRA FOR THE SERIES OF SALTS OF THE NITROANILINE DERIVATIVES

V. V. Medviediev, M. Daszkiewicz

Institute of Low Temperature and Structure Research, Polish Academy of Sciences, str. Okólna 2, 50-422 Wrocław, P.O.Box 937, Poland

Many of nitroaniline derivatives possess nonlinear optical (NLO) properties [1]. The molecules contain amino group which can be protonated and their salts can be obtained in acidic conditions. Therefore, a search of compounds with NLO properties can be expanded for a large group of organic ionic compounds. Previously, some complexes of 2-nitroaniline (2na), 3-nitroaniline (3na), 4-nitroaniline (4na) and 2-methyl-4-nitroaniline (2m4na) with inorganic acids were studied [2–5]. As a continuation of those studies, investigation for the series of new salts of 2-chloro-4-nitroaniline (2Cl4na), 2-methyl-3-nitroaniline (2m3na), 2-methyl-5-nitroaniline (2m5na) and 2-methyl-6-nitroaniline (2m6na) was performed [6–10].

Crystal structures of obtained salts were determined and their temperature stability were checked in the range of 295–100 K using XRD. Weak interactions were revealed on the Hirshfeld surfaces [11] and geometrical parameters analysis. Generally, the nitro group is engaged in a diverse interactions, which can be divided into two main groups where interacting groups are arranged parallel or perpendicular to each other.

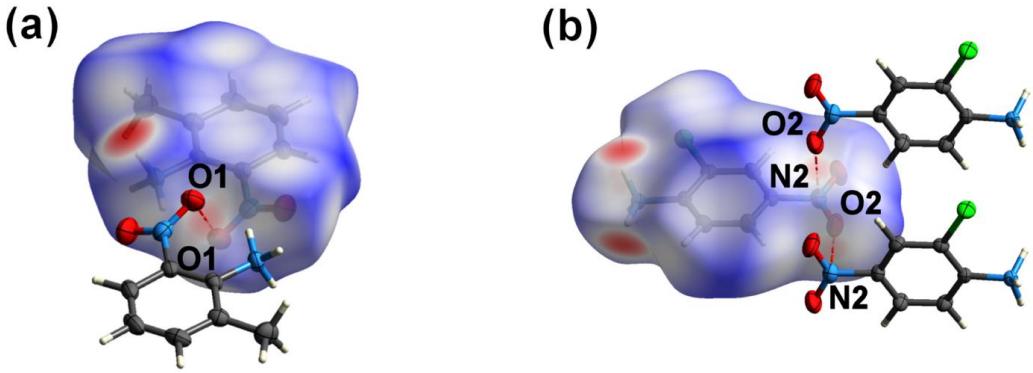

Fig. 1. The examples of the Hirshfeld surfaces for the interactions:
a) $\pi(NO_2)\cdots\pi(NO_2)$ in (H2m6na)Br and b) $O_{NO2}\cdots\pi(N)_{NO2}$ in (H2Cl4na)HSO_4.

The interactions of the nitro group were monitored by the band shift of the $\nu_s NO_2$ vibration. It was discovered that the frequency of the $\nu_s NO_2$ vibration depends on the mode of interaction [12]. Comparison of over a dozen crystal structures and their spectra showed that the $\nu_s NO_2$ band (Table 1) used to be observed at 1360 cm^{-1} for the compounds where the NO_2 groups are oriented perpendicularly (Fig.1b). The band is slightly red-shifted down to 1340–1330 cm^{-1} in the case of stronger interactions, especially for C–H···O / N–H···O hydrogen bonds or parallel oriented nitro groups (Fig. 1a). So, the mode of interaction can be identified by vibrational spectroscopy indicating the diagnostic feature of the $\nu_s NO_2$ band.

Table 1. Vibrational frequency of the $\nu_s NO_2$ mode (cm^{-1}) and intermolecular interactions of the nitro group in studied nitroaniline salts.

Compound	$\nu_s NO_2$ IR	$\nu_s NO_2$ Raman	Interaction
$(H2m3na)_2SO_4$	1361	1362	$O_{NO2}\cdots\pi(N)_{NO2}$ and C–H$\cdots O_{NO2}$
(H2m3na)I	1355	1360	$O_{NO2}\cdots\pi(N)_{NO2}$
(H2m3na)Br	1363	1359	$O_{NO2}\cdots\pi(N)_{NO2}$
$(H2m3na)H_2PO_4$	1359	1359	$O_{NO2}\cdots\pi(N)_{NO2}$ and C–H$\cdots O_{NO2}$
$(H2Cl4na)HSO_4$	1354	1361	$O_{NO2}\cdots\pi(N)_{NO2}$ and C–H$\cdots O_{NO2}$
$(H2m5na)H_2PO_4$ (RT)	1351	1352	$\pi(O)_{NO2}\cdots\pi_{ring}$ and C–H$\cdots O_{NO2}$
$(H2m5na)H_2PO_4$ (15K)	1353	-	$\pi(O)_{NO2}\cdots\pi_{ring}$ and C–H$\cdots O_{NO2}$
$(H2m3na)Cl\cdot H_2O$	1350	1350	C–H$\cdots O_{NO2}$ and $\pi(O)_{NO2}\cdots\pi_{ring}$
(H2m4na)Br	1346	1350	C–H$\cdots$O
(H2Cl4na)Br	1353	1353	C–H$\cdots$O and $\pi(O)_{NO2}\cdots\pi_{ring}$
(H2m6na)Br	-	1346	C–H$\cdots$O and $\pi(O)_{NO2}\cdots\pi(O)_{NO2}$
(H2m5na)Cl	1348	1353	C–H$\cdots$O
(H2m5na)Br	1348	1344	N–H$\cdots$O ($NH_3\cdots$O)
(H2m5na)I	1348	1344	N–H$\cdots$O ($NH_3\cdots$O)
$(H2m5na)NO_3$	1353	1346	N–H$\cdots O_{NO2}$ ($NH_3\cdots O_{NO2}$)
$(H2m5na)[I_3]\cdot H_2O$	1351	1344	N–H$\cdots O_{NO2}$ and O–H$\cdots O_{NO2}$
$(H2m6na)HSO_4$	1343	1343	N–H$\cdots O_{NO2}$
$(H2m3na)NO_3$	1343	1343	C–H$\cdots O_{NO2}$ and $NH_3\cdots O_{NO2}$
$(H2m6na)I_3$	1327	1330	2x C–H$\cdots$O

References

[1] B.F. Levine, *et al.*, *J. Appl. Phys.*, **50** (1979) 2523-2527.
[2] M. Daszkiewicz, *Cryst. Growth Des.*, **13** (2013) 2277–2285.
[3] M. Daszkiewicz, *Spectrochim. Acta A.*, **131** (2014) 335–341.
[4] M. Daszkiewicz, *Spectrochim. Acta A.*, **132** (2014) 776–785.
[5] M. Daszkiewicz, *Spectrochim. Acta A.*, **139** (2015) 102–107.
[6] V. Medviediev, M. Daszkiewicz, *Acta Cryst. B*, **75** (2019) 1003–1013.
[7] V. Medviediev, J. Baran, J.K. Zaręba, M. Drozd, M. Daszkiewicz, *Struct. Chem.*, **31** (2020) 955–964.
[8] V. Medviediev, M. Daszkiewicz, *J. Mol. Struct.*, **1211** (2020) 128073.
[9] V. Medviediev, M. Daszkiewicz, *J. Mol. Struct.*, **1229** (2021) 129577.
[10] V. Medviediev, M. Daszkiewicz, *Acta Cryst. C*, **77** (2021) 125–136.
[11] F.L. Hirshfeld, *Chim. Acta.*, **44** (1977) 129–138.
[12] V. Medviediev, Rozprawa doktorska (2021).

A-41

CRYSTALLINE STRUCTURE OF THE REACTION PRODUCTS BETWEEN AMINOISOXAZOLES AND AROMATIC ALDEHYDES

Beata Kołodziej[1], Burcu Duran[2], Maja Morawiak[3], Wojciech Schilf[3]

[1] West Pomeranian University of Technology, Szczecin; Faculty of Chemical Technology and Engineering; Department of Inorganic and Analytical Chemistry, Al. Piastów 42, 71-065 Szczecin, Poland
[2] Eskişehir Technical University, Eskişehir; Faculty of Science; Yunus Emre Kampüsü 26470 Tepebaşı / ESKİŞEHİR, Turkey
[3] Institute of Organic Chemistry, Polish Academy of Sciences, ul. Kasprzaka 44/52, 01-224 Warsaw, Poland

Heterocyclic systems are very popular organic compounds, especially in the field of medicine and pharmacy [1]. Heterocyclic compounds that exhibit high biological activity are still being searched because of their possible use in the treatment of the diseases of our time [2]. Among the heteroaromatic systems isoxazoles' derivatives are under interest of pharmaceutical environment because of their immunosuppressive activity [3]. One of the group of heterocyclic compounds having very good biological activity are Schiff bases – typical products of condensation reaction between primary amines and carbonyl compounds [4]. Sometimes the reaction of primary amines with carbonyl compounds leads to the formation of compounds different from imines [5] - secondary amines.

In this communicate, we present syntheses and results of research (NMR, ATR-FTIR, UV-Vis, and X-ray) of common (nap5AMI) and unexpected (benz3AMI, Hnap3AMI) of reaction products between aromatic carbonyls, and aminoisoxazoles: 3-amino-5-methylisoxazole (3AMI) and 5-amino-3-methylisoxazole (5AMI).

The figures below show an example of a hydrogen bond formed in the obtained Schiff bases and secondary amines.

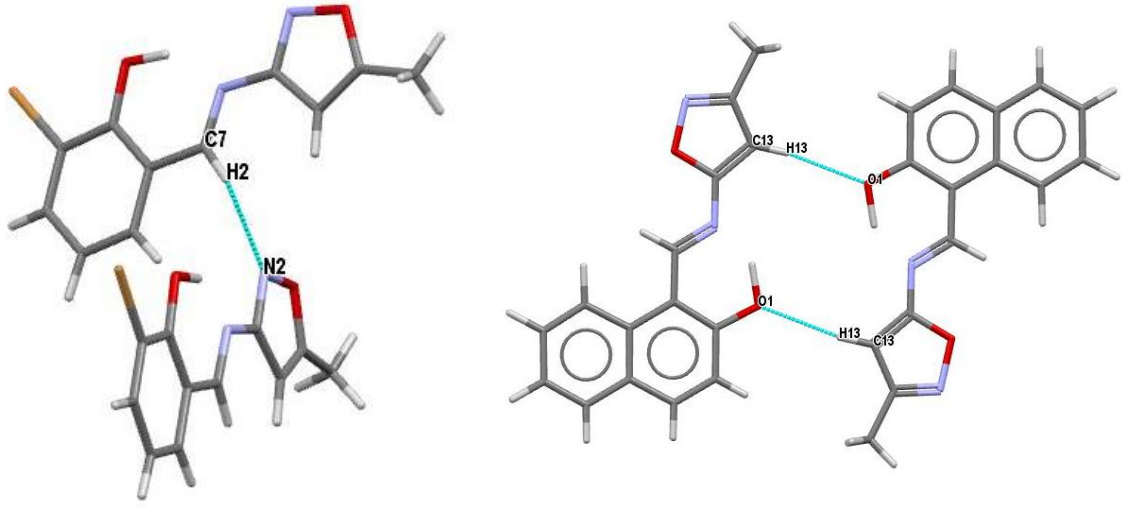

3Brsal3AMI **nap5AMI**

Figure 1. Hydrogen bonds formed in the obtained Schiff bases – common products.

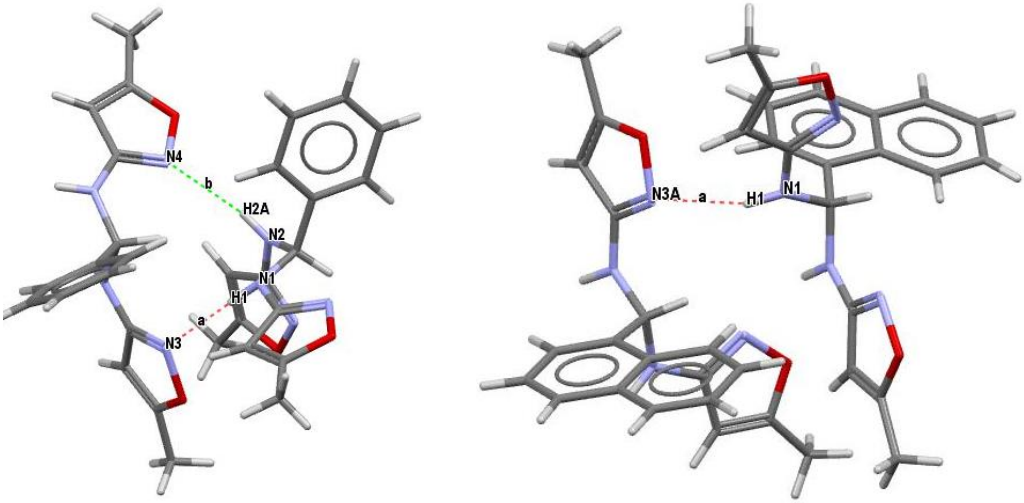

benz3AMI **Hnap3AMI**

Figure 2. Examples of hydrogen bonds formed in amines - unexpected products.

All studied derivatives of salicylaldehyde (sal) and 2-hydroxynaphthaldehyde (nap) create an intramolecular O1—H1···N1 hydrogen bond, which were described earlier [6-8]. This bond is characteristic for Schiff bases and leads to the formation of a S(6) six-membered ring [8]. The differences between conformations of molecules nap5AMI and nap3AMI are illustrated in Figure 3, showing the overlay of molecules by fitting of C1–C11 and C=N bonds.

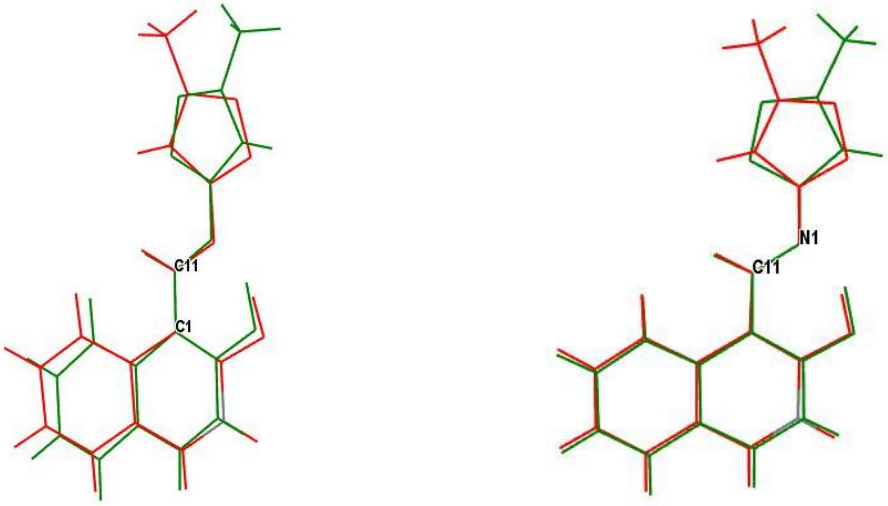

A **B**

Figure 3. Overlay of X-ray molecules of compounds nap5AMI (green) and nap3AMI (red) by least-squares fitting of the atoms: A) C1–C11 (RMS = 0.00375 Å); B) C11=N1 (RMS = 0.00574 Å).

References

[1] M.S. Saini, A. Kumar, J. Dwivendi, R. Singh, *Int. J. Pharma Sci. Res.*, **4** (2013) 66.
[2] M.A. Malik, O.A. Dar, P. Gull, M.y. Wani, A.a. Hashmi, *Med. Chem. Commun.*, **9** (2018) 409.
[3] M. Zimecki, U. Bąchor, M. Mączyński, *Molecules*, **23** (2018) 2724.
[4] K.T.A. Al-Sultani, *Int. J. Sci. Res.*, **6** (2017) 1567.
[5] B. Kołodziej, M. Morawiak, B. Kamieński, W. Schilf, *J. Mol. Struct.*, **1112** (2016) 81.
[6] A. Szady-Chełmieniecka, B. Kołodziej, M. Morawiak, B. Kamieński, W. Schilf, *Spectrochimica Acta Part A: Molecular and Biomolecular Spectridcopy*, **189** (2018) 330.
[7] R.-G. Zhao, J. Lu, J.-K. Li, *Acta Cryst.*, **E25** (2008) o499.
[8] H.-K. fun, M. Hemamalini, A.M. Asiri, S.A. Khan, *Acta Cryst.*, **E66** (2010) o1037.

A-42

NICKELOCENE MOLECULE ORDERING AT HIGH-PRESSURE CONDITIONS

Ida Moszczyńska, Andrzej Katrusiak

Department of Materials Chemistry, Adam Mickiewicz University, ul. Uniwersytetu Poznańskiego 8, 61-614 Poznań, Poland

Nickelocene and ferrocene are analogous sister sandwich compounds at ambient condition, both crystalize in monoclinic space group $P2_1/n$.[1,2] Cyclopentadienyl rings in the phase I of nickelocene crystal are disordered. However, the isothermal compression, from 0.1 MPa to 1.3 GPa in diamond-anvil cell, gradually orders the structure to the D_{5d} symmetric staggered conformation in the isostructural phase I', which appear at 1.3 GPa and is stable at high pressure. The associated anomalous crystal of nickelocene strain considerably differs from its isostructural ferrocene, where in phase I' cyclopentadienyl rings are ordered too. The ordering of structures in each crystal is associated with the gradually passing the ß angle of unit-cell through 90° by increasing pressure. Analogous ordering mechanism in nickelocene is induced by lowering temperature from 240 to 170 K,[3] while the ferrocene at low temperature undergoes a series of phase transitions by changing the crystal symmetry and leading to the eclipsed D_{5h}-symmetric conformer.

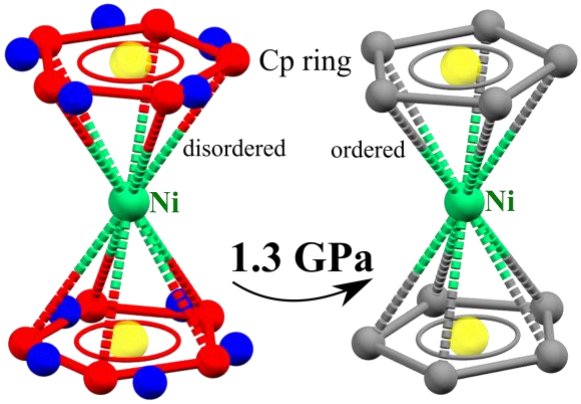

Fig. 1. Nickelocene molecule of disordered phase I and ordered phase I'.

References

[1] P. Seiler, J. D. Dunitz, *Acta Cryst. B.*, **38** (1980) 1741-1745.
[2] J. D. Dunitz, L. E. Orgel, A. Rich *Acta Cryst.*, **9** (1975) 373-375.
[3] G. Calvarin, D. Weigel, *J. Appl. Crystallog*., **9** (1976) 212-215.

A-43

ANALIZA METODAMI XRD, SEM-EDS & ICP-OES SKŁADU KOFEINOWYCH SUPLEMENTÓW DIETY SŁUŻĄCYCH DO SPORZĄDZANIA NAPOJÓW

Andrzej Żarczyński, Arkadiusz Niełacny, Waldemar Maniukiewicz, Jakub Kubicki, Małgorzata I. Szynkowska-Jóźwik

Politechnika Łódzka, Instytut Chemii Ogólnej i Ekologicznej, ul. Żeromskiego 116, 90-924 Łódź

Aktualnie na polskim rynku jest dostępnych wiele suplementów diety witaminowych oraz wzbogaconych w minerały, z których tylko niewielką część stanowią produkty zawierające kofeinę. Jednak rosnący trend spożywania kofeinowych suplementów diety, kawy, mocnej herbaty oraz innych napojów, m.in. gazowanych, prowadzi do wzrostu ilości spożywanej w nich kofeiny. Może to się - niestety wiązać z pewnymi negatywnymi konsekwencjami dla zdrowia konsumentów [1-6]. Problem ten dotyczy również proszkowych suplementów diety, które można bez ograniczeń nabywać, zarówno w sklepach jak i w aptekach. Mimo, że podczas produkcji tego typu preparatów zakłada się gwarancję bezpieczeństwa dla zdrowia i życia konsumenta, należy mieć na uwadze możliwość wystąpienia pewnych zagrożeń przy nieprawidłowym ich stosowaniu.

Celem pracy było zbadanie składu fazowego zawierających m.in. kofeinę proszkowych suplementów diety wykorzystywanych do sporządzania napojów energetycznych, mających na celu zmniejszenie uczucia zmęczenia człowieka oraz poprawę zdolności psychofizycznych. Przedmiotem badań było sześć suplementów diety służących do sporządzania napojów o nazwach handlowych: Vigor Up Fast, Sesja, Ale PowerUp, BE POWER Energy Drink, Bodymax Przypływ Energii, Plusssz Active 100% Energy Complex. Do analiz składu fazowego stosowano dyfraktometr polikrystaliczny X`PERT PRO MPD firmy PANanalytical, ze źródłem promieniowania CuKα uzyskiwanego w wyniku monochromatyzacji promieni X na filtrze niklowym. Do oceny składu fazowego próbek wykorzystano program X`Pert High Score Plus (ver. 4.9) oraz bazę standardów proszkowych ICDD PDF2 (ver. 2020). Badania morfologii lokalnych powierzchni suplementów realizowano także przy użyciu skaningowego mikroskopu elektronowego z przystawką do mikroanalizy rentgenowskiej (SEM-EDS). Analizy zawartości metali w próbach badanych suplementów wykonano metodą atomowej spektrometrii emisyjnej z plazmą sprzężoną indukcyjnie (ICP-OES), po uprzednim roztworzeniu ich w wodzie królewskiej.

Analizy suplementów diety wykazały obecność szeregu składników organicznych i nieorganicznych wymienionych przez producentów w ich specyfikacjach. Spośród związków nieorganicznych, m.in. wykryto wodorowęglan sodowy, węglan wapnia, krzemionkę i związki żelaza, a z grupy związków organicznych oprócz kofeiny tylko w części suplementów, niektóre witaminy, kreatynę, cukry proste i złożone, aspartam, kwas cytrynowy i D-sorbitol. Realizacja analizy wykazała, że dyfraktometria proszkowa może być skutecznie stosowana tylko do identyfikacji faz krystalicznych w suplementach występujących w ilości powyżej 0,5%. Badane suplementy diety można stosować do sporządzania napojów, ale należy ściśle przestrzegać zaleceń producentów i ich nie nadużywać.

A-43

Literatura
[1] H. Bojarowicz, P. Dźwigulska, *Hygeia Pub. Health*, **47(4)** (2012) 433.
[2] P. Nawrot, S. Jordan, J. Eastwood, J. Rotstein, A. Hugenholtz, M. Feeley, *Food Addit. Contam.*, **20(1)** (2003) 1.
[3] R. Wierzejska, *Rocz. Państ. Zakł. Hig.*, **63(2)** (2012) 141.
[5] M. Schlegel-Zawadzka, M. Barteczko, *Żywn. Nauk. Technol. Jakość*, **4(65)** (2019) 375.
[6] Z. Kotynia, P. Szewczyk, G. Tuzikiewicz-Gnitecka, *Kontr. Audyt*, **4** (2017) 49.

A-44

TWO POLIMORPHIC STRUCTURES OF 3-(DIETHOXYPHOSPHORYL)-1,2-DIHYDROQUINOLIN-4-OLS STABILIZED BY RESONANCE ASSISTED HYDROGEN BONDS

Przemysław Nowak[a], Anna Pietrzak[a], Jacek Koszuk[b], Tomasz Janecki[b], Wojciech M. Wolf[a]

(a) Institute of General and Ecological Chemistry, Łódź University of Technology
(b) Institute of Organic Chemistry, Łódź University of Technology
nowakprzemek0@gmail.com

Phosphonates and their aromatic derivatives are important class of compounds for medicine, the chemical industry and agriculture. Especially, they are also invaluable reagents for various synthetic routes, based on Horner-Wadsworth-Emmons (HWE) methodology.

The crystallisation of a 3-(diethoxyphosphoryl)-1,2-dihydroquinolin-4-ol derivative gave two polymorphic structures (I and II). Both have been stabilized by an intramolecular hydrogen bond defined by S(6) graph set notation. Geometrical parameters defining this intramolecular effect suggest that molecular conformations are constrained by strong planar resonance assisted hydrogen bond (RAHB) connecting phosphoryl and hydroxyl groups. RAHBs were reported in several C,H,N,O compounds, but RAHBs with phosphoryl and hydroxyl groups are rarely described in literature. Additionally, conformations of presented structures are stabilized by intramolecular hydrogen bonds provided by toluenesulphonyl (Tos) group.

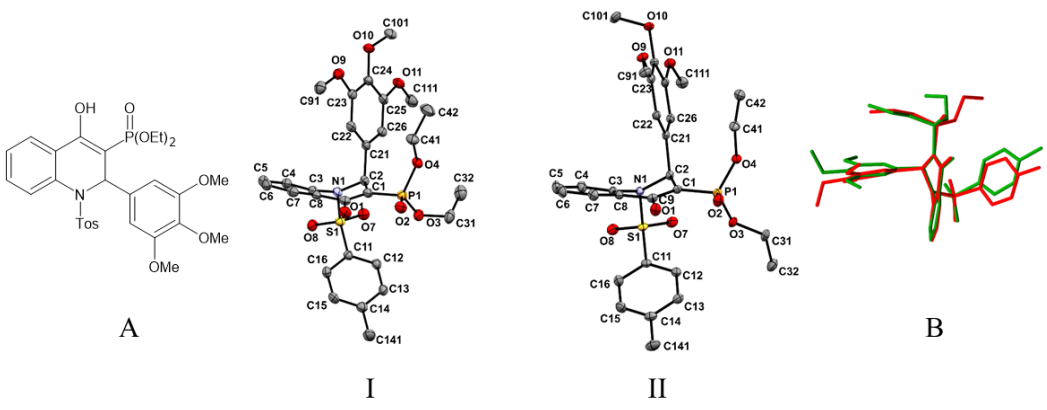

Fig. 1. Polymorphic structures **(I)** and **(II)**. Structural formula (A) and the overlay of I and II. Displacement ellipsoids are drawn at the 50% probability level; hydrogens are omitted for clarity.

Structural Data:
(I) a=15.3154(2), b=8.3635(2), c=22.9954(3) [Å], α=90 β=95.486(2) γ=90 [°], *P*-21, Z=4, R= 0.0399, S=1.040, T=100(2) K; **(II)** a=33.0671(2), b=9.9838(1), c=17.5183(1) [Å], α=90 β=95.748(1) γ=90 [°], *C*2/c, Z=8, R=0.0290 S=1.028, T=100(2) K**.**

A-45

SUPRAMOLECULAR MOTIFS IN 5*H*-PHENANTHRIDIN-6-ONE—OCTAFLUORONAPHTHALENE CO-CRYSTAL

Jan Alfuth[1], Katarzyna Kazimierczuk[2] and Teresa Olszewska[1]

[1] Department of Organic Chemistry, Faculty of Chemistry, Gdańsk University of Technology, Narutowicza 11/12, 80-233 Gdańsk
[2] Department of Inorganic Chemistry, Faculty of Chemistry, Gdańsk University of Technology, Narutowicza 11/12, 80-233 Gdańsk

Secondary amide groups participate in strong and highly directional intermolecular hydrogen bonding, facilitating formation of well-defined and stable solid-state architectures [1]. For this reason, they are relatively often studied in supramolecular chemistry, crystal engineering, and crystal design as building blocks. Studies have shown that molecules of lactams with *cis* conformation of the amide group (where the H–N–C=O torsion angle is 0°) aggregate through N−H···O bonds forming either homodimers (cyclic $R^2_2(8)$ synthons **I**) or C(4) chains (**II**) depending on the ring size (Fig. 1), the first being more common for 4- to 7-membered lactams [2].

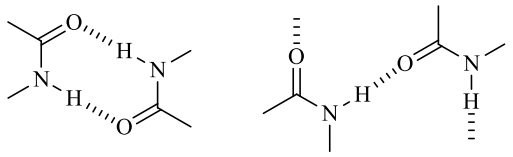

I **II**

Fig. 1. Supramolecular synthons for *cis*-amides.

2-Pyridone **1** (Fig. 2), which also belongs to the lactam family, has been obtained in two polymorphic forms: monoclinic, in which eight-membered $R^2_2(8)$ amide synthons (**I**) dominate, and orthorhombic, where the molecules form helical chains through the C=O···H–N interactions (synthon **II**) [3].

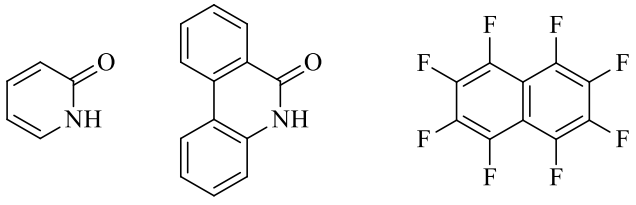

1 **2** **3**

Fig. 2. Molecular structures of **1**–**3**.

Inspired by this fact, we focused on (5*H*)-phenanthridin-6-one **2** (Fig. 2) being a lactam with an extended aromatic unit, which we previously studied. Its crystal structure comprises helices analogous to those found in **1** and a crystal where synthons **I** would form has not yet been obtained. We decided to investigate the possibility of changing the self-assembly of **2** from chains to dimers by co-crystallization with neutral

coformer. Because of its molecular size comparable to that of **2** and ability to participate in rather strong π-π stacking interactions, octafluoronaftalene **3** was chosen as the coformer. Indeed, by mixing **2** with **3** in the equimolar ratio in tetrahydrofuran we obtained a 1:1 co-crystal in which $\mathbf{2}_2$ homodimers are present (Fig. 3).

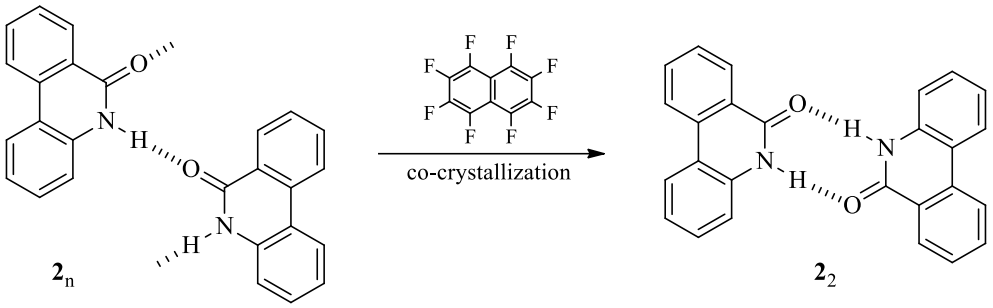

Fig. 3. Change of the crystal structure of **2** upon co-crystallization with **3**.

Additional information including crystallographic data, crystal packing and description of intermolecular interactions will be presented on the poster.

References

[1] G. R. Desiraju, *Angew. Chem. Int. Ed. Engl.*, **34** (1995) 2311–2327.
[2] C. Weck, E. Nauha, T. Gruber, *Cryst. Growth Des.*, **18** (2018) 7248−7253.
[3] H. D. Arman, P. Poplaukhin, E. R. T. Tiekink, *Acta Cryst.*, **E65** (2009) o3187.

A-46

KOOPERATYWNY EFEKT JAHNA-TELLERA WSPOMAGAJĄCY TESTOWANIE HOMOGENICZNOŚCI $LiMn_2O_4$

Jolanta Darul i Paweł Piszora

Zakład Chemii Materiałów, Wydział Chemii, Uniwersytet im. Adama Mickiewicza, Uniwersytetu Poznańskiego 8, 61-614 Poznań

Metoda Rietvelda zastosowana do udokładnienia struktury na podstawie wysokorozdzielczych dyfraktogramów proszkowych pozwala wychwycić subtelne odchylenia od nominalnej stechiometrii [1]. Również w przypadku próbek uznawanych za jednorodne przy zastosowaniu innych metod, wysokorozdzielcze pomiary w temperaturze pokojowej nie wykazały istotnych odchyleń od zadanej stechiometrii. Obniżenie temperatury powoduje jednak przemianę fazową związaną z uporządkowaniem i przestrzenną orientacją oktaedrów $Mn^{3+}O_6$. Dopasowanie kształtu refleksów dla niskotemperaturowej odmiany $LiMn_2O_4$ jest zadawalające przy zastosowaniu jednego modelu struktury $LiMn_2O_4$ o grupie przestrzennej *Fddd*. Wnikliwsza analiza pozwala uzyskać lepsze dopasowanie dla dwóch, niemal identycznych struktur. Porównanie stopnia odkształcenia regularnej sieci spinelowej dla tych faz umożliwia oszacowanie różnicy w zawartości litu. Różnica pomiędzy pseudo regularnym parametrem sieciowy dla tych faz wynosi 0.0006 Å, co przekładać się może na różnicę w zawartości litu ~0.002 w przeliczeniu na wzór $LiMn_2O_4$. Wartości te, ze względu na niepewności pomiarowe, są obecnie niemożliwe do wyznaczenia bezpośrednio z udokładnienia metodą Rietvelda w temperaturze pokojowej.

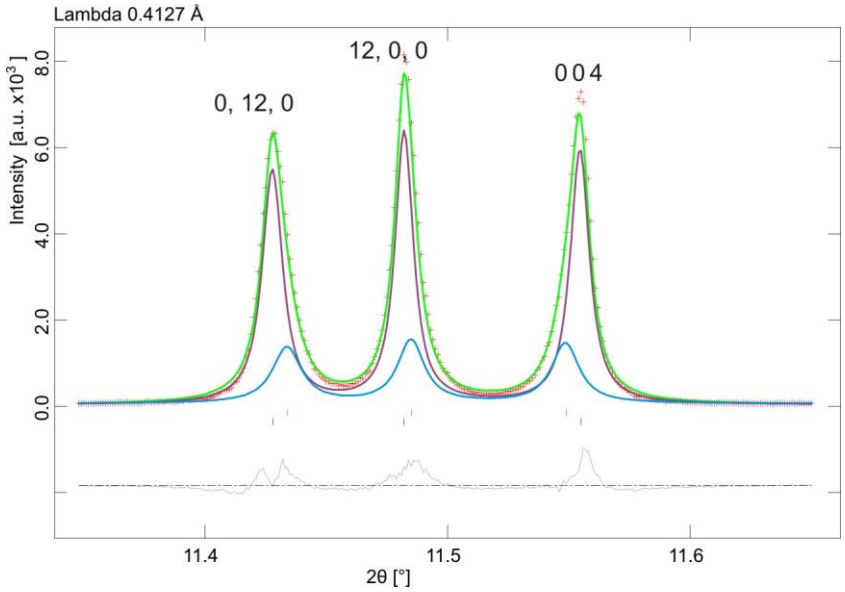

Rys. 1. Graficzny wynik dopasowania dyfraktogramu $LiMn_2O_4$ z uwzględnieniem 2 faz.

Literatura

[1] J. Darul, C. Popescu, F. Fauth, P. Piszora, *J. Phys. Chem. C*, **123**(32), (2019) 19288-19297.

A-47

SUPRAMOLECULAR APPROACH FOR FINE-TUNING OF FLUORESCENCE 8-HYDROXYQUINOLINE DERIVATIVES FROM METAL HALIDES

Marta Bogdan, Tomasz Sierański, Marcin Świątkowski, Agata Trzęsowska-Kruszyńska

Institute of General and Ecological Chemistry, Technical University of Łódź, Żeromskiego 116, 90-924, Łódź, Poland

Fine-tuning the fluorescent properties of small organic molecules using the supramolecular structure has been gaining more and more attention over the past few years [1,2,]. The use of metal halides as anions can favor the widening of the emission peaks and influences a large Stokes shift [3]. The most common central atoms are d-block elements due to the relatively small size of these atoms, while p-block elements constitute the most diverse central atoms. Moreover, the use of transition metals and p-block metals as coordination centers changes the electronic properties of the fluorophore, increasing or decreasing the emission intensity depending on the filling of the d-subshell. According to the Dexter mechanism and electron transfer mechanism, transition metal ions are notorious for their fluorescence quenching abilities [4]. In this first mechanism, an excited electron (first electron) is transferred from a donor molecule to an acceptor molecule via a non-radiative path, and the second electron from a quencher goes back to the donor. The second mechanism requires a charge transfer between donor and acceptor, leading to the formation of radical ions (cations or anions). These radicals undergo further electron transfer processes, and the final process is the restoration of the fluorophore and quencher in the ground state and the loss of excitation energy [5].

The present communication focuses on the synthesis and spectral characterization of 8-hydroxyquinoline novel derivatives with metal halides and examination of the influence of a metal halide on the emission properties of the ligand. Furthermore, halides can form polymer chains or mononuclear coordination entities, dilute the organic part in the solid phase, and influence the emission properties. The separation of 8-hydroxyquinoline cations using anionic coordination units contributes to the increase in fluorescence intensity, but it does not significantly affect the shift of the emission maximum. The emission maxima of the test compounds are in the range of 470 nm to 510 nm. The blue or cyan emission is created on 8-hydroxyquinoline molecules with π—π stacking interactions and appears during irradiation near-ultraviolet light (350-360 nm excitation wavelength). Supramolecular assembly using a fluorophore as a cation and an anion with the coordination center leads to the obtaining of structures with various spectral properties.

References

[1] X. Yu, Z. Wang, Y. Li, L. Geng, J. Ren, G. Feng, Inorganic Chemistry, **56** (2017) 7512–7518.
[2] D. Ghosh, O. Ragnarsdóttir, D. A. Tómasson K. K. Damodaran, *Symmetry*, **13** (2021) 112.
[3] V. Morad, S. Yakunin, M. V. Kovalenko, *Materials Lett*., **2** (2020) 845−852.
[4] L. Fabbrizzi, M. Licchelli, P. Pallavicini, D. Sacchi, A. Taglietti, Analyst, **121** (1996) 1763-1 768.
[5] L. Fabbrizzi, M. Licchelli, P. Pallavicini, A. Perotti, A. Taglietti, D. Sacchi, *Chemistry European Journal*, **2** (1996) 75-82.

A-48

PHOTOCRYSTALLOGRAPHIC STUDIES OF A SERIES OF COBALT (III) NITRO COMPLEXES

Patryk Borowski, Sylwia E. Kutniewska, Radosław Kamiński and Katarzyna N. Jarzembska

Department of Chemistry, University of Warsaw, Żwirki i Wigury 101, 02-089, Warsaw, Poland

Crystals which undergo light-induced photoisomerisation reaction have already found applications in optoelectronics, colour-changing materials, as high-capacity storage devices, etc. Transition-metal complexes, in which metal centre is coordinated by molecular fragments that can exist in multiple isomeric forms, are among potential functional materials of this kind. In this presentation a potential photoswitchable cobalt (III) nitro complexes will be presented. Studied compounds were prepared according to the synthesis procedure from [3]. Crystal structures of (b) and (c) have already been published in Cambridge Structural Database CCDC [4]. The nitro group is a well-known example of ambidentate ligand which may undergo photoisomerisation reaction in the solid state under certain conditions.

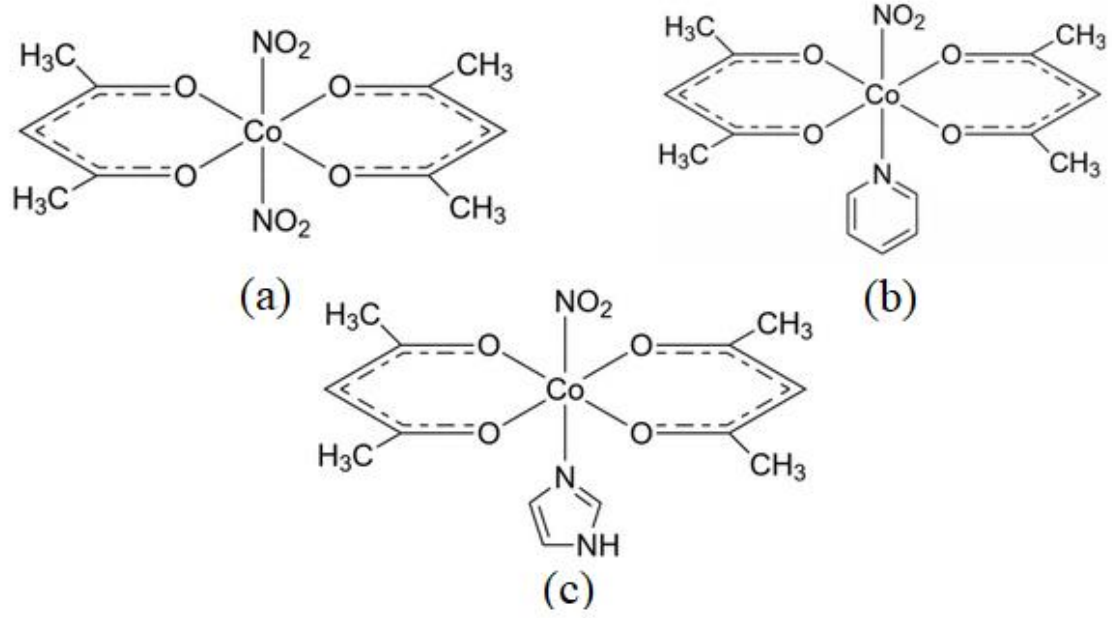

Fig. 1. Schematic representation of the studied compounds.

The main aim of this study was to examine the photoreactivity of the obtained crystal systems and understand potential linkage isomerization reaction mechanism.

All studied compounds crystallize in the monoclinic $P2_1/c$ space group. Compound (a) crystallizes with sodium positive ion between two $Co(acac)_2(NO_2)_2$ unites. The crystals are stabilized majorly by *C-H···O* hydrogen-bond-like contacts involving the nitro group and acetylacetone. All molecules presented above crystallize

forming characteristic layered network. The photoswitchable properties were confirmed by the photocrystallographic experiments using 365-470 nm LED excitation light.

The authors thank the PRELUDIUM grant (2017/25/N/ST4/02440) of the National Science Centre in Poland, University of Warsaw, for financial support. The Wrocław Centre for Networking and Supercomputing (grant No. 285) is gratefully acknowledged for providing computational facilities. The in-house X-ray diffraction experiments were carried out at the Department of Physics, University of Warsaw, on Rigaku Oxford Diffraction SuperNova diffractometer, which was co-financed by the European Union within the European Regional Development Fund (POIG.02.01.00-14.122/09).

References

[1] R.Kamiński, K.N.Jarzembska, S.E.Kutyla, M.Kamiński, *J.Appl.Cryst.*, **49** (2016), 1383.
[2] L.E.Hatcher, J.M.Skelton, M.Warren, P.R.Raithby, *Acc.Chem.Res.*, **52** (2019), 1079.
[3] L.Boucher, J.Bailrar, *J.Inorg. &Nucl.Chem*., **27** (1964), 1093.
[4] S.Ohba, M.Tsuchimoto, H.Miyazaki, *Acta Cryst. Section E*, **74** (2018), 11 1637-1642.

A-49

TUNING OF CRYSTAL STRUCTURES AND OPTICAL PROPERTIES VIA HALIDE SUBSTITUTION IN NON-CENTROSYMMETRIC 3D HYBRID PEROVSKITES COMPRISING METHYLHYDRAZINIUM CATIONS

Dawid Drozdowski,[a] **Anna Gągor**,[a] **Dagmara Stefańska**,[a] **Jan K. Zaręba**,[b] **Katarzyna Fedoruk**,[b] **Mirosław Mączka**[a] **i Adam Sieradzki**[b]

[a]*Instytut Niskich Temperatur i Badań Strukturalnych PAN, ul. Okólna 2, 50-422 Wrocław*
[b]*Politechnika Wrocławska, ul. Wybrzeże Wyspiańskiego 27, 50-370 Wrocław*

Hybrid organic-inorganic perovskites (HOIPs) have been the subject of intense studies in recent years due to their various functional and tuneable properties. General formula of HOIPs is the same as for their inorganic analogues, that is ABX_3, where "A" cations occupy 12-fold coordinated holes between the corner-sharing BX_6 octahedra [1]. In HOIPs, "A" stands for an organic cation, "B" is a metal ion and "X" can be either organic or inorganic element/group (e.g. halides, formates, azides, *etc.*) [2]. Among these systems, 3D lead halide HOIPs with methylammonium (MA^+) and formamidinium (FA^+) cations on "A" site are especially attractive from the applicational point of view. Multiple studies exposed their interesting physical and chemical properties, such as high photoluminescence (PL) yields, power conversion efficiencies around 25%, broad tunability of colours, amazing mobility of charge carriers and so on. These properties, combined with low cost and effortless synthesis, open unlimited paths of a novel applications for a photovoltaic technology, light emitting devices, photodetectors or in photodynamic therapy [3–5].

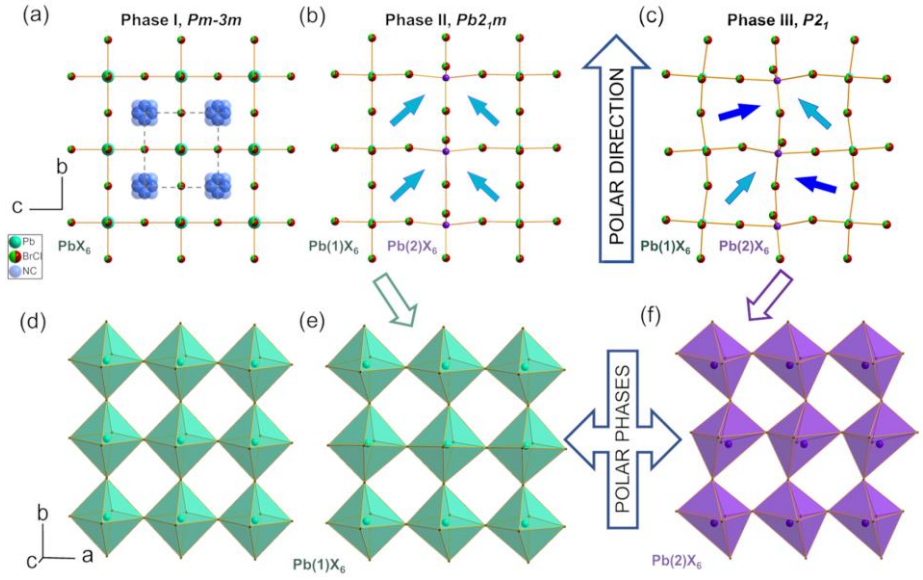

Fig. 1. (a, b, c) Crystal structures of $MHyPbBr_xCl_{3-x}$ for phase **I**, **II** and **III**, respectively. Arrows in (b, c) represent location of MHy^+ dipoles. In II and III molecules are oriented along the polar direction. (d) Single [100] layer in I built of PbX_6 (X = Br, Cl) octahedra. (e, f) [100] layers of (e) $Pb(1)X_6$ and (f) $Pb(2)X_6$ octahedra in both polar phases (**I**, **II**).

.

Another crucial advantage of lead halide HOIPs is a possibility of developing new 3D analogues via replacing organic or inorganic ions. Our group have successfully employed 3D lead halide HOIPs with methylhydrazinium (MHy^+) cation. $MHyPbBr_3$ exhibit a switchable dielectric behaviour, strong second-harmonic generation (SHG) activity and thermochromism, while in $MHyPbCl_3$ enhancement of a SHG response in the high-temperature (HT) phase is observed [6, 7]. Also, mixing halogen anions at the "X" site turned out to be a straightforward way to enhance desired optical behaviour, combining benefits of particular halides [8, 9].

We would like to present structural studies of 3D mixed-halide HOIPs, $MHyPbBr_xCl_{3-x}$ and $MHyPbBr_{2.8}I_{0.2}$. Both systems crystallize in a polar $P2_1$ structure, analogously to RT phases of $MHyPbBr_3$ and $MHyPbCl_3$. For the high-x compositions ($x \geq 1.33$) both HT phases of $MHyPbBr_3$ and $MHyPbCl_3$ are observed (cubic Pm-3m for $T_1 \geq 409$ K and orthorhombic $Pb2_1m$ for $T_2 \geq 318$ K, respectively), while for the lower bromine concentration cubic phase vanishes. An existence of the cubic phase strongly depends on the volume of the voids between the PbX_6 octahedra, in which MHy^+ cations are placed. The orthorhombic phase, which was not observed for the bromine analogue, starts to appear with a relatively low excess of Cl. Similarly to $MHyPbBr_3$, $MHyPbBr_{2.8}I_{0.2}$ undergo a direct phase transition from $P2_1$ to Pm-3m but at lower temperature T_1 = 390 K (408 K for $MHyPbBr_3$). Linear optical studies show the narrowing of energy band-gap and red shift of excitonic absorption and emission band with increasing Br concentration.

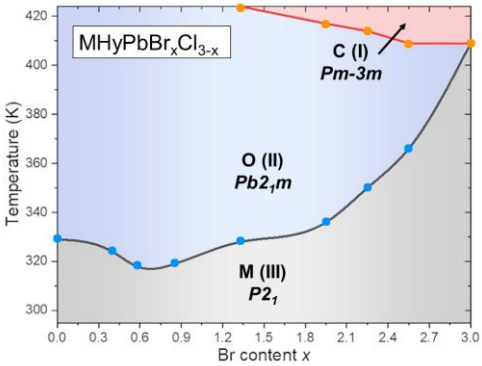

Fig. 2. Phase diagram of $MHyPbBr_xCl_{3-x}$ perovskites showing cubic (C) phase **I**, orthorhombic (O) **II** and monoclinic (M) phase **III**. The dots represent transition temperatures upon cooling obtained from the DSC measurements. The curves represent interpolation of the phase boundaries.

References

[1] D. B. Mitzi, *Progress in Inorganic Chemistry*, wiley, **48** (1999) 1–121.
[2] A. Poglitsch, D. Weber, *J. Chem. Phys.*, **87** (1987) 6373–6378.
[3] R. Lin, K. Xiao, Z. Qin, Q. Han, C. Zhang, M. Wei, M. I. Saidaminov, Y. Gao, J. Xu, M. Xiao, A. Li, J. Zhu, E. H. Sargent, H. Tan, *Nat. Energy*, **4** (2019) 864–873.
[4] H. Mehdi, A. Mhamdi, R. Hannachi, A. Bouazizi, *RSC Adv.*, **9** (2019) 12906–12912.
[5] M. Cao, J. Tian, Z. Cai, L. Peng, L. Yang, D. Wei, *Appl. Phys. Lett.*, **109** (2016) 233303.
[6] M. Mączka, M. Ptak, A. Gągor, D. Stefańska, J. K. Zaręba A. Sieradzki, *Chem. Mater.*, **32** (2020) 1667–1673.
[7] M. Mączka, A. Gagor, J. K. Zaręba, D. Stefanska, M. Drozd, S. Balciunas, M. Šimėnas, J. Banys, A. Sieradzki, *Chem. Mater.*, **32** (2020) 4072–4082.
[8] M. Liu, M. B. Johnston, H. J. Snaith, *Nature*, **501** (2013) 395–398.
[9] X. Wu, M. T. Trinh, D. Niesner, H. Zhu, Z. Norman, J. S. Owen, O. Yaffe, B. J. Kudisch, X. Y. Zhu, *J. Am. Chem. Soc.*, **137** (2015) 2089–2096.

A-50

CRYSTAL STRUCTURE OF $EuCo_{9.4}Si_{3.6}$

Bohdana Belan[1], Marek Daszkiewicz[2], Mariya Dzevenko[1], Mykola Manyako[1], Roman Gladyshevskii[1]

[1]Department of Inorganic Chemistry, Ivan Franko National University of L'viv, Kyryla i Mefodia Str. 6, 79005 L'viv, Ukraine
[2]Institute of Low Temperature and Structure Research, Polish Academy of Sciences, P. O. Box 1410, 50-950 Wrocław 2, Poland

During investigation of the isothermal section of the Eu-Co-Si ternary system in the whole concentration range by X-ray diffraction at 673 K we have found the $EuCo_{9.8}Si_{3.2}$ compound with unknown structure [1].

Therefore, we present the results of the complete crystal structure investigation of this compound. The sample with $Eu_{7.14}Co_{70}Si_{22.85}$ composition was prepared by arc-melting of the compact metals under an argon atmosphere and annealed at 673 K for 720 h. X-ray diffraction data were collected on a diffractometer Xcalibur Atlas CCD operating in kappa geometry, using Mo *K*α radiation at 293 K. The crystal structure was solved by the Patterson method and refined by full-matrix least-squares method, using the program SHELXL-2018/3 [2].

Crystallographic data and parameters for the data collection and refinement for the compound $EuCo_{9.4}Si_{3.6}$ (structure type $CeNi_{8.5}Si_{4.5}$, Pearson symbol *tI*56) are listed in the Table. The refined atomic coordinates and displacement parameters are the following: Eu 4*a* 0 0 ¼, U_{eq} = 0.0061(3) Å^2; Co1 16*l* 0.37256(12) 0.12744(12) 0.18018(12), U_{eq} = 0.0058(3) Å^2; Co2 16*k* 0.19981(17) 0.06923(17) 0, U_{eq} = 0.0055(3) Å^2; Co3 4*d* ½ 0 0, U_{eq} = 0.0050(6) Å^2; Si1 16*l* 0.1710(2) 0.3290(2) 0.1213(2), U_{eq} = 0.0058(9) Å^2, occ. = 0.914(9); Co4 16*l* 0.1710(2) 0.3290(2) 0.1213(2), U_{eq} = 0.0058(9) Å^2, occ. = 0.086(9).

Crystallographic data and parameters for the data collection and refinement

Crystallographic data	Data collection	Refinement
Space group *I*4/*mcm*	*T* = 293(2) K	25 refined parameters
a = 7.7955(6)	193 independent	240 $I > 2\sigma(I)$
c = 11.4918(15)	reflections	
V = 698.36(14)	ω-scan	*R* = 0.0484 (0.0307)
D_x = 7.659	-10≤*h*≤10,	*wR* = 0.0450
	-10≤*k*≤9,	(0.0419)
absorption coefficient	-14≤*l*≤14	analytical
μ = 30.928		absorption correction

Literature

[1] B.D. Belan, *Thesis*, Lvov State University, 1988 (in Russian).
[2] G. M. Sheldrick, *Acta Crystallogr. C***71** (2015) 3.

A-51

CRYSTAL SYMMETRY FOR INCOMMENSURATE HELICAL AND CYCLOIDAL MODULATIONS

Piotr Fabrykiewicz, Radosław Przeniosło and Izabela Sosnowska

Wydział Fizyki, Uniwersytet Warszawski, ul. Pasteura 5, 02-093 Warszawa

A classification of magnetic superspace groups [1-3] compatible with the helical and cycloidal magnetic modulations (see Fig. 1) is presented [4]. Helical modulations are compatible with groups from crystal classes with proper rotations-only i.e. 1, 2, 222, 4, 422, 3, 32, 6 and 622. Cycloidal modulations are compatible with groups from crystal classes 1, 2, m and mm2. For each magnetic crystal class, the directions of the symmetry allowed (non-modulated) net ferromagnetic moment and electric polarization are given. The proposed classification of superspace groups is tested on experimental studies including e.g. type-II multiferroics published in the literature as well as $MnAu_2$ [5], β-MnO_2 [6], $MnSO_4$ [7], Cr_2BeO_4 [8], $BiFeO_3$ [9]. The important conclusion is that cycloidal magnetic ordering is incompatible with trigonal and hexagonal lattices including the kagome one.

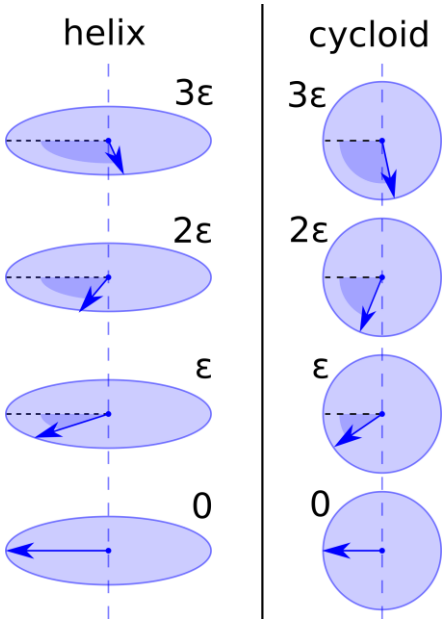

Fig. 1. Schematic picture of helical (left panel) and cycloidal (right panel) type incommensurate magnetic orderings.

Bibliography

[1] A. Janner and T. Janssen, *Acta Cryst. A*, **36** (1980) 399.
[2] P. M. de Wolff, T. Janssen and A. Janner, *Acta Cryst. A*, **37** (1981) 625.
[3] J. M. Perez-Mato, J. L. Ribeiro, V. Petricek and M. I. Aroyo, *J. Phys. Condens. Matter*, **24** (2012) 163201.
[4] P. Fabrykiewicz, R. Przeniosło and I. Sosnowska, *Acta Cryst. A.*, **77** (2021) 160.
[5] A. Herpin, P. Meriel and J. Villain, *C. R. Acad. Sci.* (Paris), **249** (1959) 1334.
[6] A. Yoshimori, *J. Phys. Soc. Jpn*, **14** (1959) 807.
[7] G. Will, *Acta Cryst.*, **19** (1965) 854.
[8] D. E. Cox, B. C. Frazer, R. E. Newnham and R. P. Santoro, *J. Appl. Phys.*, **40** (1969) 1124.
[9] I. Sosnowska, T. P. Neumaier and E. Steichele, *J. Phys. C Solid State Phys.* **15** (1982) 4835.

A-52

MODEL DEPENDENCE (IAM VS. TAAM) OF B-FACTORS – CASES OF X-RAY AND ELECTRON DIFFRACTION

Barbara Gruza, Christian Jelsch, Paulina M. Dominiak

Uniwersytet Warszawski, Wydział Chemii, Pasteura 1, 02-093 Warszawa
b.gruza@ uw.edu.pl

It is known that B-factors correlate with measurement temperature, crystals quality, disorder, etc.. They also correlate with resolution. In case of X-ray diffraction (XRD) higher values of B-factors are connected with lower resolution [1]. In case of electron diffraction (3D-ED) there are additional factors: dynamic scattering and radiation damage, so the trend in B-factors values is not so obvious as for XRD. But is there a systematic difference between sizes of B-factors if the only variable is a model of static density? Would it be the same for different crystal structures (small organic molecules, polypeptides, proteins)? How the difference would depends on resolution? Would it be the same in case of X-ray and electron diffraction?

It was also shown, that different scattering models – e.g. Independent Atom Model (IAM; spherical, not describing bonds, lone pairs, charge transfer etc.) or Transferable Aspherical Atom Model (TAAM; describing asphericity, but in fixed manner, not refined) can be used for structure refinements with diffraction data [2]–[4]. Here we present comparison of B-factors from IAM and TAAM refinements of different types of crystal structures: carbamazepine (small molecule) from XRD and 3D-ED [5], [6], peptide pseudoxylallemycin A from XRD [7] and peptide OsPYL/RCAR5 from 3D-ED [8], lysozyme from XRD and 3D-ED [9], [10]. We observe systematic difference in B-factors from these two refinements, however results still need discussion and we hoped for that during the conference.

Support of this work by the National Centre of Science (Poland) through grant OPUS No.UMO-2017/27/B/ST4/02721 is gratefully acknowledged.

Bibliography

[1] O. Carugo, *Zeitschrift fur Krist. - Cryst. Mater.*, **234** (1) (2019) 73–77.
[2] W. F. Sanjuan-Szklarz, A. A. Hoser, M. Gutmann, A. Ø. Madsen, and K. Woźniak, *IUCrJ*, **3** (2016) 61–70.
[3] K. K. Jha, B. Gruza, P. Kumar, M. L. Chodkiewicz, and P. M. Dominiak, *Acta Crystallogr. Sect. B Struct. Sci. Cryst. Eng. Mater.*, **76** (2020) 296–306.
[4] B. Gruza, M. L. Chodkiewicz, J. Krzeszczakowska, and P. M. Dominiak, *Acta Crystallogr. Sect. A Found. Adv.*, **76** (2020) 92–109.
[5] I. Sovago, M. J. Gutmann, H. M. Senn, L. H. Thomas, C. C. Wilson, and L. J. Farrugia, *Acta Crystallogr. Sect. B Struct. Sci. Cryst. Eng. Mater.*, **72** (1) (2016) 39–50.
[6] C. G. Jones *et al.*, *ACS Cent. Sci.*, **4** (11) (2018) 1587–1592.
[7] A. J. Cameron, C. J. Squire, A. Gérenton, L. A. Stubbing, P. W. R. Harris, and M. A. Brimble, *Org. Biomol. Chem.*, **17** (16) (2019) 3902–3913.
[8] M. Gallagher-Jones *et al.*, *IUCrJ*, **7** (2020) 490–499.
[9] J. Wang, M. Dauter, R. Alkire, A. Joachimiak, and Z. Dauter, *Acta Crystallogr. Sect. D Biol. Crystallogr.*, **63** (12) (2007) 1254–1268.
[10] M. J. de la Cruz *et al.*, *Nat. Methods*, **14** (4) (2017) 399–402.

PLAKATY – SESJA B
POSTERS – SESSION B

B-01

DESIGNED FUNCTIONALITIES OF MX AND SAXS ENDSTATIONS OF THE SOLCRYS BEAMLINE AT NSRC SOLARIS

Joanna Sławek, Tomasz Kołodziej, Grzegorz Gazdowicz, Maciej Kozak

National Synchrotron Radiation Centre SOLARIS, Jagiellonian University, ul. Czerwone Maki 98, 30-392 Kraków

SOLCRYS is a wiggler-based beamline, designed for operation in hard X-ray range, that is currently under construction. It is designed to perform a variety of X-ray diffraction and scattering experiments, including determination of spatial structures of biological macromolecules, atomic structures of crystalline materials, characterizations of structural phase transitions induced by high pressure or temperature, analyses of macromolecular systems in solution, and studies on the molecular organization of disordered or flexible systems. The beamline will be divided into two independent endstations: MX (macromolecular crystallography) and SAXS (small-angle X-ray scattering).

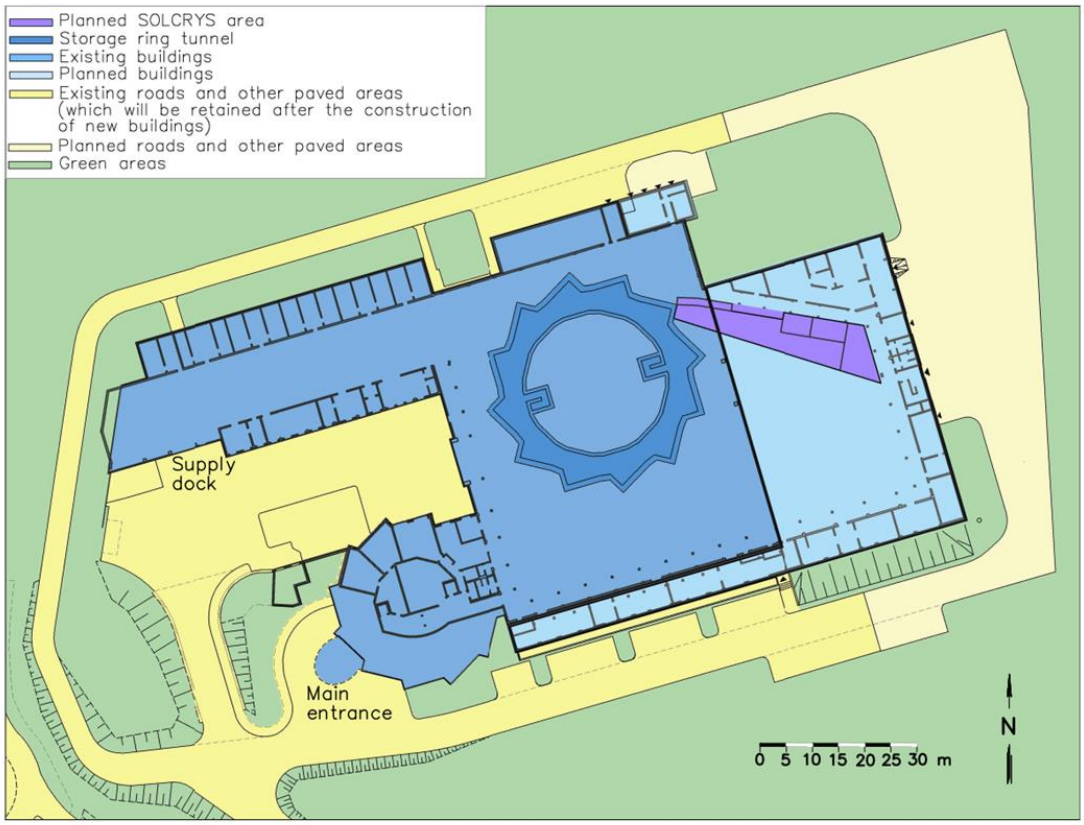

Fig. 1. Location of the SOLCRYS beamline (purple) in NSRC SOLARIS. The beamline will be located in the extended part of experimental hall.

B-01

MX endstation is designed for X-ray diffraction studies of biomacromolecules (proteins, nucleic acids) and also small molecules. In addition to standard measurement conditions, this beamline should offer future users the possibility to use a variety of tools and enhancements to customize the experiment and get high-quality data. The expected research capabilities of the MX endstation include tuneable radiation wavelength in the range 4-25 keV for multi-wavelength anomalous diffraction (MAD) experiments and high-flux mode for standard (routine) diffraction data collection on macromolecule crystals (also in He atmosphere). It is planned that the SOLCRYS beamline will be fully automated, allowing on-site and remote access. To meet the expectation of our future users, it is planned to include several functionalities to the MX endstations:

Crystallography goniometer – it is planned to equip the beamline with a microdiffractometer allowing a precise positioning of the sample and performing conventional and serial crystallography diffraction measurements in the X-ray beam. The diffractometer will be equipped with an on-axis microscope and will be compatible with a sample changing robot. The planned functionality of the goniometer will be similar to one described by Meents et al. [1].

Temperature and high pressure attachments – it is designed to equip the beamline with a high-pressure attachment allowing measurements with the pressure up to 10 GPa. This setup will be compatible with DAC and other standard pressure chambers. For the low-temperature measurements, it is planned to equip the endstation with a cryocooler, allowing to cool down the sample with LN_2 and maintain the stable cryogenic temperature.

Helium enclosure – it is planned to equip the beamline with a helium enclosure or tent, allowing the measurements in a helium atmosphere.

The SAXS endstation is intended to be applied for small-angle scattering experiments on solutions of biomacromolecules (BioSAXS) performed in the "high-flux" data collection mode and for high-resolution measurements (including anomalous scattering experiments) as well.

The BioSAXS endstation will be equipped with a fully automated autosampler for liquid samples and exposition unit with a removable sample holder adopted for the temperature or pressure measurements. It is planned to include the chromatographic system in the setup to allow performing SEC-SAXS experiments.

This project is carried out in cooperation with the Joint Institute for Nuclear Research (Dubna, Russia).

References

[1] A. Meents, et all., *Nat. Commun.*, **8** (2017) 1281.

B-02

NOVEL APPROACH TO STRUCTURE DETERMINATION OF COMPLEX PROTEIN SYSTEM HYP-1/ANS

Joanna Śmietanska[1], Joanna Śliwiak[2], Mariusz Jaskólski[2], Mirosław Gilski[2], Zbigniew Dauter[3], Ireneusz Bugański[1], Radosław Strzałka[1], Janusz Wolny[1]

[1]AGH University of Science and Technology, al. Mickiewicza 30, 30-059 Krakow, Poland,
[2]Center for Biocrystallographic Research, Institute of Bioorganic Chemistry, Polish Academy of Sciences, Zygmunta Noskowskiego 12/14, 61-704 Poznan, Poland,
[3]Synchrotron Radiation Research Section, MCL, National Cancer Institute, Argonne National Laboratory, Argonne IL 60439, USA

Newly discovered, and still uncommon, modulated crystal structure in organic systems require a deeper investigation. No exact and detailed solution of such systems has not been done up-to-date. One possibility is to use an approximation of commensurate modulation which enables constructing a supercell, extending to the case, where translational symmetry (periodicity) is recovered, and simplify the analysis. An assumption of commensurateness of the modulation is, however, questionable and rather unverifiable. The goal of our studies was to use a novel, original statistical method of structural modeling which enables a refinement based on the average unit cell with (commensurate or incommensurate) modulation without unclear assumption of commensurateness and supercell approach. The main concept of the statistical method is to express structure in terms of the statistical distribution of atomic positions concerning the periodic reference lattice with lattice constant related to characteristic length-scale present in the structure [1]. The average unit cell, defined as a probability distribution, constructed for periodic crystal is the same as the unit cell. The statistical approach was successfully used for the description of not only periodic crystals or quasicrystals, as well as it can be expanded on modulated structures as well as aperiodic structures with singular continuous components in the diffraction pattern.

Our model system is a pathogenesis-related protein (Hyp-1) complex with fluorescent probe 8-anilino-1-naphthalene sulfonate (ANS), which is a unique example of a macromolecular system with a modulated crystal structure. Previous studies have shown that Hyp-1/ANS complexes are tetartohedral twinned and crystallized in an asymmetric unit cell containing a repetitive motif of four protein molecules arranged with 7-fold noncrystallographic repetition along the **c** axis of the C2 space group [2]. Assumption of commensurate structure modulation demanded description of structure in the highly expanded unit cell with 28 unique protein molecules inside. The Hyp-1/ANS structure was solved by molecular replacement and refined using maximum-likelihood targets with reliability factors R_{work}/R_{free} of 22.3/27.8%, respectively. Our approach involved re-integration of raw data, development of the original software in Matlab environment and multidimensional analysis used to build the structure model and perform the refinement for significant improvement of results. The problem of incorporating disorder in the form of phonons into structural analysis was also carried out traditionally by the Debye-Waller factor.

B-02

Literatura
[1] J. Wolny, I. Buganski, P. Kuczera, R. Strzalka, *J. App. Cryst.* **49** (2016), 2106-2115.
[2] J. Sliwiak, Z. Dauter, M. Kowiel, A.J. McCoy, R.J. Read, M. Jaskólski, *Acta Cryst.* D**71** (2015), 829–843.

B-03

INFLUENCE OF METHYL SUBSTITUENT POSITION ON THE CRYSTAL STRUCTURES AND ANTIMICROBIAL ACTIVITY OF 4-METHYL-1,6-DIPHENYL-2[1*H*]-PYRIMIDINESELENONE DERIVATIVES

Waldemar Tejchman[a], Izabela Korona-Głowniak[b], Wojciech Nitek[c], Ewa Żesławska[a]

[a]*Institute of Biology, Pedagogical University, Podchorążych 2, 30-084 Kraków*
[b] *Department of Pharmaceutical Microbiology, Medical University of Lublin, Chodźki 1, 20-093 Lublin*
[c]*Faculty of Chemistry, Jagiellonian University, Gronostajowa 2, 30-387 Kraków*

Staphylococcus aureus is an important human pathogen which causes a range of infections from mild skin and soft-tissue infections to life-threatening endocarditis, chronic osteomyelitis, pneumonia or bacteremia. The infections are frequently associated with significant morbidity and mortality. *S. aureus* rapidly acquired resistance to antibiotics. Infections with penicillin-resistant *S. aureus*, as well as methicillin-resistant *S. aureus* (MRSA) are difficult to treat [1].

Our previous studies [2,3] allowed to identify a series of pyrimidineselonone derivatives with very good anti-staphylococcal and anti-Candida activities. As the next step in our research, we modified the previously investigated active compounds by replacing methoxy group with methyl group in aromatic ring at position 1.

In order to investigate structural properties of compounds containing methyl substituent in three different positions, we determined crystal structures of 4-methyl-1-(2'-methylphenyl)-6-phenyl-2[*1H*]-pyrimidineselenone (**1**), 4-methyl-1-(3'-methyl-phenyl)-6-phenyl-2[*1H*]-pyrimidineselenone (**2**) and 4-methyl-1-(4'-methylphenyl)-6-phenyl-2[*1H*]-pyrimidineselenone (**3**).

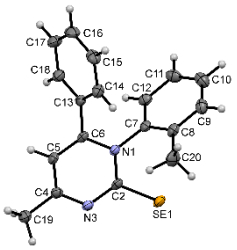

1

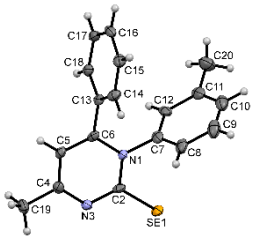

2

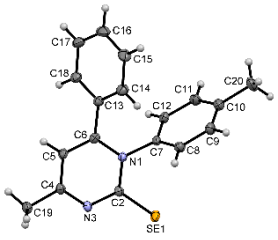

3

We analyzed the impact of methyl substituent positions (*ortho* - **1**, *meta* - **2** and *para* - **3**) on the crystal and molecular structures. The presented compounds were also evaluated towards their *in vitro* antimicrobial activity. All investigated derivatives crystallize in $P2_1/c$ space group with one molecule in the asymmetric unit. The packing of the molecules is determined by weak C-H···N and C-H···Se intermolecular interactions. The investigated methyl-containing derivatives exhibit very strong bioactivity against staphylococci and fungi, while **2** and **3** show higher activity in the tested series.

B-03

References
[1] H. F. Chambers, F. R. DeLeo, *Nat. Rev. Microbiol*., **9(629)** (2009) 641.
[2] E. Żesławska, I. Korona-Głowniak, M. Szczesio, *et al., J. Mol. Str.*, **1142** (2017) 261.
[3] E. Żesławska, I. Korona-Głowniak, W. Nitek., W. Tejchman, *Acta Cryst. C.*, **76** (2020) 359.

B-04

CAN *E.COLI* PLANT-TYPE L-ASPARAGINASE ACT AS POTASSIUM-DEPENDENT ENZYME? STRUCTURAL STUDIES OF ECAIII AND ITS NEW VARIANT

Anna Wantuch[1], Mariusz Jaskólski[2,3], Joanna Loch[1]

[1]Jagiellonian University, Faculty of Chemistry, Kraków, Poland
[2]Polish Academy of Sciences, Institute of Bioorganic Chemistry, Poznań, Poland
[3]A. Mickiewicz University, Faculty of Chemistry, Poznań, Poland

L-asparaginase is an enzyme that catalyzes the hydrolysis of L-Asn to L-Asp and ammonia. Based on phylogenetic analysis, biochemical and crystallographic data, L-asparaginases were classified into three Classes: bacterial-type (Class 1), plant-type (Class 2), and *R.etli*-type (Class 3) [1,2]. Plant-type L-aspargainases can be further subdivided into potassium-dependent and potassium-independent enzymes.

All plant-type L-asparaginases possess a sodium binding loop (often referred to as the stabilization loop), which includes residues that interact with the catalytic Thr via a hydrogen bond network. Potassium-dependent enzymes have an additional alkali metal-binding loop (activation loop) [3]. This loop regulates the activity of the enzyme by binding the Na^+ or K^+ cations, and consequently affecting the conformation of residues critical for substrate binding. Crystallographic and spectroscopic studies revealed that a Ser residue located at the activation loop of a potassium-dependent enzyme from *Phaseolus vulgaris*, PvAIII(K), is crucial for the coordination of the metal cations and enzyme activity: when Ser is replaced by Ile, the enzyme loses its dependence on potassium. Conversely, the introduction of Ser at the appropriate position of the K-independent enzyme from *P. vulgaris* resulted in the emergence of potassium sensitivity [4].

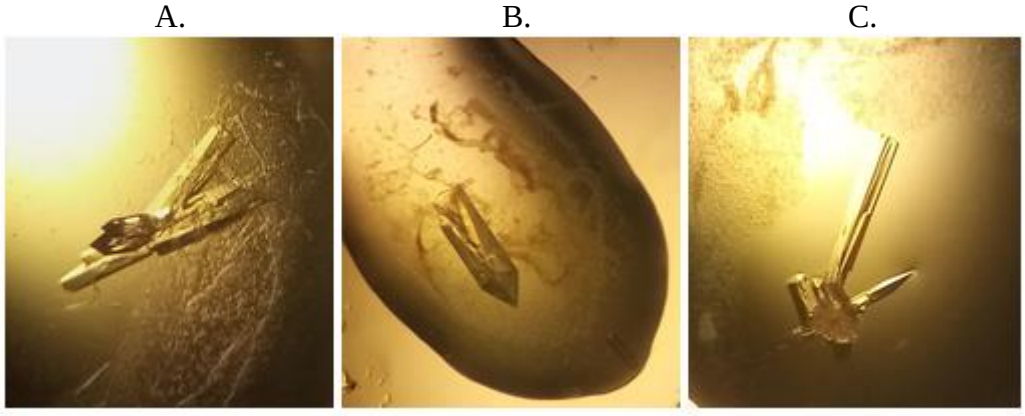

Fig. 1. Crystals of WT EcAIII (A, B) and V120S variant (C). Despite poor morphology, the crystals reach relatively large dimensions (up to 1 mm) and diffract X-rays to 1.4–1.7 Å.

EcAIII is a plant-type L-asparaginase encoded in the *E. coli* genome. EcAIII is a potassium-independent enzyme. To verify if the enzymatic activity of EcAIII can be regulated by the presence of Na^+/K^+ and modify the region corresponding to the activation loop in PvAIII(K), we prepared a V120S mutant of EcAIII. The mutant

protein was expressed, purified, and crystallized (Fig. 1) in the presence of different low-molecular-weight ligands. In parallel, similar crystallization experiments were performed for the WT protein. High-resolution X-ray diffraction data (1.4–1.7 Å) were collected for both the WT protein and the V120S mutant. The crystal structures raveled structural changes in the region of the mutation that are propagated by a series of atomic shifts to the active site. However, the character of these changes is different than observed in PvAIII(K) in the presence or absence of Na^+/K^+ ions [3].

Work supported by NCN grant 2020/38/E/NZ1/00035

References

[1] D. Borek, M. Jaskolski, *Acta Biochim. Pol.*, **48** (2001) 893–902.
[2] L. da Silva et al., *Biotechnol Appl Biochem*, **in press** (2021).
[3] M. Bejger et al., *Acta Cryst. D*, **70** (2014) 1854–1872.
[4] E. Ajewole, et al., *FEBS J*., **285** (2018) 1528–1539.

B-05

INTERACTIONS BETWEEN SELECTED TRICYCLIC DRUGS AND NEW β-LACTOGLOBULIN VARIANT I56F/L39A/I71W: CRYSTALLOGRAPHIC AND BIOPHYSICAL STUDIES

Paulina Wróbel[1], Joanna Loch[1], Piotr Bonarek[2], Krzysztof Lewiński[1]

[1]Jagiellonian University, Faculty of Chemistry, Department of Crystal Chemistry and Crystal Physics, Gronostajowa 2, 30-387 Kraków, Poland
[2]Jagiellonian University, Faculty of Biochemistry, Biophysics and Biotechnology, Department of Physical Biochemistry, Gronostajowa 7, 30-387 Kraków, Poland

β-Lactoglobulin (BLG) is a protein belonging to the family of lipocalins. BLG can bind and transport low-molecular-weight ligands, such as fatty acids, vitamins, and selected drugs. [1] A characteristic structural feature of BLG is their antiparallel β-barrel which is the primary binding site for ligands. Like many proteins from the lipocalin family, BLG can be modified by site-directed mutagenesis to change its ligand binding specificity and selectivity [2].

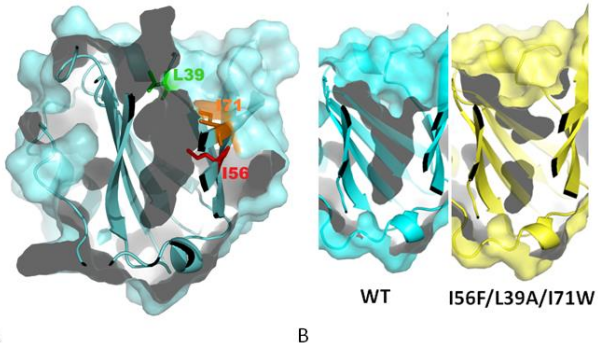

Fig. 1. (A) Structure of WT β-lactoglobulin with marked residues selected for mutagenesis. (B) The shape of the binding site of the wild-type protein (WT, cyan) with the elongated binding pocket and mutant I56F/L39A/I71W with reduced length of the binding pocket.

New BLG mutant I56F/L39A/I71W was designed to recognize drugs possessing tri-cyclic geometry (e.g. antipsychotics and antidepressants). These drugs (e.g. fluphenazine, chlorpromazine, and amoxapine) are often overdosed and might be highly toxic to humans.

Mutant I56F/L39A/I71W was co-crystallized with different ligands: tricyclic drugs and selected fatty acids, that are natural BLG ligands. Determined crystal structures revealed that substitutions at positions 56, 39, and 71 reduced the length of the binding pocket (Fig. 1). Most of the tested tricyclic drugs were bound in the β-barrel, while fatty acids were not bound to the mutated protein. Crystallographic studies were supported by biophysical studies (circular dichroism) which allowed to determine the binding constant for selected protein-drug pairs.

References

[1] J.M.Crowther, G.B.Jameson, R.C.J. Hodgkinson, A.J. Dobson (2016) Structure, Oligomerisation, and Interactions of β-Lactoglobulin. *I. Gigli (Ed.), Milk Proteins - From Struct. to Biol. Prop. Heal. Asp, IntechOpen*, pp. 33-50.

[2] F.C.Deuschle , E.Ilyukhina , A.Skerra (2020) Anticalin® proteins: from bench to bedside. *Expert Opin Biol Ther*.

B-06

ORIENTACJA NITRYLI A SIEĆ KRYSTALICZNA JAKO NARZĘDZIE DO MODYFIKOWANIA PRZEJŚĆ SPINOWYCH W JEDNOWYMIAROWYM POLIMERZE KOORDYNACYJNYM $[Fe(ebtz)_2(RCN)_2](BF_4)_2$ (RCN = nitryle)

Maria Książek[1], Joachim Kusz[1], Marcin Kaźmierczak[2], Aleksandra Tołoczko[2], Marek Weselski[2] i Robert Bronisz[2]

[1]Instytut Fizyki, Uniwersytet Śląski, ul. 75 Pułku Piechoty 1, 41 – 500 Chorzów
[2]Wydział Chemii, Uniwersytet Wrocławski, ul. F. Joliot – Curie 14, 50 – 383 Wrocław

Związek kompleksowy $[Zn(ebtz)_3](BF_4)_2$ (ebtz – 1,2-di(tetrazol-2-ylo)etan) jest pierwszym przykładem polimeru koordynacyjnego otrzymanego na bazie 2-podstawionego tetrazolu jako grupy donorowej [1]. Dzięki rozszerzeniu badań na kompleksy Fe(II) stwierdzono, że związki zawierające rdzeń $[Fe(tetrazol\text{-}2\text{-}ylo)_6]$ wykazują termicznie indukowane przejścia spinowe (SCO) [2]. W kompleksach otrzymanych na bazie tego typu ligandów jon centralny (np. Fe(II), czy Cu(II)) jest koordynowany przez cztery pierścienie tetrazolowe oraz cząsteczki nitryli. Należy podkreślić, że w kompleksach typu $[Fe(tetrazol\text{-}2\text{-}yl)_4(RCN)_2]$ zjawisko SCO jest stowarzyszone z dodatkowymi zmianami konformacyjnymi aksjalnie koordynowanych cząsteczek nitryli [3]. W przypadku kompleksu $[Fe(ebtz)_2(C_2H_5CN)_2](ClO_4)_2$ występuje szeroka pętla histerezy, która jest związana z reorientacją skoordynowanych cząsteczek propionitrylu połączoną ze znaczącymi zmianami odległości pomiędzy supramolekularnymi warstwami [4].

W celu wyjaśnienia roli skoordynowanych cząsteczek nitryli na przebieg przejścia spinowego przeprowadzone zostały badania serii układów $[Fe(ebtz)_2(RCN)_2](BF4_4)_2$ [5] ze szczególnym uwzględnieniem niezwykłego, bardzo wolnego przejścia spinowego dla pochodnej propionitrylowej. Temperaturowe badania podatności magnetycznej wykazały, że po gwałtownym schłodzeniu próbki do 10K nie występuje termiczne przełączenie HS→LS. Natomiast na podstawie pomiarów przeprowadzonych przy bardzo powolnych cyklach chłodzenia oraz grzania wykazano obecność przejścia spinowego, któremu towarzyszy histereza ($T_{1/2}^{\downarrow}$= 78 K, $T_{1/2}^{\uparrow}$=123 K). Przeprowadzone izotermiczne (80 K) czasowo-rozdzielcze monokrystaliczne badania dyfrakcji rentgenowskiej potwierdziły występowanie SCO. Początkowo obserwuje się bardzo wolne kurczenie się łańcuchów polimerycznych połączone ze zmniejszaniem się objętości komórki elementarnej (77%) w porównaniu z różnicą objętości V_{HS} - V_{LS}, podczas gdy jedynie 16% jonów Fe(II) znajduje się w stanie niskospinowym. Następnie rozpoczyna się bardzo szybkie przejście spinowe związane ze znaczącym wzrostem odległości między warstwami polimerycznymi. Reorientacja propionitryli polega na wzroście kąta Fe-N-C(nitryl) z 143.6 do 161.6°.

Badania LIESST oraz r-LIESST, przeprowadzone w 14 K metodą dyfrakcji rentgenowskiej na monokryształach, dodatkowo potwierdziły, że ilość przełączonych jonów Fe(II) koreluje z orientacją cząsteczek nitrylu. Ponadto wykazano, że stabilizacja stanu spinowego, otrzymywanego podczas naświetlania światłem, jest uzależniona od efektów sieci. Taka właściwość może być wykorzystana do modyfikowania własności przejść spinowych poprzez częściową wymianę propionitrylu na butyronitryl – im

więcej jest cząsteczek butyronitrylu, tym większy jest kąt Fe-N-C(nitryl), co skutkuje przesunięciem temperatury SCO w stronę wyższych wartości oraz zwężeniem szerokości pętli histerezy.

Literatura

[1] R. Bronisz, *Inorg. Chem. Acta*, **340** (2002) 215.
[2] R. Bronisz, *Inorg. Chem.*, **46** (2007) 6733.
[3] M. Książek, J. Kusz, A. Białońska, R. Bronisz, M. Weselski, *Dalton Trans.*, **44** (2015) 18563.
[4] A. Białońska, R. Bronisz, *Inorg. Chem.*, **51** (2012) 12630.
[5] M. Książek, M. Weselski, M. Kaźmierczak, A. Tołoczko, M. Siczek, P. Durlak, J.A. Wolny, V. Schünemann, J. Kusz, R. Bronisz, *Chem. Eur. J.*, **26** (2020) 14419.

B-07

MAGNETIC MODES COMPATIBLE WITH THE SYMMETRY OF CRYSTALS

Piotr Fabrykiewicz, Radosław Przeniosło and Izabela Sosnowska

Wydział Fizyki, Uniwersytet Warszawski, ul. Pasteura 5, 02-093 Warszawa

We present a classification of magnetic space groups which give an answer to the question: What magnetic space groups can be ascribed to a given magnetic mode? There are 32 categories of magnetic space groups which describe 64 unique different magnetic modes: 16 with a ferromagnetic component and 48 without. This classification focused on the magnetic modes is helpful for finding the magnetic space group(s) which describe(s) the observed neutron diffraction data [1]. The classification leads to a reinterpretation of the neutron powder diffraction related to collinear magnetic orderings presented by G. Shirane [2], e.g. in cubic systems any collinear ferromagnetic or antiferromagnetic ordering is not possible. The presented magnetic space groups classifcation includes also the symmetry allowed non-collinear orderings.

The classification of magnetic point and space groups can be used to select the magnetic classes and Wyckoff positions in which several magnetic phenomena can occur: collinear FM ordering, collinear AFM ordering, AFM with weak ferromagnetism (AFM-WFM), continuous spin reorientation of an FM (SR-FM) or AFM order (SR-AFM). The modes which allow these phenomena are shown schematically with coloured area boundaries in Fig. 1.

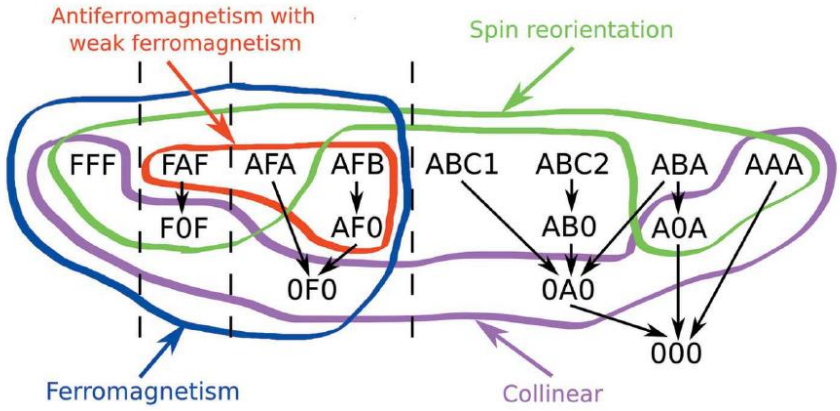

Fig. 1. (from [1]) Schematic presentation of the magnetic modes which allow selected magnetic phenomena in triclinic, monoclinic and orthorhombic systems. Modes which allow given phenomena are shown schematically with coloured area boundaries: spin reorientation - green, collinearity - purple, ferromagnetism - blue, antiferromagnetism with (weak) ferromagnetism - red.

Bibliography

[1] P. Fabrykiewicz, R. Przeniosło and I. Sosnowska, *Acta Cryst. A.*, **77** (2021) – in print DOI: https://doi.org/10.1107/S2053273321004551.
[2] G. Shirane, *Acta Cryst*. **12** (1959) 282.

B-08

NEW PHASONIC CORRECTION IN Al-Cu-Rh DECAGONAL QUASICRYSTAL

Radosław Strzałka, Ireneusz Bugański i Janusz Wolny

AGH University of Science and Technology, Faculty of Physics and Applied Computer Science, Kraków, Poland

We revisited X-ray diffraction data of decagonal Al-Cu-Rh system collected previously by Kuczera *et al.* [1] at room temperature and at 1013-1223 K. From [1] it is known, that the best quasiperiodic ordering exists most probably between 1083 and 1153 K. The stability was proven to be most likely not phason-driven entropy lowering.

In our recent studies, we tested an application of the new correction for phasons, based on the statistical approach. It was shown [2,3], that phason flips significantly change the shape of the average unit cell, and therefore influence the structure factor, and thus the diffraction diagram. These changes in the shape of the AUC can be handled analytically. During the structure refinement, the new correction for phasons gives an extra parameter to fit. The procedure was recently applied to room-temperature d-AlCuRh data [4].

We performed a series of structure refinements including a new correction term for phasons alongside the standard perp-space Debye-Waller factor for 5 sets of X-ray diffraction data at 293, 1013, 1083, 1153, and 1223 K. In the case of every dataset, we were able to achieve better *R*-factor values as compared to original results reported in [1]. As a result, phasonic ADPs were refined alongside the flip probability (measuring the phasonic contribution within the new approach), which shows a distinct minimum in the temperature plot (Figure 1). This can lead to a conclusion, that the amount of phasons is minimal at around 1153 K, which is also a temperature of maximal stability of the quasicrystal.

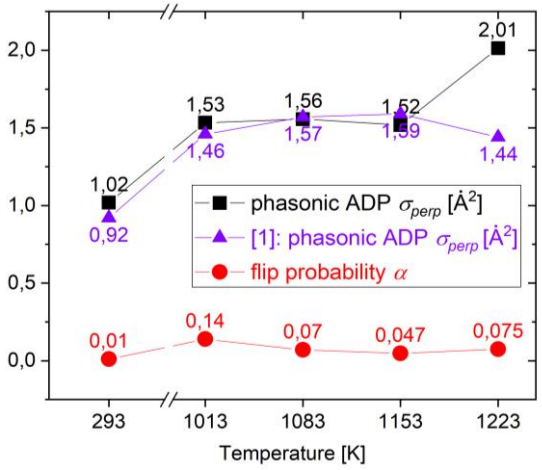

Fig. 1. Phasonic ADPs (new and from [1]) and flip probability from the refinement *vs.* temperature.

References

[1] P. Kuczera, J. Wolny, W. Steurer, *Acta Cryst. B*, **70** (2014) 306-314.
[2] J. Wolny, I. Buganski, P. Kuczera, R. Strzalka, *J. Appl. Cryst.*, **49** (2016) 2106-2115.
[3] R. Strzałka, I. Bugański, J. Śmietańska, J. Wolny, *Arch. Metall. Mater.*, **65** (2020) 291-294.
[4] I. Bugański, R. Strzałka, J. Wolny, *Acta Cryst. A*, **75** (2019) 352-361.

B-09

MEAN ATOMIC WEIGHT AND GRAIN DENSITY OF TARDA CARBONACEOUS CHONDRITE

Marian Antoni Szurgot

Łódź University of Technology, Center of Mathematics and Physics,
Al. Politechniki 11, 90 924 Łódź

Mean atomic weight, bulk and grain densities are physical properties important to characterize minerals, rocks, planets, moons and asteroids, and are important to classify meteorites. Recently interrelationships between mean atomic weight *(Amean)*, grain density *(dgr)*, and iron to silicon ratio for planetary materials were revealed and applied for predicting and verifying mean atomic weight, *Fe/Si* atomic ratio, and grain density of ordinary and enstatite chondrites, Earth, Venus, Mars, Mercury, Moon, and Vesta [1-6].

The aim of the paper was to determine mean atomic weight and grain density of Tarda chondrite. The Tarda meteorite fell on August 25, 2020, in the Moroccan Sahara. Initial petrographic and geochemical analyses suggested that Tarda corresponds to a type 2 ungrouped carbonaceous chondrite [7, 8], is characterized by a bulk oxygen isotopic composition lying between those of CI and CY chondrites [7,8], and is similar to that estimated for Tagish Lake chondrite [8,9]. Comprehensive characterization of the Tarda chondrite including petrographic observations by scanning electron microscope and electron microprobe, bulk mineralogical and chemical analyses by X-ray diffraction, inductively coupled plasma-sector field mass spectrometry, and by secondary ion mass spectrometry, and bulk isotopic measurements revealed that Tarda shares numerous similarities with Tagish Lake meteorite and thus corresponds to a D-type asteroid formed in the outer part of the solar system [8].

Literature data on chemical composition of Tarda meteorite [8] were used to calculate *Amean, Fe/Si* atomic ratio, and *dgr* values for the whole rock of meteorite. *Amean(Bulk composition), Amean(Fe/Si),* and *Amean(H_2O)* relationships were used to predict mean atomic weight. Grain density was predicted using *dgr(Fe/Si)* and *dgr(Amean)* relationships.

New relationships derived by Szurgot [10], and valid for three groups of carbonaceous chondrites: CI, CM, and CR were used in the calculations:

$$Amean(Fe/Si) = 1.434\cdot10^{7}\cdot\exp(-18.44\cdot Fe/Si) + 13.78, \quad (1)$$

$$dgr(Fe/Si)(g/cm^3) = 2.439\cdot10^{4}\cdot\exp(-12.63\cdot Fe/Si) + 2.091. \quad (2)$$

RMSE values for these equations are following: 0.72 (eq.(1)), and 0.06 */cm*^{3}(eq(2)) [10].

It was calculated that iron to silicon atomic ratio for the whole rock of Tarda meteorite is equal to *Fe/Si* = 0.813. The following values of mean atomic weight of Tarda chondrite were obtained: *Amean (Bulk composition)* = $\sum wi/\sum(wi)/Ai)$ = 18.35, and *Amean(Fe/Si)* = 18.20. Here, *wi*/*(wt%)* represents mass of *i*-th constituent (oxide, element, H_2O), *Ai* is the mean atomic weight of *i*-th constituent of the meteorite. *Amean(H_2O)*dependence recently established by Szurgot for CM2 chondrites predicts for Tarda meteorite H_2O content 8.54 wt.% [8] value of *Amean(H_2O)* = 18.73.Thus, the

range of Tarda *Amean* values is between 18.20 and 18.73, and the average value of mean atomic weight of Tarda is 18.43 ± 0.27. Tarda *Amean* and *Fe/Si* values are comparable with the *Amean* and *Fe/Si* mean values established for Murchison CM2 carbonaceous chondrite: *Amean(Bulk composition)* = 18.31, *Fe/Si* = 0.819, and those established for Flensburg ungrouped C1 carbonaceous chondrite: *Amean(Bulk composition)* = 18.33, *Fe/Si* = 0.818 [10].

It was calculated that the *dgr(Amean)* relationship [1,4]

$$dgr(Amean) = 0.133 \cdot Amean + 0.37, \quad (3)$$

leads to the grain density value of the whole rock of Tarda chondrite: 2.82±0.04 g/cm^3, and dependence *dgr(Fe/Si)* (eq.(2)) predicts the value of grain density: 2.94±0.06 g/cm^3. These predictions lead to the range of values: 2.82-2.94 g/cm^3 for Tarda chondrite. Predicted values of grain density of the whole rock of Tarda meteorite are comparable with the mean grain density of Murchison CM2 chondrite [11,12]. Macke measurements indicated for Murchison mean grain density value: 2.96±0.05 g/cm^3 [11], and the range of values: 2.87-3.05 g/cm^3 [11], and generalized relationship between bulk density and porosity *db(porosity)* applied recently by Szurgot [12] predicted for Murchison chondrite *dgr* = 2.93±0.10 g/cm^3 [12].

Conclusions: Mean atomic weight of Tarda meteorite is comparable with the *Amean* values established for Murchison and Flensburg carbonaceous chondrites, and the range of values of grain density predicted for the whole rock of Tarda carbonaceous chondrite is comparable with *dgr* values measured for Murchison CM2 chondrite.

References

[1] M. Szurgot, *46th Lunar and Planetary Science Conference* (2015) Abstract #1536.
[2] M. Szurgot, *Comparative Tectonics* and Geodynamics, (2015) Abstract #5001.
[3] M. Szurgot, *79th Annual Meeting of the Meteoritical Society* (2016) Abstract #6005.
[4] M. Szurgot, *Acta Societatis Metheoriticae Polonorum* **10** (2019) 140-159.
[5] M. Szurgot, *50th Lunar and Planetary Science Conference* (2019) Abstract #1165.
[6] M. Szurgot, R. A. Wach, O. Unsalan, C. Altunayar-Unsalan, *51st Lunar and Planetary Science Conference* (2020) Abstract #1287.
[7] H. Chennaoui Aoudjehane, C. B. Agee, K. Ziegler, *LPI **52*** (2021) 1928.
[8] Y. Marrocchi, G. Avice, J-A. Barrat, *Astrophysical Journal Letters* **913** (2021) L9.
[9] P. G. Brown, A. R. Hildebrand, M. E. Zolensky, et al., *Science* **290** (2000) 320-325.
[10] M. Szurgot, *84th Annual Meeting of the Meteoritical Society* (2021) Abstract #6006, submitted.
[11] R. J. Macke, *PhD Thesis,* (2010), Univ. Central Florida, Orlando.
[12] M. A. Szurgot, *52nd Lunar and Planetary Science Conference* (2021) Abstract #1029.

B-10

BĄBELKOWY DIAGRAM FAZOWY DLA NANOKRYSZTAŁÓW (BUBBLE PHASE DIAGRAM FOR NANOCRYSTALS)

Paweł E. Tomaszewski

Instytut Niskich Temperatur i Badań Strukturalnych, Polska Akademia Nauk, ul. Okólna 2, 50-422 Wrocław

Przemiany fazowe w kryształach są jednym z ciekawszych zjawisk w przyrodzie. Dotychczas zarejestrowano około 15 tysięcy przemian strukturalnych [1]. Warto zauważyć, że w tej bazie pominięto przemiany magnetyczne, które są jednak również przemianami strukturalnymi (choć najczęściej słabo widocznymi). Po pojawieniu się nanokryształów jako przedmiotu intensywnych badań strukturalnych okazało się, że mamy też do czynienia z rozmiarowymi przemianami fazowymi [2]. Początkowo uważano, że da się je opisać jednym schematem. Tymczasem dla części nanokryształów, które nie wykazują istnienia przemian fazowych dla wersji objętościowej (bo… nie istnieją dla nich kryształy „bulk"), należało opracować nowy rodzaj diagramu roboczo nazwanego diagramem „bąbelkowym".

Okazuje się, że przyczyną pewnego zamieszania jest błąd w nazewnictwie związany nierozerwalnie ze sposobem otrzymywania nanokryształow. Wielu badaczy nanokryształów uważa, że skoro synteza danego kryształu zachodzi w różnych temperaturach wygrzewania, to mamy przemianę fazową gdzieś pomiędzy tymi temperaturami. Tymczasem nie ma to nic wspólnego z przemianą fazową przy grzaniu próbki objętościowej. Temperatura rozumiana jako temperatura zmieniana podczas pomiaru jakiejś wielkości fizycznej to nie jest to samo, co temperatura wygrzewania/syntezy (po której następuje gwałtowne schłodzenie próbki do temperatury pokojowej). Fazy otrzymywane w różnych temperaturach są różnymi kryształami i nie ma pomiędzy nimi żadnych przemian fazowych (uwaga: dotyczy to tylko kryształów nie mających odpowiednika „bulk"). Ogrzewanie każdego z nich w normalnym procesie badawczym nie doprowadzi do jakiejkolwiek przemiany. Co jest więc wyróżnikiem danej fazy? To przede wszystkim wielkość ziaren/krystalitów charakterystyczna dla temperatury syntezy. Dopiero doprowadzenie do zmiany wielkości ziaren umożliwi przemianę do innej fazy. Należy pamiętać, że im wyższa temperatura syntezy, tym ziarna są większe.

Takie zachowanie się kryształów opisane zostało już w 1973 r. [3] dla serii pirokrzemianów $RE_2Si_2O_7$. Rysunek jest błędnie opisany – powinna być „temperatura wygrzewania" a nie zwykła „temperatura".

B-10

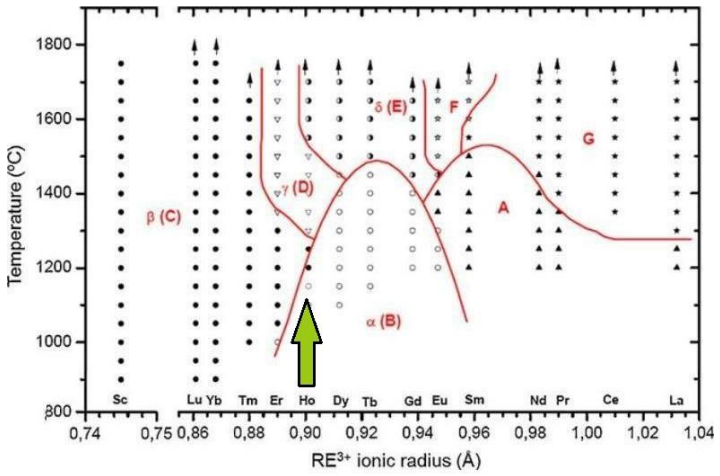

Rys. 1. Zakresy wygrzewania dla otrzymania określonych faz nanokrystalicznych $RE_2Si_2O_7$.

Podane na rysunku zakresy wskazują jedynie na granice temperatur wygrzewania potrzebnych do otrzymania określonej fazy. To nie są granice występowania, co mogłoby sugerować istnienie przemiany fazowej w określonej temperaturze. Spotykana w literaturze sekwencja faz, np. α ↔ 1225 ↔ β ↔ 1445 ↔ γ ↔ 1635°C ↔ δ, jest błędnym zapisem! Wydaje się więc, że jakaś część danych w bazie strukturalnych przemian fazowych jest błędnie opisana! Należałoby więc takie kryształy wydzielić jako osobną grupę, podobnie jak mamy do czynienia z odmianami polimorficznymi.

Dla badanego kryształu $Y_2Si_2O_7$ (to jeden z rodziny pokazanej na Rys. 1) sytuacja fazowa powinna być opisana poniższym diagramem bąbelkowym [4]. Owale na diagramie *d*-T_{calc} oznaczają zakres tworzenia danej fazy.

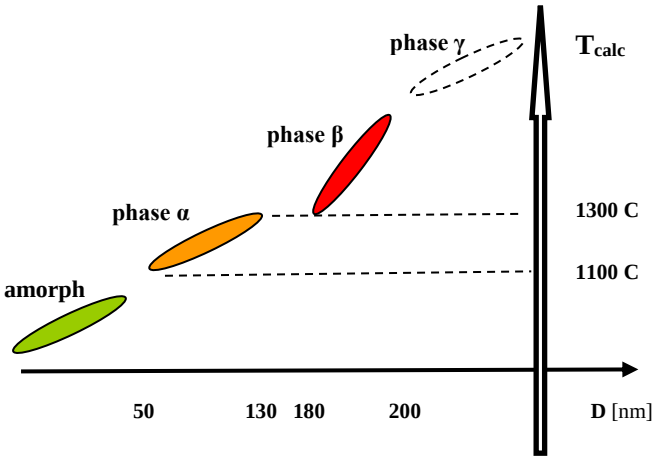

Rys. 2. Proponowany diagram fazowy dla nanokrystalicznego $Y_2Si_2O_7$.

Literatura

[1] P.E. Tomaszewski, Złota księga przemian fazowych (2002).
[2] P.E. Tomaszewski, *Ferroelectrics*, **375** (2008) 74. DOI: 10.1080/00150190802437910.
[3] J. Felsche, Struct. Bonding (Berlin) **13** (1973) 99.
[4] P.E Tomaszewski, K. Grzeszkiewicz, *Solid State Commun.* (2021).

B-11

DECOUPLING INDIVIDUAL CONTRIBUTIONS TO THE TOTAL VOLUME RESPONSE BY THE APPLICATION OF NEUTRON SCATTERING FOR IN-OPERANDO STUDIES OF HYDROPHOBIC MOFS UNDER MEDIUM WATER PRESSURE

Paweł Zajdel[1], Juscelino B. Leao[2], Markus Bleuel[2,3], Grethe V. Jensen[2,4], Craig M. Brown[2,4], Alexander R. Lowe[5], Miroslaw Chorążewski[5], Nikolay Tsyrin[6], Victor Stoudenets[6], and Yaroslav Grosu[5,7]

[1]A. Chelkowski Institute of Physics, University of Silesia, 75 Pułku Piechoty 1, 41-500 Chorzów, Poland
[2]NIST Center for Neutron Research, National Institute of Standards and Technology, Gaithersburg, Maryland 20899, United States
[3]Department of Materials Science and Engineering, University of Maryland, College Park, Maryland 20742-2115, USA
[4]Department of Chemical and Biomolecular Engineering, University of Delaware, Newark, Delaware 19716, USA
[5]Institute of Chemistry, University of Silesia, Szkolna 9, 40-006 Katowice, Poland
[6]Laboratory of Thermomolecular Energetics, National Technical University of Ukraine "Igor Sikorsky Kyiv Polytechnic Institute",Pr. Peremogy 37, 03056 Kyiv, Ukraine
[7]Centre for Cooperative Research on Alternative Energies (CIC energiGUNE), Basque Research and Technology Alliance (BRTA), Alava Technology Park, Albert Einstein 48, 01510 Vitoria-Gasteiz, Spain

In-operando studies of functional materials provide unique access to their real-time response to external stimuli. Pairing the sutdies with high penetration capabilities of neutrons allows us to reach experimental conditions that are not available using x-ray scattering methods.

In case of Metal Organic Frameworks (MOFs), neutron powder diffraction (NPD) has been routinely used to study the response of the framework to pressure, temperature as well as to locate guest molecules in the host structure. Our recent studies [1-4] extended the NPD to investigate MOFs under hydrostatic water pressures up to 30 MPa (300 bar), which constitute typical operating conditions of novel materials for energy applications. The NPD permitted the time dependent studies of the system under a wide area of a P-T phase diagram. In particular, they allowed decoupling the changes in lattice parameters from the total volume of the system, which is usually obtained from P-V isotherms. Simultaneously, the structural information encapsulated in the powder pattern connects the response of the system with the intrusion and extrusion of water into the hydrophobic framework.

The information obtained in this way also allows: (1) to connect flexibility of the framework with energy dissipation of the system, (2) estimate robustness of the time response of the material and finally (3) to propose new mechanism of nanosized thermal actuator.

References

[1] A Lowe *et al*., *ACS Appl. Mater. Interfaces*, **11** (2019) 40842-40849.
[2] M. Tortora *et al*., *Nano Letters*, **21(7)** (2021) 2848-2853.
[3] M. Chorazewski *et al. ACS Nano*, **15(5)** 9048–9056
[4] P. Zajdel *et al J. Phys. Chem. Lett.*, **12(20)** (2021) 4951–4957

B-12

TWO STRUCTURAL ISOMERS OF BIS(THIOUREA) DERIVATIVE

Weronika Hallmann, Andrzej Okuniewski

Department of Inorganic Chemistry, Chemical Faculty,
Gdańsk University of Technology, G. Narutowicza 11/12, 80-233 Gdańsk, Poland

1-Acyl-3-substituted thioureas are readily prepared by a one-pot two-step reaction of acyl chloride, thiocyanate, and primary or secondary amine in a dry solvent such as acetone (Fig. 1) [1].

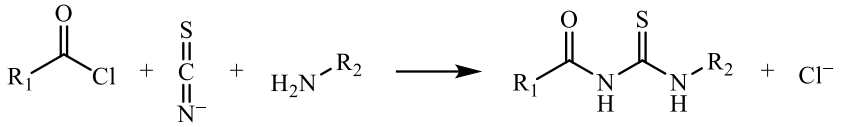

Fig. 1. The summary reaction of synthesis of 1-acyl-3-substituted thiourea derivatives.

We have successfully used this procedure in our previous research [2, 3]. Now we have used difunctional terephthaloyl chloride or *p*-phenylenediamine to obtain two isomeric bis(thioureas) of $C_{22}H_{18}N_4O_2S_2$ chemical formula:

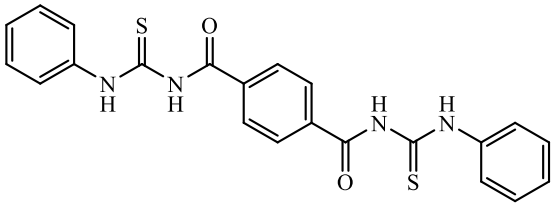

terephthaloylbis(3-phenylthiourea) – **1**

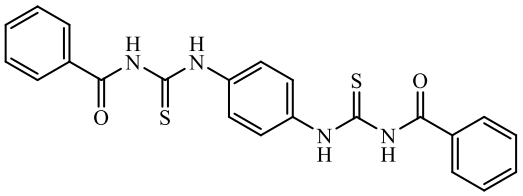

p-phenylenebis(3-benzoylthiourea) – **2**

The reaction product is isolated in the form of a fine powder, so the re-crystallization was necessary to obtain single crystals suitable for X-ray diffraction analysis. Unfortunately, the solubility of these compounds in most of the common solvents was very poor. Only low-volatile dimethylsulfoxide (DMSO, T_{bp} = 189°C) and *N*,*N*-dimethylformamide (DMF, T_{bp} = 153°C) seemed to dissolve considerable amounts of the compounds. The use of high-boiling solvents makes it difficult to concentrate the solutions. In addition, the time needed to obtain single crystals is significantly longer.

However, we have obtained single crystals of **1** from DMSO and of **2** from DMF (Fig. 2). All crystals were small and of poor quality, so even with a long time of X-ray irradiation and small scanning steps, the final refinement parameters are not satisfactory (Table 1).

After the structure solution and refinement, it turned out that in the structure of **1** additional DMSO molecules can be found. They are bonded to organic molecules with N−H···O hydrogen bonds and S···S chalcogen interactions (Table 1). The structure of **2** is solvent-free. In both structures, the molecules are centrosymmetric and adopt S-type conformation [4] that allows the formation of an intramolecular N−H···O hydrogen bond.

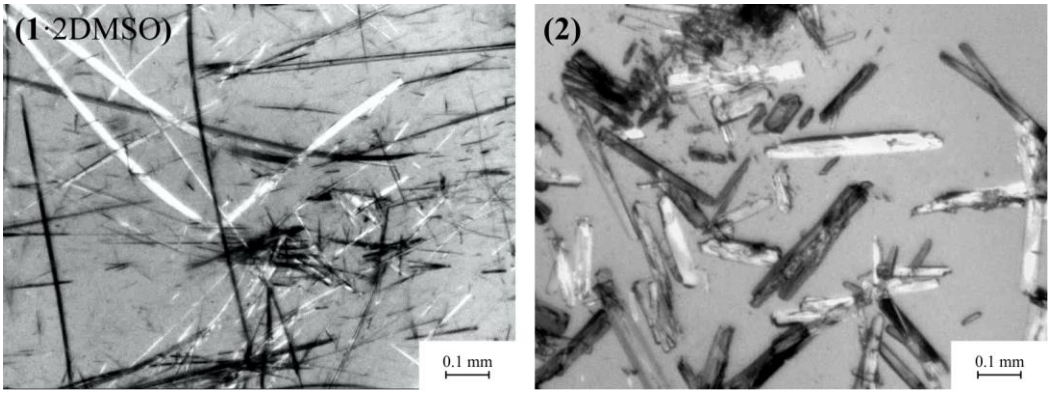

Fig. 2. Photographs of crystals of **1**·2DMSO and **2** seen under the microscope.

(1·2DMSO**)** 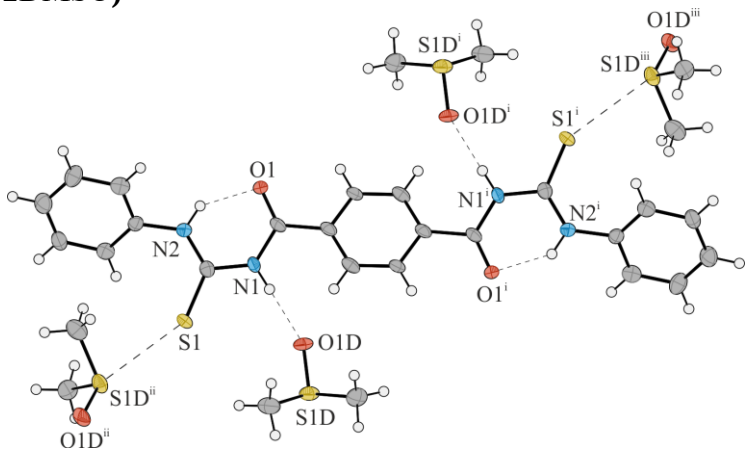	Space group: $P2_1/c$ a = 5.3064(6) Å b = 10.881(2) Å c = 24.354(3) Å β = 91.886(9)° R_1 = 14.68%
(2) 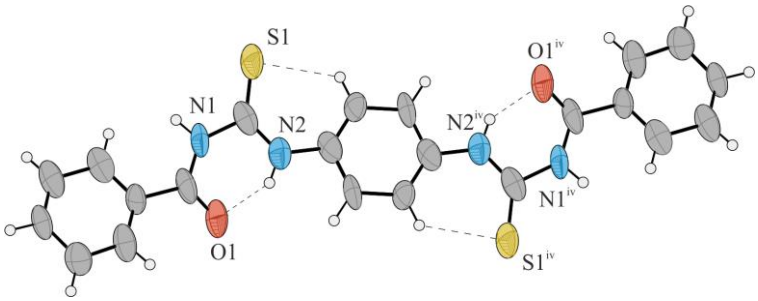	Space group: $P2_1/n$ a = 11.513(4) Å b = 4.3268(11) Å c = 20.307(8) Å β = 99.76(3)° R_1 = 21.42%

Table 1. Molecular structures of **1**·2DMSO and **2**, along with basic crystallographic data. The thermal ellipsoids are drawn at a 50% probability level. Symmetry codes: (i) $1-x, 2-y, -z$; (ii) $-x, \frac{1}{2}+y, \frac{1}{2}-z$; (iii) $1+x, \frac{3}{2}-y, -\frac{1}{2}+z$; (iv) $2-x, 2-y, 1-z$.

Acknowledgments
The authors thank Prof. Jarosław Chojnacki (GUT) for performing X-ray diffraction measurements.

References

[1] I. B. Douglass, F. B. Dains, *J. Am. Chem. Soc.*, **56** (1934) 719.
[2] D. Rosiak, A. Okuniewski. J. Chojnacki: *Acta Cryst., C* **77** (2021) 11.
[3] A. Okuniewski, D. Rosiak, J. Chojnacki, B. Becker: *Acta Cryst., C* **73** (2017) 52.
[4] M. G. Woldu, J. Dillen: *Theor. Chem. Acc.*, **121** (2008) 71.

B-13

AMIDRAZONE DERIVATIVES - STRUCTURE AND ACTIVITY

Andrzej Olczak[a], Katarzyna Gobis[b], Ewa Augustynowicz-Kopeć[c], Małgorzata Szczesio[a], Marek L. Główka[a]

[a] Institute of General and Ecological Chemistry, Faculty of Chemistry, Lódź University of Technology, Żeromskiego 116 , 90-924 Łódź, Poland
[b] Department of Organic Chemistry, Medical University of Gdańsk, M. Skłodowskiej-Curie 3a, 80-210 Gdańsk, Poland
[c] Department of Microbiology, Institute of Tuberculosis and Pulmonary Diseases, Płocka 26, 01-138 Warsaw, Poland

Tuberculosis remains a major health problem worldwide. Multi drug resistance of new strains of *Mycobacterium tuberculosis* makes it necessary to search for new active compounds. Amidrazone derivatives are known of their high potential antibacterial and, in particular, antituberculosis properties [1,2].

Three new crystal structures of amidrazone derivatives (Scheme) showing tuberculostatic activity were determined by X-ray diffraction (Table). The studied compounds can exist in various tautomeric forms, which may be important for their biological activities. Calculated energies of these tautomeric forms as well as structure-activity relationship for the tested compounds will be presented.

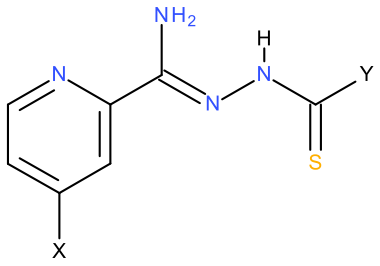

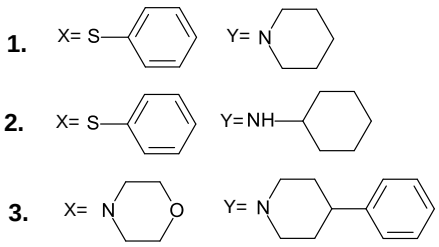

	1	2	3
Unit cell parameters	9.635, 11.571, 32.534, 90, 97.43, 90	9.961,11.480, 17.947, 79.55, 75.59, 85.16	9.128, 9.237, 35.335 90.78, 92.53, 116.79
Space Group	$P2_1/n$	P-1	P-1
R (I>2sigma)	0.06	0.05	0.07

References

[1] S.L. Dax, Antibacterial Chemotherapeutic Agents, Chapman and Hall, London, (1997).
[2] M.L. Główka, D. Martynowski, A. Olczak, C. Orlewska, H. Foks, J. Bojarska, M. Szczesio, J. Gołka, *Journal of Chemical Crystallography*, **35** (2005) 477.

This project was funded by the National Science Centre (Cracow, Poland) on the basis of decision number DEC-2017/25/B/NZ7/00124.

B-14

STRUKTURA KRYSTALICZNA CHLOROWODORKU ESTRU ETYLOWEGO L-LEUCYNY

Adam Orylski[1], Miłosz Siczek

Wydział Chemii, Uniwersytet Wrocławski, ul. F. Joliot-Curie 14, 50-383 Wrocław
[1] student studiów I stopnia (licencjackich)

Wiele substancji o działaniu farmaceutycznym wykazuje słabą rozpuszczalność w wodzie, wpływa to negatywnie na ich wchłanialność, co zmniejsza ich działanie lecznicze. Jedną z metod zwiększenia rozpuszczalności jest przygotowanie leku w postaci soli. Drugim komponentem musi być substancja, która będzie zarówno bezpieczna jak i znacząco poprawi rozpuszczalność danego związku czynnego. Aminokwasy należą do substancji powszechnie uważanych za bezpieczne (GRAS). Dodatkowo ze względu swoją chiralność mogą posłużyć do rozdziału enancjomerów leków występujących w postaci racematów.

Przedmiotem badań jest chlorowodorek estru etylowego L-leucyny. Został on otrzymany przez reakcję L-leucyny z etanolem, katalizowaną chlorkiem tionylu[1]. Badania pozwoliły otrzymać i scharakteryzować chlorowodorek estru etylowego L-leucyny, który posłuży do dalszych badań z substancjami o znaczeniu farmaceutycznym.

Związek krystalizuje w układzie rombowym w typie grup przestrzennych $P2_12_12_1$. Część asymetryczna komórki elementarnej składa się z kationu estru etylowego L-leucyny oraz anionu chlorkowego. Grupa $-NH_3^+$ zaangażowana jest w tworzenie wiązań wodorowych pomiędzy pochodną aminokwasu, a anionem chlorkowym.

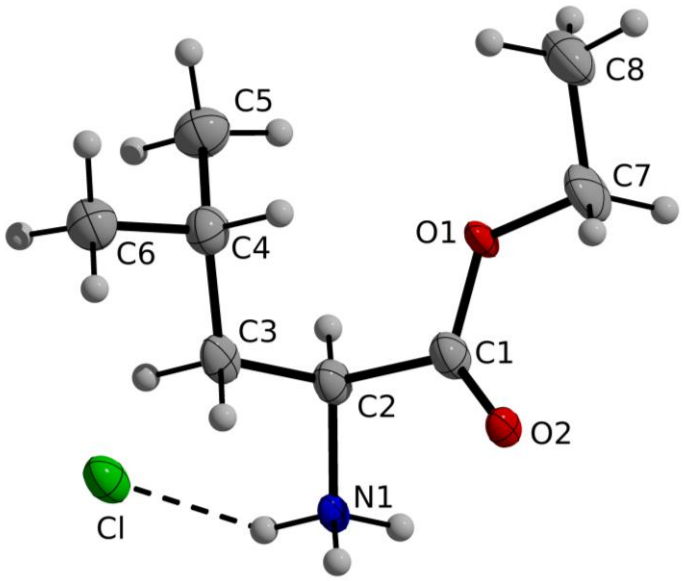

Rys. 1. Część niezależna komórki elementarnej kryształu chlorowodorku estru etylowego L-leucyny wraz ze schematem numeracji atomów.

Literatura

[1] Tian, T., Hu, X., Guan, P., Tang, Y., & Wang, H. *Sci. Ed.*, **33**(1) (2018) 249.

B-15

LOW-TEMPERATURE PHASE TRANSITIONS IN $[(CH_3)_2NH_2][Zn(DCOO)_3]$ HYBRID METAL-FORMATE PEROVSKITE

Anna Gągor[1], Paulina Peksa[2], Aneta Ciupa[1], Jan Zaręba[2], Adam Sieradzki[2]

[1]Institute of Low Temperature and Structure Research, Polish Academy of Sciences, Box 1410, 50-950 Wrocław 2, Poland
[2]Faculty of Fundamental Problems of Technology, Wrocław University of Technology, Wybrzeże Wyspiańskiego 27, 50-370 Wrocław, Poland

Metal-organic frameworks (MOFs) crystallizing in a perovskite architecture of general formula ABX_3 are intensively explored due to the possibility of ferroelectric [1] and multiferroic behaviour [2]. The crystal structure of these materials is built of metal centres coordinated octahedrally by formate linkers which also act as bridging-ligands. Organic counter ions occupy the voids within the inorganic framework. The properties of the phase transitions in $[AmineH^+][M(HCOO)_3]$, where M is a divalent metal ion highly depend on the metal centre and type of the molecular cation.

All $(CH_3)_2NH_2$ (DMA^+) templated perovskite-like M-formates, where M = Mn, Zn, Ni, Co, Fe crystallize in the trigonal space group $R\bar{3}c$ with DMA^+ being disordered along the 3-fold axis. The cooperative molecular cation ordering and framework deformation play an essential role in driving the low-temperature phase transitions. $[DMA][Zn(HCOO)_3]$ undergoes a first-order improper ferroelectric transformation at T_0~166 K. Strengthening of the hydrogen bonds leads to the polar arrangement of DMA^+ cations and appearance of long-range electric order.

The issue regarding the symmetry of low-temperature phase is complex due to the strong symmetry reduction, ferroelastic domain structure and weak deformation of the inorganic scaffold. Despite several dozen articles about $[DMA][M(HCOO)_3]$, the LT structure (with *Cc* symmetry) has been reported only for Mn analogue [3]. In this report, we show that low-temperature dielectric response may be explained basing on the triclinic *P1* crystal structure. Deuteration of the formate leads to larger deformations of the inorganic framework compared to non-deuterated crystals, which allows deconvolution of the diffraction peaks, solution and refinement of the structure.

References

[1] Xu, G.-C. et al. Coexistence of Magnetic and Electric Orderings in the Metal-Formate Frameworks of $[NH_4][M(HCOO)_3]$. *J. Am. Chem. Soc.*, **133** (2011) 14948– 14951.
[2] Jain, P. et al. Multiferroic Behavior Associated with an Order–Disorder Hydrogen Bonding Transition in Metal–Organic Frameworks (MOFs) with the Perovskite ABX_3 Architecture. *J. Am. Chem. Soc.*, **131** (2009) 13625– 13627.
[3] M. Sánchez-Andújar et al. Characterization of the order-disorder dielectric transition in the hybrid organic-inorganic perovskite-like formate $Mn(HCOO)_3[(CH_3)_2NH_2]$, *Inorg. Chem.*, **49** (2010) 1510–1516.

B-16

ANOMALOUS VOLUME CHANGES IN THE SILICEOUS ZEOLITE THETA-1 TON DUE TO THE HYDROGEN INSERTION UNDER HIGH PRESSURE, HIGH TEMPERATURE CONDITIONS

Damian Paliwoda,[1] Davide Comboni,[2] Tomasz Poręba,[2] Michael Hanfland,[2] Frederico Alabarse,[3] David Maurin,[4] Thierry Michel,[4] Umit B. Demirci,[5] Jérôme Rouquette,[1] Francesco di Renzo,[1] Arie van der Lee,[5] Samuel Bernard,[6] Julien Haines[1]

[1]ICGM, Université de Montpellier, CNRS, ENSCM, 34095 Montpellier, France
[2]ESRF, 38043 Grenoble, France
[3]Elettra Sincrotrone Trieste, 34149 Basovizza, Trieste, Italy
[4]L2C, Université de Montpellier, CNRS, 34095 Montpellier, France
[5]IEM, Université de Montpellier, CNRS, ENSCM, 34095 Montpellier, France
[6]CNRS, IRCER, UMR 7315, University of Limoges, 87000 Limoges, France

Ammonia borane (AB) is of great interest for chemical hydrogen storage as it has one of the highest releasable hydrogen content of 19.6 wt.% [1,2]. Hydrogen is released in several steps upon heating at relatively low temperature along with the polymerization of ammonia borane to form polyaminoborane, polyiminoborane and, at still increasing temperature, boron nitride [3].

Here we present our high pressure high temperature (HPHT) study on ammonia borane confinement in siliceous zeolite theta-1 (TON) porous template.

Our recent synchrotron X-ray diffraction and Raman spectroscopic experiments revealed that the compression of AB/TON or AB/MFI composite materials promotes the insertion of ammonia borane into the pores of a template. Its further high temperature treatment results in a release of a significant amount of hydrogen and in the formation of polyaminoborane and polyiminoborane polymers, both in the bulk ammonia borane outside the zeolite, as well as confined in the channels of the porous template. In consequence, strong expansion of the zeolite pores accompanied with significant increase of the unit cell volume and series of phase transitions have been observed [4].

Financial support from the Agence Nationale de la Recherche (ANR-19-CE08-0016) is gratefully acknowledged.

References

[1] C. W. Hamilton, R. T. Baker, A. Staubitz, I. Manners, *Chem. Soc. Rev.*, **38 (1)** (2009) 279.
[2] A. Staubitz, A. P. M. Robertson, I. Manners, *Chem. Rev.*, **110 (7)** (2010) 4079.
[3] F. J. Baitalow, G. Wolf, K. Jaenicke-Rossler, G. Leitner, *Thermochim. Acta*, **391 (1-2)** (2002) 159.
[4] D. Paliwoda, D. Comboni, T. Poręba M. Hanfland, F. Alabarse, D. Maurin, T. Michel, U.B. Demirci, J. Rouquette, F. di Renzo, A. van der Lee, S. Bernard, J. Haines, *J. Phys. Chem. Lett.*, **12** (2021) 5059.

B-17

2-(ALLYLTHIO)-PYRIDINE AS π,σ-LIGAND: SYNTHESIS AND STRUCTURAL FEATURES OF CU(I) HALIDE COORDINATION COMPOUNDS

Oleksii Pavlyuk, Nazariy Pokhodylo, Yurii Slyvka, Marian Mys'kiv

Ivan Franko National University of Lviv, Kyryla i Mefodiya 6, 79005 Lviv, Ukraine
e-mail: pavalex@gmail.com

Metal-organic coordination frameworks are widely used in the modern science and industrial chemistry. Among them, copper compounds possess a noticeable place in the diversity of studied substances [1–3]. In overhand, pyridine derivatives are very interesting due to their biological activity [4, 5].

Continuing our research on coordination behavior of some heterocyclic systems regarding to the Cu(I), under alternating-current electrochemical technique conditionds, novel crystalline compounds $[C_5H_4NS(C_3H_5)CuCl]$ (**I**) and $[C_5H_4NS(C_3H_5)CuBr]$ (**II**) obtained. The diffraction data were collected on New Gemini, Dual, Cu at home/near, equipped with an Atlas-CCD detector, using graphite monochromated Mo–Kα radiation.

In the structure of $[C_5H_4NS(C_3H_5)CuX]$ compounds the metal atom possesses a distorted trigonal-pyramidal coordination environment (τ'_4 = 0.77 and 0.82 for **I** and **II**, respectively [6]) formed by the nitrogen atom of organic ligand (Cu–N - 2.025 and 2.206 Å), C=C bond of allylic group of the organic ligand (Cu-*m* – 1.927 and 1.942 Å, respectively) and two halogenides atoms (Cu–Hal – 2.269 and 2.410 Å). Due to the bridging function of two Hal^- ions metal coordination polyhedra are connected to isolated $\{(C_5H_4NS(C_3H_5))_2Cu_2Hal_2\}_n$ topological units.

Interesting features of both compounds is the lack of coordination of S atom in organic moiety by copper atoms. In our point of view, the main reasons are steric hindrance from halide atoms and features of electron density distribution.

Acknowledgments
The authors are greatly thankful to National Research Foundation of Ukraine (project 2020.01/0166 "New azole and cagelike agents against cancer and pathogenic microorganisms") and the Ministry of Education and Science of Ukraine (Grant No 0120U102028) for financially support.

References

[1] Yu. Slyvka, E. Goreshnik, O. Pavlyuk, et al., *Open Chem. (Central. Eur. J. Chem.),* **11** (2013) 43.
[2] O.R. Hordiichuk, V. V. Kinzhybalo, E.A. Goreshnik, et al., *J. Organomet. Chem.,* **838** (2017) 1.
[3] Yu. Slyvka, E. Goreshnik, G. Veryasov, et al., *Polyhedron,* **133** (2017) 319.
[4] A.M. Attia, A.I. Khodair, E.A. Gendy, et al., *Lett. Drug Des. Discov.,* **17** (2020) 124.
[5] E.G. Salina, O. Ryabova, A. Vocat, et al., *J. Infect. Chemother.,* **23** (2017) 794.
[6] L. Yang, D.R. Powell, R.P. Houser, *Dalt. Trans.,* (2007) 955.

B-18

THE ISOMERISATION POTENTIAL OF NITRO-NICKEL COORDINATION COMPOUNDS WITH VARIOUS ETHYLDIAMINE DERIVATIVES

Kinga Potempa, Krystyna A. Deresz, Radosław Kamiński, Katarzyna N. Jarzembska

Department of Chemistry, University of Warsaw, Żwirki I Wigury 101, 02-089, Warsaw, Poland

Photocrystallography allows determination of structures of light-induced excited-state species formed in crystals using X-ray diffraction techniques. The presence of small, ambidentate ligands in transition metal systems opens up possibility for observation of linkage isomerism. Ligands with various donor atoms, such as NO, NO_2, SO_2 are prone to bind to metal centre in many different ways. The nitro group, which is particularly interesting in the context of this project, can form nine possible isomers [1]. Physical properties of linkage isomers may vary significantly. Materials with incorporated photoswitchable compounds can be exploited as optical switches, data storage devices, solar panels etc. [2]

The main goal of this project is to characterize physicochemical properties of a series of nickel complexes with ambidentate ligands in the solid state with the emphasis put on their photoswitchable potential. The studied compounds have metal centre coordinated by two nitro groups and various derivatives of ethylenediamine as supporting ligands.

Structures of two presented here nitro-nickel compounds $[NiL_2(NO_2)_2]$ were examined crystallographically. A thorough analysis of the crystal packing was performed to determine impact of interactions with adjacent molecules on isomeration reaction. Structural investigations were supported by Hirshfeld surface analysis and theoretical computations at the B3LYP/6-311++G** level of theory.

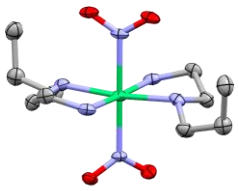

Fig. 1 Compound 1 (hydrogen atoms removed for clarity); thermal ellipsoids set at 50% probability.

Compound 1 $[NiL_2(NO_2)_2]$ L = N-(n-propyl)-1,2-diaminoethane [3], crystalizes in the C2/c space group. Examination of intermolecular interactions in the crystal structure confirms stabilizing interactions between nitro groups and amine fragments of the neighbouring/adjacent. Both of the nitro groups in the molecule form O…H-N hydrogen bonds. Reaction cavities for both nitro groups are smaller than these typically reported for photoswitchable nickel nitro complexes [4] – 22.50 $Å^3$ for the N1 group and 22.56 $Å^3$ for N2.

B-18

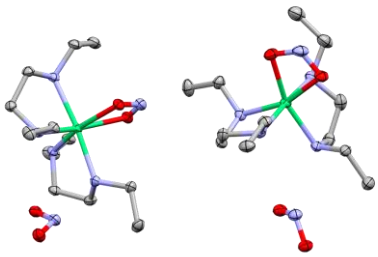

Fig. 2 Compound 2 (molecule a – left, molecule b – right, hydrogen atoms removed for clarity); thermal ellipsoids set at 50% probability

Compound 2 with L = N,N-diethylethylenediamine, crystalizes in the P-1 space group [5], and constitutes a new nitro-nickel complex. Crystallographic examination of crystal structure at 100 K revealed two nitro fragments in the asymmetric unit, among which only one is bound to the metal centre within κ-(O, O) nitrito binding mode. The second nitro group constitutes a counter ion in the crystal structure. Investigation of intermolecular contacts present in the crystal structure, revealed that **molecule a** and **molecule b** form similar interactions – weak hydrogen bonds between κ-(O, O) nitrito group and carbon atom from the amine fragments. Reaction cavities calculated for the **molecule a** and **b** are very comparable in size - 39.12 $Å^3$ and 39.35 $Å^3$, respectively.

The authors thank A. Krówczyński (Warsaw, Poland) for assistance during the syntheses of the examined compounds. The PRELUDIUM BIS grant (2019/35/O/ST4/04197) of the NCN (Poland) is gratefully acknowledged for financial support. The X-ray diffraction experiments were carried out at the Department of Physics, UW, on a Rigaku Oxford Diffraction SuperNova diffractometer, which was co-financed by the EU within the European Regional Development Fund (POIG.02.01.00-14-122/09).

Bibliography

[1] Chattopadhyay, T., Ghosh, M., Banerjee, A. et al. Syntheses, characterization and solid state thermal studies of N-propyl-1,2-diaminoethane (L) and N-isopropyl-1,2-diaminoethane (L′) complexes of nickel(II) nitrite: X-ray single crystal structure of trans-[NiL2(NO2)2]. *Transition Met. Chem.*, **32** (2007) 531–535.

[2] Cole, J. M. (2008). Applications of photocrystallography: a future perspective. *Zeitschrift Für Kristallographie*, **4-5** (2008) 223.

[3] Chattopadhyay, T., Ghosh, M., Banerjee, A. *et al.*, Syntheses, characterization and solid state thermal studies of *N*-propyl-1,2-diaminoethane (L) and *N*-isopropyl-1,2-diaminoethane (L′) complexes of nickel(II) nitrite: X-ray single crystal structure of *trans*-[NiL2(NO2)2]. *Transition Met. Chem.*, **32** (2007) 531–535.

[4] Sylwia E. Kutniewska, Adam Krowczyski, Radosław Kaminski, Katarzyna N. Jarzembska, Sebastien Pillet, Emmanuel Wenger and Dominik Schaniel, *Photocrystallographic and spectroscopic studies of a model (N,N,O)-donor square-planar nickel(II) nitro complex: in search of high-conversion and stable photoswitchable materials*, *IUCrJ*, **7** (2020) 1188–1198

[5] Goodgame, D. M. L., & Venanzi, L. M. (1963). *98. Diamine complexes of nickel (II). Part I. Complexes with NN-diethylethylenediamine. Journal of the Chemical Society (Resumed), 616.*

B-19

SYNTHESIS, STRUCTURAL CHARACTERIZATION AND ANTICANCER ACTIVITY OF NEW 5-TRIFLUOROMETHYL-2-THIOXO-THIAZOLO[4,5-*d*]PYRIMIDINE DERIVATIVES

Lilianna Becan[1], Anna Wojcicka[1], Anna Pyra[2], Nina Rembiałkowska[3], Iwona Bryndal[1]

[1]Department of Pharmaceutical Technology, Faculty of Pharmacy, Wroclaw Medical University, Borowska 211A, 50-556 Wrocław
[2]Faculty of Chemistry, University of Wroclaw, Joliot-Curie Street 14, 50-383 Wrocław
[3]Department of Molecular and Cellular Biology, Faculty of Pharmacy, Wroclaw Medical University, Borowska 211A, 50-556 Wrocław

Fluorinated organic molecules are of special interest in medicinal chemistry [1]. The addition of fluoride to the molecule often improves pharmacological properties [2]. Currently, fluorinated antitumor agents constitute an important class of anticancer drugs [3]. The trifluoromethyl moiety containing three fluorine atoms is a very lipophilic functional group of electronegative nature. Drugs with a trifluoromethyl substituent are used in the treatment of many diseases, but predominantly as neuroleptic, antiviral and anticancer agents [4].

Here we describe a structural modification of the 7-thio analogues of purines – thiazolo[4,5-*d*]pyrimidines – performed to introduce the trifluoromethyl moiety into position 5 of the scaffold. Thiazolo[4,5-*d*]pyrimidines as purine antagonists exhibit potential biological activity, including anticancer [5, 6]. It was expected that the combination of the trifluoromethyl group and the thiazolo[4,5-*d*]pyrimidine structure in one molecule would lead to an active compound with good therapeutic properties. A novel series of 5-trifluoromethyl-2-thioxo-thiazolo[4,5-*d*]pyrimidin-7(6*H*)ones was synthesized and evaluated for its *in vitro* cytotoxicity against cancer cell lines.

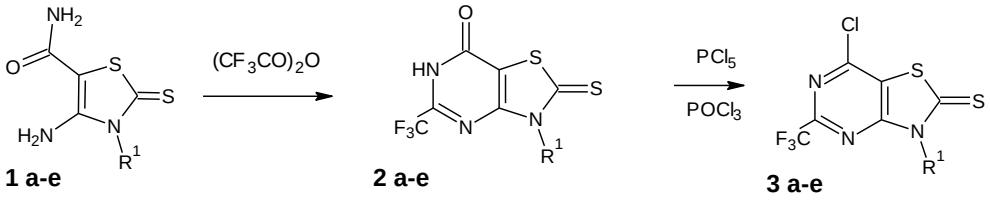

1 a-e **2 a-e** **3 a-e**

R_1: (a) C_2H_5, (b) C_6H_5, (c) 4F-C_6H_4, (d) 3F-C_6H_4, (e) 2F-C_6H_4

Scheme 1. The synthetic routes to studied compounds.

The preparation of 5-trifluoromethyl-thiazolo[4,5-*d*]pyrimidines is depicted in Scheme 1. Starting 4-amino-2-thioxo-2,3-dihydro-3-substituted-1,3-thiazole-5-carboxamides **1a-e** were prepared in a one-pot reaction from sulphur, 2-cyanoacetamide and appropriate isothiocyanate according to procedure reported by Gewald [7]. The 3-substituted-2-thioxo-5-(trifluoromethyl)-2,3-dihydro-[1,3]-thiazolo[4,5-*d*]pyrimidin-7(6*H*)-ones **2a-e** were synthesized by the cyclization of the 4-amino-2-thioxo-2,3-

dihydro-3-substituted-1,3-thiazole-5-carboxamides with trifluoroacetic acid anhydride. In the next step chlorination of **2a-e** gave the 7-chloro derivatives **3a-e**. Newly synthesized compounds were evaluated for their in vitro anticancer activity. The 7-chloro-3-phenyl-5-(trifluoromethyl)[1,3]thiazolo[4,5-*d*]pyrimidine-2(3*H*)-thione (**3b**) proved to be the most active. The single-crystal X-ray analysis was performed to confirm 3D structure for compounds **2c** (Fig. 1) and **3b**. The structures were also determined by IR, ^{1}H-NMR, ^{13}C-NMR, MS and elemental analysis.

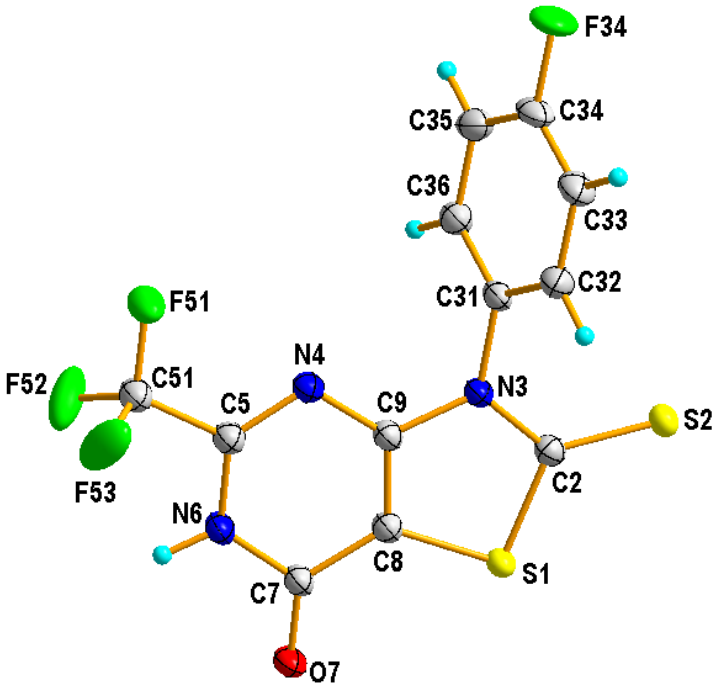

Fig. 1. View of the asymmetric unit of **2c**, showing the atom-numbering scheme and displacement ellipsoids drawn at the 50% probability level.

References

[1] S. Swallow, Fluorine in Medicinal Chemistry, in: Prog. Med. Chem., 1st ed., Elsevier B.V., United Kingdom (2015) 65.
[2] K. Müller, C. Faeh, F. Diederich, *Science*, **317** (2007) 1881.
[3] C. Isanbor, D. O'Hagan, *J. Fluor. Chem.*, **127** (2006) 303.
[4] K. L. Kirk, *J. Fluor. Chem.*, **127** (2006) 1013.
[5] B. Kuppast, H. Fahmy, *Eur. J. Med. Chem.*, **113** (2016) 198.
[6] L. Becan, E. Wagner, *Med. Chem. Res.*, **22** (2013) 2376.
[7] K. Gewald, *J. Prakt. Chem.*, **32** (1966) 26.

B-20

CRYSTAL AND MOLECULAR STRUCTURE OF TWO COORDINATION COMPOUNDS OF ZINC WITH POTENTIAL APPLICATION IN MEDICINE

Anita Raducka, Marcin Świątkowski, Agnieszka Czylkowska

Institute of General and Ecological Chemistry, Faculty of Chemistry, Łódź University of Technology, Żeromskiego 116, 90-924 Łódź, Poland

Structural studies of coordination compounds with a potential pharmacological application are an important stage in the process of designing new, effective, and safe drugs. N-heterocyclic ligands deserve special attention due to their coordination abilities. The disease that causes the highest death toll is small-cell lung cancer. The cis-platinum compounds used so far in chemotherapy also cause many side, toxic effects. In the search for new chemotherapeutic agents, new coordination compounds with potential use against A549 neoplastic cells have been designed. As a result of a slow crystallization, crystals of two zinc compounds containing biologically active organic ligands, i.e., 2-(pyridin-3-yl)-3H-imidazo[4,5-b]pyridine (L1) and 6-bromo-2-(pyridin-3-yl)-3H-imidazo[4,5-b]pyridine (L2) were obtained. In this paper, the structures of these compounds labeled C1 $[Zn_2Cl_4(L1)_2]$ and C2 $[Zn_2Cl_4(L2)_2]$ are presented (Fig. 1). Both of them are dinuclear compounds, in which the bridges are formed by L1 and L2. The mutual arrangement of organic ligand molecules is disparate in C1 and C2, which can be the main reason for differences in anticancer activity.

Crystal Data

C1: $C_{22}H_{16}Cl_4N_8Zn_2$ (M =664.97 g/mol), triclinic, space group P-1 (no. 2), a = 7.4842(2) Å, b = 8.1366(2) Å, c = 9.9889(2) Å, α = 84.703(2)°, β = 87.371(2)°, γ = 80.218(2)°, V = 596.60(3) $Å^3$, Z = 1, R1 = 0.0251 (I > 2σ(I)), wR2 = 0.0726.

C2: $C_{22}H_{14}Br_2Cl_4N_8Zn_2$ (M =822.77 g/mol), monoclinic, space group P21/c (no. 14), a = 12.9125(2) Å, b = 13.88880(10) Å, c = 15.3249(2) Å, β = 105.4830(10)°, V = 2648.61(6) $Å^3$, Z = 4, R1 = 0.0310 (I > 2σ(I)), wR2 = 0.0848.

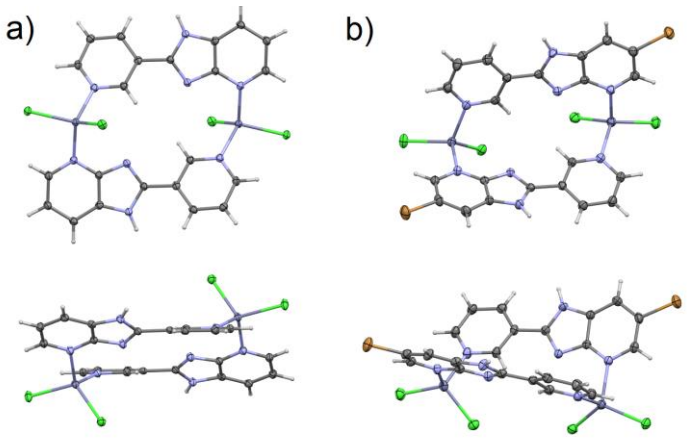

Fig. 1. Molecular structure of C1 (a) and C2 (b).

B-21

THE INFLUENCE OF VARIED METAL TO LIGAND RATIOS ON STRUCTURE DIVERSITY OF COORDINATION COMPOUNDS OF COPPER(II) 2,2-BIS(HYDROXYMETHYL)PROPIONATE WITH HEXAMETHYLENETETRAMINE

Sadaf Rauf, Agata Trzęsowska-Kruszyńska, Marcin Świątkowski, Tomasz Sierański

Institute of General and Ecological Chemistry, Łódź University of Technology, Żeromskiego 116, 90-924 Łódź, Poland

The designing and characterization of new transition metal complexes of desired structure and properties have always attracted the attention of scientists due to their diverse magnetic, photocatalytic, H_2O_2 sensing and antimicrobial properties. The properties of transition metal complexes depend upon their self-assembly, electronic configuration, non-bonding interactions and size [1-3]. Another important factor, which contributes to the structural diversity of coordination compounds, is the selection of organic ligand of appropriate symmetry, functionality, shape and adaptability to get desired geometry of coordination compound [4]. The correctly designed structure of coordination compounds together with appropriately set of parameters of single precursor method allow for example governing of size and morphology of nanoparticles, which can be obtained from these coordination compounds. The improvement of effective methods of selective synthesis of nanoparticles is one of the most important tasks of modern nanotechnology because the achievement of expected properties of nanoparticles requires precise control of their shape and size [5].

The purpose of this study is to determine the influence of different metal to ligand ratios used for synthesis and its effect on the topology of resulting coordination compounds. For this purpose**,** three different coordination compounds based on copper 2,2-bis(hydroxymethyl)propionate and hexamethylenetetramine (hmta) were designed, synthesized and investigated. The hexamethylenetetramine (hmta) was used because it can act as a multifunctional ligand due to the presence of pair of unshared electrons on each nitrogen atom. Hmta, as a heterocyclic linker, has a tendency to form wide range of coordination complexes with many transition metals using its different modes of coordination[6]. The reaction was carried out in various substrate ratios i.e.1:2, 1:1, 2:1, 3:1 for each pair of copper propionate $[Cu(dmp)_2]$-hmta respectively. Structural, spectral, and thermal properties of obtained compounds were studied in detail.

The synthesis results in the formation of three new coordination compounds with diverse structure i.e. mononuclear $[Cu(dmp)_2(hmta)_2(H_2O)]$, dinuclear $[Cu_2(dmp)_4(hmta)_2]$, and 1D coordination polymer $[Cu_2(dmp)_4(hmta)]_n$. The metal-ligand ratio in the obtained crystals exhibits similar stoichiometry as applied in the synthesis. The structural diversity of obtained coordination compounds is achieved due to the different coordination modes of tetradentate hmta and the ability of 2,2-bis(hydroxymethyl) propionic acid to coordinate *via* carboxylate group while the free hydroxyl groups play their role in stabilizing the structure through hydrogen bonding.

B-21

References
[1] K. Serbesta, T. Dural, M. Emirika, A. Zenginb , Ö. Faiza, *J. Mol. Struct*., **1229** (2020) 129579.
[2] K. Jana, R. Maity, H. Puschmann, A. Mitra, R, Ghosh, S. C. Debnath, A. Shukla, A. K. Mahanta, T. Maity, B. Chandra Samanta, *Inorganica Chim. Acta*, **515** (2021) 120067.
[3] X. X. Hao, H. Zhang, E. J. Zuo, *J. Solid State Chem*., **296** (2021) 121959.
[4] A. Alothman, M. Albaqami, R. Alshgari, *J. Mol. Struct*., **1223** (2021) 128984.
[5] M. Swiatkowski, R. Kruszynski, *Appl. Organomet. Chem*., 33 (**2019)**, e4812
[6] Y. C. Guo, S. R. Luan, Y. R. Chen, X. S. Zang, Y. Q. Jia, G. Q. Zhong and S. K. Ruan, *J. Therm. Anal. Calorim*., **68** (2002) 1025–1033.

B-22

NON-LINEAR OPTICAL PROPERTIES AND NEGATIVE AREA COMPRESSIBILITY OF (*S*)-2-AMINO-3-GUANIDINOPROPANOIC ACID MONOCHLORIDE

Piotr Rejnhardt[1], Jan K. Zaręba[2], Ida Moszczyńska[3], Marek Daszkiewicz[1]

[1] Institute of Low Temperature and Structure Research, Polish Academy of Sciences, P. O. Box 1410, 50-950 Wrocław, Poland,
[2]Advanced Materials Engineering and Modelling Group, Faculty of Chemistry, Wrocław University of Science and Technology, Wybrzeże Wyspiańskiego 27, 50-370 Wrocław, Poland
[3]Faculty of Chemistry, Adam Mickiewicz University, Umultowska 89b, 61-614 Poznań, Poland

Second harmonic generation (SHG) in organic crystals is a subject of extensive investigation for years [1]. The absence of an inversion centre in crystal is mandatory in order to obtain SHG response, although many other features play an important role and must be taken into account for synthesis of non-linear materials [2]. For example, an occurrence of delocalized π electrons and intramolecular donor-acceptor charge transfer between two molecular subparts (functional groups) is welcomed [3]. It leads to large hyper-polarizability β and this kind of materials are good candidates for second harmonic generation.

Negative area compressibility (NAC) is extremely rare phenomenon occurring under pressure and it is characterized by two-dimensional expansion of material. Most materials shrink in all directions under pressure, some of them expand in one direction (negative linear compressibility) and only few structures are capable of expanding in two directions [4]. The NAC is highly desirable for application such as pressure sensors and actuators [5].

Here we present crystal and molecular structure of a new salt of the homologue of L-arginine, (*S*)-2-amino-3-guanidinopropanoic acid monochloride (AGPA) and its deuterated analogue (DAGPA). Crystal structure were determined by X-ray diffraction at room temperature and over a dozen low-temperature conditions (down to 100 K) for both analogues. The crystals were also measured at 21 pressure points for AGPA and 10 pressure points for DAGPA. The temperature-dependent measurements showed no structural phase transition, but anomalous increase of the *c* lattice parameter upon cooling the sample. Contrary to this, the phase transition was observed by high-pressure diffraction. The isosymmetric phase transition ($P2_1$ space group) was noticed at 0.91 GPa for AGPA and 0.96 GPa for DAGPA (Figure 1 a and b). Calculations of median compressibility for the high-pressure phase of both compounds showed slight anomalous increase of *a* and *b* lattice parameters indicating the rare NAC phenomenon in the studied compounds.

Since earlier studies have shown that external pressure can tune SHG signal, diamond anvil cell (DAC) was used to investigate the pressure dependence of SHG response. The result of SHG measurements revealed that monochloride salt of (*S*)-2-amino-3-guanidinopropanoic acid and deuterated analogue have better optical non-linear properties than L-arginine chloride, $3 \cdot I_{KDP}$ *vs.* $0.3 \cdot I_{KDP}$. This fact can be associated with

shorter carbon chain (*S*)-2-amino-3-guanidinopropanoic acid and thus closer intramolecular distance between carboxyl and guanidinium groups than in L-arginine. The phase transition was also detected during the SHG measurements in the DAC. Dependence of SHG response on pressure revealed extreme decrease of the recorded SHG signal during squeezing the sample in the low region of high pressure conditions and the minimum at approximately 0.7-0.9 GPa associated with the structural phase transition (Figure 1c).

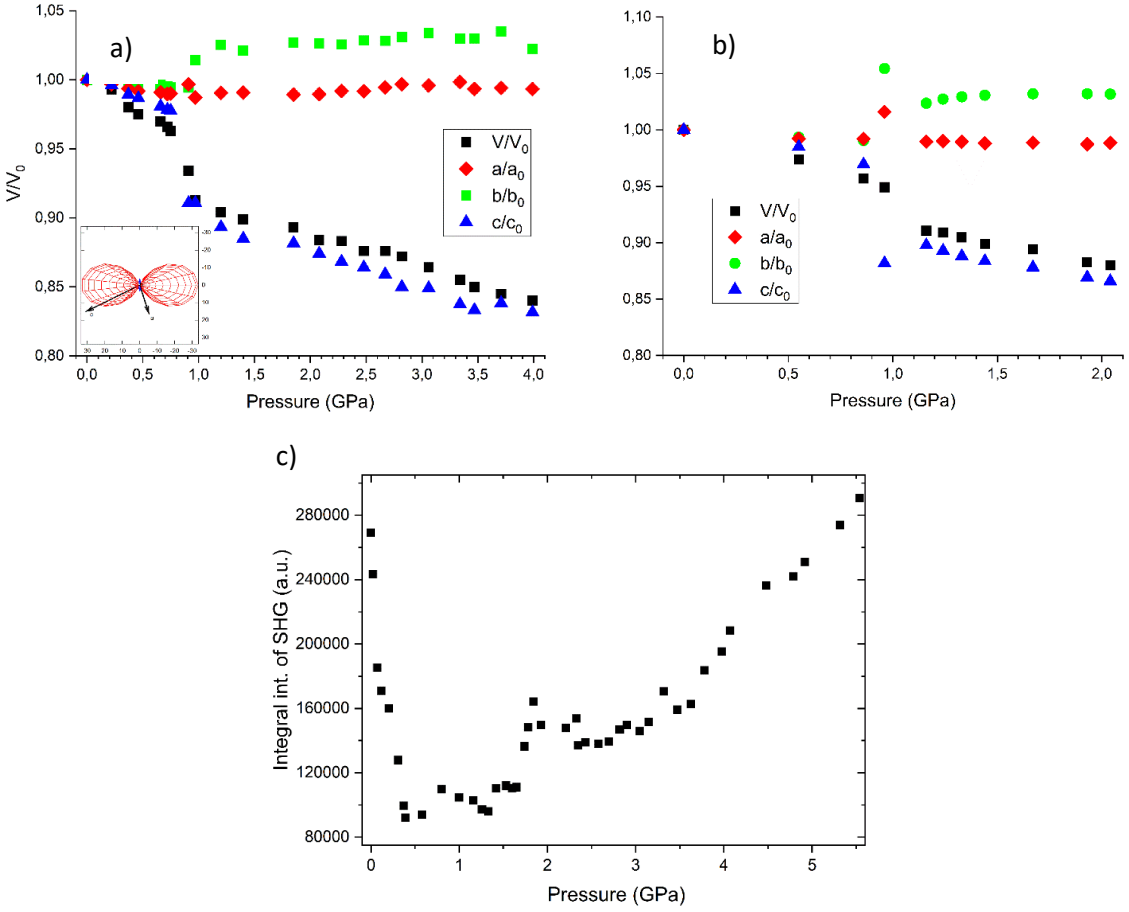

Figure 1. a) Normalized unit cell parameters and compressibility indicatrix for AGPA, b) and for DAGPA, c) dependence of the intensity of SHG response on pressure.

References

[1] Materials for Nonlinear Optics (Chemical Prospectives). Eds. S.R. Marder, J.E. Sohn, G.D. Stucky, ACS Symposium Series 455 (ACS Press Washington, DC, 1983).
[2] Elena Marelli, Nicola Casati, Fabia Gozzo, Piero Macchi, Petra Simonciccd and Angelo Sironie High pressure modification of organic NLO materials: Large conformational re-arrangement of 4-aminobenzophenone November 2011*CrystEngComm* **13(22)** (2011) 6845-6849.
[3] P.N. Prasad, D.J. Williams, Wiley, New York (1991).
[4] Cai, W., Gładysiak, A., Anioła, M., Smith, V. J., Barbour, L. J. & Katrusiak, A. *Journal of the American Chemical Society*. **137** (2015) 9296–9301.
[5] *Chem. Sci*., **10** (2019) 1309-1315.

B-23

CRYSTAL STRUCTURES, THERMAL DECOMPOSITION AND SPECTROSCOPIC PROPERTIES OF TWO NEW COPPER(II) AND ZINC(II) COMPOUNDS WITH BIOLOGICALLY IMPORTANT LIGAND

Bartłomiej Rogalewicz, Agnieszka Czylkowska, Małgorzata Szczesio

Institute of General and Ecological Chemistry, Łódź University of Technology, 116 Żeromskiego Street, 90-924 Łódź

Imipramine is currently one the most commonly used antidepressant drug. The reason behind this is its significant effectiveness. In order to increase its solubility and bioavailability for human organism, it is used in the hydrochloride form. However, treatment with imipramine hydrochloride can also result in occurrence of several side effects. One of the strategies to improve drugs' performance is to synthesize and investigate their derivatives, as some of them may exhibit either better effectiveness, or reduce the possibility of appearance of unwanted side effects.

Two new compounds have been obtained in the reaction of imipramine hydrochloride ($HIMI^+Cl^-$) with copper(II) and zinc(II) chlorides in the form of crystalline precipitates. Some of their physicochemical properties have been studied using Single-crystal X-ray diffraction analysis, thermogravimetric analysis and Fourier-transform infrared spectroscopy. For both structures melting points were determined, as well as for free imipramine hydrochloride.

Single-crystal X-ray diffraction analysis revealed that both compounds form $[HIMI^+]_2[MCl_4^{2-}]$-type systems, where M: Cu^{2+}/Zn^{2+}. Analyzed compounds are isostructural with approximately the same lattice parameters.

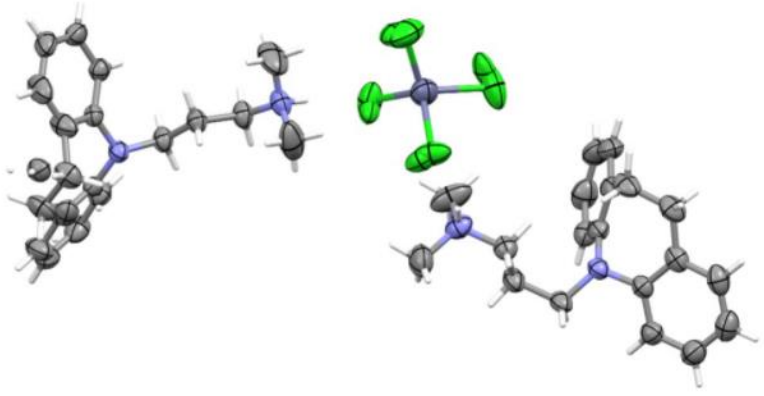

Fig. 1. Crystal structure of $[HIMI^+]_2[ZnCl_4^{2-}]$.

Both thermogravimetric analysis and Fourier-transform infrared spectroscopy provided important information about newly obtained structures. Both $[HIMI^+]_2[CuCl_4^{2-}]$ and $[HIMI^+]_2[ZnCl_4^{2-}]$ are stable at room temperature and decompose in similar manner. It is also worth mentioning, that these compounds decompose totally, due to the formation of volatile metal halide derivatives, which has already been reported [1]. FT-IR spectra of these compounds are in very good agreement with crystallographic

data. Also DTA peaks derived from thermogravimetric analysis confirm correctness of measured melting points.

Literatura

[1] S. Zhou, S. Shen, D. Zhao, Z. Zhang, S. Yan, *J. Therm. Anal. Calorim.*, **129** (2017) 1445-1452.

B-24

THE INFLUENCE OF HALIDE TYPE ON THE REACTION OF COPPER(I) HALIDES WITH 1-BENZOYL-3-(5-METHYLPYRID-2-YL)THIOUREA

Damian Rosiak, Andrzej Okuniewski, Jarosław Chojnacki

Department of Inorganic Chemistry, Faculty of Chemistry, Gdansk University of Technology, G. Narutowicza 11/12, 80-233 Gdańsk

Thiourea and its derivatives are soft Lewis bases and readily form complexes with soft Lewis acids such as copper, gold, and mercury ions [1], where they serve as *S*-donor ligands.

During our research, we react d^{10} metal halides (i.e. HgX_2 and CuX, where X = Cl, Br, I) with various 1-benzoylthioureas obtaining mono- and dinuclear complexes, coordination polymers, and hybrid inorganic chains [2-4]. To increase the probability of coordination polymers formation, we have used a ligand that contains an additional *N*-donor atom – 1-benzoyl-3-(5-methylpyrid-2-yl)thiourea (**L**). Within this communication we would like to present the products of the reaction of **L** with CuX (where X = Cl, Br, I) – **I**, **II**, and **III** respectively. When we used CuCl and CuBr, the ligand has been oxidized and cyclized. This could be due to the fact that the reaction was carried out in the presence of oxygen (air) and the copper(I) ions have oxidized to copper(II) ions. This caused the ligand molecules to undergo oxidative heterocyclization. Subsequently, the resulting compound reacted with excess of CuCl or CuBr forming complexes (see Fig. 1).

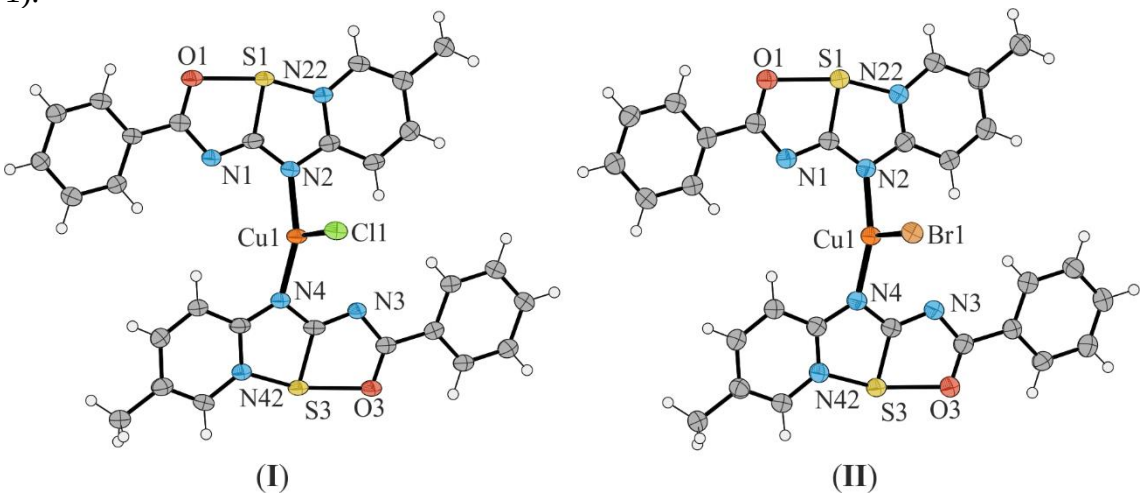

Fig. 1. Molecular structure of **I** and **II**. Ellipsoids are drawn at 50% probability level.

Although the synthetic procedure of **III** was identical to that of **I** and **II**, the iodide ions have such strong reducing properties that we do not find products of the oxidative cyclization of the ligand. Instead, a coordination polymer is formed in which the ligand molecules (as intended) connects to copper ions not only by the sulphur atom but also by the nitrogen atom of the pyridine ring.

I and **II** are mononuclear coordination compounds and their crystals are isostructural. In these complexes, central atoms have the coordination number of 3 and

$Cu(Cl/Br)N_2$ coordination centres adopt trigonal planar geometry. In the crystal structures of these compounds, C−H···(Cl/Br) hydrogen bonds can be distinguished, which cause the formation of chains. Extension of the structure in two successive dimensions is ensured by the presence of weak C−H···O hydrogen bonds with simultaneous participation of S···S chalcogen interactions (see Fig. 2).

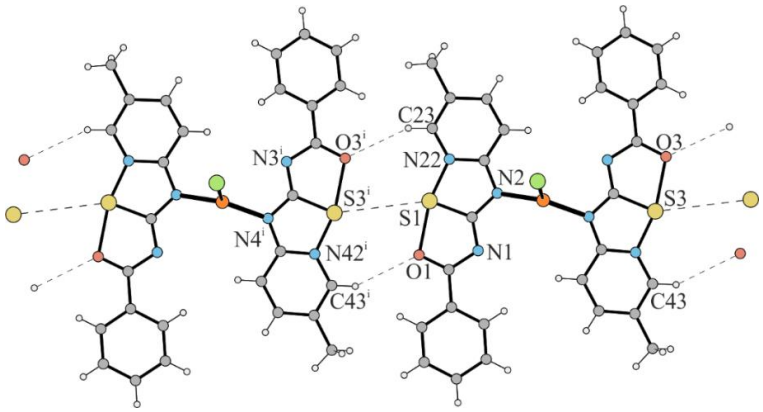

Fig. 2. Main interactions present in the crystal structures of **I** and **II**; on the example of **I**. Symmetry codes: (i) $x, -1 + y, -1 + z$.

In the case of **III**, the CuI_2NS coordination centre adopts the geometry of a distorted tetrahedron ($\tau_4' = 0.82$ [2]). The ligand molecules do not behave as chelating ligands but act as bridging ligands, linking two binuclear coordination centres. As a result of the above interactions, two alternately occurring centrosymmetric rings are formed: small Cu_2I_2 (with short Cu···Cu contacts – 2.8407(2) Å) and large $Cu_2(\mathbf{L})_2$ (see Fig. 3).

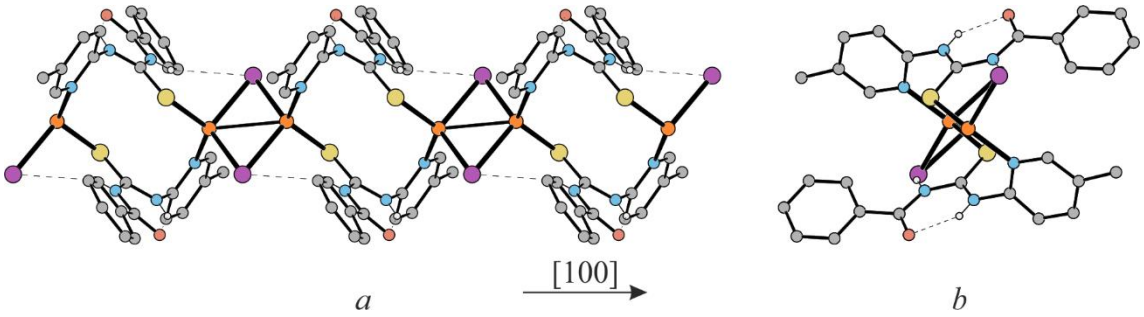

Fig. 3. A fragment of the **III** chain seen (a) perpendicularly; (b) along the propagation direction; with marked hydrogen bonds and an emphasized coordination centre.

References

[1] M. Mirzaei, H. Eshtiagh-Hosseini, M. Mohammadi Abadeh, M. Chahkandi, A. Frontera, A. Hassanpoor: *CrystEngComm*, **15** (2013) 1404.
[2] A. Okuniewski, D. Rosiak, J. Chojnacki, B. Becker: *Polyhedron*, **90** (2015) 47.
[3] D. Rosiak, A. Okuniewski, J. Chojnacki: *Polyhedron*, **146** (2018) 35.
[4] D. Rosiak, A. Okuniewski, J. Chojnacki: *Acta Cryst. C*, **74** (2018) 1650.

B-25

AN INTERPRETATION OF ELECTRON DENSITIES OF ATOM TYPES IN MULTIPOLAR ATOM TYPES FROM THEORY AND STATISTICAL CLUSTERING (MATTS) DATABANK

Paulina Rybicka, Marta Kulik, Michał L. Chodkiewicz i Paulina M. Dominiak

Centrum Nauk Biologiczno-Chemicznych Uniwersytetu Warszawskiego, Wydział Chemii, Uniwersytet Warszawski, ul. Żwirki i Wigury 101, 02-089 Warszawa

Independent Atom Model (IAM) is the most commonly used model in crystal structure refinement on X-ray or electron diffraction data. It assumes spherical symmetry of atomic densities, disregarding the charge redistribution due to chemical bonding. However, more accurate models of electron densities are available, such as the Multipole Model (MM). It introduces an aspherical approach that describes the surrounding of the nucleus far more accurately by using the Hansen-Coppens pseudoatom formalism[1]. In the MM, the electron density parameters of pseudoatoms appeared to be almost identical for atoms of one element located in similar chemical environment. For that reason, banks of transferable aspherical atoms with universal parameters were created. MATTS (Multipolar Atom Types from Theory and Statistical Clustering) databank is one of them and supersedes previously used UBDB (University at Buffalo DataBank)[2]. It contains over 600 different atom types categorized by central element type and the topology of chemical surroundings, with the information about the electron density distribution. However, such atom types are defined in only one of many possible local coordinate systems determined by the position of coordinate axes towards neighboring atoms. As the axis position changes, the multipole parameters present in MM also can change. The main idea behind the project was to get the comprehensive and detailed image of the electron density for atom types present in MATTS databank and also, to determine and understand the relationships and similarities between different atom types. Primarily, clustering based on topology or density parameters was the main tool used to group similar atom types. The topology clustering took into account the information about the number and type of atoms' neighbors, local symmetry and planarity. It allowed to visualize the databank as a series of trees. For electron density clustering, Density-Based Spatial Clustering of Applications with Noise (DBSCAN) method was used to do multidimensional clustering of all parameters. The results from topology and density clustering were compared searching for common features. Such analysis allowed to capture similarities in the spatial distribution of electron density for atom types, identify errors and made it possible to categorize atom types into general and specific ones. Finally, it helped to understand which topology features differentiate atom types and influence the electron density the most.

The authors acknowledge NCN UMO-2017/27/B/ST4/02721 grant.

References

[1] N. K. Hansen, P. Coppens, *Acta Cryst A.*, **34** (1978) 909–921.
[2] P. Kumar, B. Gruza, S. A. Bojarowski, P. M. Dominiak, *Acta Cryst. A.*, **75** (2019) 398-408.

B-26

CRYSTAL STRUCTURES OF ENISAMIUM HALOGENIDES

Anna Shaposhnyk[a], Vitalii Rudiuk[b], Igor Levandovskiy[c], Vyacheslav Baumer[a], Viktor Margitich[b]

[a]SSI "Institute for Single Crystals" NAS of Ukraine,
60 Nauky Avenue, 61001,Kharkiv, Ukraine
[b]Farmak JSC, 63 Kyrylivska Street, Kyiv 04080, Ukraine
[c]National Technical University of Ukraine "Igor Sikorsky Kyiv Polytechnic Institute",
37 Prospect Peremohy, 03056, Kyiv, Ukraine

At present, the synthesis of effective antiviral molecules is an essential direction in pharmaceutical science. One of such compounds is enisamium (IUPAC name: 4-[(benzylamino)carbonyl]-1-methylpyridinium; hereafter 4-BACMP) iodide which directly inhibits viral RNA-dependent RNA polymerase of influenza virus and SARS-CoV-2. Enisamium cation is stable enough due to the localization of the positive charge at the pyridine nitrogen atom substituted by the methyl group. The attempts to replace iodide anion in a crystal by chloride- and bromide were performed to study the enisamium capability to form different salts. The obtained crystal structures are reported in the present work.

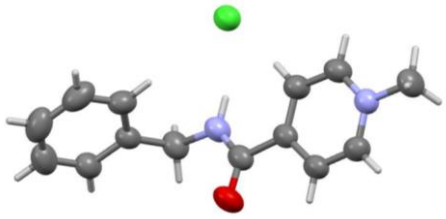

Fig. 1. Molecular stucture of 4-BACMP halohenide.

The main crystallographic data for different salts of enisamium are presented in Table 1.

Table 1
Crystalline lattice characteristics of chloride, bromide, and iodide salts of 4-BACMP

Salt	Sp. gr.	Unit cell, Å, °	V, Å^3	d_{calc}, Mg·m^{-3}
4-BACMP-Cl	$P2_1/n$	a=8.5222(7) b=5.6875(3) c=27.172(1) β=91.243(6)	1316.71(15)	1.325
4-BACMP-Br	$P2_12_12_1$	a=9.417(3) b=11.099(5) c=14.363(6)	1501.2(10)	1.390
4-BACMP-I	$P2_12_12_1$	a=10.8801(4) b=14.3044(5) c=9.2869(3)	1445.36(8)	1.628

It was shown that enisamium bromide and enisamium iodide crystal structures are iso-structural having a similar packing motif. Furthermore, the enisamium cation does not contain any asymmetric centre but its salts with bromide and iodide are crystallized in the Soncke chiral space group (Table 1). Enisamium chloride crystal structure is centrosymmetric and differs significantly from bromide and iodide analogs.

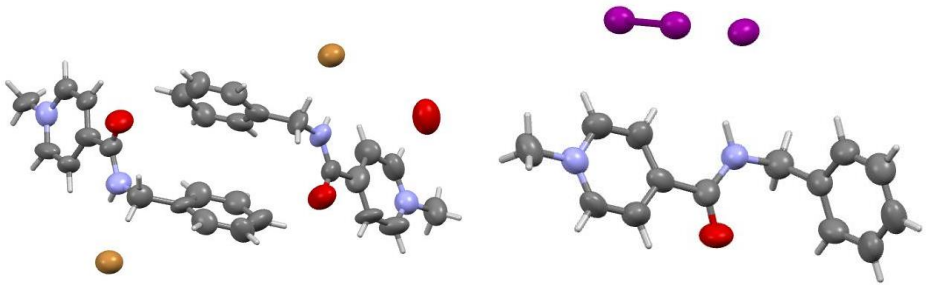

(a) *(b)*

Fig. 2. Molecular stucture of *(a)* 4-BACMP-Br hemihydrate and *(b)* 4-BACMP-I·I_2.

The main crystallographic data for 4-BACMP-Br hemihydrate and 4-BACMP-I_3 are presented in Table 2.

Table 2
Crystalline lattice characteristics of 4-BACMP bromide hemihydrate and 4-BACMP iodide·I_2

Salt	Sp. gr.	Unit cell, Å, °	V, Å^3	d_{calc}, Mg·m^{-3}
4-BACMP-Br·0.5H_2O	P-1	a=5.854(3) b=14.733(6) c=17.744(8) α=65.74(4) β=85.64(4) γ=85.26(4)	1388.8(12)	1.512
4-BACMP- I·I_2	P2$_1$/n	a=14.407(3) b=8.849(1) c=14.555(4) β=119.63(3)	1613.0(7)	1.981

It is important to detect possible polymorphs of the same salts for well- known pharmaceutical reasons. No polymorph for the enisamium salts was obtained. Nevertheless, as a result of crystallization, 4-BACMP-Br hemihydrate and 4-BACMP-I_3 were received. The mentioned compounds were analyzed by the method of single crystal diffraction.

No crystalline polymorphs of different salts of enisamium (iodide, bromide, and chloride) were found. Instead, 4-BACMP-Br hemihydrate and 4-BACMP-I·I_2 were detected depending on the conditions of the crystallization of the corresponding salts.

B-27

CRYSTAL STRUCTURE OF A PRODUCT OF SELF-CYCLIZATION OF A SCHIFF BASE

Magdalena Siedzielnik, Anna Dołęga

Department of Inorganic Chemistry, Faculty of Chemistry, Gdansk University of Technology, G. Narutowicza 11/12, 80-233 Gdańsk

Schiff bases were received for the first time in 1864 by Hugo Schiff and since then, a variety of methods for the synthesis of imines have been described.[1] Schiff bases are compounds of big importance, as evidenced by the number of publications published annually on the topic. Such a great interest can be explained by the fact that they are widely used in organic synthesis, chemical catalysis, and they occur in many biologically active compounds.[2-7] The special properties of Schiff bases are related to the simultaneous presence of proton-donor and proton-acceptor groups, the possibility of formation of inter- and intramolecular hydrogen bonds and possible participation in proton transfer processes.[7] The electrophilic carbon and nucleophilic nitrogen within the imine bond provides good binding properties with different nucleophiles and electrophiles. The imine nitrogen atom is acting as a Lewis base (electron donor) toward metal ions, thus, Schiff bases can form complexes.

However our preliminary studies to obtain a cobalt(II) complex with Schiff base (**L1**, shown in Figure 1), confirms that the **L1**, can undergo self-cyclization with the formation of a multi-cyclic compound (**C1**, shown in Figure 1). As the compound crystallises very well from the reaction mixture, this allowed us to perform X-ray diffraction analysis and determine the molecular structure (Figure 2). The reaction was catalysed in this case by cobalt(II) chloride. It is worth mentioning that preliminary studies show that the reaction takes place in an aprotic solvent (acetonitrile), while the formation of compound **C1** was not observed in a protic solvent (methanol). Moreover the reaction additionally proceeds with the formation of an ionic pair of cobalt(II) complex with 2-aminopyridine, o-vanillin and **L1**. A preparative TLC technique was used to separate the products.

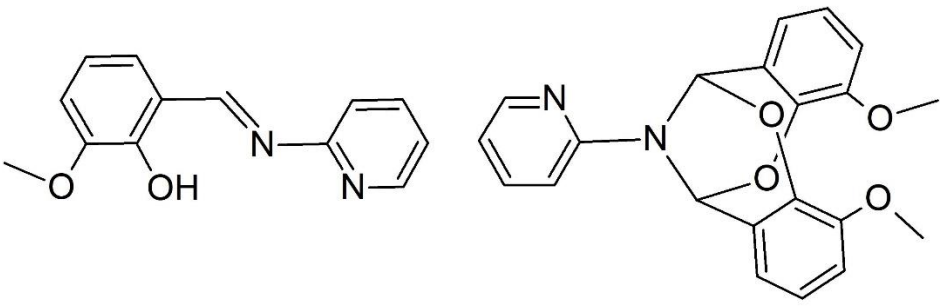

L1 **C1**

Figure 1. Formulas of Schiff base **L1** and obtained cyclic product **C1**

B-27

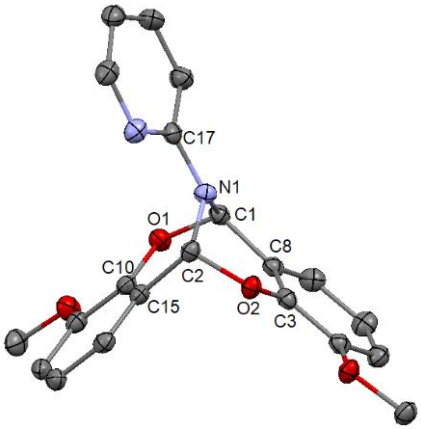

Figure 2. Molecular structure of **C1**. Thermal ellipsoids at 50%. Hydrogen atoms have been omitted for clarity. Bond lengths [Å]: O1—C1 1.4556(14), O2—C2 1.4436(14), N1—C1 1.4419(16), N1—C2 1.4544(16), N1—C17 1.4061(16). Angles [°]: C1—N1—C2 109.17 (10), C17—N1—C1 121.13 (10), C17—N1—C2 119.56 (10), C10—O1—C1 112.81(9), C3—O2—C2 112.87(9).

The crystallographic data for the title compound were collected on an STOE IPDS II diffractometer. at 120.0 K using Mo *K*α radiation of a microfocus X-ray source. **C1** crystallizes in a triclinic system in *P*-1 space group. The unit cell parameters are as follows: a= 9.2880(5) Å, b= 9.6491(5) Å, c= 10.2198(5) Å, α= 66.574(4)°, β= 82.570(4)°, γ= 84.516(4)°, V= 832.37(8) Å^3 and Z= 2. Quality parameters of the solution are $R_1[I > 2\sigma(I)]$= 0.0333, wR_2 (all data)= 0.0400, R_{int}= 0.025, GOOF= 1.043. Asymmetric unit contains one molecule.

The compound consists of six connected rings, including two benzene rings, one pyrimidine ring, two six-membered heterocyclic rings and one eight-membered heterocyclic ring. The rings are either fused or bridged and the pyridine ring in attached to the bridging nitrogen. The geometry around the nitrogen atom is flat, and the sum of the corresponding angles is approximately 360°. This demonstrates the sp^2 hybridisation of the nitrogen atom.

Literature

[1] H. Schiff, *Justus Liebigs Ann. Chem*., **131** (1864) 118.
[2] A. Hameed; M. al-Rashida; M. Uroos; S.A. Ali; K.M. Khan, *Expert Opin. Ther. Pat*., **27** (2017) 63.
[3] A. Mielcarek; A. Bieńko; P. Saramak; J. Jezierska; A. Dołęga, *Dalton Trans*., **48** (2019) 11780.
[4] A. Mielcarek; A. Wiśniewska; A. Dołęga, *Struct. Chem*., **29** (2018) 1189.
[5] W.-G. Jia; H. Zhang; T. Zhang; D. Xie; S. Ling; E.-H. Sheng, *Organometallics*, **35** (2016) 503.
[6] M. Siedzielnik; D.A. Pantazis; J. Bruniecki; K. Kaniewska-Laskowska; A. Dołęga, *Crystals*., **11** (2021) 512.
[7] C.M. Silva; D.L. Silva; L.V. Modolo; R.B. Alves; M.A. Resende; C.V.B. Martins; A. Fatima, *J. Adv. Res*., **2** (2011) 1.

B-28

STRUCTURAL CHEMISTRY OF Cu*X* (*X* = CF_3COO^-, NO_3^-, ½SO_4^{2-}) π,σ-COMPLEXES WITH SOME 1,2,4-TRIAZOLE AND 1,3,4-THIADIAZOLE ALLYL DERIVATIVES

Yurii Slyvka[1], Vasyl Kinzhybalo[2], Marian Mys'kiv[1]

[1]Ivan Franko National University of Lviv, 79005 Lviv, Ukraine
[2]Institute of Low Temperature and Structure Research, 50-422 Wrocław, Poland
e-mail: yurii.slyvka@lnu.edu.ua

1,2,4-Triazole and 1,3,4-thiadiazole derivatives have a wide range of applications in pharmaceutical chemistry and also were found to be excellent precursors for the crystal engineering of organometallic materials, possessing potential luminescent, catalytic, magnetic activities etc. Among these allyl-substituted 1,2,4-triazole and 1,3,4-thiadiazole compounds were recently used for the construction of heterometallic and mixed-valence copper(I/II) chloride π-complexes with interesting magnetic and non-linear optical properties and also they have proven to be a convenient scaffold for a design of novel copper(I) π,σ-coordination compounds [1, 2]. In our present work, using alternating-current electrochemical technique [3] and basing on 3-phenyl-4-allyl-5-allylsulfanyl-4*H*-1,2,4-triazole (**L1**) & 5-methyl-*N*-allyl-1,3,4-thiadiazol-2-amine (**L2**) ligands, five new copper(I) π,σ-complexes have been synthesized (Table 1). The diffraction data were collected on Oxford Diffraction Xcalibur (Atlas CCD detector) and Kuma KM4CCD diffractometers.

Table 1. Selected crystal data for copper(I) π,σ-complexes with **L1** and **L2** ligands.

	Composition	Space group	*V*, Å^3	*Z*	Density, g/cm^3	Coordination
1	$[Cu_2(\mathbf{L1})_2(CF_3COO)_2]$	$P2_1/c$	1771.6(11)	2	1.63	π, σ
2	$[Cu_2(\mathbf{L1})_2(H_2O)(NO_3)](NO_3)$	$P2_1/c$	3194.2(16)	4	1.63	π, σ
3	$[Cu_2(\mathbf{L1})_2(SO_4)]\cdot 4H_2O$	$P2_12_12_1$	3242.6(19)	4	1.66	π, σ
4	$[Cu_2(\mathbf{L2})_2(CF_3COO)_2]$	*P*-1	571.7(4)	1	1.93	π, σ
5	$[Cu_2(\mathbf{L2})_2(H_2O)(SO_4)]\cdot H_2O$	*P*-1	943.7(6)	2	2.01	π, σ

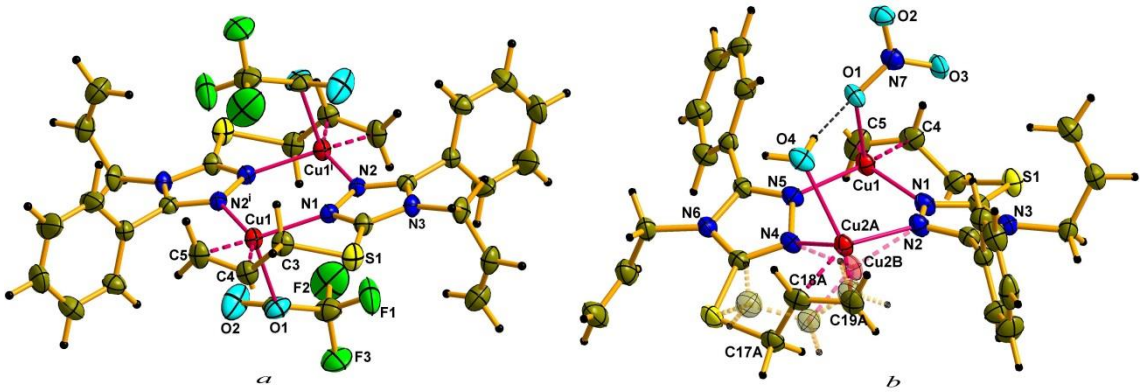

Figure 1. Centrosymmetric fragment in the structure **1** (*a*) and cationic dimeric moiety in the structure **2** (*b*). Symmetry code: **1**: (*i*) –*x*, –*y*+2, –*z*+1.

B-28

In the structures of **1**-**5** the organometallic part is represented by the $\{Cu_2(\mathbf{L})_2\}^{2+}$ dimers which are formed due to the chelating-bridging coordination behaviour of the ligands **L1** or **L2** (Fig. 1 & Fig. 2). The dimeric moieties contain six-membered ring comprised of two pairs of [*–N–N–*] azole fragments and two Cu(I) cations.

In all complexes the π-coordinated Cu(I) cation adopts a close to a trigonal pyramidal coordination environment (2N, (C═C) + O). The corresponding four-coordinate geometry indexes τ_4 are 0.83 (**1**), 0.83/0.84 (**2**), 0.82/0.81 (**3**), 0.82 (**4**) and 0.83/0.82 (**5**). The basal plane of the coordination arrangement consists of two N atoms and the η^2-allyl group. The axial site is occupied by O atom of the corresponding anion or H_2O molecule.

Similarly to previously studied complex $[Cu_2(\mathbf{L2})_2(NO_3)_2]$ [4] with thiadiazole ligand, in **1** and **4** structures centrosymmetric dimeric fragments are formed. In structure of **2** there are two crystallographically independent Cu(I) ions and two organic ligands, what is forced by the presence of two different apical ligands – H_2O molecule and NO_3^- anion. Non-equivalent effect of these apical ligands on the central ions leads to a significant distortion of the organometallic moiety and thus one of the coordinated allyl groups (C17, C18 and C19 atoms) is disordered over two sites with an occupancy ratio of 0.781(6) : 0.219(6).

Quite different coordination behaviour of the SO_4^{2-}anion in complexes **3** & **5** most probably is forced by the nature of the substituents at azole rings. In the case of more bulky **L1** ligand sulfate anion binds two copper(I) ions of the acentric $\{Cu_2(\mathbf{L1})_2\}^{2+}$ dimer in a bridging mode (Fig. 2a) and incorporates four H_2O molecules that participate in branched H-bonded network formation. In contrast to **3**, in the structure of **5** the presence of –NH- group in organic ligand significantly changes the geometry of hydrogen-bonded network, allowing H_2O molecule to compete with the anion at apical coordination of the metal ions.

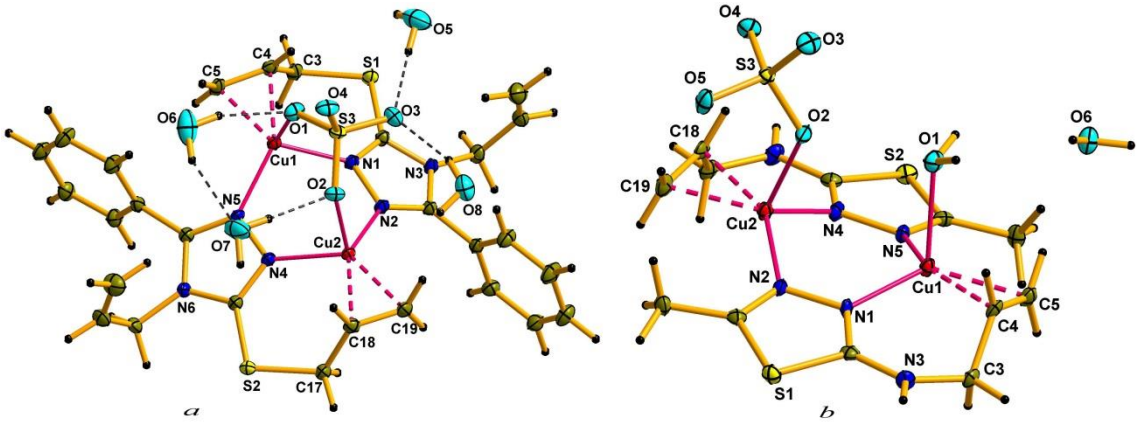

Figure 2. Different copper(I) coordination environments in the structures of **3** (*a*) and **5** (*b*).

Literature

[1] Yu. Slyvka, V. Kinzhybalo, O. Shyyka, M. Mys'kiv, *Acta. Crystalogr. Sect. C.*, **77** (2021) 249–256.

[2] O.R. Hordiichuk, Yu.I. Slyvka, V.V. Kinzhybalo, E.A. Goreshnik, T.J. Bednarchuk, O. Bednarchuk, J. Jedryka, I. Kityk, M.G. Mys'kiv, *Inorg. Chim. Acta.*, **495** (2019) 119012-9.

[3] Yu.I. Slyvka, O.V. Pavlyuk, M.Yu. Luk'yanov, M.G. Mys'kiv, *Ukraine Patent UA 118819*, Bull. № 16 (2017).

[4] B. Ardan, V. Kinzhybalo, Yu. Slyvka, O. Shyyka, M. Luk'yanov, T. Lis, M. Mys'kiv, *Acta Cryst. Section C.*, **73** (2017) 36–46.

B-29

SCHIFF BASE AND ITS SALTS EXHIBITING FLUORESCENCE IN THE SOLID-STATE

Paulina Sobczak, **Agata Trzęsowska-Kruszyńska**

Institute of General and Ecological Chemistry, Faculty of Chemistry, Łódź University of Technology, Żeromskiego 116, 90-924 Łódź

Compounds exhibiting fluorescence in the solid-state are increasingly a subject of interest among researchers in many fields of science. Due to the advantages of fluorescence, the scientific community focuses on the discovery of new fluorescent materials with different emission wavelengths with disparate applications, e.g. in optoelectronics [1] and forensics [2]. The fluorescence of organic compounds in a solid-state depends not only on the structure of the fluorophore, but also on the packing of the molecules in the crystal net and the intermolecular interactions. Understanding the role of the molecule packing, as well as the presence of weak intermolecular interactions and relating them to fluorescence properties is essential for efficient solid-state fluorescence. It also allows us to consciously modify the fluorescent properties and obtain structures with the desired light emission properties.

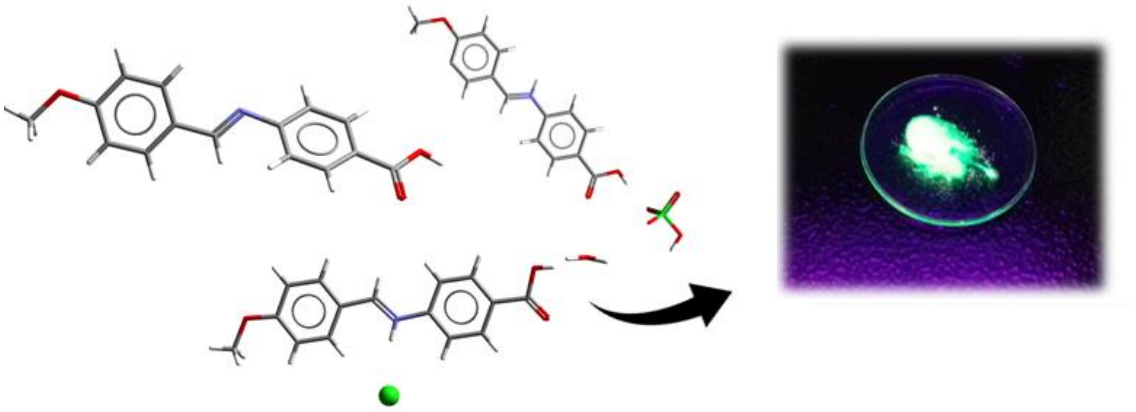

Fig. 1. Molecular structures of Schiff base and its salts exhibiting fluorescence.

The main aim of the research was to investigate the relationship between the structural properties of the obtained compounds and the exhibited fluorescent properties.

The study includes the syntheses of Schiff's base and its salts, their structural and spectroscopic characterization using respectively X-ray diffraction, infrared (IR), and fluorescence spectroscopy methods (including excitation—emission matrix–EEM).

References

[1] C.C. Vidyasagar, B.M. Munoz Flores, V.M. Jimenez-Perez, P.M. Gurubasavaraj, *Materials Today Chemistry*, **11** (2019**)**, 133-155.

[2] X. Zhu, R. Liu, Y. Li, H. Huang, Q. Wang, D. Wang, X. Zhu, S. Liuc, H. Zhu, *Chemical Communications*, **50** (2014), 12951-12954.

B-30

STRUCTURE AND ACTIVITY OF BENZIMIDAZOLE DERIVATIVES

Jarosław Sukiennik[a], Katarzyna Gobis[b], Adam Truchlewski[a], Andrzej Olczak[a], Małgorzata Szczesio[a]

[a] Institute of General and Ecological Chemistry, Faculty of Chemistry, Łódź University of Technology, Żeromskiego 116, 90-924 Łódź, Poland
[b] Department of Organic Chemistry, Medical University of Gdansk, M. Skłodowskiej-Curie 3a, 80-210 Gdańsk, Poland

Benzimidazoles are widely used in medicine [1-5]. Their derivatives show very diverse biological activity, such as antitumor, antiviral, antibacterial and antifungal properties. They also have a potential to cross the blood-brain barrier and show neuroprotective activity that may help in the treatment of the Alzheimer's disease.

X-ray analysis of three new derivatives (Scheme, Table) showing antibacterial activity, in particular anti-tuberculosis, was performed. One of these compounds containing the piperazine group is shows significant activity against bacteria.

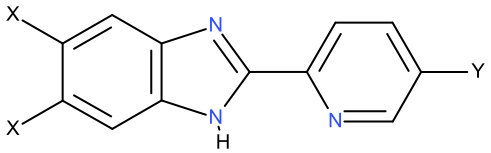

X=H, Me
Y=PhO, F-C_6H_4O, Ph-$C_4N_2H_8$

No	a, b, c [Å]	α, β, γ [°]	Space group	R [%]
1	11.0255(3) 13.8022(3) 10.1885(3)	90 115.648(3) 90	$P2_1/c$	5.03
2	9.9036(2) 9.9008(2) 29.6419(5)	90 90 90	Pbca	5.6
3	11.20050(10) 13.57840(10) 28.5911(4)	90 90 90	Pbca	5.95

Literature

[1] Laudy A.E., Moo-Puc R., Cedillo-Rivera R., Kazimierczuk Z., Orzeszko A., *Journal of Heterocyclic Chemistry* **49**(5) (2012) 1059-1065.
[2] El Rashedy, Aboul-Enein H.Y., *Current Drug Therapy* **8**(1) (2013) 1-14.
[3] Alamgir M., Black D. S. C., Kumar N., *Topics in Heterocyclic Chemistry*, **9** (2007) 87-118.
[4] K.Gobis; H. Foks; M. Serocki; E. Augustynowicz-Kopeć; A. Napiórkowska, *European Journal of Medicinal Chemistry*, **89** (2015) 13-20.
[5] Yuying Fang, Huihao Zhou, Qiong Gu, Jun Xu, *European Journal of Medicinal Chemistry* **167** (2019) 133-145.

B-31

REFINING ANHARMONIC MOTION OF H-ATOMS BASED ON NEUTRON DATA COLLECTED FOR GLYCINE

Szymon Sutula[1], Maura Malińska[1], Laura Canadillas Delgado[2], Oscar Ramon Fabelo Rosa[2], Krzysztof Woźniak[1]

[1] Department of Chemistry, University of Warsaw, Pasteura 1, 02-093 Warsaw, Poland,
[2] Institute Laue-Langevin, 71 Ave Des Martyrs, 38042, Grenoble, France

In our study we have collected neutron diffraction data sets on α-glycine ($P2_1/n$) at two temperatures – 90 K and 200 K – using nuclear reactor source at ILL, Grenoble, France. The resolutions for the data are 0.925 and 1.02 $Å^{-1}$ for 90 K and 200 K, respectively, and with these diffraction data we tried to refine anharmonic motion of H-atoms with Gram-Charlier coefficients up to the 3rd level. Collected data were then cut down into sets with limited $\sin\theta/\lambda$ values for comparison how some parameters depend on the resolution. The analysed parameters are: cell parameters, bond lengths, ADPs, C_{ijk}, refinement descriptors values and additionally 3D probability density function shapes.

The refinements were carried out in Jana2020 on F^2 using sigma weighting. Obtained results for the refinements on the full resolution data sets were then compared with results for model obtained when H-atoms were treated harmonically anisotropically with no Gram-Charlier coefficients. Those two approaches were tested with the Prince-Spiegelman test to see if introduction of anharmonic motion for H-atoms is justified. Additionally, those results have been confronted with the Kuhs'[1] formula for estimating the necessary resolution of the data needed for proper Gram-Charlier coefficients introduction, as it has been shown by Kuhs, that these are the higher angle reflections, where the information about anharmonic motion is mainly contained.

This work was supported by the Foundation for Polish Science, TEAM-TECH Core facility for crystallographic and biophysical research to support the development of medicinal products (co-financed by the European Union under the Regional Development Fund).

References

[1] Kuhs, W. F., *Acta Cryst. A*, **48** (1992) 80.

B-32

HYDRAZIDE DERIVATIVES - STRUCTURE AND ACTIVITY

Małgorzata Szczesio[a], Katarzyna Gobis[b], Izabela Korona Głowniak[c], Andrzej Olczak[a], Marek L. Główka[a]

[a] Institute of General and Ecological Chemistry, Faculty of Chemistry, Łódź University of Technology, 116 Żeromskiego Street, 90-924 Łódź, Poland
[b] Department of Organic Chemistry, Medical University of Gdańsk, M. Skłodowskiej-Curie 3a Street, 80-210 Gdańsk, Poland
[c] Department of Pharmaceutical Microbiology, Medical University of Lublin, Chodźki 1, 20-093 Lublin, Poland

Hydrazine derivatives are the interesting groups of compounds, and among them hydrazides and amidrazones (Scheme), which are widely studied in terms of their biological activity [1, 2]. Hydrazine derivatives are tested as anti-tuberculosis agents.

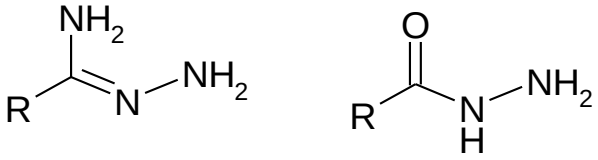

The studied hydrazide derivatives contain three flat fragments whose modification affects conformation and activity (Fig.). Besides the flexible dithioester groups, the remaining parts of the studied molecules consists of three conjugated π-systems, namely phenyl, amide and methyleneamine, which promotes their coplanarity.

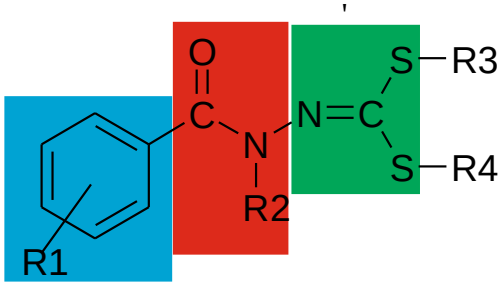

Fig. Structures of hydrazide derivatives contain three essential flat fragments.

References

[1] S.L. Dax, Antibacterial Chemotherapeutic Agents, Chapman and Hall, London, (1997).
[2] J. Bertrand, C. Dobritz, H. Beerens, *Bull. Soc. Pharm.*, **39** (1956) 1168.

This project was funded by the National Science Centre (Cracow, Poland) on the basis of decision number DEC-2017/25/B/NZ7/00124.

B-33

STUDY OF STRUCTURE AND ABILITY TO THERMALLY INDUCED SPIN CROSSOVER IN 2D AND 3D Fe(II) COORDINATION POLYMERS BASED ON 1,ω-DI(AZOLYL)ALKANES WITH DINITRILES AS COLIGANDS

Aleksandra Tołoczko[1], Marcin Kaźmierczak[1], Marek Weselski[1], Maria Książek[2], Joachim Kusz[2], Robert Bronisz[1]

[1]*Wydział Chemii, Uniwersytet Wrocławski, ul. F. Joliot-Curie 14, 50-383 Wrocław*
[2]*Instytut Fizyki, Uniwersytet Śląski, ul. 75 Pułku Piechoty, 1, 41-500 Chorzów*

In the coordination compounds of $3d^4$-$3d^7$ metal ions the electronic configuration can be reversibly switched between the high (HS) and low (LS) spin state, using an external stimulus such as temperature, pressure, or light. In Fe(II) complexes the typical coordination number accommodated by metal ion is 6, and the surrounding ligands form octahedral geometry. The transition from high-spin ($t_{2g}^4e_g^2$) to low-spin (t_{2g}^6) state is accompanied by transformation from paramagnetic to diamagnetic form, as well as a shortening of the Fe-ligand bond length by about 0.2 Å [1]. Our research showed that reactions between 1,ω-di(azolyl)alkanes (azolyl = 1,2,3-triazol-1-yl, tetrazol-1-yl, tetrazol-2-yl) and Fe(II) ions lead to the formation of coordination polymers showing the spin crossover phenomenon [2,3]. Due to the monodentate type of coordination, N-substituted tetrazoles can be successfully used as donors in construction of bridging ligand molecules. Depending on the substitution site, the formation of both homo- and heteroleptic complex compounds is possible. The coordination sphere of the metal ion in heteroleptic systems can contain, apart from tetrazole rings, also molecules of alcohols and nitriles [4]. At the moment, the conducted studies have shown, that the use of nitriles as coligands leads to formation of compounds of a formula [Fe(1,ω-di(azolyl)alkane)$_2$(RCN)$_2$]X_2 (X = BF_4^- or ClO_4^-), in which the coordination sphere of the metal ion, apart from the in-plane azole rings, contains also axially coordinated nitriles. Work with 1,2-di(tetrazol-2-yl)ethane has led to the creation of a series of 1D coordination polymers [5], while 1,6-di(tetrazol-2-yl)hexane is a component of 2D coordination networks [6].

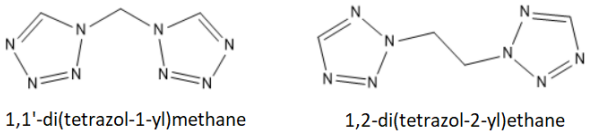
1,1'-di(tetrazol-1-yl)methane

1,2-di(tetrazol-2-yl)ethane

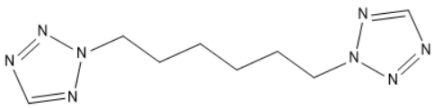
1,6-di(tetrazol-2-yl)hexane

The above presented outcomes were an encouragement to continue the research on implementing dinitrile molecules as coligands into the synthesis of the new coordination polymers. Dinitriles are a group of bidentate ligands, so in the contrary to mononitriles they are able to connect Fe(II) ions. It was confirmed by obtaining 2D and 3D coordination polymers with the coordinated dinitrile molecules. Reactions were conducted for: 1,1'-di(tetrazol-1-yl)methane (1,1'-mbtz), 1,2-di(tetrazol-

2-yl)ethane (ebtz) and 1,6-di(tetrazol-2-yl)hexane (hbtz) with Fe(II) tetrafluoroborate. Adiponitrile and 1,6-dicyjanohexane were used both as coligands and solvents.

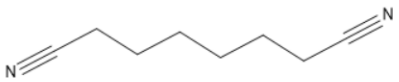

1,6-dicyanohexane

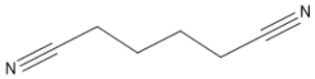

adiponitrile

As expected, in case of using ebtz and hbtz, the coordination environment of Fe(II) ions is consisted of four tetrazole rings and axially coordinated dinitriles, which are also the bridging molecules. The general formula of these compounds is $[Fe(ebtz/hbtz)_2(NC-(CH_2)_4-CN)](BF_4)_2$. On the contrary the octahedral coordination sphere of 1,1'-mbtz systems comprise four tetrazole rings, one dinitrile molecule connecting two polymeric layers and one monodentantly coordinated dinitrile molecule. Moreover, there are uncoordinated dinitrile molecules in the crystal lattice. The resulting compounds formulas are: $[Fe_2(1,1'\text{-mbtz})_4(\mu\text{-NC-}(CH_2)_4\text{-CN})(NC\text{-}(CH_2)_4\text{-CN})_2](BF_4)_4*2NC\text{-}(CH_2)_4\text{-CN}$ and $[Fe_3(1,1'\text{-mbtz})_6(\mu\text{-NC-}(CH_2)_6\text{-CN})_2(NC\text{-}(CH_2)_6\text{-CN})_2](BF_4)_6*3NC\text{-}(CH_2)_6\text{-CN}$. For compounds exhibiting the spin crossover phenomenon the crystal structures were determined both for HS and LS form. Transformation from paramagnetic to diamagnetic form is accompanied by shortening of the Fe-ligand bond length by about 10%. The specific research results will be shown at the poster.

References

[1] M. A. Halcrow, *Spin-Crossover Materials: Properties and Applications*, Wiley, 2013.
[2] R. Bronisz, *Inorg. Chem*., **44(13)** (2005) 4463–4465.
[3] R. Bronisz, *Inorg. Chem*., **46** (2007) 6733-6739.
[4] A. Białońska, R. Bronisz, *Inorg. Chem*., **49** (2010) 4534-4542.
[5] M. Książek, M. Weselski, M. Kaźmierczak, A. Tołoczko, M. Siczek, P. Durlak, J. A. Wolny, V. Schünemann, J. Kusz, R. Bronisz, *Chem. Eur. J*., **26** (2020) 14419-14434.
[6] M. Książek, J. Kusz, A. Białońska, R. Bronisz, M. Weselski, *Dalton Trans.*, **44** (2015) 18563-18575.

B-34

POLIMER KOORDYNACYJNY MIEDZI (II) – SYNTEZA SOLWOTERMALNA W REAKTORACH BERGHOF

Kamil Twaróg, Andrzej Kochel

Uniwersytet Wrocławski, Wydział Chemii, F. Joliot-Currie 14, 50-383 Wrocław

Polimer koordynacyjny o wzorze $[Cu(bptc)(H_2O)_2]_n$ otrzymano na drodze syntezy solwotermalnej w reaktorze ciśnieniowym Berghof. Związek krystalizuje w układzie jednoskośnym, grupie punktowej $P2_1/n$, a = 10,093(3) Å, b = 11,299(3) Å, c = 10,403(3) Å, β = 100,82(2)°, V = 1160,2(5) Å^3, Z = 4.

Sferę koordynacyjną wokół jonu Cu^{2+} wypełniają dwie cząsteczki wody, oraz dwa ligandy z których jeden koordynuje przez atom tlenu O1 pochodzący z grupy karboksylowej a drugi poprzez dwa atomy azotu N1 i N2 pochodzące z bipirydylu. Poprzez tak ułożone ligandy sfera koordynacyjna jonu miedzi(II) zbliżona jest do piramidy tetragonalną z parametrem S równym 0,17 (gdzie S=0 jest dla idealnej piramidy tetragonalnej a S=1 dla bipiramidy trygonalnej) [1]. W rezultacie polimer ten tworzy jednowymiarową sieć koordynacyjną.

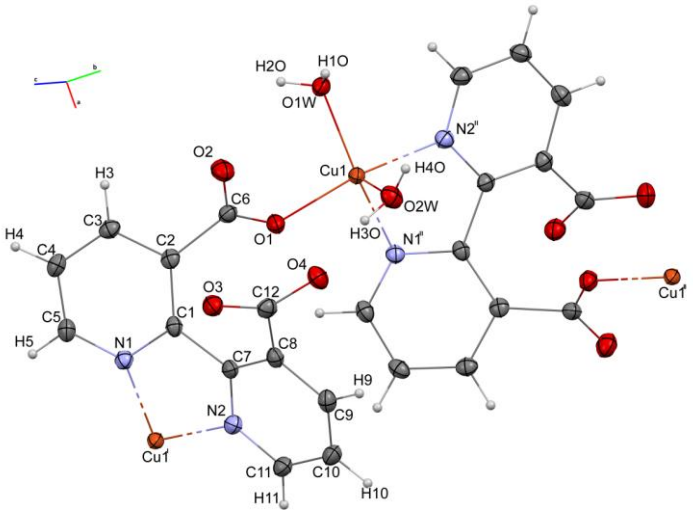

Rys. 1. Polimer koordynacyjny $[Cu(bptc)(H_2O)_2]_n$, kody symetrii: [i] *-x+3/2, y-1/2, -z+1/2*; [ii] *-x+3/2, y+1/2, -z+1/2*.

Literatura

[1] A. W. Addison, T. N. Rao, J. Reedijk, J. van Rijn, G. C. Verschoor. *J. Chem. Soc., Dalton Trans.*, **7** (1984) 1349.

B-35

HYDROPHILIC ORGANOBORON COMPLEXES AS EFFECTIVE PHOTOSENSITIZERS FOR APPLICATION IN MICROORGANISM PHOTOINACTIVATION

Karolina Anna Urbanowicz[a], Paulina H. Marek[a,b], Jolanta Mierzejewska[a], Krzysztof Woźniak[b], Krzysztof Durka[a]

[a] *Faculty of Chemistry, Warsaw University of Technology, Warsaw*
[b] *Faculty of Chemistry, University of Warsaw, Warsaw*

Singlet oxygen ($^1O_2$) is one of the reactive oxygen species (ROS) and can be formed due to the interaction between oxygen in its ground triplet state ($^3O_2$) and photosensitizer upon its light excitation to triplet state. That reactive form of oxygen could be used in the photodynamic therapy (PDT), which is a modern technique of treating skin cancers as well as other malignant and non-malignant dermal diseases [1], or in the antimicrobial photodynamic therapy (APDT) against pathogens like bacteria, viruses or fungi [2, 3]. Efficient singlet oxygen photosensitizers usually includes in their structures heavy atom (i.e. Ir cation or I substituents) what enables intersystem crossing (ISC) between singlet and triplet excited states. Due to their toxicity, application of such compounds in biological environment is limited and the need of search for new heavy-atom free sensitizers emerges. The most exploited approach to facilitate ISC is separation of donor and acceptor in the photosensitizer molecule. According to recent studies performed in our group, introduction of boracyclic moiety into the BODIPY dyes (derivatives of 4,4-difluoro-4-bora-3a-4a-diaza-*s*-indacene) enables ISC in the molecules.

In this work I present series of BODIPY complexes with borafluorene moiety. In order to enhance their water solubility, I have introduced into the structure cationic (NEt_2Me^+), anionic (SO_3^-) and zwitterionic groups ($-NMe_2^+(CH_2)_2SO_3^-$) presented on Figure 1. BODIPY complexes were comprehensively characterized by X-ray diffraction and initially tested as homogeneous photocatalysts. Their potential in the antimicrobial photodynamic therapy against *Escherichia coli*, *Staphyloccocus aureus* and *Candida albicans* was tested. In order to attempt understand mechanism of generation of triplet states, structural studies and theoretical calculations were performed.

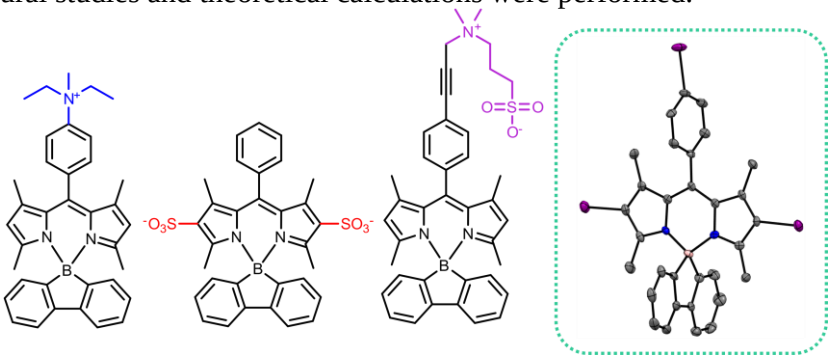

Fig. 1. Scheme of obtained and analyzed structures of borafluorene modified BODIPY dyes and one of analyzed structures.

References

[1] B. Carpenter, et al., *Molecules*, **20** (2015) 10604–10621.
[2] A. Wiehe, *Photochem. Photobiol. Sci.*, **18** (2019) 2565–2612.
[3] T. N. Singh-Rachford, *J. Am. Chem. Soc.*, **130** (2008) 16164–16165.

B-36

ANALIZA PREPARATÓW NIE BAZUJĄCYCH NA ZWIĄZKACH MIEDZI I OGRANICZAJĄCYCH EMISJĘ ZANIECZYSZCZEŃ Z PIECÓW NA PALIWA STAŁE METODAMI XRD, SEM-EDS & ICP-EOS

Andrzej Żarczyński, Katarzyna Wieczorek, Waldemar Maniukiewicz, Jakub Kubicki, Wojciech M. Wolf, Małgorzata I. Szynkowska-Jóźwik

Politechnika Łódzka, Instytut Chemii Ogólnej i Ekologicznej, ul. Żeromskiego 116,90-924 Łódź

W Polsce dominuje energetyka konwencjonalna, która wykorzystuje głównie paliwa kopalne takie jak: węgiel kamienny, węgiel brunatny, ropę naftową i gaz ziemny [1]. Niestety spalanie paliw kopalnych, zwłaszcza stałych, powoduje duże emisje zanieczyszczeń do powietrza atmosferycznego. Jednak w Polsce elektrownie i elektrociepłownie zwykle są wyposażone w wydajne systemy usuwania zanieczyszczeń. Z kolei prywatne paleniska przydomowe nie są wyposażone w systemy usuwania zanieczyszczeń i ich funkcjonowanie skutkuje emisją licznych substancji do powietrza, w tym sadzy. Ów produkt uboczny spalania często możemy zaobserwować w kominach przydomowych pieców, w których ciężko jest uzyskać optymalne warunki spalania paliw stałych [2, 3]. Sadza jest to produkt niecałkowitego spalania lub pirolizy paliw takich jak: drewno, węgiel kamienny lub brunatny i ropa naftowa. Sadza głównie składa się z węgla (ok. 96%), a pozostałe jej składniki to: wodór, tlen, azot i siarka. Możemy wyróżnić dwa rodzaje sadzy: płomieniową i techniczną. Pierwsza z nich powstaje w wyniku niecałkowitego spalania paliw, z którym najczęściej mamy do czynienia podczas spalania w przydomowych kotłowniach. Z uwagi na to, ze sadza zwykle zawiera węglowodory aromatyczne, w tym benzo-α-piren, może mieć szkodliwy a nawet kancerogenny wpływ na zdrowie człowieka [3-5]. Zapobieganie powstawaniu sadzy jest wysoce uzasadnione, bowiem stanowi ona zagrożenie pożarowe, hamuje wypływ spalin z komina, co może spowodować zatrucie mieszkańców spalinami w ekstremalnych sytuacjach, a także zmniejsza efektywność procesu spalania paliw przez co obniża wydajność pieców i zwiększa zużycia paliwa.

Celem pracy było zbadanie składu i wybranych właściwości preparatów handlowych (Kalnit, Kominiarz Extra Strong, AnLen, SP Nitrolen oraz Diavolina) nie bazujących na związkach miedzi, przeznaczonych do usuwania sadzy w piecach na paliwa stałe. Aktualnie na polskim rynku jest dostępnych szereg preparatów opartych na miedzi, ale badania naukowe wskazują, iż obecność tego pierwiastka o właściwościach katalitycznych może skutkować powstawaniem i emisją znaczących ilości polichlorowanych dibenzo-p-dioksyn i polichlorowanych dibenzofuranów (PCDD/Fs), powszechnie nazywanych dioksynami, w produktach reakcji spalania [6]. Z kolei związki azotu i siarki ograniczają powstawanie dioksyn w procesach spalania [7-9].

Badania obejmowały analizy próbek preparatów, metodami rentgenowskimi (XRD i SEM-EDS), innymi instrumentalnymi (ICP-OES, pH) i fizykochemicznymi. Do analiz składu fazowego stosowano dyfraktometr polikrystaliczny X`PERT PRO MPD firmy PANanalytical, ze źródłem promieniowania CuKα uzyskiwanego w wyniku monochromatyzacji promieni X na filtrze niklowym. Do oceny składu fazowego próbek

wykorzystano program X`Pert High Score Plus (ver. 4.9) oraz bazę standardów proszkowych ICDD PDF2 (ver. 2020). Badania lokalnych powierzchni materiałów realizowano także przy użyciu skaningowego mikroskopu elektronowego z przystawką do mikroanalizy rentgenowskiej (SEM-EDS). Analizy zawartości metali w próbach badanych preparatów wykonano metodą atomowej spektrometrii emisyjnej z plazmą sprzężoną indukcyjnie (ICP-OES), po uprzednim roztworzeniu ich w wodzie królewskiej.

Badania metodami XRD i SEM-EDS prób preparatów Kalnit i Kominiarz Extra Strong wykazały znaczne podobieństwo rodzajów ich faz krystalicznych i morfologii powierzchni. Stwierdzono obecność: KNO_3, NaCl i siarki (S). Podobieństwo to może mieć związek z otrzymywaniem ich przez tego samego producenta. Preparat AnLen zawierał większe zróżnicowanie składu, bowiem zidentyfikowano następujące związki: $CaMg(CO_3)_2$, $CaCO_3$, NH_4Cl, SiO_2 oraz ślady soli żelaza i miedzi. Próba preparatu SP Nitrolen zawierała dwie główne fazy, tj. KNO_3 i S, a próba Diavoliny - NaCl oraz S.

Wykazano, że wszystkie preparaty są mieszankami związków nieorganicznych. Stwierdzono, że celu redukcji powstawania sadzy do preparatów dodawane są związki siarki lub azotu. Dodatkowo stwierdzono za pomocą aparatu Scheiblera, że preparat AnLen wykazywał dużą zawartość węglanów, co potwierdza wyniki badań krystalograficznych. W preparatach wykazano także obecność chlorków, które potencjalnie mogą mieć wpływ na korozję instalacji grzewczej. Termiczny rozkład Kalnitu wskazuje na tworzenie się tlenków azotu i siarki mogących ograniczać powstawanie dioksyn w procesach spalania paliw stałych.

Literatura

[1] J. Kotowicz, K. Janusz, *Rynek Energii*, **1** (2007) 10.
[2] M.R. Chyc, B. Burzała, *Arch. Gosp. Odpad. i Ochr. Środ.*, **14(3)** (2012) 65.
[3] H. Richter, J. Howard, *Prog. Energy Combust. Sci.*, **26** (2000) 565.
[4] K. Wieczorek, Praca dyplomowa magisterska (w przygotowaniu), IChOiE PŁ, Łódź 2021.
[5] H.B. Al-Wakeel, Z.A.A. Karim, H.H. Al-Kayiem, M.H.M. Jamlus, *J. Appl. Sci*., **12(23)** (2012) 2338.
[6] A. Grochowalski, M. Węgiel, A. Maślanka A., R. Chrząszcz, M. Chyc, *Organohalogen Comp*., **77** (2015) 202.
[7] Z. Makles, A. Świątkowski, S. Grybowska, *Niebezpieczne dioksyny*, Arkady, Warszawa 2001.
[8] Y.T. Chin, C. Lin, G.P. Chang-Chieng, Y.M. Wang, J. Environ. *Sci. Health, Part A*., **46(5)**, (2011) 465.
[9] Wielgosiński G. *Emisja dioksyn z procesów termicznych i metody jej ograniczania,* Polska Akademia Nauk, Oddział w Łodzi 2009.

B-37

EXPERIMENTAL CHARGE DENSITY STUDY FOR SULPHOHALITE – $Na_6(SO_4)_2FCl$, A MINERAL BELONGING TO THE PEROVSKITE FAMILY

Agata Wróbel[1], Roman Gajda[1], Krzysztof Woźniak[1]

[1]Department of Chemistry, Biological and Chemical Research Centre, University of Warsaw, Poland

Based on high-resolution X-ray diffraction data collected for a suitable crystal of *sulphohalite* [$Na_6(SO_4)_2FCl$], the experimental distribution of electron density was modelled. Annotated data set was gathered at 100K employing AgKα radiation (λ = 0.56087 Å), to a resolution of 0.3941 Å. The Hansen-Coppens formalism[1] was implemented through consecutive least-square refinements. **QTAIM** *topological analysis*[2] revealed interesting features appertaining to the distribution of charge in the mineral's structure. Full-volume property integration of *atomic basins* (**AB's**) was undertaken. The corresponding individual charges [$Q_{AB\text{-}Cl}$ = -0.836e$^-$; $Q_{AB\text{-}S}$ = 03.168e$^-$; $Q_{AB\text{-}Na}$ = 0.910e$^-$; $Q_{AB\text{-}F}$ = -1.334e$^-$ and $Q_{AB\text{-}O}$ -1.227e$^-$] and volumes [$V_{AB\text{-}Cl}$ = 38.920Å^3; $V_{AB\text{-}S}$ = 5.656 Å^3; $V_{AB\text{-}Na}$ = 7.931 Å^3; $V_{AB\text{-}F}$ = 14.178 Å^3 and $V_{AB\text{-}O}$ = 17.416Å^3] were reported. The percentage of unaccounted electrons and volume per unit cell resulting from performed numerical integration can be unheeded within the uncertainty range of such procedure. A number of *critical points* (**CP's**) were identified. Among them: **6**·*bond* **CP's** [$\nabla^2\rho(r_{Cl\text{-}S})$ = 0.120e$^-$ Å^{-5}; $\nabla^2\rho(r_{Cl\text{-}Na})$ = 0.575e$^-$·Å^{-5}; $\nabla^2\rho(r_{S\text{-}O})$ = -31.00e$^-$·Å^{-5}; $\nabla^2\rho(r_{Na\text{-}O})$ = 1.931e$^-$·Å^{-5}; $\nabla^2\rho(r_{Na\text{-}F})$ = 3.022e$^-$·Å^{-5} and $\nabla^2\rho(r_{F\text{-}O})$ = 0.868e$^-$·Å^{-5}], **5**·*ring* **CP's** [$\nabla^2\rho(r_I)$ = 0.912e$^-$·Å^{-5}; $\nabla^2\rho(r_{II})$ = 0.332e$^-$·Å^{-5} and $\nabla^2\rho(r_{III,IV,V})$ = 0.201e$^-$·Å^{-5}] and **4**·*cage* **CP's** [$\nabla^2\rho(r_{I,II})$ = 0.514e$^-$ ·Å^{-5} and $\nabla^2\rho(r_{III,IV})$ = 0.401e$^-$ Å^{-5}] – as illustrated in (Fig.1). Morse's 'characteristic set' condition was met[3]. The interconnection between **AB's** and **CP's** was examined– as proposed by Pendás[4]. Basins of attraction and basins of repulsion were denoted.

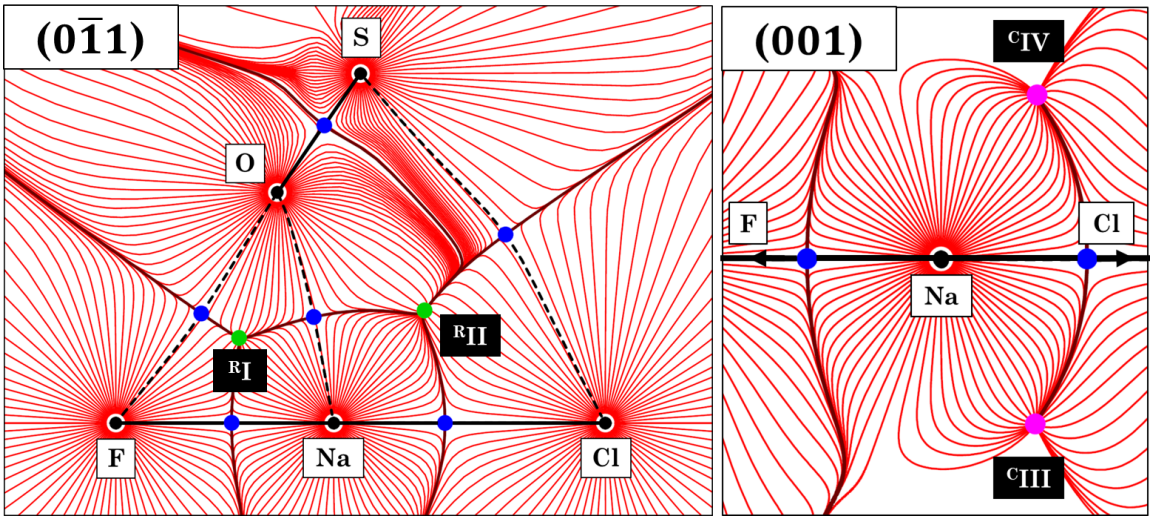

Fig. 1. Gradient vector field of electron density, mapped for two selected planes in the *sulphohalite* crystal. BCP's – (3, -1), RCP's – (3, +1) and CCP's – (3, -3) are respectively denoted by blue, green, and magenta circles. Interatomic bonding is presented by black lines; whereas bonding paths are depicted by black dashed lines.

Finally, the nature of interatomic interactions was assessed through the dichotomous classification[3]. The **S–O** contact was acknowledged as a covalent with a shared-shell. The remaining contacts were characterized as non-covalent closed-shell (**Cl···Na**, **Na···O** and **Na···F**) or weak van der Waals closed-shell (**Cl···S** and **F···O**).

References

[1] Hansen, N. K.; Coppens, P. Testing Aspherical Atom Refinements on Small-Molecule Data Sets. *Acta Crystallographica Section A*, **34 (6)** (1978) 909–921. https://doi.org/10.1107/S0567739478001886.
[2] Bader, R. Atoms in Molecules: A Quantum Theory.; Oxford University Press: USA, 1994.
[3] Chemical Bonding in Crystals: New Directions. *Zeitschrift für Kristallographie* - Crystalline Materials, **220 (5-6)** (2005), 399–457. https://doi.org/doi:10.1524/zkri.220.5.399.65073.
[4] Martín Pendás, A.; Costales, A.; Luaña, V. Ions in Crystals: The Topology of the Electron Density in Ionic Materials. I. Fundamentals. *Phys. Rev. B*, **55 (7)** (1997) 4275–4284. https://doi.org/10.1103/PhysRevB.55.4275).

B-38

COBALT(II) COORDINATION COMPOUNDS OF HOMOCHIRAL 3+3 MACROCYCLIC AMINE

Karol Wydra, Jerzy Lisowski

University of Wrocław, Department of Chemistry, 14 F. Joliot-Curie, 50-383 Wrocław

Cobalt(II) ions exhibit strong first order spin-orbit coupling and large magnetic anisotropy which makes them attractive candidates for the construction of novel magnetic materials [4]. Encapsulation of several Co^{II} ions close together in the core of large chiral macrocycles may result in the formation of polynuclear species with fascinating architecture and uncommon magnetic properties. For instance, homochiral 3+3 macrocycle H_3L composed of three phenolic and three diamine units constitute a versatile platform for the construction of di-, tri- and even tetranuclear cobalt(II) coordination compounds [1-3].

Here we describe the synthesis, solution characterization and crystal structures of three novel cobalt(II) macrocyclic complexes with ligand H_3L (Fig. 1). The magnetic properties of these coordination species were also preliminarily investigated.

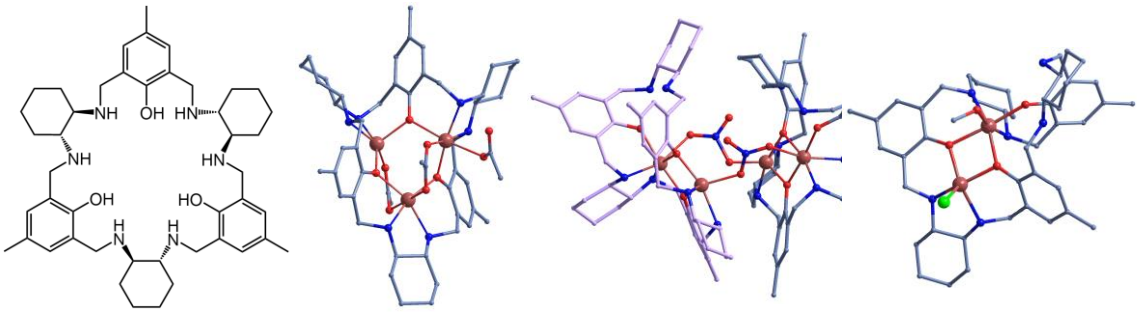

Fig. 1 (From left) Structure of ligand H_3L. X-ray structures of $[Co_3(L)(CH_3COO)_3]$, $[Co_4(NO_3)_2(H_2L)_2](NO_3)_4$ and $[Co_2(H_2L)Cl(CH_3OH)][CoCl_4]$, respectively (hydrogen atoms and counteranions are omitted for clarity).

References

[1] K. Wydra, M. J. Kobyłka, T. Lis, K. Ślepokura, J. Lisowski, Eur. J. *Inorg. Chem.*, (2020) 2096-2104.
[2] M. J. Kobyłka, K. Ślepokura, M. A. Rodicio, M. Paluch, J. Lisowski, *Inorg. Chem.*, **52** (2013) 12893-12903.
[3] M. J. Kobyłka, J. Janczak, T. Lis, T. Kowalik-Jankowska, J. Kłak, M. Pietruszka, J. Lisowski, *Dalton Trans.*, **41** (2012) 1503-1511.
[4] A. Sarkar, S. Dey, G. Rajaraman, *Chem. Eur. J.*, **26** (2020) 14036-14058.

B-39

BADANIA STRUKTURALNE POCHODNYCH 1-(4-FLUOROFENOKSY)ACETYLO-4-(ARYLO)TIOSEMIKARBAZYDU

Waldemar Wysocki[1], Monika Pitucha[2], Zbigniew Karczmarzyk[1], Adrian Borzęcki[2]

[1]Wydział Nauk Ścisłych i Przyrodniczych,Uniwersytet Przyrodniczo-Humanistyczny w Siedlcach, ul. 3 Maja 54, 08-110 Siedlce
[2]Samodzielna Pracownia Radiofarmacji, Wydział Farmaceutyczny z Oddziałem Analityki Medycznej, Uniwersytet Medyczny w Lublinie, ul. Chodźki 4a, 20-093 Lublin

Pochodne tiosemikarbazydu zawierające w swojej budowie ugrupowanie fenoksyoctowe wykazują cytotosyczność wobec linii komórek raka żołądka MKN74 bez znaczącej toksyczności wobec normalnych komórek [1].

Kontynuując nasze badania w tej grupie związków przedstawiamy syntezę i struktury krystaliczne dwóch nowych pochodnych tiosemikarbazydu: 1-(4-fluoro-fenoksy)acetylo-4-(2-chlorofenylo)tiosemikarbazydu (**1**) oraz 1-(4-fluorofenoksy) acetylo-4-(2,4-dichlorofenylo)tiosemikarbazydu (**2**), które zostały otrzymane w wyniku reakcji hydrazydu 4-fluorofenoksyostowego z odpowiednim aryloizotiocyjanianem.

Badania rentgenowskie tych związków potwierdziły ich drogę syntezy oraz struktury molekularne. Otrzymane dane strukturalne zostały użyte w obliczeniach teoretycznych na poziomie DFT/B3LYP/6-311++G(d,p) i pozwoliły wyznaczyć parametry geometryczne i elektronowe cząsteczek do wykorzystania w badaniach SAR w grupie pochodnych tiosemikarbazydowych.

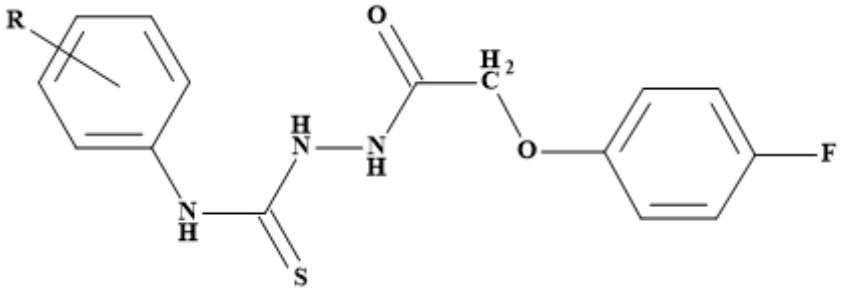

(1) R = 2-Cl

(2) R = 2,4-diCl

Dane krystalograficzne:

Związek (***1***): $C_{15}H_{13}ClFN_3O_2S$, M_r = 353.79, układ trójskośny, $P\bar{1}$, a = 8.6773 (15), b = 9.3488 (16), c = 10.6905 (15) Å, α = 89.835 (13), β = 70.387 (14), γ = 76.972 (15)°, V = 793.79 (15) Å^3, Z = 2, D_x = 1.481 gcm^{-3}, μ = 0.395 mm^{-1}, *MoKα*, λ = 0.71073 Å, T = 296 (2) K, R = 0.0522 dla 3395 refleksów

Związek (***2***): $C_{15}H_{12}Cl_2FN_3O_2S$, M_r = 388.24, układ trójskośny, $P\bar{1}$, a = 8.7526 (8), b = 9.5122 (6), c = 10.7018 (9) Å, α = 86.446 (6), β = 72.915 (7), γ = 77.803 (6)°, V = 830.4 (4) Å^3, Z = 2, D_x = 1.547 gcm^{-3}, μ = 0.538 mm^{-1}, *MoKα*, λ = 0.71073 Å, T = 296 (2) K, R = 0.0503 dla 2650 refleksów

Literatura

[1] M. Pitucha, A. Korga-Plewko, P. Kozyra, M. Iwan, A.A. Kaczor, *Biomolecules*, **10** (2020) 296.

B-40

INFLUENCE OF FLUORINE SUBSTITUENT ON THE CRYSTAL AND MOLECULAR STRUCTURE OF ARYLPIPERAZINE DERIVATIVES OF 3-(2,4-DICHLOROBENZYL)-5,5-DIMETHYLHYDANTOIN

Ewa Żesławska[1], Wojciech Nitek[2], Jadwiga Handzlik[3]

[1] Institute of Biology, Pedagogical University, Podchorążych 2, 30-084 Kraków
[2] Faculty of Chemistry, Jagiellonian University, Gronostajowa 2, 30-387 Kraków
[3] Jagiellonian University Medical College, Department of Technology and Biotechnology of Drugs, Medyczna 9, 30-688 Kraków

The arylpiperazine derivatives of hydantoin (imidazolidine-2,4-dione) display a variety of biological actions, especially, promising for the treatment of circulation [1] and CNS diseases [2]. Recently, a series or arylpiperazine-hydantoin derivatives with a different fluorine-substitution was obtained. The compounds displayed significant affinity for α_1-adrenergic receptors and antagonistic action in particular towards the subtype 1A with respect to 1B. Specifically, the 2,4-difluorosubstituted derivative showed beneficial pharmacological profile *in vitro* and *in vivo*, promising for the treatment of patients with benign prostatic hyperplasia (BPH)/lower urinary tract syndrome (LUTS), while its 2- or 4-monosubstituted analogues were less active. These results need wider analysis to rationalize the future search for therapeutically useful BPH/LUTS agents.

In order to extend knowledge about newly synthesized arylpiperazine derivatives of 3-(2,4-dichlorobenzyl)-5,5-dimethylhydantoin containing one or two fluorine substituents in aromatic ring, we performed crystal structure analysis for three hydrochlorides of 3-(2,4-dichlorobenzyl)-1-[3-(4-(2-fluorophenyl)piperazin-1-yl)-2-hydroxypropyl]-5,5-dimethylimidazolidine-2,4-dione (**I**), 3-(2,4-dichlorobenzyl)-1-[3-(4-(4-fluorophenyl)piperazin-1-yl)-2-hydroxypropyl]-5,5-dimethylimidazolidine-2,4-dione (**II**) and 3-(2,4-dichlorobenzyl)-1-[3-(4-(2,4-difluorophenyl)piperazin-1-yl)-2-hydroxypropyl]-5,5-dimethylimidazolidine-2,4-dione (**III**).

I **II** **III**

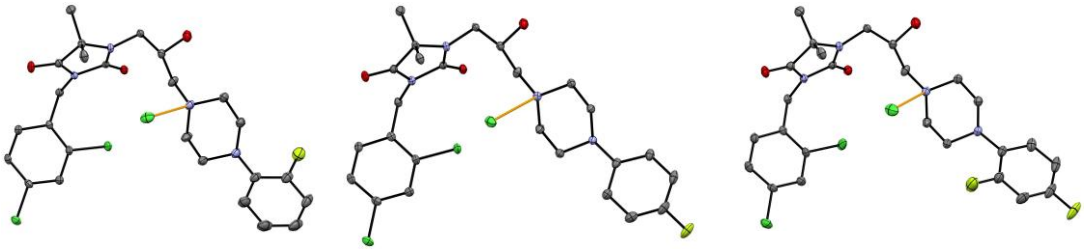

In the presented crystal structures, the chlorine anion is involved in a charge assisted hydrogen bond with protonated N atom. The overall shape of these three molecules is very similar. The conformation of the linker, consisting of three methylene units with hydroxy group located at the second carbon atom, is bent. The intermolecular interactions in the crystals are dominated by N-H···Cl, O-H···Cl, C-H···Cl and C-H···O

contacts. Additionally, C-H···F contacts are observed for structures containing fluorine substituent in position 4 of aromatic ring (**II** and **III**).

References

[1] J. Handzlik, M. Bajda, M. Zygmunt et al. *Bioorg. Med. Chem*. **20** (2012) 2290.
[2] J. Handzlik, A.J. Bojarski, G. Satała et al. *Eur J Med Chem.* **78** (2014) 324.

B-41

DISPERSION OF GOLD ON SURFACE OF CERIUM (IV) OXIDE RESPONSIVE TO GAS ADSORPTION

Maciej Zieliński[a,b], Wojciech Juszczyk[a], Zbigniew Kaszkur[a]

[a]Instytut Chemii Fizycznej Polskiej Akademii Nauk, ul. M. Kasprzaka 44/52, 01-224 Warszawa, Poland
[b]Narodowe Centrum Badań Jądrowych, ul. A. Sołtana 7, 05-400 Otwock, Poland

We took under investigation the CO oxidation reaction (sCOOX) on supported gold catalyst (Au/CeO_2) by acquisition of a series of powder diffraction patterns (DPs) under controlled gas atmosphere (Fig. 1) [1-3], i.e. we performed an *in-opernado* PXRD-MS experiment. We discovered that AuNPs have very mobile surface. All kinds of gold nanoparticles – nanocrystals (AuNP – NCrs) and smaller just a-few-atom clusters anchor to ceria on Ce^{3+} and oxygen vacancies (V_O^{++}) sites that are naturally present in cerium (IV) oxide (CeO_2) making it slightly unstoichiometric by default. Ce^{3+} ions and V_O^{++} spontaneously accumulate at the surface of ceria rather than in the particle's core (what is represented by the black curve in Fig. 2).

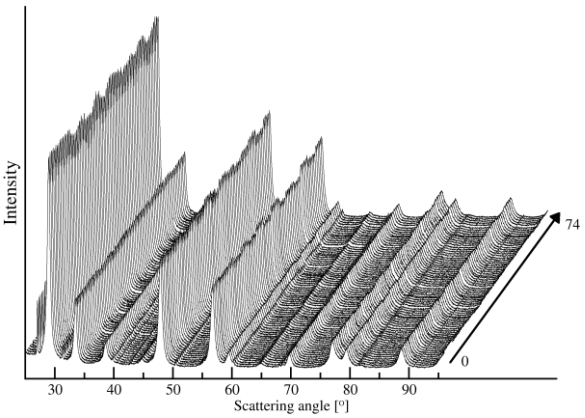

Fig. 1. A series of collected diffraction patterns (DPs) of the 9.4%$_{wt.}$ Au/CeO_2 catalyst under different gas atmospheres: He, H_2, He, CO, He, O_2, He, sCOOX, He, PROX, sCOOX, PROX, He, CO_2, He.

Adsorption of CO and H_2 on oxygen groups on the surface of CeO_2 causes Ce^{3+} and V_O^{++} to temporarily migrate to the particle's core, so their distribution looks then like the red curve in Fig. 2.

This reversible change of distribution implies 3 observations:

1. The Apparent Lattice Parameter (ALP) of ceria increases markedly under H_2 and CO comparing to He (what is reflected in the diffraction peaks positions).
2. The intensities of Au diffraction peaks rise, too.
3. CeO_2 lattice oxygen does <u>not</u> directly oxidise CO to CO_2 as it is assumed many times, but has been also already suggested [4].

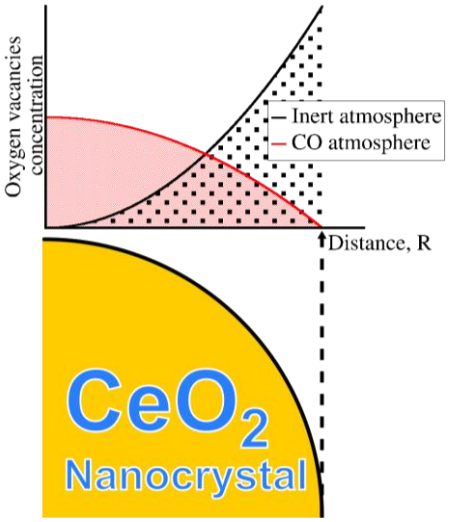

Fig. 2. The schematic illustration of the redistribution of the oxygen vacancies, V_O^{++}, (analogous case for Ce^{3+} ions) inside a CeO_2 nanocrystal exposed to an inert atmosphere and CO.

References
[1] M. Zielinski, W. Juszczyk, J. W. Sobczak, Z. Kaszkur, *J. Mater. Chem. A*, submitted for publication.
[2] W. Y. Hernandez,* F. Romero-Sarria, M. A. Centeno, J. A. Odriozola, *J. Phys Chem. C*, **114** (2010) 10857.
[3] M. Zielinski, PhD thesis, Institute of Physical Chemistry, Polish Academy of Sciences, ul. Kasprzaka 44/52, 01-224 Warszawa, Poland, 2019.
[4] H. Y. Kim, H. M. Lee, G. Henkelman, *J. Am. Chem. Soc.*, **134** (2012) 1560.

B-42

THE STRUCTURE OF SELECTED PICOLINOHYDRAZONAMIDE DERIVATIVES AND THEIR POTENTIAL AS TUBERCULOSTATICS

Dagmara Ziembicka[a], Katarzyna Gobis[a], Małgorzata Szczesio[b]

[a]Department of Organic Chemistry, Medical University of Gdańsk, Gen. J. Hallera 107, 80-416, Gdańsk
[b]Institute of General and Ecological Chemistry, Technical University of Łódź, Żeromskiego 116, 90-924, Łódź

The urgent need to develop new potent tuberculostatic agents has been caused by the steadily increasing rates of drug-resistant strains of *Mycobacterium tuberculosis* [1].

Our team's study of compounds exhibiting anti-tuberculosis activity focused on picolinohydrazonamide derivatives as structural analogues of the clinically used drug isoniazid. The synthesized compounds **1–3** possess a phenoxy moiety at the 6-position on the pyridine ring and a thiosemicarbazide chain terminated with appriopriate amine at the 2-position (Fig. 1). Because derivatives showed good *in vitro* tuberculostatic activity (MIC 4−16 μg/ml), we attempted to solve the crystal structure in a search for relationships between activity and specific intramolecular interactions causing the conformation of the molecule.

Determination of the spatial structure revealed that the molecules crystallize in the zwitterionic form (Fig. 1). The zwitterionic species were observed probably due to the formation of an intramolecular hydrogen bond. Therefore, the zwitterionic structure tends to enhance planarity of a molecule, which in turn correlates well with its tuberculostatic activity. The studies reported allowed to confirm our previous hypothesis by which only derivatives whose molecules are capable of adopting a planar conformation may show tuberculostatic activity [2].

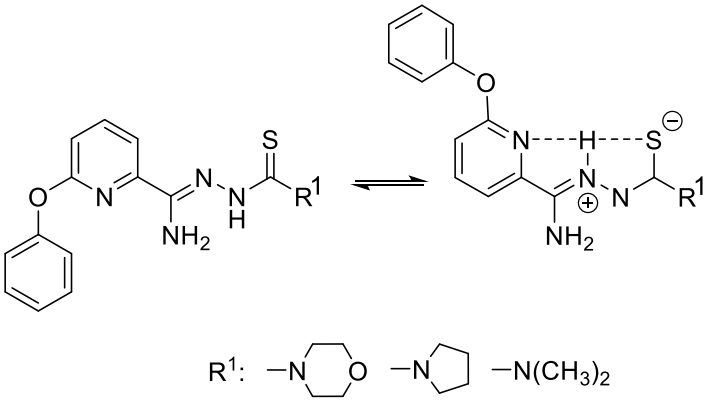

Fig. 1. The structure of compounds **1–3** and their zwitterionic form.

The main crystallographic parameters of the obtained compounds are summarized in Tab. 1.

Tab. 1. Crystallographic parameters of compounds **1**–**3**.

Compound	R^1	Space group	Unit cell parameters [Å,°]	R1 [%]
1	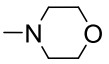	Pcnn	38.0219(5), 12.3665(2), 7.9201(2)	4.0
2		$P2_1/c$	5.0283(1), 22.5544(3), 14.5985(2) 97.451(1)	4.0
3	$-N(CH_3)_2$	Ia	7.9681(2), 10.9473(2), 18.4774(3) 96.245(2)	2.5

References

[1] Global Tuberculosis Report 2020. Geneva: World Health Organization (2020).
[2] M. L. Główka, D. Martynowski, A. Olczak, C. Orlewska, H. Foks, J. Bojarska, M. Szczesio, J. Gołka, C. Cabacka, *Journal of Chemical Crystallography*, **35** (2005) 477–480.

B-43

PHOTOREACTIVITY OF CHALCONE DERIVATIVES IN CRYSTALS

Przemysław Zima, Krzysztof A. Konieczny and Ilona Turowska-Tyrk

Advanced Materials Engineering and Modelling Group, Faculty of Chemistry, Wrocław University of Science and Technology, Wybrzeże Wyspiańskiego 27, 50-370 Wrocław, Poland

Photochemical reactions of chalcones are intensively studied for the potential pharmacological use of these compounds [1]. Some chalcone derivatives can undergo [2+2] photodimerization in a solid state, however this depends, besides other factors, on the mutual orientation of reactant molecules [2]. In general, during the [2+2] photodimerization two different products can be obtained. Products A and B are formed when molecules in crystal lattices are situated head-to-tail or head-to-head, respectively (Fig. 1).

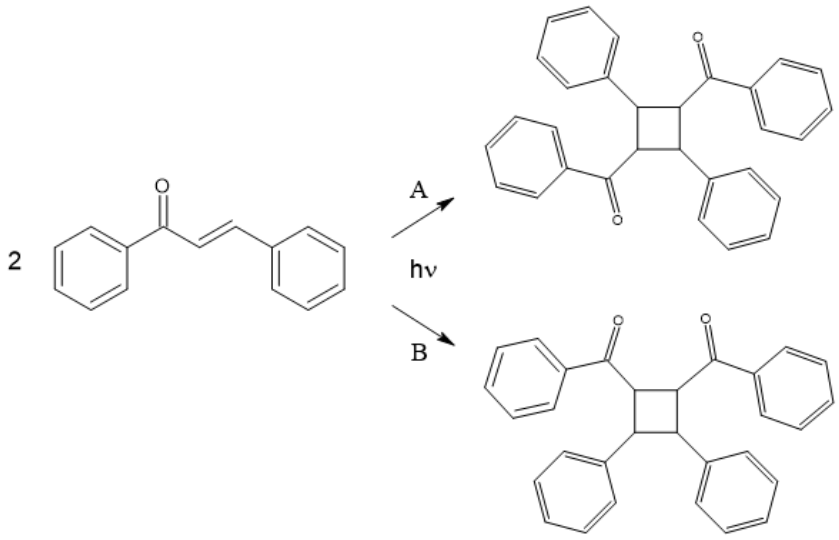

Fig. 1. Two possible [2+2] photodimerization paths in chalcones.

The crystal structures of two chalcone derivatives were determined: 3-(4-methylphenyl)-1-phenylprop-2-en-1-one (I) and 1-(2,4-difluorophenyl)-3-phenylprop-2-en-1-one (II). The values of the intermolecular geometrical parameters important in terms of the reactivity were calculated and analysed. The crystals of the above-mentioned compounds were irradiated in the UV-vis range. The X-ray structures of the irradiated crystals were determined. For compound I no structural changes were observed after irradiation, despite the values of the intermolecular geometrical parameters did not exclude the reaction. The crystal of compound II contains two molecules in the asymmetric unit, but the geometry allowed for the reaction of only one of them (Fig. 2).

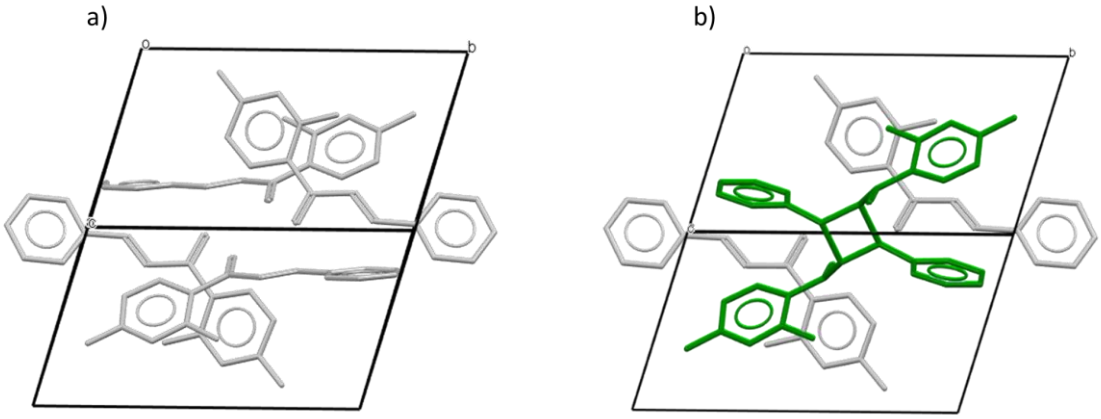

Fig. 2. The crystal structure of 1-(2,4-difluorophenyl)-3-phenylprop-2-en-1-one: a) before and b) after irradiation.

References

[1] A. Rammohan, J. S. Reddy, G. Sravya, C. N. Rao, and G. V. Zyryanov, "Chalcone synthesis, properties and medicinal applications: a review," *Environ. Chem. Lett.*, **18 (2)** (2020) 433–458.
[2] T. Galica and I. Turowska-Tyrk, "Influence of pressure on molecular packing and photochemical properties in three chalcone analogs," *Z. Kristallogr.*, **230 (2)** (2015) 131–137.

B-44

SYNTHESIS AND STRUCTURAL AND SORPTION PROPERTIES OF SILVER(I) COMPLEX SALT WITH 2,4-DICHLOROBENZALDEHYDE DERIVATIVE

Michał Kula, Agata Białońska

Wydział Chemii, Uniwersytet Wrocławski, ul. F. Joliot-Curie 14, 50-383 Wrocław

Capabilities of a system for a response on external stimuli always fascinated scientists. Breathing materials, which undergo structural reorganization owing to sorption or desorption process, belong to the system able to respond on external stimuli. One of them is the crystalline system of copper(I) complex salt with 4-chlorobenzaldehyde derivative, N-[(*E*)-(4-chlorophenyl)methylidene]-4*H*-1,2,4-triazol-4-amine [1-3]. The system is built up of X-shape binuclear cationic units self-assembled in such a way that one dimensional channels are formed between them. The systematic studies revealed that the system is able absorbing a wide range of compounds varied by size and functional groups. Guest release from the system results in huge structural changes related to closure the channels preliminary occupied by the guest molecules. Inspired by the breathing material, we started to study an influence of various factors on structure and properties of resulted analogues. Among them there is the system of silver(I) complex salts with the Schiff base of 2,4-dichlorobenzaldehyde with 4*H*-1,2,4-triazol-4-amine, N-[(*E*)-(2,4-dichlorophenyl)methylidene]-4*H*-1,2,4-triazol-4-amine presented in the poster.

The crystal structure of the silver(I) complex salt reveals a great resemblance to the known copper(I) analogue. It is also built up of the X-shape binuclear cationic units, which self-assembly resulted in the one dimensional channels formation. In both cases anions are located in the external parts of the channels, and solvent molecules occupy the internal part of the channels. Structural similarity of both the systems suggest their similar sorption capabilities. Surprisingly, the sorption capabilities of the both systems are different. Presence of the additional chlorine atom bonded to the phenyl ring of the ligand in orto-position caused that the silver(I) system reveals a greater selectivity in regard to functional groups. Simultaneously, it is still able to absorb a wide range of compounds of various size.

Literatura

[1] K. Drabent, Z. Ciunik and P. J. Chmielewski, *Eur. J. Inorg. Chem.*, (2003) 1548.
[2] Drabent, A. Białońska,Z. Ciunik, *Inorg. Chem. Commun.*, **7** (2004) 224.
[3] A. Białońska, K. Drabent, B. Filipowicz, M. Siczek, *CrystEngComm*, **15** (2013) 9859.

B-45

SYNTEZA I BADANIA METODĄ XRD STAŁYCH NOŚNIKÓW TLENU O STRUKTURZE TYPU PEROWSKITU OTRZYMYWANYCH NA BAZIE TLENKÓW MIEDZI I ŻELAZA WYKORZYSTYWANYCH W PROCESACH CLC

Rafał Łysowski[1], Ewelina Ksepko[1]

[1]Politechnika Wrocławska, Katedra Chemii i Technologii Paliw
rafal.lysowski@pwr.edu.pl

Proces CLC *(Chemical looping combustion*) jest procesem spalania bezpłomieniowego, w którym źródłem niezbędnego dla paliwa tlenu są substancje zwane stałymi nośnikami tlenu. Substancje te, zdolne są do przyłączania oraz oddawania tlenu, przy różnej wartości parametrów fizycznych, takich jak ciśnienia parcjalne tego gazu lub temperatury panującej wewnątrz reaktora. Nośniki utleniane są wewnątrz reaktora powietrznego, a następnie transportowanie do reaktora paliwowego. Wydzielony wewnątrz reaktora tlen może być wykorzystywany do spalania paliw ciekłych, stałych i gazowych [1].

Związki o strukturze typu perowskitu o ogólnym wzorze ABO_3, ze względu na dużą zdolność do oddawania tlenu, są obiecującymi kandydatami do roli stałych nośników tlenu wykorzystywanych w CLC oraz CLOU (*Chemical looping with oxygen uncoupling).* Ważną cechą związków o strukturze typu perowskitu, w porównaniu do konwencjonalnych stałych nośników tlenkowych, jest ich wysoka wytrzymałość termiczna oraz mechaniczna [2]. Ponadto, inną ich zaletą jest także duża swoboda w projektowaniu nowych typów związków, poprzez podstawianie w miejsca A i B różnych kationów metali.

W ramach przeprowadzonych badań, otrzymywano żelazowo-miedziane związki proszkowe o strukturze typu perowskitu, o wzorze ogólnym $A(Fe_xCu_{1-x})O_3$. Wykorzystano w tym celu prekursory tlenkowe i metodę mieszania mechanicznego oraz kalcynacji [3]. Dla syntetyzowanych materiałów obliczono także współczynnik tolerancji Goldschmidta, celem teoretycznego oszacowania możliwości otrzymania związków o spodziewanej strukturze typowej dla perowskitu [4].

Badania struktury krystalicznej oraz stopnia czystości otrzymanych materiałów przeprowadzono za pomocą proszkowego dyfraktometru rentgenowskiego (XRD) MiniFlex marki Rigaku. Związki wykazujące strukturę typową dla perowskitu, były następnie kierowane, w celu oceny zdolności przenoszenia tlenu, do badań które przeprowadzono przy pomocy analizatora termograwimetrycznego (TGA) Luxx STA 449 F5 Jupiter marki Netzsch.

Podziękowanie: Praca została sfinansowana w ramach projektu NCN nr 2020/37/B/ST5/01259.

Literatura

[1] Adanez J. *et all*, Chemical looping combustion of solid fuels, Progress in Energy and Combustion *Science* **65** (2018) 6, 66.
[2] Mattison, T., Materials for Chemical-Looping with Oxygen Uncoupling, ISRN Chemical Engineering (2013).
[3] Ksepko, E., Perovskite $Sr(Fe_{1-x}\ Cu_{\ x})O_{3-d}$ materials for chemical looping combustion applications, *International journal of hydrogen energy* **43** (2018) 9622 -9634.
[4] Goldschmidt, V.M. Die Gesetze der Krystallochemie. *Naturwissenschaften* **14** (1926) 477–485.

B-46

CRYSTAL STRUCTURE OF $LaNi_{11.8}Si_{1.2}$

Bohdana Belan, Mariya Dzevenko, Svitlana Pukas, Roman Gladyshevskii

Ivan Franko National University of L'viv,
Kyryla i Mefodia Str. 6, 79005 L'viv, Ukraine

The twenty ternary compounds with various compositions and crystal structures exist in the La-Ni-Si system [1]. However, this system is still remains incompletely studied. There are some "white area" with phases with unknown or partially determined crystal structures, for example, the ternary compounds, which exist at the section 7.14 at. % La [2]. One of them namely $LaNi_9Si_4$ is isotypic to $CeNi_{8.5}Si_{4.5}$-type [3]. The crystal structure of the other two compounds $LaNi_{11.6\text{-}9.5}Si_{1.4\text{-}3.5}$ and $LaNi_{8.8\text{-}8.4}Si_{4.2\text{-}4.6}$ are known to be derived from the $NaZn_{13}$-type [4]. Therefore, we present the results of the complete crystal structure investigation of the $LaNi_{11.8}Si_{1.2}$.

The samples has been prepared by arc-melting of the compact metals under an argon atmosphere and annealed at 600°C for 720 h. The crystal structure has been investigated using X-ray powder data: diffractometer STOE STADI P with a linear PSD detector ($CuK\alpha_1$- radiation, curved germanium [1 1 1] monochromator; 2θ-range $6.0 \le 2\theta \le 111.060°$ 2θ with step 0.015° 2θ; PSD step 0.480° 2θ, scan time 250 s/step). The crystal-structure refinement was performed using the DBWS software. The compound crystallize in the $CaCu_{6.5}Al_{6.5}$, which is a partially ordered ternary derivative of the $NaZn_{13}$-type: space group *Fm*-3*c*, Pearson code *cF*112, $Z = 8$; $a = 11.25486(8)$ Å, $V = 1425.68(2)$ Å^3; $R_p = 4.17$ %, $R_{wp} = 5.85$ %, $R_B = 3.44$ %. The parameters of atoms are listed in the Table. All the crystallographic positions are fully occupied, but atomic position (96*j*) is occupied by mixture of the nickel and silicon atoms. These data lead to the refined composition $LaNi_{11.8}Si_{1.2}$ for the investigated compound.

Atomic coordinates and thermal parameters for $LaNi_{11.8}Si_{1.2}$

Atom	WS	Occupation	*x*	*y*	*z*	B_{iso}, Å^2
La	8*a*	1	1/4	1/4	1/4	0.56(3)
Ni	8*b*	1	0	0	0	0.83(6)
M	96*i*	0.897(6)Ni+0.103(6)Si	0	0.1178(1)	0.1798(1)	0.88(3)

Most of interatomic distances in the structure of $LaNi_{11.8}Si_{1.2}$ are in good agreement with the atomic sizes. The coordination spheres of La and Ni atoms are formed only by the mixture of Ni/Si atoms. The lanthanum atom is in the center of a 24-vertex snub cubes. The nickel atom are located inside the icosahedra. The environment of the mixture of Ni/Si atoms consist of atoms of all sorts and the coordination polyhedron has 12 vertices.

References

[1] O.I. Bodak, E.I. Gladyshevskii, *Ternary systems containing rare earth metals*, Vyshcha shkola, Lvov **(**1985) 328.
[2] O.I. Bodak, E.I. Gladyshevskii, *Dopov. Akad. Nauk Ukr. RSR, Ser. A*, **12** (1969) 1125.
[3] O. Kasaraba, S. Pukas, B. Belan, M. Manyako, R. Gladyshevskii *Coll. Abs. XIII Int. Conf. Cryst. Chem. Intermet. Compd., Lviv*, (2016) 137.
[4] E. Parthé, L. Gelato, B. Chabot, M. Penzo, K. Cenzual, R. Gladyshevskii, *TYPIX. Standardized Data and Crystal Chemical Characterization of Inorganic Structure Types*, Springer, Berlin, Heidelberg (1993) 1596 p.

B-47

CIAŁOSTAŁOWE PROTONOWO PRZEWODZĄCE KOMPOZYTY NA BAZIE NANO I MIKRO WŁÓKNISTEJ CELULOZY JAKO MATRYCY POLIMEROWEJ

Iga Jankowska[(a)*], Katarzyna Pogorzelec-Glaser[(a)], Radosław Pankiewicz[(b)], Jadwiga Tritt-Goc[(a)]

[(a)] *Institute of Molecular Physics, Polish Academy of Sciences, M. Smoluchowskiego 17, 60-179 Poznań, Poland*
[(b)] *Faculty of Chemistry, Adam Mickiewicz University in Poznań, Umultowska 89b, 61-614 Poznań, Poland*

W celu uzyskania nowych kompozytów wykazujących protonowe przewodnictwo w temperaturach powyżej temperatury wrzenia wody, włókniste materiały celulozowe zostały sfunkcjonalizowane molekułami imidazolu [1-3].

Prowadzone badania dotyczyły porównania strukturalnych i termicznych właściwości różnych rodzajów włókien celulozowych: mikrowłókien i nanowłókien. Stopień krystaliczności badanych materiałów celulozowych został sprawdzony przy użyciu dyfrakcji rentgenowskiej (XRD). Powierzchnie kompozytów zostały zobrazowane za pomocą skaningowej mikroskopii elektronowej (SEM). Włókniste celulozy zostały zbadane za pomocą analizy termograwimetrycznej (TGA + DTG) oraz skaningowej kalorymetrii różnicowej (DSC) w celu określenia ich właściwości termicznych, ze szczególnym uwzględnieniem procesów ewaporacji wody z materiałów oraz ich stabilności termicznej.

Właściwości matrycy polimerowej, w tych przypadku różnych celulozowych materiałów włóknistych, użytych do syntezy nowych kompozytów wydają się być kluczowe dla właściwości zsyntezowanych kompozytów. Wyniki potwierdzają różnice we właściwościach strukturalnych i termicznych między nano i mikrowłóknami celulozy, których przyczyną są różne wielkości ziaren celulozowych oraz stopień ich krystaliczności.

Projekt finansowany przez Narodowe Centrum Nauki, 2017/24/C/ST5/00156

Literatura

[1] S. Ü. Celik, A. Bozkurt, S.S. Hosseini, Alternatives toward proton conductive anhydrous membranes for fuel cells: Heterocyclic protogenic solvents comprising polymer electrolytes, *Progress in Polymer Science*, **37** (2012) 1265–1291.

[2] I. Jankowska, R. Pankiewicz, K. Pogorzelec-Glaser, P. Ławniczak, A. Łapiński, J. Tritt-Goc. Comparison of structural, thermal and proton conductivity properties of micro- and nanocelluloses. *Carbohydrate Polymers*, **200** (2018) 536–542.

[3] I. Jankowska, P. Ławniczak, K. Pogorzelec-Glaser, A. Łapiński, R. Pankiewicz, J. Tritt-Goc, Cellulose microfibers surface treated with imidazole as new proton conductors, *Materials Chemistry and Physics*, **239** (2020) 122056.

B-48

ENVIRONMENT SENSITIVE SELF-HEALING FERROELASTIC METAL-ORGANIC FRAMEWORK

Aleksandra Półrolniczak and Andrzej Katrusiak

Department of Materials Chemistry, Faculty of Chemistry, Adam Mickiewicz University, Uniwersytetu Poznańskiego 8, 61-614 Poznan, Poland
**E-mail: aleksandra.polrolniczak@amu.edu.pl*

A new porous metal-organic framework, $[Cd(BDC)(AZPY)]_n$ (BDC = terephthalic acid; AZPY=4,4'-azobispyridine), hereafter AMU3 (Fig.1a), displays several potentially useful properties, such as pleochroism (Fig.1a), ferroelasticity, self-healing property (Fig.1b), and sensitivity to chemical composition of the liquid environment. Most importantly some of these properties are activated by pressure, whereas temperature induces no analogous transformations. The AMU3 crystals undergo a ferroelastic transition between orthorhombic (space group *Cmce*) and monoclinic ($P2_1/n$) phases. The transition can be induced by high pressure, but at 0.1 MPa the crystal remain orthorhombic. The critical pressure of the ferroelastic transition depends both on the guests in the AMU3 pores and on the pressure-transmitting medium. For example, AMU3·DMF compressed in methanol:ethanol:water (16:3:1 vol.) mixture transforms at 0.4 GPa, and when compressed in glycerin it transforms at 0.8 GPa. The crystal broken under the ferroelastic strain self-heal the cracks when the pressure is released.

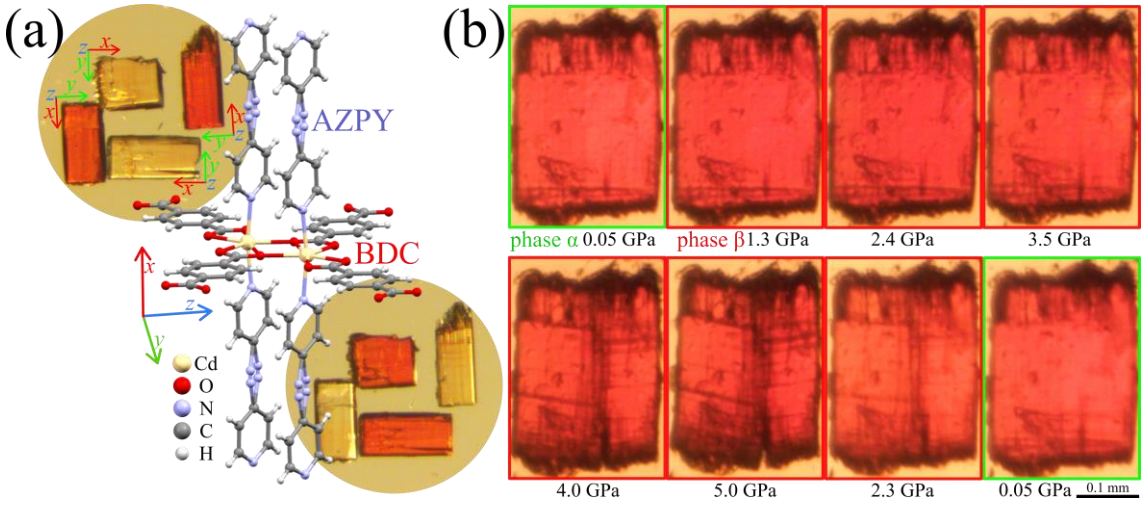

Fig. 1. (a) The double Cd(II) centre coordinated by AZPY and BDC linkers in AMU3 at normal conditions, including both sites of disordered AZPY linkers. In the first inset, several single-crystal AMU3 samples are aligned parallel and perpendicular to the polarized light and then rotated by 90° in the second inset; (b) Photographs of a sample crystal with defects appearing in the compressed β phase along planes (100) and (010), and the cleavage of the crystal along (010).

Literature

[1] A. Półrolniczak, A. Katrusiak, *Mater. Adv.*, (2021) Accepted Manuscript.

B-49

3D ARCHITECTURE OF CERIUM FORMATE-DERIVED CeO_2 HIERARCHICALLY STRUCTURED STAR-SHAPED PARTICLES

Piotr Woźniak, Małgorzata Małecka

Institute of Low Temperature and Structure Research, Okólna 2, 50-422 Wrocław

Cerium oxide due to its exceptional redox capabilities has been an object of structural and catalytic research since its introduction in motor industry as a three-way catalyst [1]. High oxygen storage capacity (OSC) facilitating CO oxidation and shape-dependent nanoparticle activity in soot combustion allow to design highly active ceria catalysts [2,3]. However, the low active site availability due to agglomeration and sintering of the powdered samples may limit ceria nanoparticles commercial utilization. One of possible solutions to this problem is designing hierarchically structured porous micro-sized particles composed of active well-organized nanosized crystallites [4]. In this study, 3D hierarchical architecture of such ceria-based material is presented.

Star-like CeO_2 particles were synthesized by oxidative thermolysis of $Ce(HCOO)_3$ formate precursor. Scanning Electron Microscope (SEM) was used to image the changes of particle morphology induced by thermal treatment. Electron Tomography (ET) followed by volume reconstruction allowed to get insight into the 3D porosity distribution within the star-shaped particle arm. The investigation was accompanied by TEM, HRTEM, SAED and PXRD characterization. Based on the obtained results and chemical considerations the model of approximate pore distribution was constructed.

In conclusion, the 3D mesoscale architecture of the porous CeO_2 oxide arm of the star-shaped particle is imprinted in the $Ce(HCOO)_3$ formate crystal structure. Due to that the pore channel distribution within the hierarchically structured ceria catalytic support is encoded in its synthetic precursor. This knowledge opens up a new perspective to design materials with highly defined pore layout via thermal decomposition of organic acids ceria precursors**.**

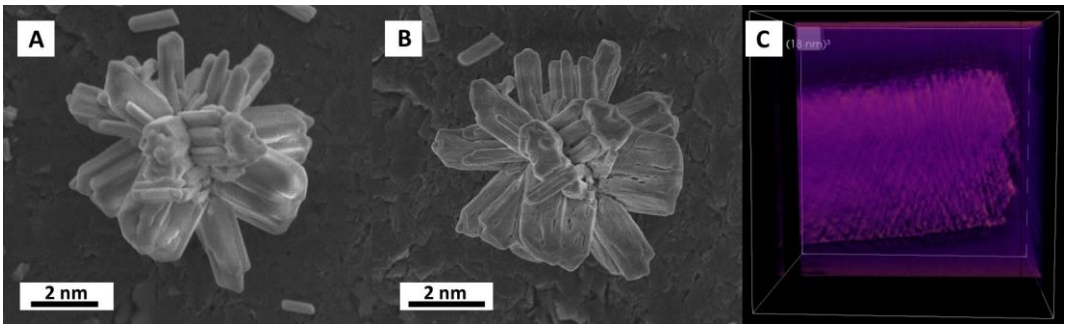

Fig. 1 A) SEM image of star-shaped $Ce(HCOO)_3$ particle; B) SEM image of star-shaped CeO_2 particle after oxidative thermolysis; C) ET volume reconstruction of the arm showing pore distribution.

References

[1] A. Trovarelli, P. Fornasiero, *Catalysis by Ceria and Related Materials, 2nd ed.*, Imperical College Press, London, 2013.
[2] P. Bharali, P. Saikiaac, B. M. Reddy, *Catal. Sci. Technol*., **2** (2012) 931–933.
[3] E. Aneggi, D.Wiater, C. de Leitenburg, J. Llorca, A. Trovarelli, *ACS Catal*., **4** (2014) 172-181.
[4] P. Woźniak, W. Miśta, M. A. Małecka, *CrystEngComm*, **22** (2020) 5914–5930.

B-50

CRYSTAL STRUCTURE AND ELECTRIC PROPERTIES OF NEW PROTON CONDUCTING PYRAZOLIUM SALT

P. Ławniczak[a], S. Zięba[a], A. Piotrowska[b], A.T. Dubis[c], A.K. Gzella[d], K. Markiewicz[c], A. Mizera[a], A. Łapiński[a]

[a]Institute of Molecular Physics, Polish Academy of Sciences, ul. Mariana Smoluchowskiego 17, 60-179 Poznań
[b]Poznań University of Technology, Piotrowo 3, 60-965 Poznań
[c]Institute of Chemistry, University of Bialystok, ul. Ciołkowskiego 1K, 15-245, Białystok
[d]Department of Organic Chemistry, Poznan University of Medical Sciences, ul. Grunwaldzka 6, 60-780 Poznań

Proton conducting materials belongs to a very interesting group of ionic conductors. They are applied as a membrane between electrodes in proton exchange membrane (PEM) and solid oxide fuel cells (SOFC) [1-2] or electrochemical sensors [3]. We can distinguish few branches of proton conductors due to operating temperature. Low-temperature proton conductors work usually at the temperature above 100^{o}C and often processes responsible for the migration of protons are related to the water molecules that are part of the material. However, water brings thermal limitations to the application of the material. Kreuer suggested using an alternative to water molecules, but that act similarly to water (can act as proton-acceptor, easily creates hydrogen bonds, etc.) [4]. To such molecules belongs imidazole and its derivatives (pyrazole, triazole, benzimidazole). Compounds based on imidazole and organic acids, introduced by MacDonald for the first time, are a very interesting and promising group of proton conducting materials [5-9].

Here we present detailed studies of a newly synthesized organic compound based on pyrazole and hemimellitic acid. Hemimellitic acid is a benzene derivative with three carboxylic acid groups. Structural investigations of new salt shows, that pyrazolium hemimellitate crystallized in the monoclinic system and space group C2/c with lattice parameters a = 31,2140(9) Å, b = 11,7836(4) Å, c = 6,8121(2) Å, $\alpha = \gamma = 90^{\circ}$, $\beta = 91{,}394(2)^{\circ}$. The volume of a unit cell is V = 2504.84(13). A view of molecular structure is presented in figure 1.

Studies of electric properties, based on impedance and dielectric spectroscopy, show some interesting and non-trivial results (see figure 2). In the case of linear dicarboxylic acids, the dc conductivity increases with temperature and no changes in the mechanism of charge migration are observed [5-7]. However, different behavior we observed for the pyrazolium hemimellitate. DC conductivity increases with temperature but above 90^{o}C reaches a plateau and is almost temperature independent up to 110^{o}C.

The origin of a plateau at the conductivity dependence in pyrazolium hemimellitate is caused by the evaporation of water, detected at thermal (DSC and TGA) studies. The influence of water molecules on impedance properties (i.e. Nyquist's plots) is visible in the inset in figure 2.

Acknowledgment
The scientific work was financed from budget Funds for Science in 2017-2021 as a research project under the "Diamentowy Grant" program (DI2016 015846).

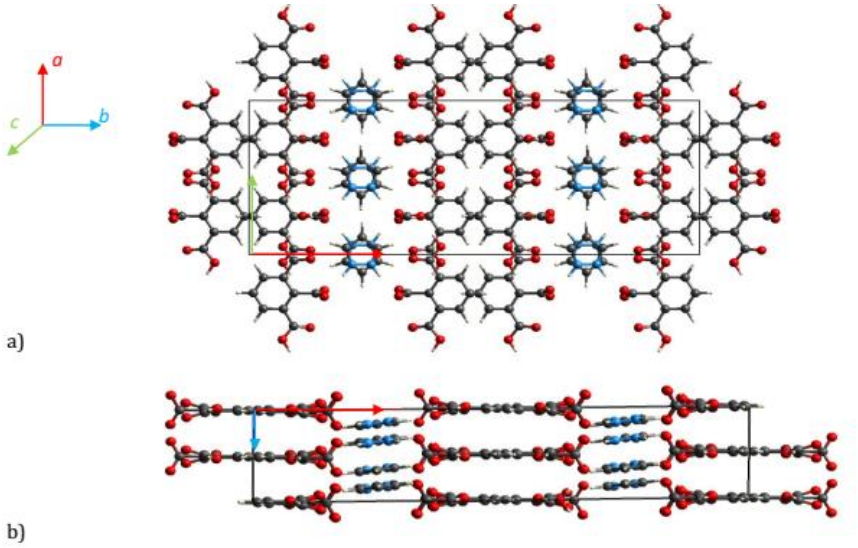

Fig. 1. A view of the molecular structure of pyrazolium hemimellitate on ab plane (top) and ac plane (bottom).

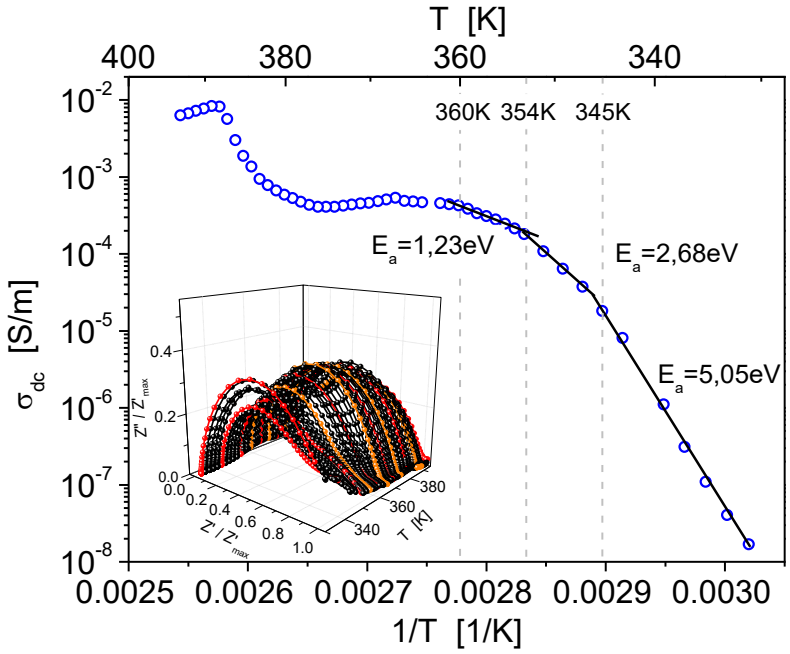

Fig. 2. The Arrhenius plot of dc conductivity of pyrazolium hemimellitate. Inset present the scaled Nyquist plots in the temperature range from 333K up to 393K.

References

[1] L. Bi, E. H. Da'as, S. P. Shafi *Electrochemistry Communications*, **80** (2017) 20.
[2] Y. Li, S. Wang, P.-C. Su *Scientific Reports*, **6** (2016) 22369.
[3] A.Vourros, V.Kyriakou, I.Garagounis, E.Vasileiou, M.Stoukides *Solid State Ionics*, **306** (2017) 76.
[4] K.D. Kreuer, A. Fuchs, M. Ise, M. Spaeth, J. Maier *Electrochimica Acta*, **43** (1998) 1281.
[5] J.C. MacDonald, P.C. Dorrestein, M.M. Pilley, *Crystal Growth & Design*, **1** (2001) 29.
[6] S.K. Callear, M.B. Hursthouse, T.L. Threlfall, *CrystEngComm*,**12** (2010) 898.
[7] K. Pogorzelec-Glaser, A. Rachocki, P. Ławniczak, A. Pietraszko, C. Pawlaczyk, B. Hilczer, M. Pugaczowa-Michalska, *CrystEngComm*, **15** (2013) 1950.
[8] S. Zięba, A. Dubis, P. Ławniczak, A. Gzella, K. Pogorzelec-Glaser, A. Łapiński, *Electrochimica Acta*, **306** (2019) 575.
[9] P. Ławniczak, K. Pogorzelec-Glaser, A. Pietraszko, B. Hilczer, *Acta Crystallographica B*, **77** (2021) 31.

B-51

COMPLETENESS IN HIGH-PRESSURE XRD EXPERIMENTS

Daniel Tchoń and Anna Makal

Biological and Chemical Research Centre, Faculty of Chemistry,
University of Warsaw, Żwirki i Wigury 101, 02-089 Warsaw, Poland

Quality of data obtained from high-pressure diffrac\tion experiments has become a sort of a taboo topic in the community. Any mentions of high-pressure in experimental tables tend to be followed with higher discrepancy factors, and it is so not without reason [1]. Presence of bulky steel body and two diamonds does not only affect the reliability of collected data, but more importantly limits the number of collectable reflections altogether. This often hampers investigation and forces researchers to rely on distorted or restrained models, which may lead to oversights and false conclusions.

While anvil cell is expected to increase background noise, and diamond signals can be considered a necessary evil, the completeness of obtained datasets can be vastly improved by carefully planning experimental strategy. The most straightforward way to do that is to increase coverage of reciprocal space using a cell with higher aperture [2], though this may come with a cost of limiting maximum attainable pressure. A much more affordable approach relies on utilising internal sample symmetry and increasing the final completeness by exposing as much independent reciprocal space as possible.

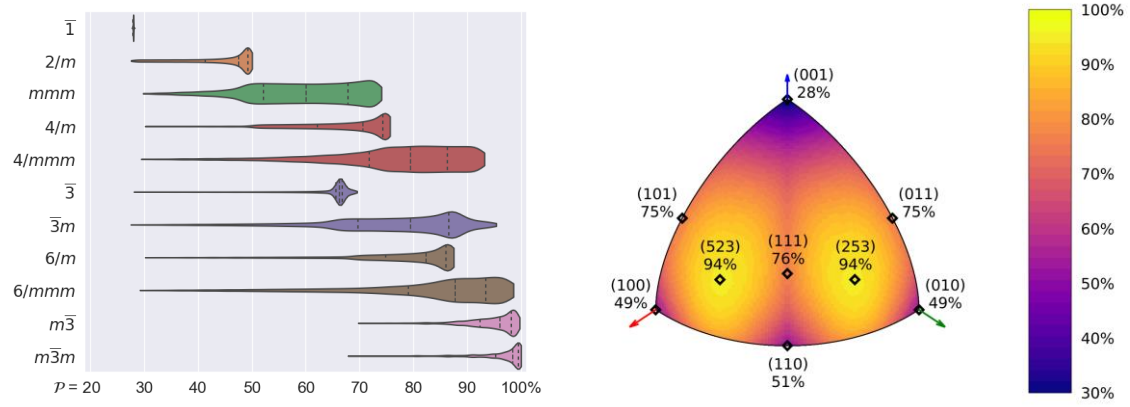

Fig. 1. Distribution of data completeness obtainable in high-pressure experiments: integrated (left) and as a function of crystal orientation (right), simulated assuming MoKα radiation and 35° anvil cell aperture. In some cases well-thought sample placement may increase completeness even by a factor of 4.

In this work an impact of diamond anvil cell aperture, incident radiation wavelength and sample placement on completeness of collected data is discussed. Range of data completeness obtainable using the most common incident sources and anvil cells, predicted using new software designed with this task in mind, is presented. Sample preparation protocols and data collection strategies, allowing to obtain the highest quality of results at virtually no expense, are suggested.

References

[1] a) N. Casati *et al.*, Nat Commun **7**, 10901 (2016); b) A. Jaffe *et al.*, ACS Cent. Sci., **2**, 201 (2016); c) S. A. Moggach *et al.* Crystallogr. Rev., **14**, 143 (2008)
[2] L. Merrill and W. Basset, Rev. Sci. Instrum. **45**, 290 (1974).

B-52

REFINED PROJECT OF THE SOLCRYS BEAMLINE OPTICS

Tomasz Kołodziej[1]*, Joanna Sławek[1], Grzegorz Gazdowicz[1], and Maciej Kozak[1]

[1]National Synchrotron Radiation Centre SOLARIS, Jagiellonian University, Czerwone Maki 98, 30-392 Kraków, Poland
**e-mail: t.kolodziej@uj.edu.pl*

In August 2020 started the design and construction process of superconducting wiggler by the Budker Institute of Nuclear Physics (Novosibirsk, Russian Federation). After the reception of the preliminary design of the photon source, the refined project of the optical scheme of the SOLCRYS beamline could be drafted.

The current project of the insertion device consists of the ~25 periods of superconducting magnet working at the magnetic field of 4 T. This device will be mounted in the straight section 02 of the SOLARIS storage ring. With the stored current of the electron beam of 500 mA, the emitted power should not exceed 14 kW.

Photon beam coming out of the front section will be split into two parallel branches:
- Macromolecular branch (MX) will use central portion of the beam with the opening of 1 mrad x 0.3 mrad.
- BioSAXS branch will use side part of the beam of the opening of 0.5 mrad x 0.3 mrad centered at the 0.75 mrad (horizontally).

In the current design, X-ray beams are crossed after BioSAXS beam is reflected sideways by the vertically collimating mirror, which can decrease angular separation of the beams at the beginning. Thanks to that, image of the beam at the focus of BioSAXS is not enormously elongated horizontally. Simplified scheme of the beamline is shown in Figure 1.

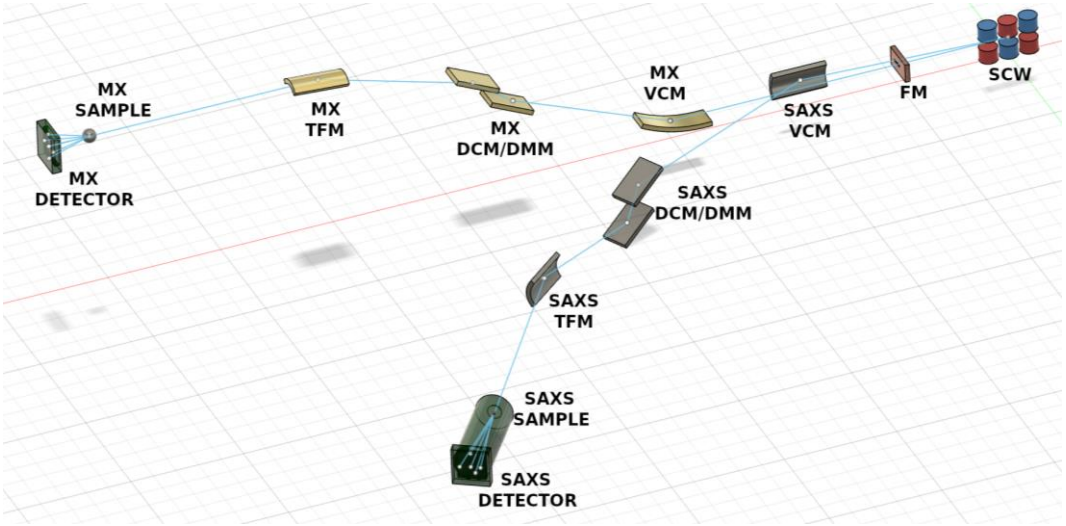

Fig. 1. Simplified optical scheme of the SOLCRYS beamline.

Both branches are designed in a similar manner from the optical point of view:
- First mirror (cylindrical) serve as the beam collimator in the vertical direction, initial heat load absorber and cutter of the higher photon energies (to avoid the contamination with the higher harmonics in the crystalline monochromator)
- In both branches there are hybrid Double Crystal/ Multilayer Monochromators serving as the energy/wavelength selector. Bandwidth of a Si(111) monochromator is $\delta E/E = 1.4 \cdot 10^{-4}$, while that of the multilayers should not exceed 0.5 %.
- Second mirror (toroidal) focuses the photon beam onto the sample position.

In both branches the beam shaping elements (slits) and diagnostic (fluorescent screens, intensity monitors) are planed as well.

Beamline design is supported with the geometrical ray tracing simulations. It was done with the use of most popular codes: XOP/Shadow [1] and OASYS/ ShadowOui [2]. Codes allow to simulate the performance of the complete setup, beginning with the generation of the radiation in the insertion device, to the propagation of the beam through the optical system including interaction of the radiation with the element (e.g. absorption in the elements); with the assumption of the realistic parameters of the elements (slope errors of the mirrors, reflectivity of the surfaces, etc.). The procedure can help to determine not only geometrical parameters of the beam size, angular divergence and energy resolution, but also flux (in photons/s), especially at the sample position.

Current design of the beamline give the following estimated numbers for the spot sizes and fluxes (here given for the 12 keV photon energy, with the Si(111) DCM):
- MX: size 290×79 μm^2, divergence 1.9×0.2 $mrad^2$, ΔE = 1.56 eV, $F=9 \cdot 10^{12}$ ph/s
- BioSAXS: size 604×44 μm^2, divergence 0.4×0.3 $mrad^2$, ΔE = 1.56 eV, $F=4 \cdot 10^{12}$ ph/s

Results of the simulation for the BioSAXS branch are shown in Figure 2.

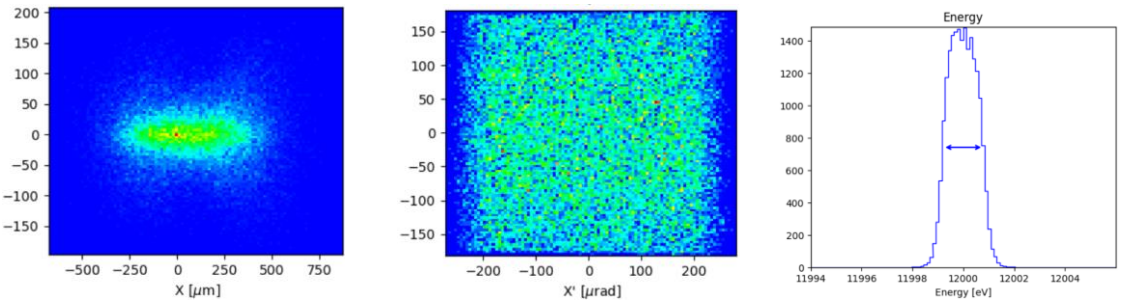

Fig. 2. Results of the simulation of the BioSAXS branch at the 12 keV photon energy. a) Spot size: 604 x 44 μm^2 (FWHM), b) Divergence 0.4 x 0.3 $mrad^2$, c) Energy resolution at 12 keV: 1.56 eV. Calculated flux: ~$4 \cdot 10^{12}$ ph/s.

References

[1] M. Sánchez del Río and R. J. Dejus. "XOP v2.4: recent developments of the x-ray optics software toolkit" *SPIE proceedings* **8141** (2011).
[2] L. Rebuffi, M. Sanchez del Rio, "ShadowOui: A new visual environment for X-ray optics and synchrotron beamline simulations", *J. Synchrotron Rad.* **23** (2016).

LISTA ZAREJESTROWANYCH UCZESTNIKÓW KONWERSATORIUM
LIST OF THE REGISTERED PARTICIPANTS

Jan	**Alfuth**	mgr inż.	Politechnika Gdańska
Beata	**Barszcz**	student	Instytut Niskich Temperatur i Badań Strukturalnych PAN, Wrocław
Elżbieta	**Bartoszak-Adamska**	Prof. UAM dr hab	Adam Mickiewicz University in Poznań
Julia	**Bąkowicz**	dr inż.	Wydział Chemiczny, Politechnika Wrocławska
Tamara	**Bednarchuk**	dr	Instytut Niskich Temperatur i Badań Strukturalnych PAN
Bohdana	**Belan**	Dr	Ivan Franko National University of L'viv
Michał J.	**Białek**	dr	University of Wrocław
Agata	**Białońska**	dr hab.	Uniwersytet Wrocławski
Weronika	**Bodylska**	student	Politechnika Wrocławska
Marta	**Bogdan**	mgr inż.	Politechnika Łódzka
Joanna	**Bojarska**	dr inż.	Politechnika Łódzka, Wydział Chemiczny
Patryk	**Borowski**	student	University of Warsaw, Department of Chemistry
Iwona	**Bryndal**	dr	Uniwersytet Medyczny im. Piastów Śląskich we Wrocławiu
Urszula	**Budniak**	mgr	Uniwersytet Warszawski
Daria	**Budzikur**	mgr	Uniwersytet Wrocławski
Ireneusz	**Bugański**	dr	Akademia Górniczo-Hutnicza
Anna	**Bujacz**	Dr hab. inż. prof. uczelni	Politechnika Łódzka, Instytut Biotechnologii Molekularnej i Przemysłowej
Grzegorz	**Bujacz**	Prof. dr hab. inż.	Politechnika Łódzka, Instytut Biotechnologii Molekularnej i Przemysłowej
Maciej	**Bujak**	dr hab.	Wydział Chemii, Uniwersytet Opolski
Helena	**Butkiewicz**	Eng MSc	Institute of Physical Chemistry Polish Academy of Sciences
Małgorzata	**Cabaj**	doktor	Uniwersytet Warszawski, Wydział Chemii
Jarosław	**Chojnacki**	Prof.	Politechnika Gdańska
Anna	**Ciborska**	dr inż.	Katedra Chemii Nieorganicznej, Wydział Chemiczny, Politechnika Gdańska
Anna	**Cociurovscaia**	mgr inż.	Instytut Biotechnologii Molekularnej i Przemysłowej, Politechnika Łódzka / Institute of Molecular and Industrial Biotechnology, Lodz University of Technology
Agnieszka	**Czapik**	doktor	Uniwersytet im. Adama Mickiewicza w Poznaniu, Wydział Chemii
Marek	**Daszkiewicz**	dr hab. inż.	Instytut Niskich Temperatur i Badań Strukturalnych PAN we Wrocławiu
Zbigniew	**Dauter**	Dr	National Cancer Institute, USA
Aleksandra	**Deptuch**	Dr	IFJ PAN
Paulina	**Dominiak**	Prof. dr hab.	Uniwersytet Warszawski
Jakub	**Drapała**	mgr inż.	Wydział Chemiczny Politechniki Warszawskiej
Dawid	**Drozdowski**	mgr inż.	INTiBS PAN

Henryk	**Drozdowski**	Prof.	Uniwersytet im. Adama Mickiewicza w Poznaniu, Wydział Fizyki
Michał	**Duda**	dr	Uniwersytet Jagielloński w Krakowie, Wydział Chemii
Kajetan	**Duszyński**	mgr inż.	Instytut Biotechnologii Molekularnej i Przemysłowej, Wydział Biotechnologii i Nauk o Żywności ,Politechnika Łódzka
Grzegorz	**Dutkiewicz**	mgr	Uniwersytet im. Adama Mickiewicza w Poznaniu
Viktoriya	**Dyakonenko**	PhD	SSI "Institute for Single Crystals" National Academy of Sciences of Ukraine
Konrad	**Dyk**	Magister	Uniwersytet Marii Curie-Skłodowskiej w Lublinie
Mariya	**Dzevenko**	PhD	Ivan Franko National University of L'viv
Piotr	**Fabrykiewicz**	mgr (doktorant)	Wydział Fizyki, Uniwersytet Warszawski, ul. Pasteura 5, 02-093 Warszawa
Marzena	**Fandzloch**	doktor	Instytut Niskich Temperatur i Badań Strukturalnych PAN, Wrocław
Anna	**Froelich**	dr	Uniwersytet Medyczny im. K. Marcinkowskiego w Poznaniu
Emilia	**Ganczar**	magister	Uniwersytet Wrocławski, Wydział Chemii
Anna	**Gągor**	dr hab	Instytut Niskich Temperatur i Badań Strukturalnych PAN
Maria	**Gdaniec**	Prof.	Wydział Chemii, Uniwersytet im. Adama Mickiewicza w Poznaniu
Mirosław	**Gilski**	prof. UAM dr hab.	Zakład Krystalografii, Wydział Chemii, Uniwersytet im. A. Mickiewicza, Poznań
Tadeusz	**Glenc**	Dr	Testchem sp. z o.o.
Mateusz	**Gołdyn**	M. Sc.	Adam Mickiewicz University
Barbara	**Gruza**	magister	Uniwersytet Warszawski, Wydział Chemii
Marlena	**Gryl**	dr hab.	Uniwersytet Jagielloński w Krakowie
Anita	**Grześkiewicz**	dr	UAM
Piotr	**Guńka**	dr inż.	Wydział Chemiczny Politechniki Warszawskiej
Karolina	**Gutmańska**	student	Katedra Chemii Nieorganicznej, Wydział Chemiczny, Politechnika Gdańska
Andrzej	**Gzella**	Profesor	Uniwersytet Medyczny im. Karola Marcinkowskiego w Poznaniu
Felix	**Hennersdorf**	Dr.	Rigaku Europe SE
Anna	**Hoser**	dr	University of Warsaw, Faculty of Chemistry
Jan	**Janczak**	profesor	Instytut Niskich Temperatur i Badań Strukturalnych, polska Akademia Nauk
Dominika	**Jankowska**	magister	Uniwersytet Mikołaja Kopernika w Toruniu, Katedra Chemii Analitycznej i Spektroskopii Stosowanej, Zespół Naukowy Chemii Bionieorganicznej i Koordynacyjnej
Irena	**Jankowska-Sumara**	dr hab.	Instytut Fizyki, Uniwersytet Pedagogiczny
Mariusz	**Jaskólski**	Prof.	A. Mickiewicz University
Teresa	**Jaworska-Gołąb**	dr	Instytut Fizyki im. M. Smoluchowskiego, UJ
Grzegorz	**Jędrzejczyk**		Faculty of Chemistry, Warsaw University of Technology
Kunal	**Jha**	PhD	University of Warsaw
Karolina	**Kałduńska**	Magister	Wydział Chemii, Uniwersytet Mikołaja Kopernika w Toruniu

Michał	**Kamiński**	Student (III rok studiów licencjackich)	Wydział Chemii, Uniwersytet Warszawski
Zbigniew	**Karczmarzyk**	dr hab. inż.	Wydział Nauk Ścisłych i Przyrodniczych, Uniwersytet Przyrodniczo-Humanistyczny w Siedlcach
Zbigniew	**Kaszkur**	Dr hab.	Instytut Chemii Fizycznej PAN, Warszawa
Oskar	**Kaszubowski**	Licencjat	Wydział Chemii Uniwersytetu Wrocławskiego
Marcin	**Kaźmierczak**	mgr	Wydział Chemii, Uniwersytet Wrocławski, ul. F. Joliot-Curie 14, 50-383 Wrocław
Vasyl	**Kinzhybalo**	Dr	Instytut Niskich Temperatur i Badań Strukturalnych PAN
Agnieszka	**Klonecka**	licencjat	Uniwersytet Jagielloński
Andrzej	**Kochel**	dr hab.	Wydział Chemii UWr.
Tomasz	**Kołodziej**	dr inż.	Narodowe Centrum Promieniowania Synchrotronowego SOLARIS UJ
Sebastian	**Koniarz**	mgr	Uniwersytet Wrocławski, Wydział Chemii
Krzysztof	**Konieczny**	Dr inż.	Advanced Materials Engineering and Modelling Group, Faculty of Chemistry, Wrocław University of Science and Technology
Irina	**Konovalova**	Dr.	STC “Institute for Single Crystals”, National Academy of Science of Ukraine, 60 Nauki ave., Kharkiv, 61001, Ukraine.
Daria	**Kowalkowska-Zedler**	dr inż.	Katedra Chemii Nieorganicznej, Wydział Chemiczny, Politechnika Gdańska
Dorota	**Kowalska**	Dr	Instytut Niskich Temperatur i Badań Strukturalnych PAN
Maciej	**Kozak**	Prof. dr hab	1) SOLARIS National Synchrotron Radiation Centre Jagiellonian University, Czerwone Maki 98, 30-392 Kraków, Poland 2) Department of Macromolecular Physics, Adam Mickiewicz University, Uniwersytetu Poznańskiego 2, 61-614 Poznań
Anna	**Kozakiewicz**	dr	Faculty of Chemistry, Nicolaus Copernicus University in Toruń
Marcin	**Kozieł**	doktor	Politechnika Łódzka, Instytut Biotechnologii Molekularnej i Przemysłowej
Monika	**Krawczyk**	doktor	Instytut Fizyki Doświadczalnej Uniwersytet Wrocławski, Pl. M. Borna 9, 50-204 Wrocław
Marta	**Krawczyk**	doktor	Wydział Farmaceutyczny, Uniwersytet Medyczny im. Piastów Śląskich we Wrocławiu, ul. Borowska 211, 50-556 Wrocław
Jacek	**Krawczyk**	dr	Institute of Materials Engineering, Faculty of Science and Technology, UNIVERSITY of SILESIA in Katowice
Ewelina	**Ksepko**	dr hab.	Politechnika Wrocławska
Maria	**Książek**	doktor	Instytut Fizyki, Uniwersytet Śląski
Michał	**Kula**	Pan	Uniwersytet Wrocławski
Marta	**Kulik**	dr	Uniwersytet Warszawski
Joachim	**Kusz**	profesor	Instytut Fizyki, Uniwersytet Śląski w Katowicach
Sylwia	**Kutniewska**	mgr	Department of Chemistry, University of Warsaw,
Iwona	**Lazar**	dr	Instytut Fizyki Uniwersytetu Śląskiego

Barbara	**Leśniewska**	Dr	Instytut Chemii Fizycznej PAN
Maciej	**Lewandowski**	Magister	Uniwersytet Mikołaja Kopernika w Toruniu
Zofia	**Lipkowska**	Prof.	Instytut Chemii Organicznej PAN
Tadeusz	**Lis**	Prof. dr hab.	Uniwersytet Wrocławski
Joanna	**Loch**	dr	Jagiellonian University
Wiesław	**Łasocha**	prof	Wydzial Chemii UJ
Paweł	**Ławniczak**	dr	Instytut Fizyki Molekularnej Polskiej Akademii Nauk ul. Mariana Smoluchowskiego 17, 60-179 Poznań
Rafał	**Łysowski**	mgr.inż	Politechnika Wrocławska
Sebastian	**Machowski**	magister	TESTCHEM sp. z o.o.
Izabela	**Madura**	dr hab. inż.	Wydział Chemiczny Politechniki Warszawskiej
Vladyslav	**Maliuzhenko**	licencjat	Uniwersytet Wrocławski
Waldemar	**Maniukiewicz**	Dr inż.	Politechnika Łódzka, Instytut Chemii Ogólnej i Ekologicznej
Paulina	**Marek**	MSc	Faculty of Chemistry, Warsaw University of Technology
Volodymyr	**Medviediev**	mgr	Instytut Niskich Temperatur i Badań Strukturalnych im. Włodzimierza Trzebiatowskiego Polskiej Akademii Nauk
Adrian	**Mermer**	MSc	University of Wrocław
Maja	**Morawiak**	dr inż.	Instytut Chemii Organicznej PAN
Ida	**Moszczyńska**	magister	Uniwersytety im. Adama Mickiewicza w Poznaniu
Tadeusz	**Muzioł**	dr	Nicolaus Copernicus University in Toruń Faculty of Chemistry
Arkadiusz	**Niełacny**	inżynier	Politechnika Łódzka, Instytut Chemii Ogólnej i Ekologicznej, ul. Żeromskiego 116, 90-924 Łódź
Wojciech	**Nitek**	dr	Uniwersytet Jagielloński, Wydział Chemii
Przemysław	**Nowak**	inżynier	Politechnika Łódzka, Wydział Chemiczny, Instytut Chemii Ogólnej i Ekologicznej
Weronika	**Nowak**	master	Adam Mickiewicz University in Poznań
Andrzej	**Okuniewski**	dr inż.	Katedra Chemii Nieorganicznej, Wydział Chemiczny, Politechnika Gdańska
Andrzej	**Olczak**	dr hab.	Politechnika Łódzka
Marta	**Orlikowska**	dr	Uniwersytet Gdanski
Adam	**Orylski**	brak	Wydział Chemii, Uniwersytet Wroclawski
Marta	**Otręba**	mgr	Uniwersytet Wrocławski, Wydział Chemii
Damian	**Paliwoda**	Dr	CNRS, ICGM, Universite de Montpellier, France
Jesica	**Pantaz**	Chemical Analyst	Antofagasta University
Wojciech	**Paszkowicz**	Profesor	Instytut Fizyki PAN, Warszawa
Robert	**Paszkowski**	dr inż.	University of Silesia in Katowice
Ewa	**Patyk-Kaźmierczak**	Doktor	Uniwersytet im. Adama Mickiewicza w Poznaniu
Olek	**Pavlyuk**	Dr.	Ivan Franko National University of Lviv
Adam	**Pietraszko**	Prof.	INTiBS PAN, Wrocław
Anna	**Pietrzak**	dr inż.	Politechnika Łódzka

Agnieszka	**Pietrzyk-Brzezińska**	Dr inż.	Instytut Biotechnologii Molekularnej i Przemysłowej, Politechnika Łódzka / Institute of Molecular and Industrial Biotechnology
Karolina	**Pioruńska-Sędłak**	mgr	Narodowy Instytut Leków
Paweł	**Piszora**	prof. UAM dr hab.	Uniwersytet im. Adama Mickiewicza w Poznaniu
Katarzyna	**Pogorzelec-Glaser**	dr hab.inż.	Instytut Fizyki Molekularnej PAN
Paulina	**Poniatowska**	Licencjat	Uniwersytet Adama Mickiewicza w Poznaniu
Kinga	**Potempa**	BSc	University of Warsaw
Aleksandra	**Półrolniczak**	magister	Uniwersytet im. Adama Mickiewicza / Adam Mickiewicz University
Radosław	**Przeniosło**	Prof.	Wydział Fizyki, Uniwersytet Warszawski
Anna	**Pyra**	dr	Uniwersytet Wrocławski
Anita	**Raducka**	mgr inż.	Politechnika Łódzka, Instytut Chemii Ogólnej i Ekologicznej, Wydział Chemiczny
Sadaf	**Rauf**	M.Sc.	Institute of General and Ecological Chemistry, Lodz University of Technology, Zeromskiego 116, 90-924 Lodz, Poland
Piotr	**Rejnhardt**	Magister inż.	Instytut Niskich Temperatur i Badań Strukturalnych
Bartłomiej	**Rogalewicz**	Inżynier	Politechnika Łódzka
Damian	**Rosiak**	dr inż.	Katedra Chemii Nieorganicznej, Wydział Chemiczny, Politechnika Gdańska
Paulina	**Rybicka**	mgr	Centrum Nauk Biologiczno-Chemicznych Uniwersytetu Warszawskiego, Wydział Chemii, Uniwersytet Warszawski, ul. Żwirki i Wigury 101, 02-089 Warszawa
Aron	**Rynkiewicz**	licencjat	Wydział Chemii, Uniwersytet Adama Mickiewicza w Poznaniu
Wojciech	**Rypniewski**	Professor	Insittute of Bioorganic Chemistry, Polish Academy of Sciences
Jarosław	**Serafińczuk**	dr hab. inż., prof. PWr	Politechnika Wrocławska
Anna	**Shaposhnyk**	PhD	SSI "Institute for Single Crystals" NAS of Ukraine
Svitlana	**Shishkina**	PhD	SSI "Institute for Single Crystals" NAS of Ukraine
Miłosz	**Siczek**	dr	Wydział Chemii, Uniwersytet Wrocławski
Magdalena	**Siedzielnik**	mgr inż.	Politechnika Gdańska, Wydział Chemiczny, Katedra Chemii Nieorganicznej
Yurii	**Slyvka**	Dr	Ivan Franko National University of Lviv
Joanna	**Sławek**	dr inż.	Narodowe Centrum Promieniowania Synchrotronowego SOLARIS, Uniwersytet Jagielloński
Wojciech	**Sławiński**	dr hab.	Uniwersytet Warszawski, Wydział Chemii
Paulina	**Sobczak**	inżynier	Politechnika Łódzka
Szymon	**Stolarek**	MSc	Rigaku Europe SE
Dominik	**Straszak**	Mgr/doktorant	Uniwersytet Medyczny w Lublinie
Radosław	**Strzałka**	dr inż.	AGH University of Science and Technology

Jarosław	**Sukiennik**	magister inżynier	Instytut Chemii Ogólnej i Ekologicznej Politechniki Łódzkiej
Szymon	**Sutuła**	mgr	University of Warsaw
Kinga	**Suwińska**	profesor	Uniwersytet Kardynała Stefana Wyszyńskiego w Warszawie
Daniel	**Szczerba**	magister inzynier	Universite Bourgogne Franche Comte
Małgorzata	**Szczesio**	dr hab. inż.	Politechnika Łódzka, Wydział Chemiczny, Instytut Chemii Ogólnej i Ekologicznej
Marian	**Szurgot**	Dr	Politechnika Łódzka
Andrzej	**Szytuła**	prof. dr hab.	Instytut Fizyki, Uniwersytet Jagielloński
Katarzyna	**Ślepokura**	dr hab.	Uniwersytet Wrocławski
Joanna	**Śmietańska**	mgr	Wydział Fizyki i Informatyki Stosowanej, Akademia Górniczo-Hutnicza im. Stanisława Staszica w Krakowie
Wiesław	**Świętnicki**	Dr.	IITD PAN
Daniel	**Tchoń**	mgr	Centrum Nauk Biologiczno-Chemicznych, Wydział Chemii Uniwersytetu Warszawskiego
Waldemar	**Tejchman**	dr hab.	Uniwersytet Pedagogiczny w Krakowie
Aleksandra	**Tołoczko**	mgr	Wydział Chemii, Uniwersytet Wrocławski, ul. F. Joliot-Curie 14, 50-383 Wrocław
Paweł	**Tomaszewski**	dr	Instytut Niskich temperatur i Badań Strukturalnych, Polska Akademia Nauk
Ilona	**Turowska-Tyrk**	Prof. dr hab.	Advanced Materials Engineering and Modelling Group, Faculty of Chemistry, Wrocław University of Science and Technology
Kamil	**Twaróg**	Magister	Uniwersytet Wrocławski, Wydział Chemii
Karolina	**Urbanowicz**	Inżynier	Wydział Chemiczny, Politechnika Warszawska
Yevhenii	**Vaksler**	PhD	SSI “Institute for Single Crystals” NAS of Ukraine
Anna	**Wantuch**	Licencjat	Uniwersytet Jagielloński, Wydział Chemii,
Katarzyna	**Wieczorek**	Inżynier	Politechnika Łódzka, Wydział Chemiczny, Instytut Chemii Ogólnej i Ekologicznej, ul. Żeromskiego 116, 90-924 Łódź
Ewa	**Wieczorek-Dziurla**	Magister	Uniwersytet Medyczny im. Karola Marcinkowskiego w Poznaniu
Marcus	**Winter**	Dr.	Rigaku Europe SE
Alexander	**Wlodawer**	Prof.	Center for Structural Biology, National Cancer Institute, Frederick, MD, USA
Andrzej	**Wojtczak**	Profesor dr hab.	Wydział Chemii, Uniwersytet Mikołaja Kopernika w Toruniu
Marek	**Wołcyrz**	Prof.	Instytut Niskich Temperatur i Badań Strukturalnych PAN, Wrocław
Piotr	**Woźniak**	mgr	Instytut Niskich Temperatur i Badań Strukturalnych PAN, Wrocław
Krzysztof	**Woźniak**	Prof. dr hab.	Wydział Chemii, Uniwersytet Warszawski
Agata	**Wróbel**	Bachelor of Science	Faculty of Chemistry, University of Warsaw
Paulina	**Wróbel**	magister	Uniwersytet Jagielloński
Karol	**Wydra**	mgr	Uniwersytet Wrocławski
Piotr	**Wyputa**	mgr inż.	Testchem Sp. z o.o.

Waldemar	**Wysocki**	dr	Wydział Nauk Ścisłych i Przyrodniczych, Uniwersytet Przyrodniczo-Humanistyczny w Siedlcach, ul. 3 Maja 54, 08-110 Siedlce
Paweł	**Zajdel**	dr hab.	Instytut Fizyki im. A. Chełkowskiego, Uniwersytet Śląski w Katowicach
Maciej	**Zieliński**	dr inż./PhD Eng.	Narodowe Centrum Badań Jądrowych / National Centre for Nuclear Research
Dagmara	**Ziembicka**		Katedra i Zakład Chemii Organicznej, Wydział Farmaceutyczny, Gdański Uniwersytet Medyczny
Przemysław	**Zima**	Inżynier	Politechnika Wrocławska, Wydział Chemiczny
Aleksandra	**Zwolenik**	student	Uniwersytet Warszawski
Andrzej	**Żarczyński**	Dr inż.	Politechnika Łódzka, Wydział Chemiczny, Instytut Chemii Ogólnej i Ekologicznej, ul. Żeromskiego 116, 90-924 Łódź
Ewa	**Żesławska**	dr hab.	Uniwersytet Pedagogiczny, Kraków

INDEKS AUTORÓW PRAC / INDEX OF AUTHORS

Normalną czcionką zaznaczono autorów prezentujących*, czcionką pochyłą współautorów.*
Presenting authors are shown in normal font, *co-authors in italics*.

Mirosława D.	***Ossowska-Chruściel***	*A- 8*
Marcin	***Oszajca***	*O- 21*
Marta	**Otręba**	A- 9, O- 4
Ibrahim I.	***Ozturck***	*A- 10*
Damian	**Paliwoda**	B- 16
Radosław	***Pankiewicz***	*B- 47*
Jan	***Parafiniuk***	*O- 16*
Marek	***Paściak***	*O- 25*
Oleksii	**Pavlyuk**	B- 17
Paulina	***Peksa***	*B- 15*
Adam	***Pietraszko***	*A- 15*
Anna	***Pietrzak***	*A- 1*, *A- 44*
Agnieszka	***Pietrzyk-Brzezińska***	*O- 15*
A.	***Piotrowska***	*B- 50*
Paweł	**Piszora**	A- 46
Monika	***Pitucha***	*B- 39*
Katarzyna	**Pogorzelec-Glaser**	B- 47
Nazariy T.	***Pokhodylo***	*A- 34*, *B- 17*
Aleksandra	**Półrolniczak**	B- 48
P.	***Poniatowska***	*A- 3*
Tomasz	***Poręba***	*B- 16*
Kinga	**Potempa**	B- 18
Radosław	**Przeniosło**	*A- 51*, B- 7
Svitlana	***Pukas***	*A- 50*
Anna	**Pyra**	*A- 16*, B- 19
Anita	**Raducka**	B- 20
Sadaf	**Rauf**	B- 21
Piotr	**Rejnhardt**	B- 22, O- 20
Nina	***Rembiałkowska***	*A- 16*, *B- 19*
Milan	***Remko***	*A- 1*
Francesco di	***Renzo***	*B- 16*
Bartłomiej	**Rogalewicz**	B- 23
Krystian	***Roleder***	*O- 24*
Oscar Ramon Fabelo	***Rosa***	*B- 31*
Damian	**Rosiak**	B- 24
Jérôme	***Rouquette***	*B- 16*
Vitalii	***Rudiuk***	*B- 26*
Bernhard	***Rupp***	*O- 12*
Paulina	**Rybicka**	B- 25
A.	***Rynkiewicz***	*A- 3*
Wojciech	***Rypniewski***	*O- 9*
Wojciech	***Rżysko***	*O- 26*
Volodymyr	***Sashuk***	*A- 19*
Wojciech	***Schilf***	*A- 41*

ISBN 978-83-939559-5-4